9TH INTERNATIONAL
ACID SULFATE SOILS CONFERENCE
26-31 MARCH, 2023
HOTEL GRAND CHANCELLOR, ADELAIDE

9TH INTERNATIONAL ACID SULFATE SOIL CONFERENCE ADELAIDE AUSTRALIA 2023

FIELD TOURS GUIDEBOOK

R.W. FITZPATRICK, E. LEYDEN, L.M MOSLEY & B. THOMAS

Contents

Participant to bring	Organisers to provide
Hat (wide brim recommended)	Water for refilling and cups
Sturdy shoes	Sunscreen
Water bottle to refill	First aid kits
Long pants	Insect repellent
Sun protective clothing	Shade tents if hot weather /rain forecast
	Transport as close as practicable to sites for mobility impaired attendees

Purpose of Field Trips

The purpose of the 3 field trips is to see and observe a wide range of acid sulfate soils (ASS) in coastal and inland environments across South Australia. The three field trips described in this guidebook have been made possible only because of help provided by many individuals from several agencies across Australia and overseas who have made valuable contributions to the understanding of the nature and occurrences of ASS in South Australia. We will not attempt to name all the individuals who have helped because we would without doubt forget someone. The information synthesized in this guidebook has been drawn from many sources, which we have attempted to cite throughout the guidebook. Where possible, we have used diagrams, sketches and photographs to better illustrate and represent huge volumes of data and text in the form of simplified visual representations. We apologise in advance for any oversimplification and omissions, which inadvertently may have crept into the guidebook.

This updated Post Conference website version of the guidebook was revamped by including additional explanations, references, data, land-use recommendations, and photographs taken during the 3 field trips to better clarify questions asked by delegates at several field sites. This current version of the field trip guidebook can be used as a teaching aid for student field excursions and self-guided field tours.

Health and Safety

We are looking forward to the upcoming 3 field trips. While we hope that it will be a safe and enjoyable experience for everyone, we want to make you aware of some of the potential hazards you may encounter during the 3 field trips. Please read the following information carefully and take appropriate precautions to ensure your safety.

Hazards:

The following hazards have been identified for this field trip:

- *Rough and uneven terrain*
- *Snakes*
- *Sun exposure and hot weather*
- *Proximity to water*
- *Mosquitoes*
- *Trucks and other vehicles*
- *Slippery surfaces*
- *Bushfire*

RISK ASSESSMENT:

The following risk assessment has been conducted for each hazard:

ROUGH TERRAIN AND UNEVEN GROUND

The rough terrain may pose a risk of trips, slips, and falls. Wear sturdy, comfortable shoes with good grip to prevent slipping and tripping. If you are unsure about a particular area, please ask the trip leader for guidance.

SNAKES

There may be snakes in the area, so be vigilant and stay away from tall grass and underbrush. Wear long pants and closed-toe shoes to protect yourself, and do not touch or try to catch any snakes you may encounter. If you see a snake, move away slowly and inform the trip leader. If you are bitten, remain calm and stationary and inform field trip leaders immediately so medical attention immediately administered.

SUN EXPOSURE AND HOT WEATHER

Participants are at risk of sunburn and heat exhaustion due to the high temperatures and exposure to the sun. Participants are advised to wear sunscreen, a hat, and protective clothing, and to drink plenty of water. The field trip leaders will provide shade tents in the event of hot weather. Sunscreen will be available at all times for participants.

PROXIMITY TO WATER

Participants may be at risk of drowning or other water-related injuries. Participants are advised to be careful near the water edge, stay within designated areas, and to follow all safety rules and instructions provided.

MOSQUITOS

Mosquitos can be a nuisance, but they can also transmit diseases. Wear long-sleeved shirts and pants and apply insect repellent to exposed skin. Insect repellent will be available at all times.

TRUCKS AND OTHER VEHICLES

There may be trucks and vehicles passing at speed beside the stops during the field trips. Please stay on the designated paths and be alert at all times. Avoid standing or walking close to the road, and never cross the road unless you are directed to do so by the trip leader.

WEATHER: RAIN

We recommend raincoats if rain is scheduled. Please take particular care on muddy and uneven surfaces following rain.

BUSHFIRE:

There may be a risk of bushfires in the area. Participants are advised to follow all instructions provided by local authorities, and to evacuate immediately if instructed to do so. See below for relevant numbers to report bushfire.

SLIPPERY SURFACES

There may be areas with slippery surfaces due to water or other factors. Participants are advised to watch their step, wear appropriate footwear with good grip, and to walk slowly and carefully.

Please note that this document is not an exhaustive list of all the hazards you may encounter during the field trip. It is your responsibility to take precautions and exercise good judgment to ensure your safety at all times. If you have any concerns or questions, please do not hesitate to contact the trip leader (see below for phone numbers).

Reporting injury and hazards

Please report any injuries or hazards, no matter how small, to the field trip leaders. First aid kits will be available at all times. If you see a hazard, please inform field trip leaders so steps can be taken to make the area safe.

Important Phone Numbers	
Emergency: Fire (including bushfire), Ambulance, Police	**000**
Police Assistance (non-urgent matters)	**13 14 44**
Bushfire information	**1800 362 361**
SES (Flood and fire rescue)	**132 500**
Prof Rob Fitzpatrick	**0408 824 215**
A/Prof Luke Mosley	**0428103563**
Dr Brett Thomas	**0438 844 298**
Dr. Emily Leyden	**0401 181 085**

Sponsors

PLATINUM SPONSOR

SOIL SCIENCE AUSTRALIA

THE UNIVERSITY of ADELAIDE

Government of South Australia
Coast Protection Board

EAL Environmental Analysis Laboratory

ENVIROLAB SERVICES

SOUTH AUSTRALIA

Government of South Australia
Department for Environment and Water

Conference organising committee: Prof. Rob Fitzpatrick & A/Prof. Luke Mosley (co-chairs), Dr Brett Thomas, Dr Emily Leyden, All Occasions Group (Patti Sbrissa, Amy Mitchell)

International Union of Soil Sciences Acid Sulfate Soils Working Group: Dr Anton Boman (Chair)**,** A/Prof. Vanessa Wong (Vice Chair)

International Scientific Committee: Australia – Laurance Fox, Prof. Leigh Sullivan, Phil Mulvey, Bernie Powell, Robert Quirk; Finland – Dr Peter Österholm; UK – Dr David Dent; USA – Prof. Martin Rabenhorst, Dr Mike Melville; Germany – Dr Angelika Kölbl; Indonesia – Dr Wirastuti Widyatmanti; China – A/Prof. Chaolei Yuan, Changxun Yu

Cover photo: (credit: Rob Fitzpatrick)**:** *Acid sulfate soil profile from Gillman (site on mid-conference field trip) showing: sulfuric material in contact with acidic drain water, with schwertmannite, an iron-oxyhydroxysulfate mineral coating surfaces.*

Conference Program Overview

Time	Sunday 26th	Monday 27th (Day 1)	Tuesday 28th (Day 2)	Wednesday 29th (Day 3)	Thursday 30th (Day 4)	Friday 31st
9:00-9:15am	**Pre-Conference**	**Opening Addresses**	**Keynote 3**	**Mid-Conference**	**Keynote 5**	**Post-Conference**
9:15-9:30am	**Field Trip**	**Keynote 1**	**Martin Rabenhorst**	**Field Trip**	**Angelika Kolbl**	**Field Trip**
9:30-9:45am		**Del Fanning**				
9:45-10:00am			Anton Boman		Emily Leyden	
10:00-10:30am		***Morning tea***	***Morning tea***		***Morning tea***	
10:30-10:45am		Anton Boman	Virginia Estévez		Rob Fitzpatrick	
10:45-11:00am		Graham Lancaster	Alexandra Nyman		Nicolaas Unland	
11:00-11:15am		Tapio Sutela	Vanessa Wong		Adrian Bonica	
11:15-11:30am		Michelle Martens	Michael Melville		Niloofar Karimian	
11:30-11:45am		Robert Quirk	Federico Alvarellos		Martin Rabenhorst	
11:45-12:00pm		Chrisy Clay	Makruf Nurudin		Phil Mulvey	
12:00-1:00pm		***Lunch***	***Lunch***		***Lunch***	
1:00-1:45pm		**Keynote 2**	**Keynote 4**		**Keynote 6**	
		Peter Osterholm	**Andrea Gerson**		**Andrew Coward**	
1:45-2:00pm		Leigh Sullivan	Rong Fan		Chaolei Yuan	
2:00-2:15pm		Colee Quayle	Gujie Qian		Andrew Grigg	
2:15-2:30pm		Alan Foley	Andrea Stiglingh		Eko Hanudin	
2:30-2:45pm		Navjot Kaur	Niloofar Karimian		Anders Johnson	
2:45-3:00pm		Thomas Kronberg	Jason Reynolds		Li Bi	
3:00-3:30pm		***Afternoon tea***	***Afternoon tea***		***Afternoon tea***	
3:30-3:45pm		Laurie Fox	Seija Virtanen		Leigh Sullivan	
3:45-4:00pm		Silvana Santomartino	Jeremy Manders		Liubov Kononova	
4:00-4:15pm		Miriam Nystrand	**Special Discussion**		Ruby Hume	
4:15-4:30pm		**Special Discussion**	**ASS classification**		Vanessa Wong	
4:30-4:45pm		**ASS management triggers**	**& mapping**		**Closing Addresses**	
4:45-5:00pm			**EJSS Special Issue**			
	Welcome Reception 6-7:30pm (Hotel Grand Chancellor)	**IUSS Acid Sulfate Soil working group meeting 5-6pm**	**Early Career Researcher Networking and EJSS Publishing Event 5-6 pm**	**Conference Dinner 7pm (Hotel Grand Chancellor)**		

Program Monday 27th March 2023

Time	Presenter	Presentation Title
9:00-9:15am	**Opening Addresses**	**Welcome (Prof. Rob Fitzpatrick), President of Soil Science Australia (Ed Scott)**
9:15-10:00am	**Keynote - Del Fanning**	**Historical Developments in the Understanding of Acid Sulfate Soils**
10:00-10:30am	***Morning tea***	
10:30-10:45am	Anton Boman	Potential acid sulfate soils in Arctic regions of Finland: A first survey
10:45-11:00am	Graham Lancaster	ASPAC Global Proficiency Testing, Acid Sulfate Soils Interlaboratory Testing Data and Analytical Methods for the National Guidelines
11:00-11:15am	Tapio Sutela	The effect of acid sulfate soils on river water quality and fish assemblages in Finland
11:15-11:30am	Michelle Martens	Packaging Acid Sulfate Soil (ASS) science for First Nations storytelling and ecotourism engagement
11:30-11:45am	Robert Quirk	Managing "The soils from Hell"
11:45-12:00pm	Chrisy Clay	28 years of managing broadacre acid sulfate soils on the North Coast of NSW: what have we done and what's left to do?
12:00-1:00pm	***Lunch***	*Formal Poster Session (will be up during whole conference)*
1:00-1:45pm	**Keynote - Peter Osterholm**	**Can identification and risk assessment of acid sulfate soils be simplified?**
1:45-2:00pm	Leigh Sullivan	Formal Assurance of professional competence in acid sulfate soil management
2:00-2:15pm	Colee Quayle	Identifying non coastal ASS and the Implications for beneficial reuse in NSW
2:15-2:30pm	Alan Foley	Case Study: Ellenbrook Residential Development, Perth, Western Australia 1994–2020
2:30-2:45pm	Navjot Kaur	Coastal Acid Sulfate Soils Assessment and Management – Story of Removal of Two Rail Crossings in Victoria, Australia
2:45-3:00pm	Thomas Kronberg	Stabilization of sulfide-bearing clays as a new building ground
3:00-3:30pm	***Afternoon tea***	
3:30-3:45pm	Laurie Fox	Assessing Acidic Soils versus Acid Sulfate Soils – Some Case Studies
3:45-4:00pm	Silvana Santomartino	Modifications to Accepted Acid Sulfate Soil Management Practices to Address External Risk Factors
4:00-4:15pm	Miriam Nystrand	An accelerated incubation method for the identification of acid sulfate soils
4:15-5:00pm	**Facilitated by Luke Mosley**	**Special discussion session on triggers for acid sulfate soils assessment and management** Fenn Hinhcliffe & Gunnar Haid - Net environmental benefit of ASS assessment - discussion primer (5 mins) Phil Mulvey - Kinetics and Nature of ASS Systems is Equally Important as Thermodynamics - discussion primer (5 mins) Chris Auricht - Management of peaty soils - discussion primer (5 mins)
5:00-6:00pm	**Anton Boman**	**International Union of Soil Science (IUSS) acid sulfate soil working group meeting**

Program Tuesday 28th March 2023

Time	Presenter	Presentation Title
9:00-9:45am	**Keynote - Martin Rabenhorst**	**The Evolving Classification of Acid Sulfate Soils**
9:45-10:00am	Anton Boman	Classification of acid sulfate soils and materials in Finland and Sweden: Re-introduction of pseudoacid sulfate soil materials
10:00-10:30am	***Morning tea***	
10:30-10:45am	Virginia Estévez	Improving prediction accuracy for acid sulfate soil mapping by means of variable selection
10:45-11:00am	Alexandra Nyman	Mapping and geochemical characterization of Acid Sulfate Soils throughout the Swedish coastline – a cost effective and rapid approach to determine environmentally relevant features over a large area
11:00-11:15am	Vanessa Wong	Acid sulfate soil characteristics in a large embayment under different vegetation types in southern Australia
11:15-11:30am	Michael Melville	Changes in cationic plant nutrient availability during Acid Sulfate Soil pedogenesis
11:30-11:45am	Federico Alvarellos	Geochemical and mineralogical composition of acid sulfate soils in Luleå, northern Sweden.
11:45-12:00pm	Makruf Nurudin	Early indications on potential acid sulphate soils formation in the Opak River Lagoon, Bantul, Yogyakarta, Indonesia
12:00-1:00pm	***Lunch***	
1:00-1:45pm	**Keynote – Andrea Gerson**	**Acid mine drainage: source control, standard testing methodologies and a case study of unexpected non-acid drainage**
1:45-2:00pm	Rong Fan	Evolution of pyrite oxidation from a 10-year kinetic leach study: Implications for mineralogical characterisations of secondary sulfate minerals
2:00-2:15pm	Gujie Qian	Dissolution of sulfide minerals in single and mixed sulfide systems under simulated acid and metalliferous drainage conditions
2:15-2:30pm	Andrea Stiglingh	Corrosion of zinc-aluminium and galvanised-steel fencing in Anthropogenic sulfuric soils
2:30-2:45pm	Niloofar Karimian	Arsenic and antimony co-sorption onto jarosite: An X-ray absorption spectroscopic study of retention mechanisms
2:45-3:00pm	Jason Reynolds	The geochemistry of arsenic in acid mine drainage: the role of pharmacosiderite
3:00-3:30pm	***Afternoon tea***	
3:30-3:45pm	Seija Virtanen	The effects of soil ripening on saturated hydraulic conductivity in cultivated acid sulfate soils in Finland
3:45-4:00pm	Jeremy Manders	How does potential and actual acidity of Acid Sulfate Soils (ASS) change over twenty years of soil storage?
4:00-4:45pm	**Facilitated by Prof. Rob Fitzpatrick**	**Special discussion session on international acid sulfate soil classification systems and mapping**
4:45-5:00pm	**Mark Farrell**	**Presentation on Special Issue from 9th IASSC on 'New Horizons in Acid Sulfate Soils Research' in European Journal of Soil Science**
5:00-6:00pm	**Early Career Researcher Event**	**Networking and discussion targeted at Early Career Researchers on advice for publishing in European Journal of Soil Science (EJSS) by Dr Mark Farrell, CSIRO, Deputy Editor of EJSS & Luke Mosley, Associate Editor of EJSS**

Program Thursday 30th of March 2023

Time	Presenter	Presentation Title
9:00-9:45am	**Keynote - Angelika Kolbl**	**Importance of mineral-organic matter interactions for remediation of acid sulfate soils by submergence and organic matter addition**
9:45-10:00am	Emily Leyden	Iron and sulfate reduction dynamics in coastal soils undergoing seawater inundation from sea level rise
10:00-10:30am	***Morning tea***	
10:30-10:45am	Rob Fitzpatrick	Acid sulfate soil change processes during wetting-drying cycles in peaty wetlands on Norfolk Island and impact of climate change
10:45-11:00am	Nicolaas Unland	Managing acid sulfate soil wetlands in a world of changing needs, values and climate
11:00-11:15am	Adrian Bonica	Salinization and Sulfide Distribution in Coastal Freshwater Wetlands: Gippsland Lakes
11:15-11:30am	Niloofar Karimian	Variations in Fe/S speciation and trace metals mobilisation in fresh water re-flooded ASS wetlands in a highly dynamic climate
11:30-11:45am	Martin Rabenhorst	Impact of Water Halinity on the Occurrence of Hypersulfidic Materials in Estuarine Tidal Marsh Soils of Chesapeake Bay (USA)
11:45-12:00pm	Phil Mulvey	Australian response to ASSs in regulating regional off-farm impacts is a template for measurably responding to climate change
12:00-1:00pm	***Lunch***	
1:00-1:45pm	**Keynote - Andrew Coward**	**How the zebra rock got its stripes: the formation of hematite banding from acid-sulfate fluid-rock interactions**
1:45-2:00pm	Chaolei Yuan	Effect of organic matter addition on cadmium and arsenic mobility in paddy soil
2:00-2:15pm	Andrew Grigg	Stability of jarosite in acid sulfate paddy soil from Central Thailand
2:15-2:30pm	Eko Hanudin	Interactive Effects of Nanozeolite and Ca-Humate in Alleviating Acidity and Al Toxicity of Sulfate Acid Soil from Segara Anakan Island, Indonesia
2:30-2:45pm	Anders Johnson	Survey of Swedish acid sulfate soils - microbiology
2:45-3:00pm	Li Bi	Unravelling the diversity and ecological roles of viruses in acid sulfate soil of Australia
3:00-3:30pm	***Afternoon tea***	
3:30-3:45pm	Leigh Sullivan	Behaviour of biogenic and geologic carbonates in disturbed sulfidic and sulfuric soil materials: particle size effects
3:45-4:00pm	Liubov Kononova	Effect of limestone amount and grain size on acid neutralization and metal release in dredged sulfide-bearing sediments: laboratory oxidation experiment
4:00-4:15pm	Ruby Hume	Monitoring lime application and movement using mid infrared spectroscopy
4:15-4:30pm	Vanessa Wong	Effect of inundation and lime amendments on greenhouse gas emissions from acid sulfate soils
4:30-5:00pm	**Closing Addresses**	**Discussion on host country and lead for 10th International Acid Sulfate Soils Conference (2026/2027). Pons Medal Presentation. Conference Closing Address.**

South Australia

Physiography

The Adelaide region is situated on the eastern edge of the Great Australian Bight and is dominated by the Mount Lofty Ranges, which run parallel to the coast. The ranges are composed of a series of sedimentary and volcanic rocks, including sandstone, shale, and basalt, which were formed during the Paleozoic and Mesozoic eras. In the modern landscape, the Mount Lofty Ranges form a prominent escarpment, rising sharply from the coastal plain to an elevation of over 700 meters at their highest point. Much of the ranges are forested and are home to a diverse range of flora and fauna, including many species that are endemic to the region. A series of river systems, including the Torrens River and the Onkaparinga River, which flow from the Mount Lofty Ranges to the coast, carving out valleys and gorges.

Geology

South Australia has a diverse geology, shaped by a complex history of tectonic activity, volcanic eruptions, and sedimentation over millions of years. The oldest rocks in South Australia are found in the Gawler Craton, which forms the central part of the state. The craton is composed of a variety of metamorphic and igneous rocks, including granites, gneisses, and schists, which were formed over 1.6 billion years ago during the Proterozoic era. To the east of the Gawler Craton, the Adelaide Geosyncline was formed during the Cambrian period, around 540 million years ago. The geosyncline is a sedimentary basin that contains a variety of rock types, including sandstone, shale, and limestone. Fossilized remains of marine life are common in these rocks, providing valuable insights into the evolution of life on Earth.

In the northern part of the state, the Stuart Shelf is composed of a mix of ancient rocks that were formed during the Proterozoic and Archean eras. The region is home to a number of mineral deposits, including copper, gold, and uranium, which have been mined for many years. In the southeast of the state, the Mount Gambier Volcanic Complex is a series of volcanic craters and lava flows that were formed during the Tertiary period, around 4-5 million years ago. The region is also home to a number of limestone caves, including the Naracoorte Caves, which contain a wealth of fossilized remains of ancient animals.

The Mount Lofty Ranges are a complex geological feature in South Australia, characterized by a diverse range of rock types and structures. The core of the Mount Lofty Ranges is composed of ancient, metamorphosed rocks that are around 1.6 billion years old. These rocks include granites, gneisses, and schists, which were formed deep within the Earth's crust and subsequently uplifted and exposed by tectonic activity. Surrounding the core of the range are a series of younger sedimentary rocks, which were deposited during the Paleozoic and Mesozoic eras (between around 541 million and 66 million years ago). These sedimentary rocks include sandstones, shales, and limestones, which were deposited in a range of different environments, including river deltas, shallow seas, and coral reefs. During the Tertiary and Quaternary periods (between around 66 million years ago and the present), the Mount Lofty Ranges underwent a series of deformation and uplift events, leading to the formation of the mountain range as we see it today. This uplift was accompanied by extensive erosion, which has resulted in the exposure of the underlying rock

formations and the formation of a range of distinctive landforms, including steep-sided valleys, gorges, and rocky outcrops.

The Adelaide Plains are composed of a thick layer of unconsolidated sediments, consisting of mainly of sands, silts, clays, and gravels that have been eroded from the Mount Lofty Ranges and transported by rivers and streams to the coast. The oldest rocks that underlie the plains are around 500 million years old and consist of sedimentary rocks such as sandstone, shale, and limestone. These rocks were deposited in shallow seas and have been uplifted and eroded over time to form the Mount Lofty Ranges. During the Quaternary period the Adelaide Plains were subjected to repeated cycles of marine transgression and regression, resulting in the deposition of thick layers of sediments.

The Murray Plains are located to the east of the Mount Lofty Ranges in South Australia. The area is dominated by a flat, low-lying landscape, which is generally suitable for agriculture. The Murray Plains consist of a thick layer of sedimentary rocks that were deposited during the Cenozoic era (65 MYA). The Murray Plains are underlain by a series of sedimentary basins which consist mainly of sandstones, shales, and limestones, deposited in a variety of environments, including river deltas, coastal plains, and shallow seas. These basins are separated by structural features, such as faults and folds, which have influenced the distribution and composition of the sedimentary rocks. The rocks are generally flat-lying, but they may be gently folded or faulted in places. The Murray River and its tributaries have played a significant role in shaping the landscape of the Murray Plains. The river has carved out deep valleys and gorges and has deposited alluvial sediments along its banks. The alluvial sediments are often highly fertile and have been extensively used for agriculture.

The South Australian landscape has also been impacted by a series of glacial and interglacial cycles during the Quaternary (2.8 m to present). During the early part of the Quaternary, South Australia was characterized by a relatively arid and flat landscape, with a series of shallow lakes and swamps occupying the low-lying areas. Over time, the climate became cooler and wetter, leading to the formation of extensive grasslands and woodlands. Around 1 million years ago, the first major glaciation occurred, with ice sheets extending from the southern polar region as far north as southern Australia. This period was marked by the deposition of large amounts of sediment, including glacial till, which forms the basis of many of the landscape features in South Australia today. Over the next several hundred thousand years, the climate fluctuated between periods of glaciation and interglacials, with the most recent glacial period occurring around 20,000 years ago. During this time, much of South Australia was covered by a large ice sheet, which carved out the landscape and left behind a series of glacial landforms, such as moraines and eskers. As the climate warmed and the ice sheets retreated, the landscape of South Australia began to take on its current form, with many of the rivers and valleys that exist today being formed during this time. The interglacial period also saw the evolution of modern humans and the development of indigenous cultures in the region.

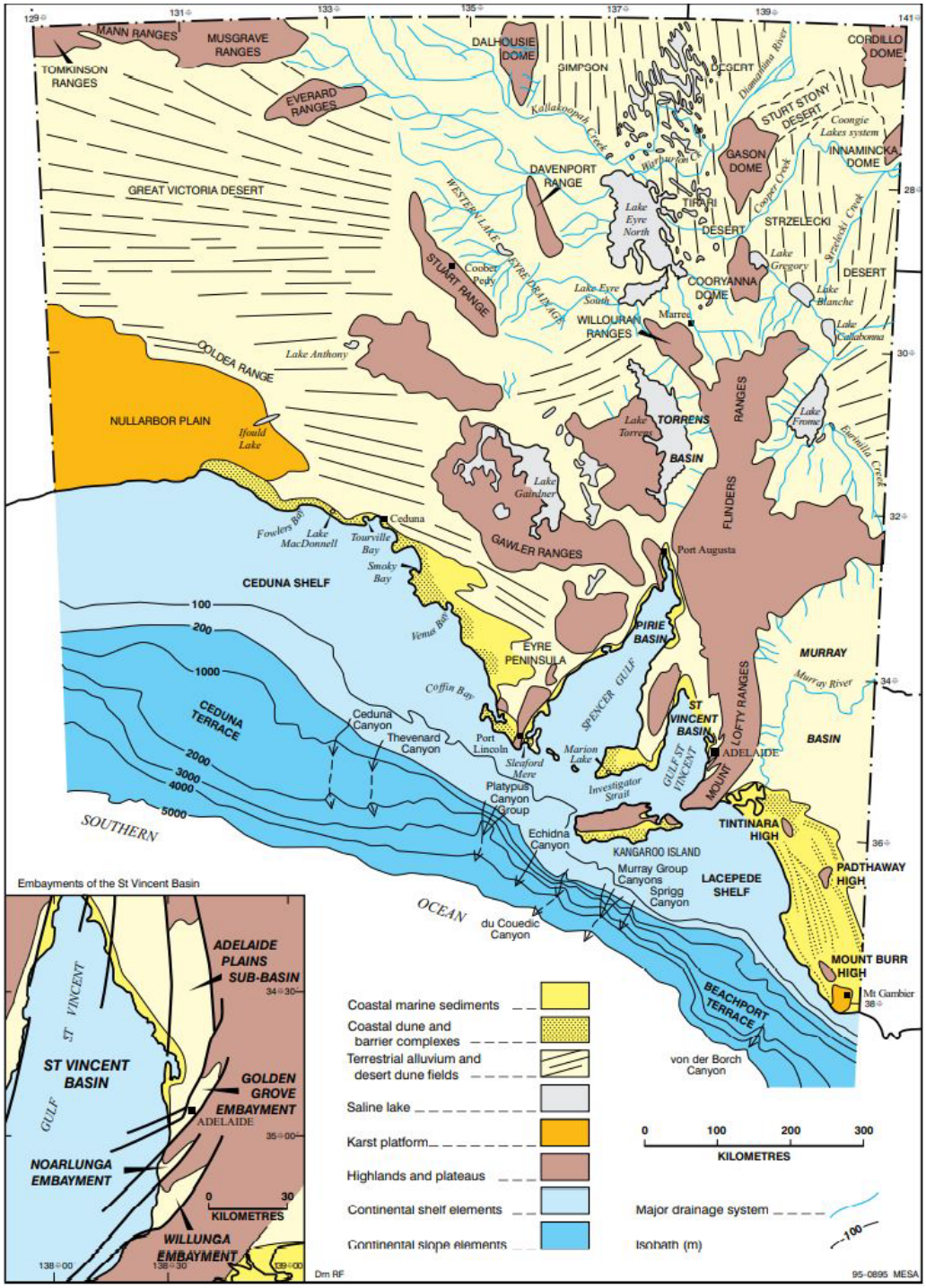

Figure 1: The Quaternary morphological elements of South Australia (Drexel & Preiss, 1995)

Climate:

Adelaide has a Mediterranean climate characterized by warm to hot summers, mild winters, and moderate rainfall throughout the year. The city is located in a coastal region, which moderates the temperature and brings some rainfall throughout the year. During the summer months of December to February, temperatures in Adelaide typically range from around a minimum of 16°C (61°F) to an average maximum of 30°C (86°F). Heatwaves can occur during this period, with temperatures

occasionally exceeding 40°C (104°F) for several days in a row. Humidity is generally low during the summer, which can exacerbate the feeling of heat. Winter in Adelaide is mild, with temperatures ranging from around 8°C (46°F) to 16°C (61°F). Rainfall is more common during the winter months of June to August, with occasional thunderstorms and periods of heavy rain. Spring and autumn are transitional seasons in Adelaide, with temperatures generally mild. During these seasons, temperatures can range from around 12°C (54°F) to 22°C (72°F). According to the Bureau of Meteorology, the average annual rainfall in Adelaide is around 537 mm (21.1 inches), with the majority of this falling during the winter months. In contrast, the summer months are generally dry, with little rainfall.

Water:

South Australia's water supply is primarily sourced from two major river systems: the River Murray and the Adelaide Hills catchments. The River Murray is a major source of water for the state, providing around three-quarters of the water used for irrigation, as well as a significant proportion of the water used for domestic and industrial purposes. Water from the Murray is transported to various parts of the state via a network of channels and pipelines, with the majority of the water used for agriculture in the Murray-Darling Basin region. The Adelaide Hills catchments provide a smaller, but still significant, proportion of the state's water supply. The catchments are located in the hills to the east of Adelaide and are primarily used for urban water supply, providing water for domestic and industrial purposes in the Adelaide metropolitan area. In addition to these major sources of water, South Australia also relies on a number of smaller groundwater sources, particularly in rural and remote areas of the state. Groundwater is typically used for irrigation and stock watering, as well as for domestic and industrial purposes. Managing the state's water resources is a complex task, and requires careful planning and management to ensure that water is used efficiently and sustainably. In recent years, South Australia has invested in a range of initiatives aimed at improving water use efficiency, reducing waste, and increasing the use of recycled water. These initiatives include the construction of new water treatment plants, the development of water recycling schemes, and the implementation of water pricing and allocation systems designed to encourage sustainable use of the state's water resources.

Soils:

South Australia's soils are diverse, reflecting the state's varied geology, climate, and land use history. The state can be divided into several broad soil regions, each characterized by its unique combination of soil and substrate types and properties. A great diversity of substrate materials occurs in South Australia—from ancient bedrock formed over three thousand million years ago (Fraser et al. 2008) to unconsolidated coastal and alluvial sediments deposited over the last few thousand years. The properties of many South Australian soils have also been affected by later accessions of wind or water borne substances (e.g. fine carbonate), which are often dissimilar in origin and nature to both the original substrate and soil materials (Hall et al., 2009)

Thirty-seven substrate types are described in Hall et al. (2009) and grouped into ten broad categories as listed below. The below section has been adapted from Hall et al. (2009):

1. **Recent coastal deposits and sediments associated with inland saline depressions**: including wind deposited, coastal siliceous and carbonate sands; the sediments of coastal swamps,

often including shell-rich layers; gypsum-rich loams and sands derived from, and adjacent to, coastal and inland saline depressions; and the sediments of inland saline depressions.

2. **Volcanic ash:** sediments derived from volcanic eruptions in the Lower South East.
3. **Unconsolidated aeolian deposits:** including siliceous sand, carbonate sand, and finer grained calcareous material (loess), but not including recently deposited aeolian sediments of modern coastlines and adjacent areas.
4. **Calcrete:** consolidated, terrestrial, carbonaterich materials, including 'mallee' calcrete and calcreted calcarenite.
5. **Buried soils:** a range of buried-soil profiles forming the substrate of overlying soils.
6. **Pleistocene to Holocene age alluvium:** sediments associated with modern watercourses as well as older outwash sediments derived from adjacent basement rock highlands.
7. **Clay, sand and till sediments**: mostly unconsolidated clays, sandy clays, sandy clay loams or clayey sands of ancient coastal, lacustrine, lagoonal, estuarine, fluvial, glacial or in situ weathering origin. Sediments of obvious recent to relatively recent alluvial origin are not included (see 6)
8. **Tertiary to Pleistocene age limestone**: semiconsolidated to consolidated limestones, but not including the partially metamorphosed to metamorphosed ancient bedrock limestone or dolomite of earlier periods (see 10).
9. **Kaolin clay, ferricrete and silcrete**: materials characterised by formation during extended periods of deep weathering.
10. **Weathering bedrock:** including all major igneus, sedimentary and metamorphic basement rocks commonly found as substrates in Southern South Australia.

Some materials have only minor occurrence as soil substrates, either because of limited extent or deep burial by other sediments. For example, the Wisanger Basalt on Kangaroo Island has very limited occurrence both as a sediment and as a substrate, while the calcareous Coomandook Formation of the South East Coastal Plain is extensive, but is generally too deeply buried to act as a soil substrate. The properties of many soils in Southern South Australia have been affected by accessions of younger materials. The process involves the deposition of substances contained in dust or dissolved in rain drops, and their subsequent leaching within profiles via internal wetting fronts. In higher rainfall districts, such substances are typically leached beyond the soil profile (except where drainage is restricted); however, in moderate to lower rainfall districts they commonly accumulate within the soil. The most readily observable of these materials is fine carbonate, usually evident as an accumulation of whitish material within the subsoil. In such cases, these substances are not parent or substrate material, but later additions which nonetheless influence soil properties.

More detail on these groups (including photos) can be found in (Hall et al., 2009) from Page 323 using the QR code below.

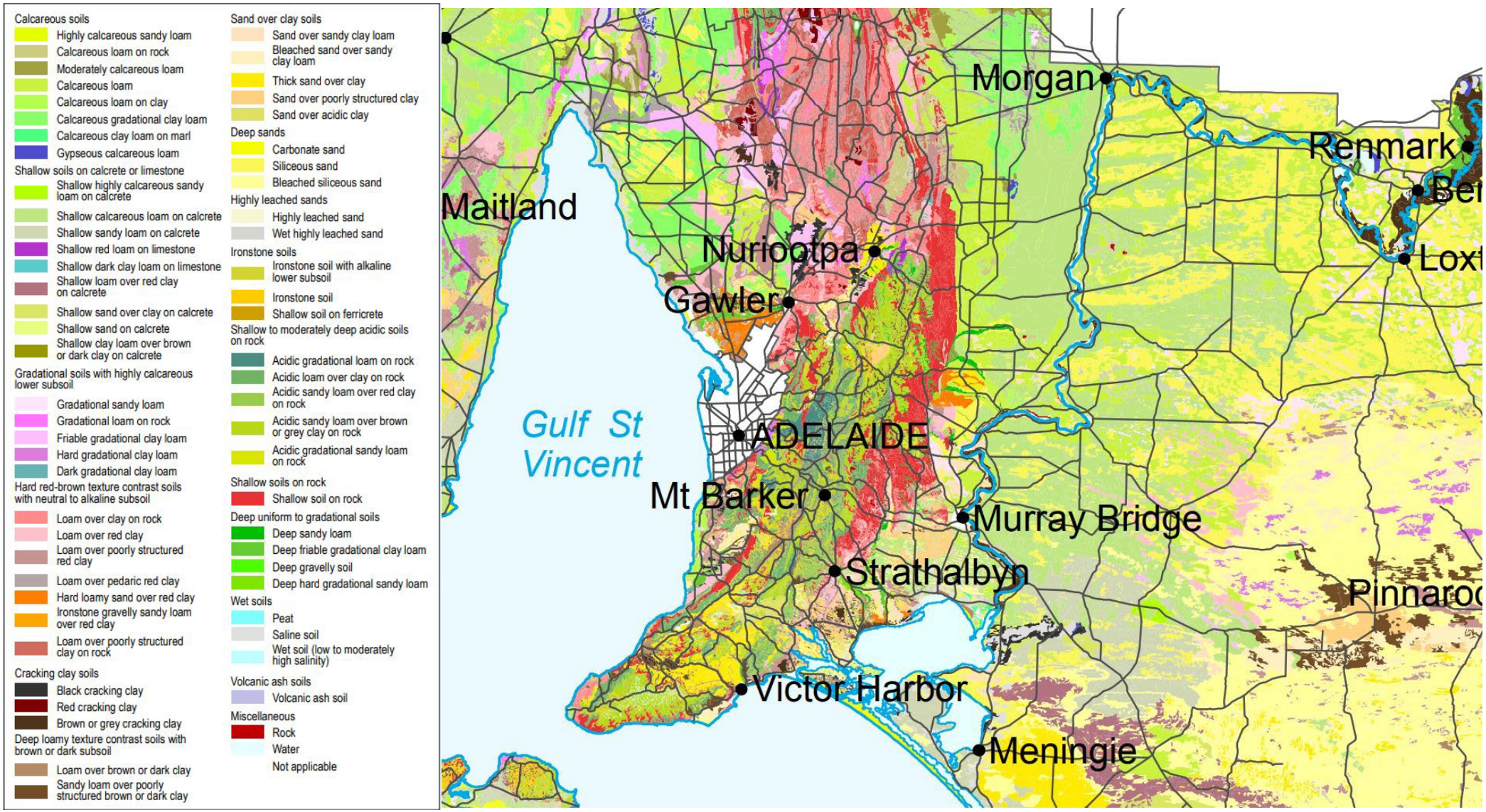

Figure 2: General Soil Map of Adelaide, Mount Lofty and Surrounds – from Department of Environment and Water

Land use:

The land use in Adelaide and the Mount Lofty Ranges is diverse, reflecting the region's mix of urban, peri-urban, and rural landscapes. In the urban areas of Adelaide, land use is dominated by residential, commercial, and industrial development, with a significant proportion of the population living in the metropolitan area. The city also has a number of parks and open spaces, including the Adelaide Park Lands, which are used for recreational purposes by residents and visitors.

Outside the urban areas, the Mount Lofty Ranges are characterized by a mix of agricultural, forestry, and conservation land uses. The region is home to a number of vineyards and orchards, which produce a range of crops including wine grapes, apples, and pears. The hills and forests of the Mount Lofty Ranges also provide opportunities for forestry and timber production.

The land use in the Lower Murray area is dominated by agriculture, with the region being one of the most important agricultural areas in South Australia. The majority of the land in the Lower Murray area is used for dryland cropping, with wheat, barley, and other cereals being the main crops grown. Other important crops include legumes, such as chickpeas and lentils, as well as oilseeds like canola. In addition to dryland cropping, the Lower Murray area is also an important horticultural region, with citrus fruits, stone fruits, and almonds being among the main crops grown. These crops are typically grown using irrigation, which is sourced from the River Murray and other local water sources. Livestock grazing is also an important land use in the Lower Murray area, with sheep and cattle being the main livestock species raised. Grazing typically occurs on native pastures, which are found in the region's more marginal areas.

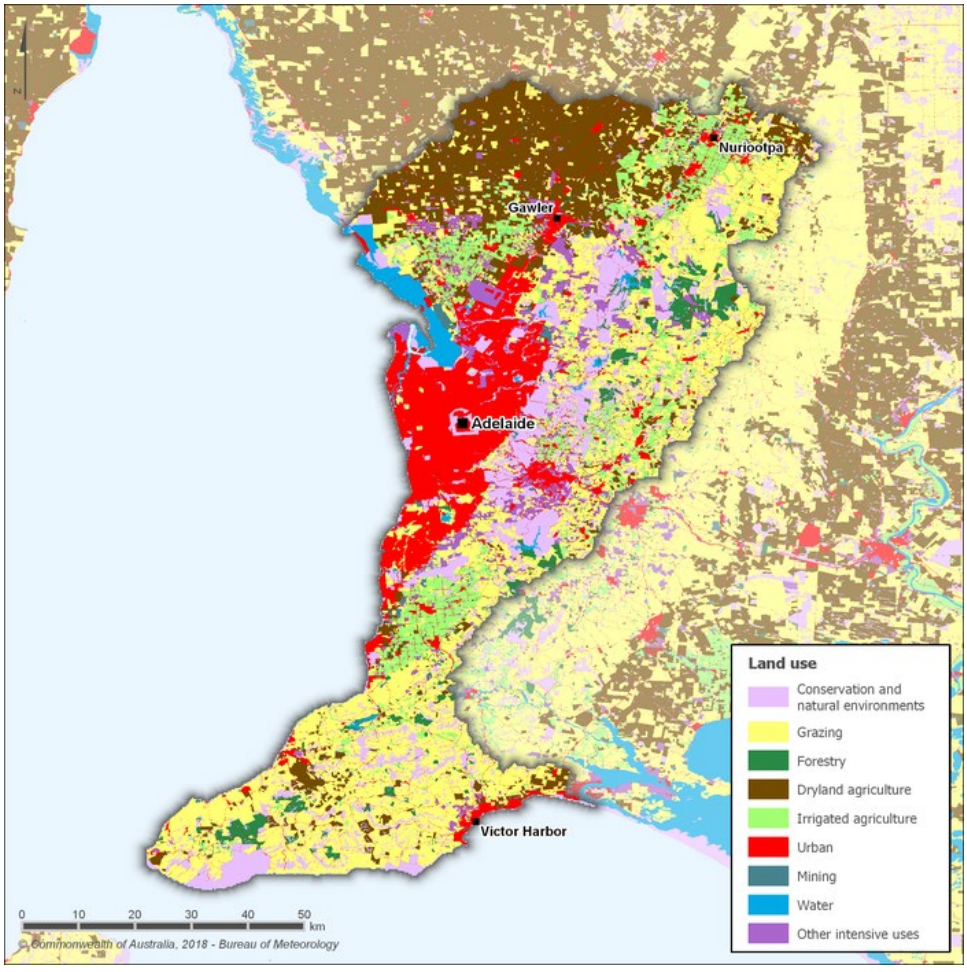

Figure 3: Generalised land use in the region

PRE-CONFERENCE FIELD TRIP

WALLY'S LANDING - FINNISS RIVER & JERVOIS - LOWER MURRAY RECLAIMED IRRGATION AREA

SUNDAY 26TH MARCH 2023

FIELD TRIP ITINERARY

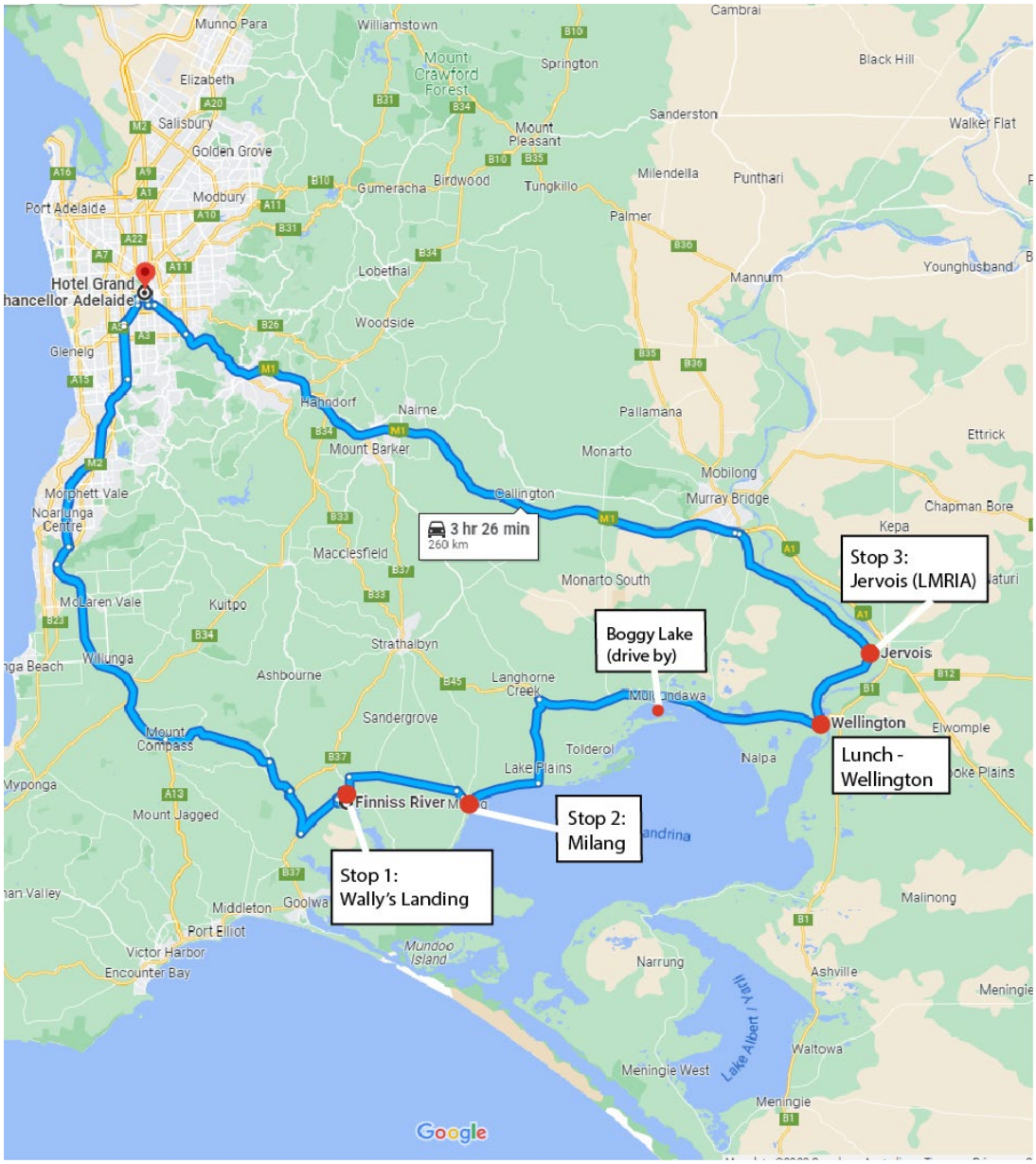

Location	Time
Meet in lobby	8:45 am
Leave Hotel Grand Chancellor	9:00 am
Arrive Stop 1: Wally's Landing Finniss River	10:30 am
Morning tea	10:30 am
Leave Stop 1	12:00 am
Arrive Stop 2: Milang to view Lake Alexandrina	12:15 am
Drive by Boggy Lake	12.30
Arrive Wellington for lunch	12:45 pm
Leave Wellington	1:30 pm
Arrive Stop 3: Jervois	2:00 pm
Leave Jervois	3:30 pm
Arrive at Hotel Grand Chancellor	4:30 pm

Figure 4: Google Earth Map of Field Trip sites

Summary

Adapted from ***(Fitzpatrick et al., 2018)****.*

This Field Trip will take attendees to several sites (Figure 4) which were severely affected by the Millennium Drought. The Millennium drought was a prolonged period of severe drought in Australia, which began in the early 2000's and lasted until mid-2010. The drought had a significant impact on the River Murray Catchment, which is one of Australia's most important river systems. The River Murray is a major source of water for irrigation, urban water supply, and environmental flows, and the drought had a profound impact on the basin, in particular the lower sections. The Millennium drought was caused by a combination of factors, including a decrease in rainfall, higher temperatures, and increased evaporation rates. The drought was also exacerbated by the over-extraction and over-allocation of water from the river system for irrigation and other uses.

Before European arrival, the traditional owners of the land we are visiting on this field trip were the Ngarrindjeri people. The Ngarrindjeri people recorded creation stories about the remarkable changes that occurred both when the sea level began rising ~18 000 years ago and when the current sea level stabilised ~5 000 years ago. At the same time, rainfall and inland lake levels were initially low, followed by cycles of brief highs and extended dries. By 5 000 years ago, rainfall was marginally higher than it is today. During wetter periods, lake levels filled, while dune building dominated in dry periods (Bowler et al., 1976). The creation stories and oral traditions of Indigenous people have been passed down from generation to generation, especially about the detailed knowledge of the nurseries, i.e. wetlands (reed beds were much more extensive in the past), many of which contain acid sulfate soils. The Coorong is also an archaeological site of national importance with shell middens and burial sites throughout the area, giving evidence of Aboriginal occupation for >5 000 years. For example, the Ngarrindjeri believe that the land and waters is a living body and that they are a part of its existence (Ngarrindjeri Nation, 2007). In the Ngarrindjeri Nation Yarluwar-Ruwe plan (Ngarrindjeri Nation 2007, p. 13) it is stated: 'The land and waters must be healthy for the Ngarrindjeri people to be healthy. We say that if wetlands/nurseries die, our Ngartji (totem or special friend) die, then Ngarrindjeri will surely die'.

The first European explorers also possessed great skills of observation. The early explorers were usually not trained scientists, as their primary concerns were to delineate the major terrain features of the interior, and to survive. Moreover, many of the early explorers originated or worked in environments quite different from Australia. The early explorers used mainly horses for transport, and their observations and reports on soils had mainly to do with pastoral or agricultural potential rather than with the natural history of wetlands or back swamps. Nevertheless, the following observations remain of interest with regard to past and current known occurrences of inland acid sulfate soils:

Captain Charles Sturt was one of the earliest European recorders of soil information in southern Australia. Following his previous experience along the Murrumbidgee, Murray and Darling Rivers from 1828 to 1829, Sturt explored from Cawndilla near the Menindee Lakes westward into the north-eastern deserts of South Australia in 1844-1846. His journals (Sturt 1833) reveal him to be an observant and inquisitive explorer. Quotations from his published journals reveal a few of his perceptions about the possible natural occurrences of inland acid sulfate soils in wetlands. Sturt was the first known European to have travelled down the Murray River to its mouth in 1830, when he noted in his journal that 'the shores of the lakes were densely covered with fresh water reeds in one continuous belt as far as the eye could see'. (These are suitable conditions for the formation of

sulfidic material, because of the considerable build-up of organic matter in the dense reeds in waterlogged soils.) This was confirmed by Sturt's observations of subaqueous soils in Lake Alexandrina: 'Its bottom was one of black mud, and weeds of enormous length were floating on its surface, detached by the late gales, and which, from the shallowness of the lake, got constantly entangled with our rudder'. The black mud description is still apt today, but the aquatic plants (macrophytes) described are largely absent from the Lakes.

Geomorphic settings, distribution and properties of soils within land types

(section adapted from (R. Fitzpatrick et al., 2018)

The diversity of soil types in the Coorong, the Lower Lakes (Lake Alexandrina, 649 km2, and Lake Albert, 320 km2) and the Murray Mouth (CLLMM), which comprise the Murray-Darling Basin terminal lake-estuary system, is attributable to the wide variety of soil-forming factors over time and landscape types in the region (e.g. Baker et al. 2013; de Mooyi 1959; Fitzpatrick & Shand 2008; Fitzpatrick et al. 2009a; 2018; Maschmedt 2009). These varied soil-forming factors are expressed over a wide range of (i) natural environments (geology, geomorphology, climate, vegetation, fresh and saline water conditions) (ii) anthropogenically modified environments (barrages, blocking banks and irrigation) (iii) changing climatic environments (e.g. increased hydrological droughts, sea level rise and decreased winter rainfall).

The Lower Lakes area is characterized by a series of interconnected lakes and lagoons, including Lake Alexandrina, Lake Albert, and the Coorong. The geology of the Lower Lakes area is dominated by sedimentary rocks, including sandstones, shales, and limestones, which were deposited during the Paleozoic era, around 300-500 million years ago. These sedimentary rocks were subsequently uplifted and eroded by the Murray River, which has been flowing through the area for millions of years. During the Quaternary period (2.6 million years ago), the climate in the Lower Lakes area changed from a warm and humid climate to a cooler and drier climate. This change in climate caused the Murray River to deposit large quantities of sediment, which eventually formed the lakes and lagoons that are visible today. The Lower Lakes area is also home to a number of significant geological features, including the Murray Mouth, which is the point at which the Murray River meets the Southern Ocean. The Murray Mouth has been a significant feature of the landscape for thousands of years and has been shaped by a combination of river and ocean currents.

The CLLMM was designated in 1985 as a Wetland of International Importance under the Ramsar Convention on Wetlands, reflecting the region's ecological significance.

We provide here an overview of various soil change processes and management strategies, especially during drying and wetting cycles.

Linkages between the geology, geomorphology and soils in the region are further described by Maschmedt (2009) and de Mooy (1959). Most soils in the CLLMM immediate catchment area are sandy and/or calcareous from aeolian (wind-derived) sources (Baker 2013; de Mooy 1959; Fitzpatrick & Shand 2008; Fitzpatrick et al. 2008a, 2009b, 2010a, 2010b, 2011b, 2018; Maschmedt 2009). However, wherever the aeolian deposits have been eroded to re-expose the older Tertiary and Pleistocene sediments, more clayey or weakly calcareous to non-calcareous soils predominate. The dominant soil types occurring in the CLLMM, which mostly comprises the Ramsar wetland complex, are subaqueous acid sulfate soils. These ASS are typically formed in Holocene sediments in

aqueous environments that provide anoxic conditions; that have high concentrations of sulfate, soluble iron and labile organic matter; and that are widespread in the region.

The earliest research on the nature and distribution of subaqueous soils and sediments in Lake Albert was completed by Taylor and Poole (1931) prior to barrage construction. At this time the levels of both Lake Albert and Lake Alexandrina changed seasonally, periodically exposing acid sulfate soils with hypersulfidic and hyposulfidic materials. Taylor and Poole were assessing the agricultural potential of Lake Albert, which was being considered for drainage and development for irrigated pastures and cropping. At that time they noted the presence of what we now call acid sulfate soils, because one of the soils sampled had a pH of 3.9 after drying, and they argued (successfully and accurately in hindsight) that the Lake should not be drained for agriculture (Taylor & Poole 1931). Their original 1930s soil samples were retrieved from the CSIRO Land and Water soil archive in 2007, and reanalysed for pH for comparison with the original measurements made 78 years previously (Fitzpatrick et al. 2008b). In this case, the original 1930s results can be taken as the original pH values (pH 8.5); the pH values for 2007 were much lower (pH 2 to 4) than when the samples were collected, confirming the acidifying effects of exposure to the atmosphere of the subaqueous acid sulfate soils (ASS) with hypersulfidic material Fitzpatrick et al. 2008b).

Acid Sulfate soils in the CLLMM region

(section adapted from (R. Fitzpatrick et al., 2018)

Most soils in the CLLMM immediate catchment area are sandy and/or calcareous from aeolian (wind-derived) sources (Baker 2013; de Mooy 1959; Fitzpatrick & Shand 2008; Fitzpatrick et al. 2008a, 2009b, 2010a, 2010b, 2011b, 2018; Maschmedt 2009). However, wherever the aeolian deposits have been eroded to re-expose the older Tertiary and Pleistocene sediments, more clayey or weakly calcareous to non-calcareous soils predominate. The dominant soil types occurring in the CLLMM, which mostly comprises the Ramsar wetland complex, are subaqueous acid sulfate soils. These ASS are typically formed in Holocene sediments in aqueous environments that provide anoxic conditions; that have high concentrations of sulfate, soluble iron and labile organic matter; and that are widespread in the region.

The earliest research on the nature and distribution of subaqueous soils and sediments in Lake Albert was completed by Taylor and Poole (1931) prior to barrage construction. At this time the levels of both Lake Albert and Lake Alexandrina changed seasonally, periodically exposing acid sulfate soils with hypersulfidic and hyposulfidic materials. Taylor and Poole were assessing the agricultural potential of Lake Albert, which was being considered for drainage and development for irrigated pastures and cropping. At that time they noted the presence of what we now call acid sulfate soils, because one of the soils sampled had a pH of 3.9 after drying, and they argued (successfully and accurately in hindsight) that the Lake should not be drained for agriculture (Taylor & Poole 1931). Their original 1930s soil samples were retrieved from the CSIRO Land and Water soil archive in 2007, and reanalysed for pH for comparison with the original measurements made 78 years previously (Fitzpatrick et al. 2008b). In this case, the original 1930s results can be taken as the original pH values (pH 8.5); the pH values for 2007 were much lower (pH 2 to 4) than when the samples were collected, confirming the acidifying effects of exposure to the atmosphere of the subaqueous acid sulfate soils (ASS) with hypersulfidic material Fitzpatrick et al. 2008b).

Since the 1940s, water levels in the River Murray, adjacent wetlands and Lower Lakes have been maintained and managed using locks, barrages and levee banks along the river channel, with seawater exclusion being their main function. The construction of locks, barrages and levee banks has allowed artificially stable water conditions in the Lower Murray regions to be maintained for over 80 years with a normal pool level of c.+0.75 m AHD (Australian Height Datum; 0 m AHD corresponds approximately to mean sea level). This likely resulted in considerable build-up of hyposulfidic, hypersulfidic and monosulfidic materials in the Lower Lakes and adjacent wetlands because of:

- less frequent and lower magnitude wetting and drying cycles that would have prevented build-up (particularly on the Lake margins) of acid sulfate soils (due to the fluctuations creating frequent oxidising conditions in sediments)
- the evaporative concentration of sulfate from river nutrient/salt loads during the period of stable pool level and from groundwater sources
- the lack of natural scouring and seasonal flooding, which occurred during the time prior to major pre-European water resource development (5 000 BP to 1920s)
- the plentiful supply of organic matter from Phragmites australis reed beds and dairy farming activities.

The following are typical contemporary features of acid sulfate soils from the Lower Lakes containing pyrite (FeS2) in clays, sands and peats:

- black clayey hypersulfidic material (e.g. Finniss River regions, Figure 5)
- dark grey sandy hypersulfidic material (e.g. Goolwa Channel regions)
- black organic-rich or peaty hypersulfidic material (also known as Coorongite) (e.g. Lakes Alexandrina and Albert; Fitzpatrick et al. 2017).

These hypersulfidic and hyposulfidic materials also contain abundant live and relict plant material [see Figure 5 (b)], mainly *Phragmites australis* (Common Reed) and/or *Typha latifolia* (Bulrush) roots and root channels, but also laminae and other detritus, which provide evidence of freshwater deposition. Other features of ASS with hypersulfidic and hyposulfidic materials in the Lower Lakes are the widespread presence of freshwater shells and shell detritus in layers down to a depth of 1 m, which also points to a freshwater environment.

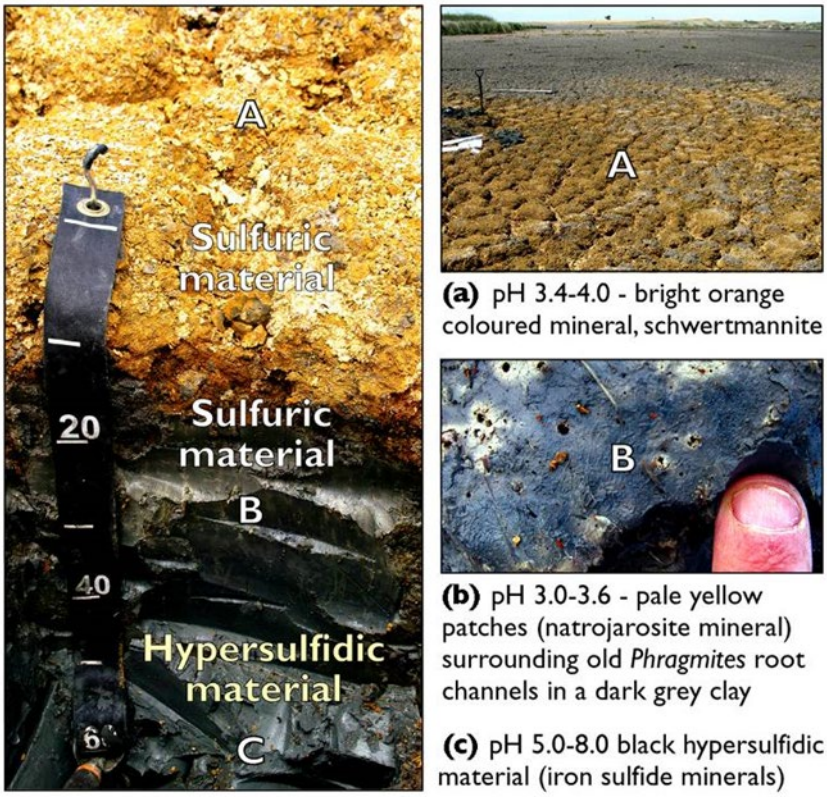

Figure 5: Acid sulfate soil showing the presence of hypersulfidic and sulfuric materials in a dry river bed of the Finniss River, South Australia. (Modified from Fitzpatrick et al. 2009b, 2018)

Black monosulfidic material with gel-like consistency is also common in areas adjacent to the barrages in Lake Alexandrina and in the Coorong (Fitzpatrick et al. 2008b, 2011c). In most cases, all three of these acid sulfate soil materials are permanently saturated or are subaqueous soils and are benign unless disturbed.

Formation and rewetting of sulfuric (pH <4) materials during the Millennium Drought

(section adapted from (R. Fitzpatrick et al., 2018)

The extreme Millennium Drought period had its biggest impact in the Lower Murray from 2006 to 2010, and considerably reduced the freshwater inflows from the River Murray to the Lower Lakes. As such, water levels declined from the typical pre-drought water level of c.+0.5 m AHD to, at lowest, c.-1 m AHD for Lake Alexandrina during autumn 2009 and c.-0.8 m for Lake Albert during late summer 2010.

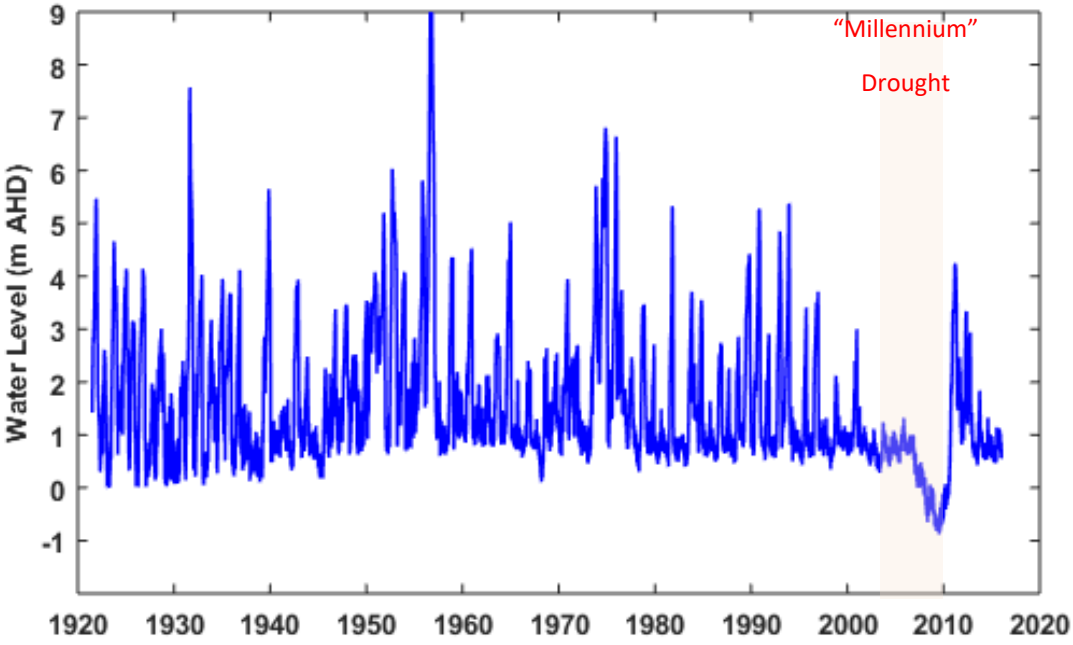

Figure 6: Water level (mAHD) in Lower Lakes from 1920 to 2020 showing the drought period

The lowering of Lake water levels, combined with the extensive shallow fringing bathymetry of the Lakes, incrementally exposed and drained large new areas of lake margins, and with this there was widespread formation of sulfuric (pH <4) soil materials (Fitzpatrick et al. 2008a, b, c). Accompanying these highly acidic soil conditions there were consequent accumulations of the pale-yellow iron oxy-hydroxysulfate mineral jarosite shown in Figure 5. In addition, there were common occurrences of greenish-yellow and orange-yellow coloured surface crusts of salt efflorescences, comprising sulfate-rich evaporite minerals of sideronatrite (yellow) and schwertmannite (Figure 5).

The Lower Lakes are shallow-water bodies, with a mean depth of ~2.4 m and 1.5 m, for Lake Alexandrina and Lake Albert respectively, at a normal operating level of c.+0.75 m AHD (Mosley et al. 2012). Bathymetry was used to model the extent and formation of different acid sulfate soil types as water levels declined in the Millennium Drought. As water level receded, sulfuric soil formation followed the sequence:

subaqueous sulfidic soils (<2 m deep to near to or at the waterline, waterlogged)

↓

sulfidic soils (near to or at the waterline, very moist to mostly waterlogged)

↓

sulfuric soils (drying or dry)

Figure 7: (Top) Photo illustrating the area of dry lake bed in Lake Alexandrina; (Bottom) Aerial view of Currency Creek river bed (tributary adjacent Finniss River), with Goolwa Channel in background

The proportions of acid sulfate soil types and deep-water distributions for the +0.5 and -1.5 m AHD scenarios for each Lake are presented in Figure 8. Computer projections to plot the incremental spread of acid sulfate soils with sulfuric materials by combining lakebed bathymetry and water level scenarios (normal +0.5m to -1.5 m AHD) showed the potential for 32 699 ha of shoreline and lake bed to convert from subaqueous sulfidic soils to sulfidic soils and to sulfuric soils.

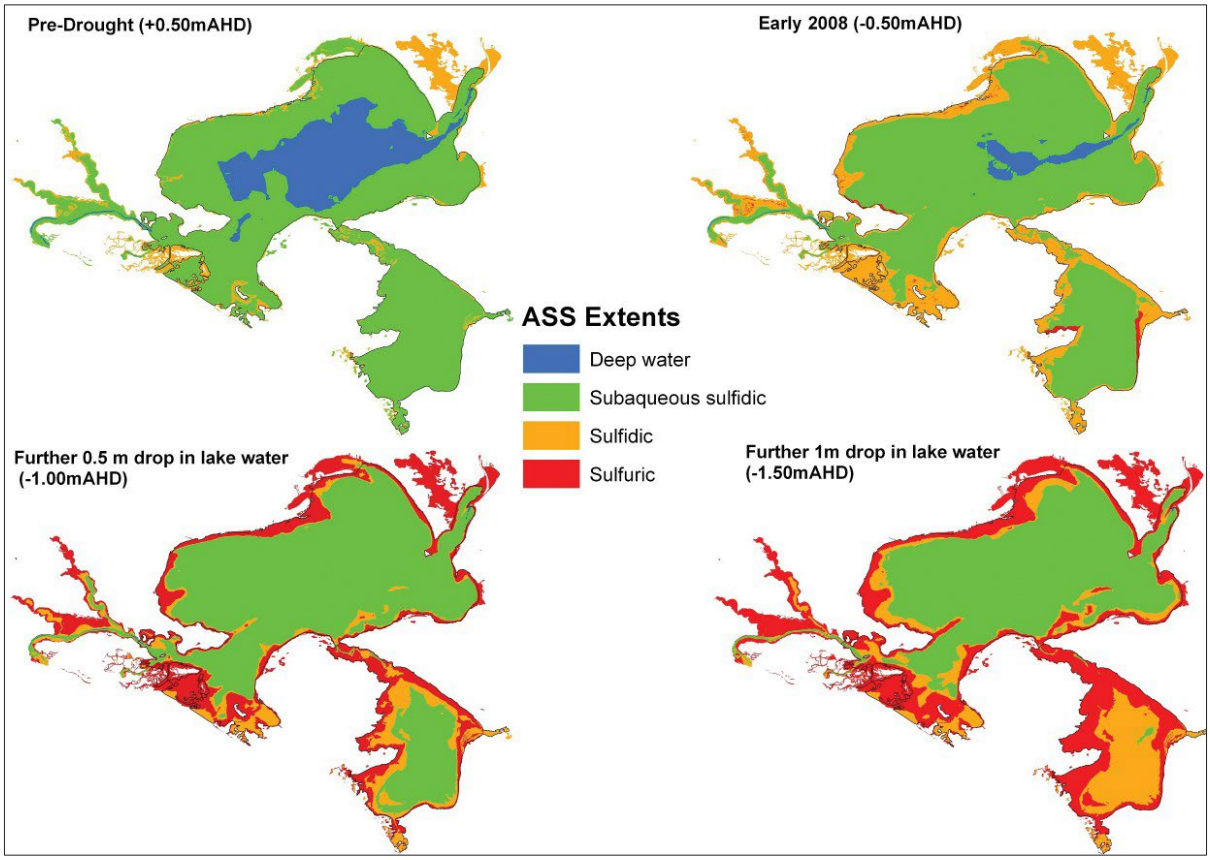

Figure 8: Predictive scenario maps depicting changes in acid sulfate soil materials at different water levels in the Lower Lakes (+0.5 m AHD, -0.5 m AHD and -1.5 m AHD), based on regional soil investigations and bathymetry (modified from Fitzpatrick et al. 2008a, 2008b, 2008c, 2009a, 2009b). Finniss River, Currency Creek and Goolwa Channel are the three extensions occurring on the left side of Lake Alexandrina. The term 'sulfidic', used in 2008, was replaced by Isbell and National Committee on Soils & Terrain (2016 and 2021) with 'hypersulfidic'.

As a result of these predictions, grave concerns grew that without significant new river inflows to the Lakes, the ASS trajectories (Figure 8 and Figure 9) could eventually be realised, along with the associated environmental degradation. In August 2009, the predictions were indeed verified based on extensive field investigations and laboratory analyses across the Lower Lakes region, where 330 sites were described and sampled, resulting in 706 samples being analysed for pH and acid base accounting parameters (Fitzpatrick et al., 2010). About **85% of the lake surface soil/sediment had a positive net acidity** (i.e. total acidity minus soil- neutralising capacity), with highest net acidities **(>500 mol H+ t-1)** occurring in clay-rich sediments in the middle of Lakes Albert and Alexandrina. These results showed that an extensive acid sulfate soil hazard was present in the Lower Lakes. About **82% (67 087 ha)** of the total lake area (82 219 ha) had potential for developing sulfuric (pH <4) materials in the soils/sediments if water levels continued to decline. The median net acidity measured (10 mol H+ t-1) was below guideline levels (18 mol H+ t-1; Dear et al. 2002) for when management of soils is recommended. However, a large area of the inundated soil/sediments of both Lakes and tributaries, particularly Lake Albert, contained very high levels of net acidity (>250 mol H+ t-1). This is well in excess of the (Dear et al., 2002) guideline and indicated a very severe

hazard. The southern and north-eastern regions of Lake Alexandrina and some marginal areas around both Lakes were a lower hazard.

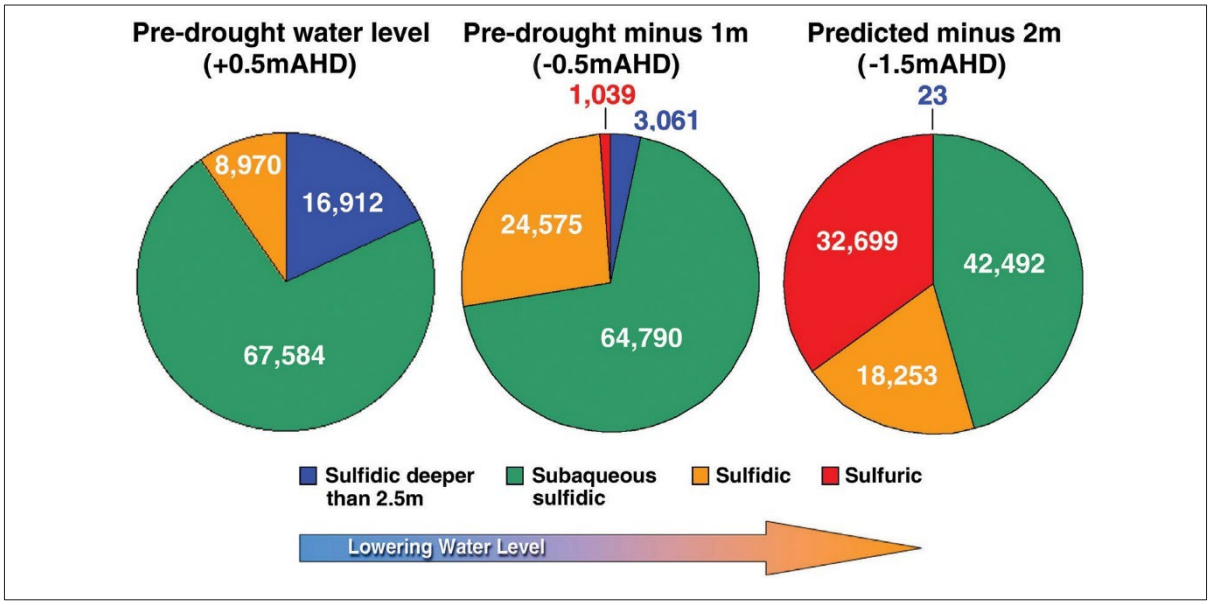

Figure 9: Pie charts showing changes in predicted areal extents for the Lower Lakes in hectares for various ASS types corresponding to pre-drought conditions (+0.5 m AHD), drought conditions in 2008 (-0.5 m AHD), and conditions that would occur were the drought to be prolonged and cause the Lower Lakes' water level to drop to -1.5 m AHD (modified from Fitzpatrick et al. 2008a, b, c).The term 'sulfidic', used in 2008, was replaced by Isbell and National Committee on Soils & Terrain (2016) with 'hypersulfidic'.

As shown in Figure 11, there was a large variability, or heterogeneity, in the properties of acid sulfate soil types mapped. The net acidity (Figure 10) and acid sulfate soil (Figure 11) maps showed that sulfuric soils were especially prevalent in tributary regions with poor connection to the main lake bodies, such as Currency Creek, Finniss River, Loveday Bay, the body of water at Tolderol and Boggy Creek. The rate of oxidation of hypersulfidic material was found to be high, with up to 2% of available pyrite able to be oxidised per day in the sandy sediments to form sulfuric material. The rewetting of these materials via rainfall and tributary inflow resulted in widespread surface water acidification (pH 2-5) in the Currency and Finniss tributary areas and other shallow embayments around the lake margins in 2009-2010. Metal and metalloid contaminants that were released from the sediment matrix by extreme acidification (e.g. pH <2) posed risks to the public and the environment (Mosley et al., 2014a; Simpson et al., 2010). Other hazards included noxious (hydrogen sulphide) gas release as well as mobilisation of dust from exposed acid sulfate soil areas, which led to community concern.

Many research studies were undertaken during this time, coordinated in a major integrated acid sulfate soil research program. The research program informed the geochemical modelling by (Hipsey et al., 2011, 2014), which indicated that acidification of the main lake areas could occur if water levels fall below c.-1.75 m AHD for Lake Alexandrina and -0.75m AHD for Lake Albert. The risk profile was predicted to substantially increase past these lower water levels and/or with prolonged time near these levels. This was predicted to be due to the acidic groundwater seepage becoming much greater, due to an increase in exposed sediment area and higher hydraulic head gradients. Localised acidic 'hotspots' were also predicted to occur around the lake margins.

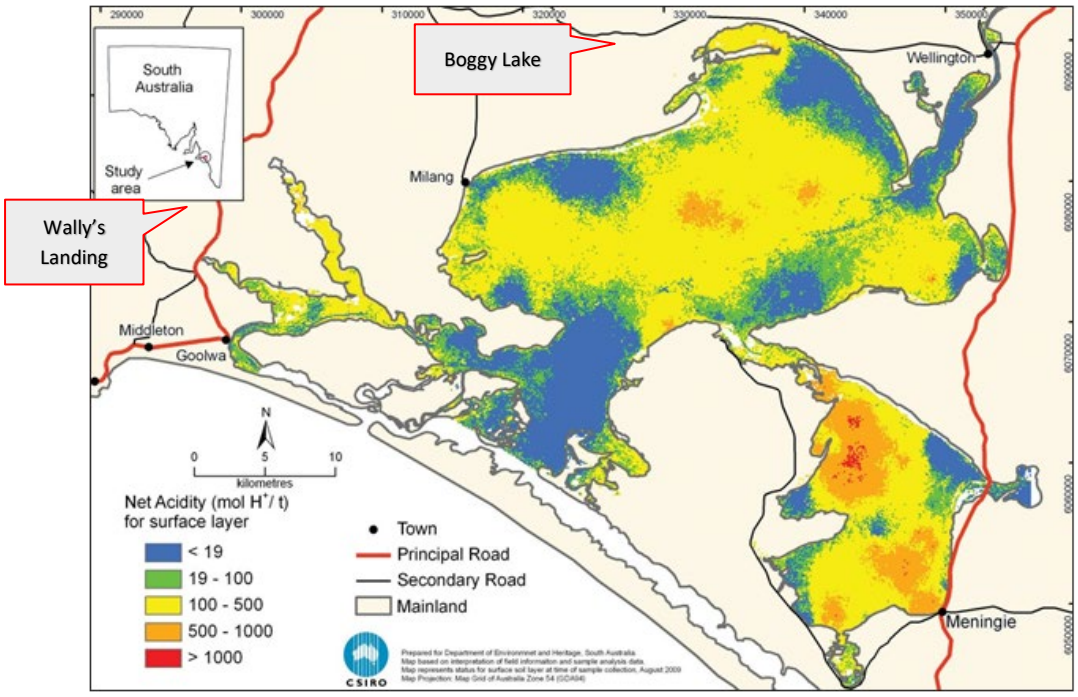

Figure 10: Net acidity map showing data grouped into five classes for the upper soil layer (0 to 10 cm). (After Fitzpatrick et al. 2010)

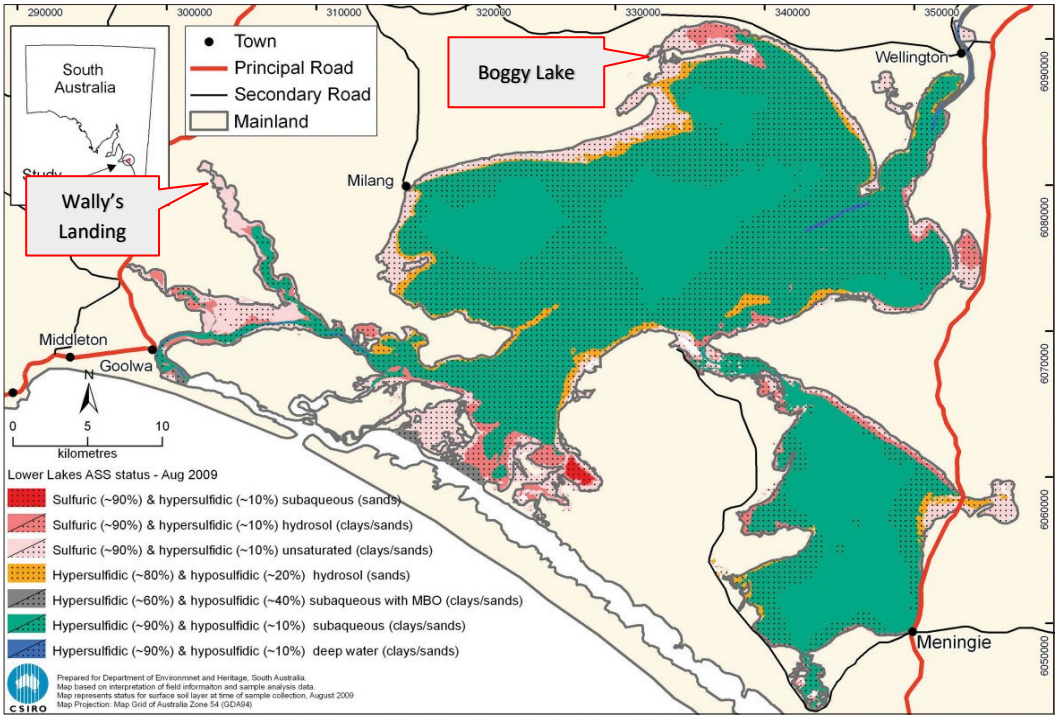

Figure 11: Soil classification map of the distribution of the following wide range of acid sulfate soil subtypes: (i)acid sulfate soil materials with sulfuric, hypersulfidic, hyposulfidic and monosulfidic (MBO) materials; (ii) depth of water with deep water, subaqueous, hydrosols (saturated to a depth of 50 cm below the mineral soil surface) and unsaturated (unsaturated to a depth of 50 cm below the mineral soil surface); (iii) soil texture with sands, loams and clays. (After Fitzpatrick et al. 2010).

Summary of Field Sites

Stop 1: Wally's Landing**,** located in the top reaches of the Finniss River.

The Finniss River is 64 km long, has a catchment area of around 750 square km and flows into the Goolwa channel to the south. The soil material in the Finniss River is described as a "sulfuric subaqueous clay soil". The Millennium drought caused severe drying of the river and subsequent acidification (pH < 4) of hypersulfidic material in the soils. After river levels returned to normal in 2011, the site is permanently flooded and the pH values have slowly recovered to neutral pH values (Fitzpatrick et al., 2009; Kölbl et al., 2017). We will see the site where soils were collected for these two studies.

Stop 2: Milang Jetty

We will see comparison of water level from now (during a flood) and the photograph below showing conditions during the drought.

Drive By: Boggy Lake

Embayment which had very low pH soil and water, heavy cracking clays and was the site of aerial limestone dosing in 2009.

Stop 3. Jervois – Lower Murray Reclaimed Irrigation Area.

Jervois is one section of the Lower Murray Reclaimed Irrigation Area (LMRIA), flood irrigated agricultural land on the former floodplain of the River Murray in South Australia, south of Murray Bridge. Drought conditions and low inflows from 2006 to early 2010 in the Murray–Darling system in Australia led to unprecedented low water levels in the lower reaches of the river below Lock 1 at Blanchetown, South Australia. This resulted in groundwater tables falling up to 2 m in sites such as Jervois. The heavy clay soils subsequently salinised, dried and cracked, resulting in pyrite oxidation of previously waterlogged, anaerobic hypersulfidic material approximately 1–3 m below ground level (bgl). The return of the river to normal pool levels and subsequent recovery of groundwater levels in late 2010 resulted in the appearance of acid drainage across an area of 3,300 ha and resultant river water quality risks (Mosley et al., 2012). Soil remain acidic over 13 years since oxidation, with transport of acidic water from porewaters to drains.

Stop 1: Wally's Landing Finniss River

Figure 12: Google Earth Map of Wally's Landing with red circle illustrating Stop 1

At Wally's Landing (Figure 12), extreme drought conditions between 2007 and 2009 and the partial drying of the wetland caused hypersulfidic subaqueous clays to oxidise and transform to sulfuric clays. When the sulfuric clays were rewetted, after summer rainfall in 2009, surface water in the channel became acidic (pH < 3.5). Further inundation, following winter rainfall in 2009, neutralised the surface water acidity and caused the formation of sulfuric subaqueous clays. Prolonged inundation most likely encouraged reducing conditions resulting in sulfate reduction and the formation of hypersulfidic subaqueous clays. Although sampling sites remained subaqueous for a period of 3 years, net acidities remained very high and TAA and RA was still present in the soil profiles. Neutralisation of acidity was limited at this site and the soil material was considered to pose a high acidification hazard. On drying, soil material is likely to re-acidify rapidly and may impact surface waters upon rewetting.

The Wallys landing study area LF01 is located on the northern side of the Finniss River (Figure 13). Sampling were conducted in the drainage ditch to the north east of the Finniss River itself, at Wallys Landing (jetty site LF01-D) during the following 9 sequential wet-drying-rewetting periods: (h1) Pre-drought/flooded in Winter 2007 (Figure 14a); (h2) drought/drying in Summer 2008 Figure 14b) (h3)

drought/drying in Summer 2009 (Figure 14b), (a) reflooding in September 2009, (b) reflooding in March 2010, (c) reflooded in February 2011, (d) reflooded in June 2011, (e) reflooded November 2012 and (f) reflooded in June 2012.

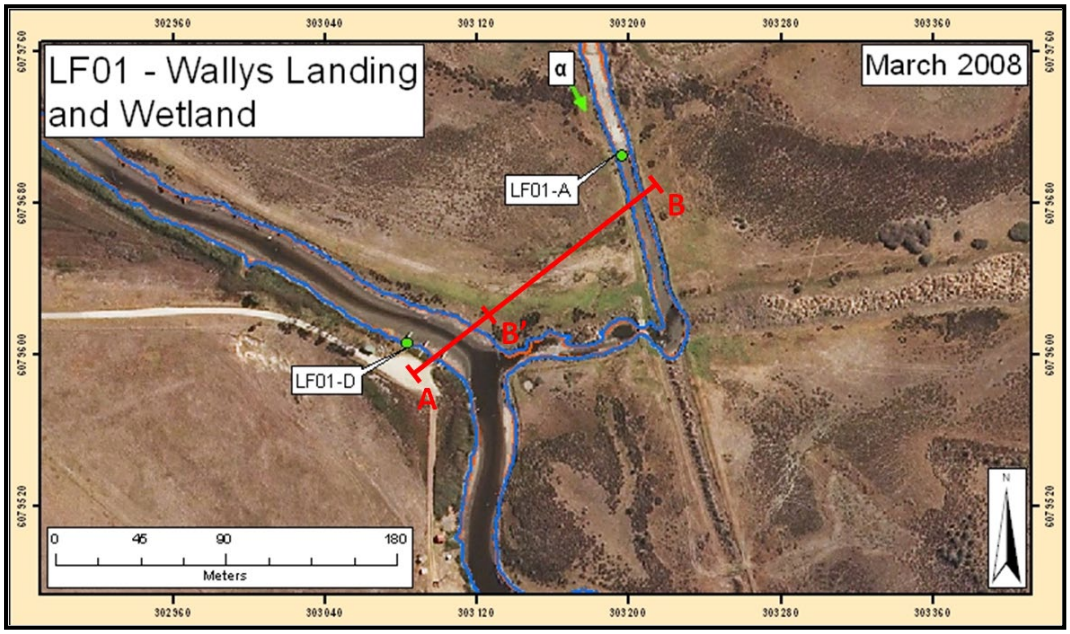

Figure 13: Sample location map. Aerial photograph taken in March 2008 (Orange line: sampling-a & b water level, Blue line: sampling-c, d, e & f water level). Red line indicates cross section presented in the construction of conceptual soil-landscape cross-section models (see below). (from Baker et al. 2013)

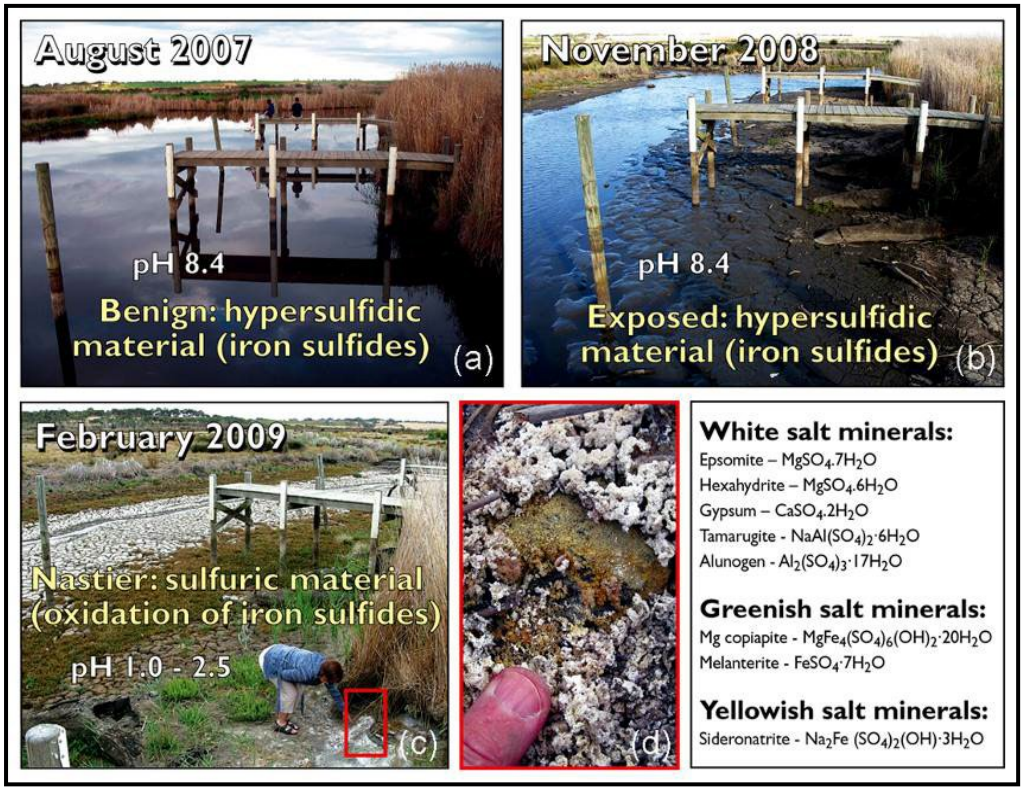

Figure 14: Wally's Landing showing changes in water level and soil pH during August 2007, November 2008 and February 2009 (modified from Fitzpatrick et al. 2009a).

The August 2007 photograph shows the Finniss River with benign hypersulfidic subaqueous clay under 80 cm of water at the end of the jetty (Figure 14a). Benign hypersulfidic organic clay was sampled in the *Phragmites* reeds four metres from the bank/water's edge. The November 2008 photograph shows substantial lowering of water levels to produce mainly waterlogged benign hypersulfidic cracking clay (Figure 14b; end of jetty). The February 2009 photograph shows further lowering of water levels to expose a dry clay river-bed with cracks and salt efflorescences (sulfuric cracking clay) (Figure 14c). The red square shown in the February 2009 photograph in Figure 14c indicates the location of white fluffy acidic salts adjacent to Phragmites reeds. This is shown in close-up on the lower right hand side photograph.

Table 1: Soil profile description of core sampled in June 2012 from channel on western side of Wallys Jetty, approximately one metre from the bank (modified from Baker et al. 2012). Soil Classification: [2]Typic Sulfiwassent; [3]Hypersulfidic subaqueous soil; [4]Hypersulfidic, Subaqueous Hydrosol; [5]Subaquatic Gleysol (Hypersulfidic) (see also Table 2)

[6]Sample ID	Horizon	Depth (cm)	Description
LFf01-D.1	Ase	0 -15	Very dark brown (10YR 2/2) mixed materials, upper few cm decomposing organic matter, gravel and clay grading to decomposing peaty material, approaching sapric (very little coarse material after light rubbing); medium and fine roots and a few coarse (~ 1.5 cm) *Phragmites* roots; clear boundary.
LFf01-D.2	2Btseg1	15-41	Dark brown (7.5Y 3/2) sapric peat, clayey towards the base; darker in parts with some coarse plant remnants that break to very fine organic matter; common medium root remnants and few coarse roots; few coarse quartz gravel; moderate sulfidic smell in lower part; boundary clear to gradual, but sharp in one core. [1]Hypersulfidic material
LFf01-D.3	2Btseg2	41-60	Black (5Y 2.5/1) heavy clay, organic towards the upper part; sub-rounded coarse to ~ 1cm and bands of coarse sand with clay; few medium (live?) roots; weak sulfidic smell; gradual boundary. [1]Hypersulfidic material
LFf01-D.4	2Ctseg	60-90+	Very dark greyish brown (2.5Y 3/2) heavy clay, spongy; few medium roots. [1]Hypersulfidic material.

[1]Where acid sulfate soil material is based on the definition in the 2nd and 3rd editions of the Australian Soil Classification (Isbell and National Committee on Soils & Terrain, 2016 and 2021)

[2]Soil Taxonomy (Soil Survey Staff ,2014)

[3]Acid Sulfate Soil classification (Soil identification key) used in Australia (Fitzpatrick *et al.* 2010; Fitzpatrick, 2013).*Where the soil classification is a Hypersulfidic soil, hypersulfidic material (pH decreased to <4 after incubation of at least 16 weeks) has been identified in a layer or horizon (at least 10cm thick) within 150 cm of the soil surface.

[4]Australian Soil Classification (Isbell and National Committee on Soils & Terrain, 2021).

[5]IUSS Working Group WRB (2014): World Reference Base for Soil Resources 2014. World Soil Res. Report 106, FAO, Rome. http://www.fao.org/3/a-i3794e.pdf

[6]Wally's Landing (Finness River) sampled on 6th November, 2015. However, after drying between 2008 to early 2010 during the Millennium drought this soil profile classified as a [2]Hydaquentic Sulfaquept and [3]Sulfuric soil. After reflooding / rewetting between 2010 to 2015 this soil classified as a [2]Hydraquentic Sulfowassept (i.e. proposed new Inceptisol Suborder: Sulfowassepts and Inceptisol Great Groups & Subgroups for Hydraquentic Sulfowassept) and Sulfuric subaqueous soil.

Table 2: pH values of re-saturated soil after Millennium drought from Kolbl et. al (2017, 2018) showing time course of pH values during oxic incubation, Acid sulfate soil material classification, Soil Taxonomy, ASS subtype classification, WRB and acidification OC and N concentrations, C/N ratios and FeDCB concentrations. Where SD = standard deviation; OC = organic carbon, N = nitrogen) and FeDCB= Dithionite-citrate-bicarbonate (modified from Kolbl et. al 2017, 2018)

No.	Depth (cm)	[1]Material	pH_{H2O} 1:1 soil:solution, oxic conditions				OC mg g^{-1}	*SD*	N mg g^{-1}	*SD*	C/N	Fe_{DCB} mg g^{-1}	*SD*
			day 0	8 weeks	16 weeks	**24 weeks**							
[6]Wally's Landing: [2]Typic Sulfiwassent; [3]Hypersulfidic subaqueous soil, [4]Hypersulfidic, Subaqueous Hydrosol; [5]Subaquatic Gleysol (Hypersulfidic)													
Fi Ri 1.1	0-10	Hyposulfidic	**7.1**	5.2	4.2	**3.9**	**58.4**	*2.0*	**5.55**	*0.11*	10.5	**15.77**	*0.21*
Fi Ri 1.2	10-25	Hyposulfidic	**6.8**	5.0	4.6	**4.1**	**51.5**	*0.5*	**4.46**	*0.04*	11.6	**11.22**	*0.37*
Fi Ri 1.3	25-55	Hyposulfidic	**6.8**	6.0	4.6	**4.4**	**45.0**	*0.3*	**3.83**	*0.01*	11.8	**11.39**	*0.18*
Fi Ri 1.4	55-80	Hyposulfidic	**6.9**	5.5	4.4	**4.3**	**46.7**	*0.4*	**3.93**	*0.04*	11.9	**11.39**	*0.17*
Fi Ri 1.5	80-130	**Hypersulfidic**	**7.7**	3.6	2.4	**2.0**	**28.5**	*0.9*	**2.27**	*0.01*	12.5	**2.91**	*0.02*
Fi Ri 1.6	130-180	**Hypersulfidic**	**8.4**	2.6	1.9	**1.7**	**34.3**	*1.4*	**2.85**	*0.01*	12.0	**1.47**	*0.02*

[1]Where acid sulfate soil material is based on the definition in the 2nd edition of the Australian Soil Classification (Isbell and National Committee on Soils & Terrain, 2016)

[2]Soil Taxonomy (Soil Survey Staff ,2014)

[3]Acid Sulfate Soil classification (Soil identification key) used in Australia (Fitzpatrick *et al.* 2010; Fitzpatrick, 2013).[*]Where the soil classification is a Hypersulfidic soil, hypersulfidic material (pH decreased to <4 after incubation of at least 16 weeks) has been identified in a layer or horizon (at least 10cm thick) within 150 cm of the soil surface.

[4]Australian Soil Classification (Isbell and National Committee on Soils & Terrain, 2021).

[5]IUSS Working Group WRB (2014): World Reference Base for Soil Resources 2014. World Soil Res. Report 106, FAO, Rome. http://www.fao.org/3/a-i3794e.pdf

[6]Wally's Landing (Finness River) sampled on 6th November, 2015. However, after drying between 2008 to early 2010 during the Millennium drought this soil profile classified as a [2]Hydaquentic Sulfaquept and [3]Sulfuric soil. After reflooding / rewetting between 2010 to 2015 this soil classified as a [2]Hydraquentic Sulfowassept (i.e. proposed new Inceptisol Suborder: Sulfowassepts and Inceptisol Great Groups & Subgroups for Hydraquentic Sulfowassept) and Sulfuric subaqueous soil.

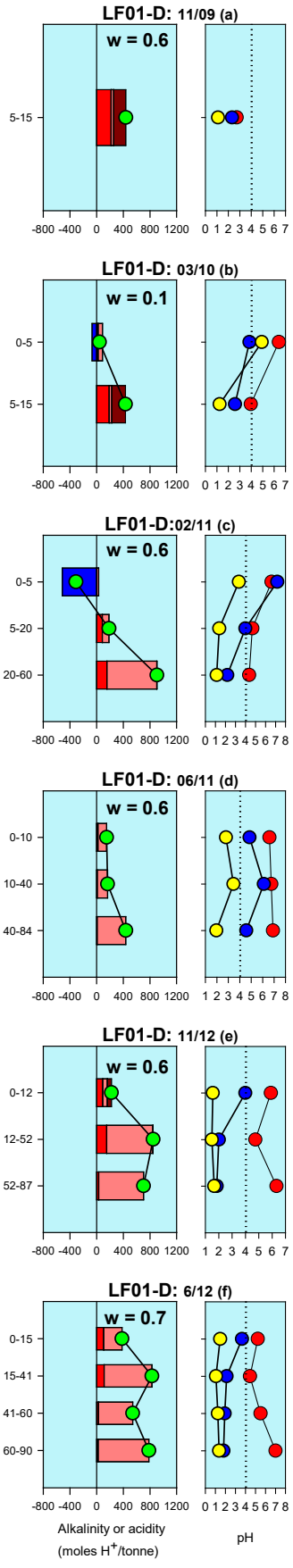

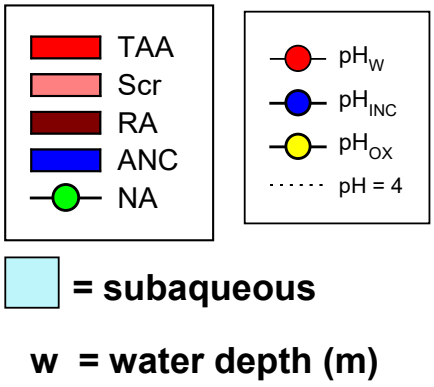

Figure 15: pH and acid-base accounting data plotted against depth (cm) for soil profiles collected during the following periods (from Baker et al. 2013):

(a) September 2009

(b) March 2010

(c) February 2011

(d) June 2011

(e) November 2012

(f) June 2012

Soil acidity and acid-base accounting

Acid-base accounting analyses was carried out for sulfide-S (S_{CR} or Cr-reducible S), Retained Acidity (RA), Titratable Actual Acidity (TAA), Acid Neutralising Capacity (ANC) and Net Acidity (NA). Acid-base accounting and pH data (pH_{OX}, pH_{INC} & pH_W), for each soil layer, are presented in Figure 15. These data were used to inform the acidification hazard assessment. Acidification hazard assessment and ASS subtype classification were carried out for each soil profile collected. Acidification hazard assessment was based on: (i) landscape position, (ii) soil morphology, (iii) acid-base accounting (Figure 15), (iv) pH data (Table 2), (v) acidification potential (Figure 15) and (vi) ASS material and subtype classification (Table 2). Acidification hazard categories were: (i) very low, (ii) low, (iii) medium and (iv) high. A summary of ASS subtype classification and acidification hazard for each profile is presented in Baker et al. (2013).

Soil profiles sampled at Wallys Landing comprised hypersulfidic and sulfuric subaqueous clay soils with high acidification hazard (Table 3). At each site, net acidity was very high (maximum of 1100 moles H+/tonne) and increased with depth (Figure 15). There was little ANC (Figure 15) and acidification potentials were generally medium and high (Figure 15).

During extreme drought conditions, between 2007 and 2009, the partial drying of the wetland caused the hypersulfidic subaqueous clays to oxidise and transform to sulfuric clays. When the sulfuric clays were rewetted, after summer rainfall in 2009, surface water in the channel became acidic (pH < 3.5). Further inundation, following winter rainfall in 2009, neutralised the surface water acidity and caused the formation of sulfuric subaqueous clays. Prolonged inundation most likely encouraged reducing conditions, leading to sulfate reduction and the formation of hypersulfidic subaqueous clays (Table 3).

At Wallys Landing, at the foot of the jetty, hypersulfidic subaqueous clays transformed to sulfuric clays. On rewetting, sulfuric subaqueous clays were formed. Prolonged inundation most likely encouraged reducing conditions, leading to sulfate reduction and the formation of hypersulfidic and hyposulfidic subaqueous clays (Table 2).

At Wallys Landing, since 2009, sampling sites remained subaqueous for a period of 3 years. Soils converted from sulfuric to hypersulfidic and hyposulfidic subaqueous and the proportion of TAA and RA, relative to SCr, decreased in the upper part of the profile. However, net acidities remained very high, TAA was present throughout the profile and RA was present at intermediate depths (consistent with visual observations of pale yellow mottles, possible natrojarosite). Neutralisation of acidity was limited, little or no ANC was present in the profiles and the soil material was considered to pose a high acidification hazard (Table 2). On drying, soil material is likely to re-acidify rapidly and may impact surface waters upon rewetting.

Mineralogy

At several sites, abundant minerals were recorded in salt efflorescences and sub-surface horizons by Fitzpatrick et al. (2009a). In the bright yellowish green and orange surface salts shown in Figure 14, and pale yellow mottles in subsoils (see Figure , X-ray diffraction analyses identified sideronatrite, schwertmannite and jarosite/natrojarosite minerals, respectively. The pH values of the bright yellowish green surface efflorescences was very acidic (pH < 2) and the orange and pale yellow minerals were acidic (pH < 3 to 4). The presence of all these minerals indicates high contents of iron sulfides (principally pyrite) in the original materials. Where winter rainfall has rewet previously identified sandy sulfuric soils with pH values of 1.6 to 2.5, the mineral tamarugite [$NaAl(SO_4)2.6H_2O$], with traces of sideronatrite were subsequently identified with extremely acidic pH values ranging from 0.5 to 0.8 during slight rewetting of the mineral surfaces.

Table 3: Summary of temporal and spatial variations and changes in ASS subtypes at Wallys Landing site D in winters and summers during 2007, 2008, 2009, 2010, 2011 and 2012 Note: (i) Cells bordered in blue indicate subaqueous (From Fitzpatrick et al. (2010b; 2009a; 2008a; 2008b; 2009b; 2008c) and Baker et al. 2013)

Wallys Landing Site		Pre-drought Winter 2007 (h_1)	Drought Summer 2008 (h_2)	Drought Summer 2009 (h_3)	Drought End winter 2009 (a)	Drought End summer 2010 (b)	Post-drought Summer 2011 (c)	Post-drought Winter 2011 (d)	Post-drought start summer 2012 (e)	Post-drought start winter 2012 (f)	Summary
LF01-D	[1]Classification & [2]Acid hazard	Hypersulfidic subaqueous clay (H)	Hypersulfidic subaqueous clay (H)	Sulfuric clay (H)	Sulfuric* subaqueous clay (H)	Sulfuric* subaqueous clay (H)	Hypersulfidic subaqueous clay (H)	Hyposulfidic subaqueous clay (M)	Hypersulfidic subaqueous clay (H)	Hypersulfidic subaqueous clay (H)	During the extreme drought (2007 to 2009) the partial drying of the wetland caused the Hypersulfidic subaqueous clays transform to Sulfuric clays. When the Sulfuric clays were rewetted after summer rainfall in 2009, acidic pools of water (pH <3.5) formed. Further inundation following winter 2009 neutralised the acidic pools and caused the formation of Sulfuric subaqueous clays. Prolonged inundation encouraged sulfate reduction and caused the formation of Hypersulfidic subaqueous clays.
	Dominant water and ASS process	UW & Sulfide	LW & Sulfide	LW & Sulfuric	RF &Sulfuric	RW & Sulfuric	RW & Sulfide	UW & Sulfide	UW & Sulfide	UW & Sulfide	

[1] **Classification – Acid Sulfate Soil subtype classification**
[2] **Acid hazard – Acidification hazard: H = High; M = medium; L = Low; VL = Very Low**
Dominant Water process
LW – Lowering water level regime to expose soil to air due to drought conditions and water evaporation
UW – Unchanged water regime, which had not yet evaporated to expose soil to air
RW – Rising water level regime to inundate and saturate soils by reflooding (e.g. due to pumping, regulator installation, river flow and groundwater)
RF – Rain fall rewetting and natural reflooding to inundate and saturate soils

Dominant ASS – process
Sulfuric – Sulfuricization - oxidation of pyrite in hypersulfidic material due to onset of aerobic conditions to form sulfuric material
Sulfuric* – As above with acidic minerals and/or salt efflorescences noted (i.e. measurable RA)
Sulfide – Sulfidization due to sulfide accumulation to form hypersulfidic material
Monosulfide – Monosulfidization due to monosulfide accumulation to form monosulfidic material
Leach – Leaching of acid from soil by winter rain fall
Sulfuric **subaqueous** with **overlying circa neutral water** pH >4: = font coloured blue or default
Sulfuric **subaqueous** soil with **overlying acid water** pH <4: = font coloured red
Where h_1 to h_3 = historical sampling; (a) – (f) sampling conducted following rewetting

Hydrogeochemistry

While still connected, the alkalinity of Lake Alexandrina (> 250 mg/L) has helped to maintain the alkalinity of the remnant Finniss River and Currency Creek waters, along with local contributions from alkaline ground waters and evaporation. ASS impacts are most likely to have an effect where net acidities are high and surface water alkalinities are low, such as in Currency Creek, where alkalinities are lower than in Lake Alexandrina (200 to 250 mg/L).

The data from Wallys Landing in May 2009 showed that the pH in the flowing river was circumneutral following rewetting from winter rainfall. However, water in cattle pugs close to the river was found to be very acidic (pH 3.2). In a major anabranch of the Finniss River, the flowing stream water was found to produce acidic pulses (pH 3.3. to 4.0) with relatively high specific electrical conductance (SEC) of 13300 µS cm-1 (reflecting presence acidic sulfate salts).

Finniss River detailed predictive soil-regolith models

Predictive soil-regolith models illustrating the formation and transformation of hypersulfidic material were constructed for the Finniss River and adjacent wetlands in the area near Wally's Landing (Figure 16, Figure 17). These models provide an additional understanding of how and why the nature of soil materials has changed over time, especially in describing the spatial heterogeneity of ASS property variation described in Table 1. Based on field investigations and historical/soil knowledge of the Finniss River wetlands, a sequence of seven conceptual soil-regolith models (Fitzpatrick et al. 2009a) have been reconstructed in Figure 16 and Figure 17. This is elaborated in the following text.

5,500 BC to 1920s. Following stabilisation of sea level to about its present position 5,500BC, the lower Finniss River cycled between natural wetting and flushing, and partial drying conditions in response to seasonal and climatic cycles occurring in the upper Murray-Darling Basin and its own catchment. During wetter periods, the river accumulated sulfidic materials from sulfate contained in surface waters and groundwaters. However, during periods when river flows were lower (Figure 16 - middle panel), the river and adjacent wetlands partially dried causing oxidation of hypersulfidic material, especially on the dry margins with the potential formation of sulfuric material. In wetter times and during floods, the acidic material was resubmerged causing dilution or neutralisation of acidity, entrainment of soluble materials in the river waters or the reformation of sulfidic material. The build-up of hypersulfidic material in the Finniss River was thus regularly kept in check by oxidation and removal during scouring floods.

(i) Pre-drought, modified by barrages from the 1920s to 2006. Since the 1920s water levels in Lake Alexandrina, The Finniss River and adjacent wetlands have been managed using locks and barrages and this continues to the present, with seawater exclusion being their main function. The installation of locks and barrages has allowed considerable build-up of sulfidic, hypersulfidic and monosulfidic material in the lower lakes and tributaries due to: firstly the evaporative concentration of sulfate from river nutrient/salt loads during periods of stable pool levels and from groundwater sources, and secondly, the lack of scouring and seasonal flooding. This has led to the formation of subaqueous ASS (i.e. hypersulfidic subaqueous clay soils) with ultra-fine monosulfidic material accumulating in low-flow backwaters and along the vegetated edges of the wetlands [see panel (i) in Figure 17].

(ii) Drought with drying from 2006 to November 2008. During this drought period, partial drying of the river [panel (ii) in Figure 17 took place and the river and lake levels continued to

decrease. The subaqueous ASS (hypersulfidic subaqueous clayey soils) transformed to waterlogged ASS (hypersulfidic clayey soils).

(iii) Drought with extreme drying from November 2008 to February 2009. During the November 2008 to February 2009 period, extreme drying of Lake Alexandrina and adjacent wetlands took place because of the extended drought conditions and lower lake levels (Lake Alexandrina had almost lowered to minus 1.0m AHD). Most wetlands adjacent to Lake Alexandrina effectively became hydraulically disconnected from the lake. These conditions also permitted oxidation of sulfides due to increased soil aeration from deepening of desiccation cracks (> 50cm), especially in areas that are organic-rich (> 10 % organic carbon) and clayey (> 35 % clay). This resulted in the formation of sulfuric material up to 75 cm into the subsoil (sulfuric clayey soils). Under these low pH conditions, acid dissolution of the layer silicate soil minerals caused the release of substantial soluble Fe, Al, Mg, Si (and other elements). The continued drying of the Finniss River and the adjacent wetlands caused further desiccation and the precipitation of sulfate-rich salt efflorescences in desiccation cracks and on the sandy edges of the river [see panel (iii) in Figure 17]. Areas with monosulfidic material continued to dry out, with the formation of desiccation cracks in the fine textured material.

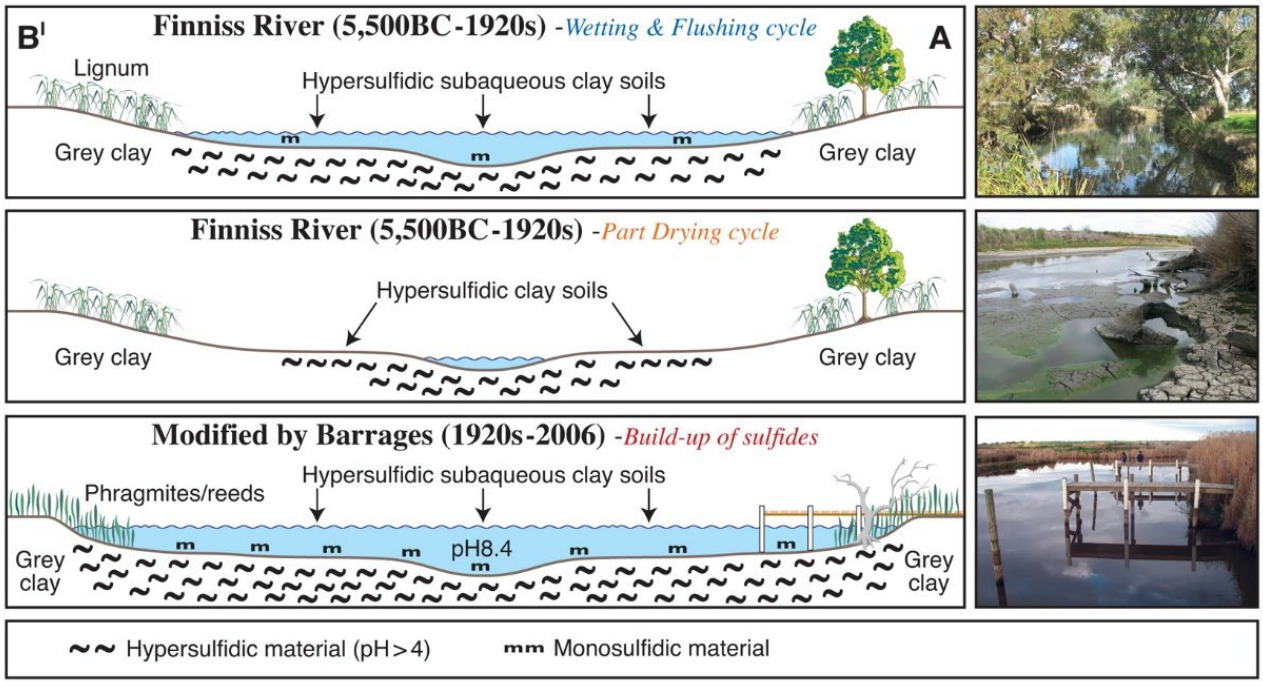

Figure 16: Predictive soil-regolith models for Finniss River (A – B' transect in Figure 13 illustrating natural wetting and flushing (upper panel), and partial drying (lower panel) cycles during the time prior to major pre-European development (5,000 BC to 1880s). The first picture taken upstream of Wally's Landing to represent its possible original condition (modified from Fitzpatrick et al. 2009a).

(iv) Winter rains causing rewetting in May 2009. During May 2009, the river and adjacent wetlands (cracks and areas pugged by cattle) were rewet [see panel (iv) in Figure 17]. This caused sulfate-rich salt efflorescences to dissolve and wash into cracks and cattle pugs (pH 1.3 to 2.5). Rewetted soil surfaces with extremely low pH values (pH 0.5 to 0.8) were also recorded. Strongly flowing extremely acidic water (pH 3.3) was observed in the adjacent anabranches and wetlands draining former channels of the lower alluvial plain. In contrast, at the same time the adjacent river

channel water had a pH of 7.0 to 7.5. The higher river pH values on the southern side were likely partly maintained by the discharge of alkaline ground water. The submerged sulfuric subaqueous clay soil in the wetlands contained vertical cracks that were coated in jarosite and infilled with medium sand.

(v) and (vi) Post drought flooding from end winter, 2009 to autumn 2010. During this extensive period of rewetting both the river and adjacent wetlands remained submerged with the sulfuric subaqueous clay soils containing vertical cracks that were coated in jarosite and infilled with medium sand [see panel (v) & (vi) in Figure 17].

(vii) Post drought continued flooding from February 2011 to June 2012. In sampling no jarosite mottling was observed, leaving most of this area comprising predominantly hypersulfidic subaqueous clay soils [see panel (vii) in Figure 17].

Degree of external and internal factors controlling pedogenic pathways and processes of soil evolution

The soil-regolith models displayed in Figure 16 and Figure 17 were used as a framework or basis to illustrate some of the key intrinsic features and external drivers that render the various subtypes of acid sulfate soils relatively stable or susceptible to rapid change (Fitzpatrick et al. 2012). Fitzpatrick et al. (2012) define Extrinsic and Intrinsic pedogenic thresholds (Muhs 1984) rather loosely as a circumstance by which a "relatively modest change" in an environmental driver can cause a major change in soil subtype alteration (i.e. soil evolution) and soil properties. The degree of external and internal factors, which control pedogenic pathways of soil evolution at Wally's Landing are shown in Figure 18.

The dominant pedogenic processes are assigned to: (i) each sequential hydro-toposequence model in Figure 18 and (ii) the summary Table 1 for Wally's Landing using the following 3 pedogenic concepts:

(a) Extrinsic and intrinsic pedogenic thresholds (Muhs 1984). The pedogenic threshold is a value, unique to a particular soil system, beyond which the system adjusts or changes, not just in rate but also in soil type. In an extrinsic pedogenic threshold, an external factor changes progressively, which triggers abrupt, fast or slow pedogenic changes. This is usually caused by climatic, geomorphic or human-made changes. In contrast intrinsic pedogenic thresholds occur when a system changes without a change in external variable.

(b) Pedogenic rates [e.g. dynamic balance of thickness (Johnson and Watson-Stegner 1987)].

(c) Acid sulfate soil processes (e.g. sulfidization and sulfuricization).

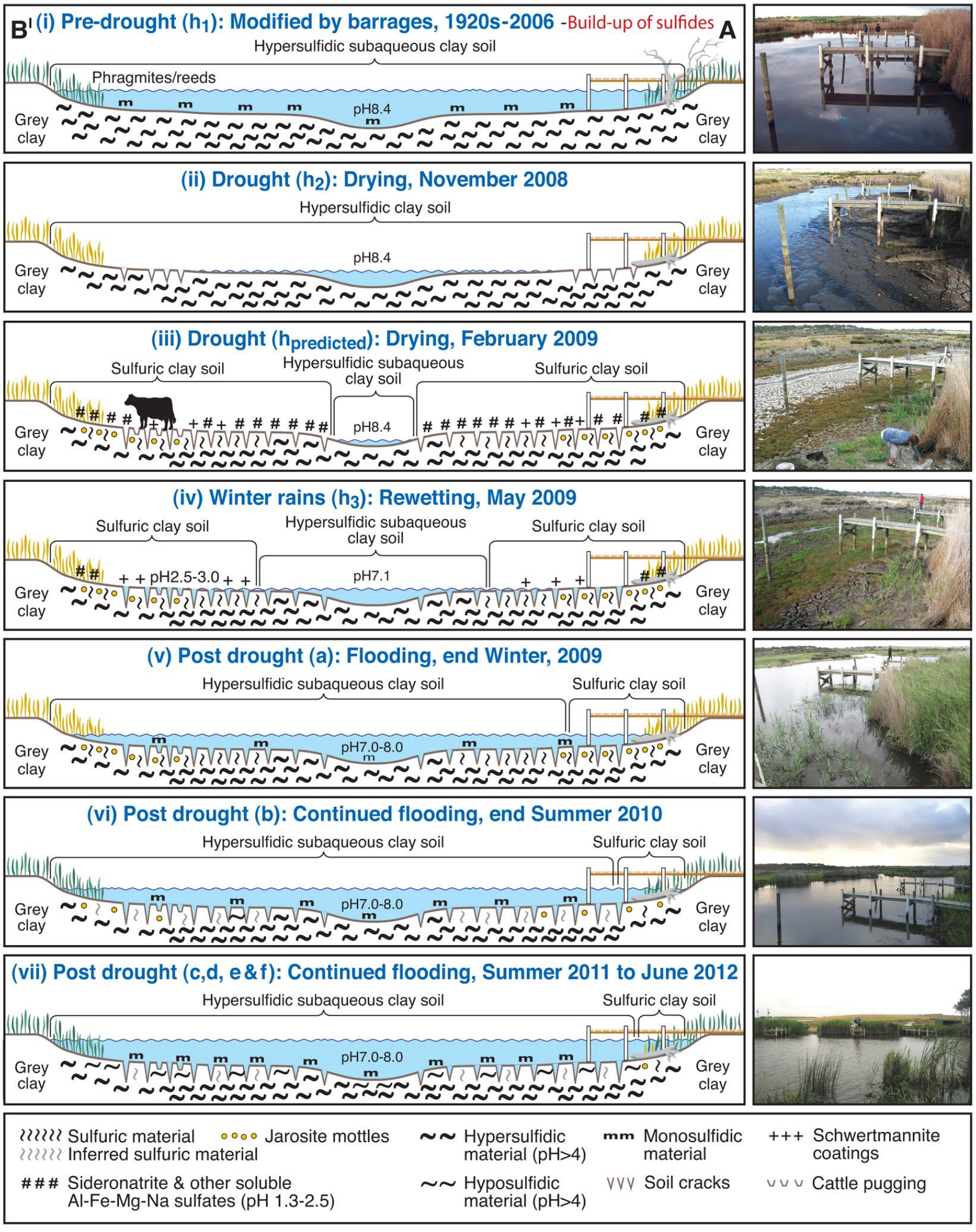

Figure 17: Predictive soil-regolith models for the Finniss River at Wally's Landing (A – B' transect in Figure 13) illustrating modification of water levels by barrage installations causing the build up of sulfides under continuous subaqueous ASS conditions from 1920s-2006 followed by progressive drying [panels (ii) and (iiii)] and a rewetting phase in May 2009 [panel (iv)], which resulted in acidic pools and flowing water (pH 3.3. to 4) in the cracks and cattle pugs (pH 0.5 to 0.8); and finally post drought flooding resulting in the sequential transformation of jarosite to sulfide under subaqueous conditions after at least 3 years (modified from Fitzpatrick et al. 2009a)

Generalised predictive hydro-toposequence model

All this information was used to construct a **generalised predictive soil-regolith model** for the Lower Lakes and River Murray regions as shown in Figure 18, which illustrates the lowering of water levels due to drought, followed by winter rainfall rewetting and flooding in 2010 (Fitzpatrick et al. 2008b, 2009a, 2009b, 2011b). The soil-regolith model outlines sequential transformations progressively through five sediment/soil types from:

1. alkaline deeper water sediments →
2. alkaline subaqueous soils →
3. neutral waterlogged soils containing 'benign' hypersulfidic material →
4. acidic drained soils containing 'nasty' sulfuric material (pH <4) →
5. rewetted acidic subaqueous soils with sulfuric material and water.

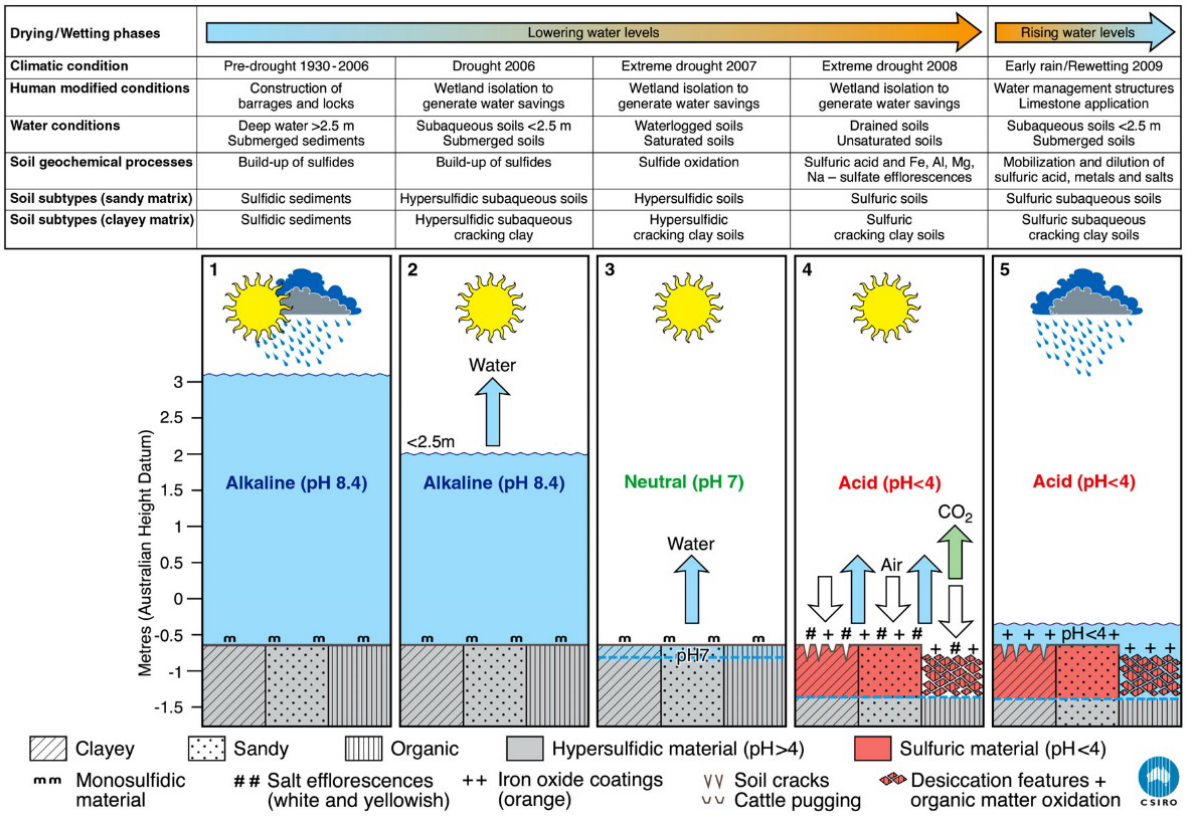

Figure 18: Generalised predictive soil-regolith model illustrating the role of climate variability (drought triggered and early winter rains), environmental conditions imposed by humans (i.e. modifications from barrages, isolating wetlands and weirs) and water conditions (subaqueous, waterlogged, dried and rewetted), which play a vital role in the alteration of soil geochemical processes and sequential transformation of various sandy, clayey and organic acid sulfate soil subtypes. (Modified from Fitzpatrick et al. 2008b, 2009b, 2011d).

Management response, implications and strategies

While increased disturbance of hypersulfidic material is the principal cause of the formation of sulfuric materials, one would expect that the principal management option would be to reverse the situation (i.e. keep conditions anoxic or under-anaerobic, in order to slow or stop the rate and extent of pyrite oxidation). This can be achieved either by keeping hypersulfidic material anaerobic under saturated conditions or by rapid drying of hypersulfidic material to slow the biologically mediated oxidation processes, which are responsible for the formation of sulfuric acid. However, the selection of appropriate management options to prevent oxidation of sulfides depends on the nature and location of the various types of acid sulfate soil materials, their position in the landscape, and availability and ability to deliver sufficient amounts of water to either maintain or generate anoxic or waterlogged conditions. Reversing the process by rewetting, once oxidation has occurred, is not straightforward, however, because it is at this time that the risks from acid and metal mobilisation are highest. This is why reliable acid sulfate soil hazard maps, at appropriate scales, along with characterising landscapes are so important (e.g. Figure 11). Understanding the soil properties and chemistry, rates of chemical processes and hydrogeological parameters is key to selecting the best options for drainage and the most appropriate management of the soils when they are drained. Appropriate management of acid sulfate soil types during their formation can improve discharge water quality and protect infrastructure and the environment. Such improvements can generally be achieved by applying low-cost land management strategies (e.g. Dear et al. 2002).

Limestone application at Wallys Landing

Applications of fine limestone ($CaCO_3$) were applied to the upper Finniss River in the form of a barrier across the river below Wally's Landing jetty, as shown in Figure 19, to neutralise potential acidic waters from the wetland and channel. Larger areas of exposed acid sulfate soils with sulfuric (pH<4) materials and associated acid water bodies in two key 'hotspots' (Currency Creek and Boggy Lake) were managed via aerial dosing of limestone. This option involved precision application of limestone into the water body using a crop-dusting plan. The amount and location of limestone dosed was informed by measurements of acidity already present in the water body (Mosley et al. 2014b,c,d).

Figure 19: Applications of fine limestone in the Finniss River below Wally's Landing jetty to acidic waters flowing from the wetland and channel in May 2009. (From Fitzpatrick et al. 2011d)

Clayton Embankments, regulators and pumping: Goolwa Channel

As a consequence of the widespread occurrence of sulfuric material and acidic waters in the Goolwa Channel, Finniss River and Currency Creek areas (Figure 20), the federal government, in response to a Referral under the *Environment Protection and Biodiversity Conservation Act* 1999 EPBC Reference Number 2009/4833, gave approval for the South Australia Government to undertake a set of emergency actions to undertake management measures to mitigate acid sulfate soils (Natural Resources SA Murray-Darling Basin, 2009). First, a temporary flow regulator across the Goolwa Channel at Clayton was constructed (Figure 20) to allow water levels in the Goolwa Channel, Finniss River and Currency Creek to be raised. This strategy aimed to saturate the exposed sulfuric and hypersulfidic materials to minimise further sulfide oxidation and to allow the early season flows (which would have mobilised acid and heavy metals) to be held back, allowing natural in situ bioremediation to proceed. The constructed height of the regulator was c.+2.5 m AHD (to allow sufficient freeboard), but the water level was managed to a maximum level of +0.7 m AHD. The pool level was initially raised to +0.7m AHD by pumping water from Lake Alexandrina. This action required ~20 GL of water. In addition, a low-level regulator (0 m AHD) was constructed across the mouth of Currency Creek to permit continued saturation of sulfidic, hypersulfidic and sulfuric materials.

Figure 20; The main temporary flow regulator across the Goolwa Channel was completed in early August 2009, allowing water levels in the Goolwa Channel, Finniss River and Currency Creek to be raised and to saturate the existing exposed sulfuric material shown in the soil map (see Figure 5). The regulator was about 400 m long and 40 m wide, and was constructed as an earth-fill embankment. The photographs show two angles of the same public notice in the foreground, explaining the 'Goolwa Channel Water Level Management Project', with information on acid sulfate soils, which included the following statement: 'Keeping acid sulfate soils with hypersulfidic material wet is a proven and effective management technique'. (From Fitzpatrick et al. 2011d)

As well, construction of a large bund across the Narrung Narrows and pumping water from Lake Alexandrina to Lake Albert to maintain water levels successfully prevented more hypersulfidic material in Lake Albert oxidising to form sulfuric material.

Stop 2: Milang Jetty.

The water level at Milang Jetty illustrated the water level reduction of Lake Alexandrina as shown in Figure 21. It was the source of much distress in the local community as water level dropped to their lowest level in recorded history (see Figure 22). The bus will stop briefly to see the difference at this location now the River Murray is still in flood as shown in the two photographs taken during the field trip on 26th March 2023 (Figure 23). The photograph in Figure 24 shows the River Murray in flood near Murray Bridge at Long Flat on 28th January, 2023 illustrating widespread flooding of fields, roads and infrastructures due to bursting of the levee banks with extensive fish kills as the water levels recede due to anoxic blackwater events together with likely contributions from anoxic monosulfidic material (or monosulfidic black ooze).

Figure 21: (top) Photo illustrating extent of drying of shoreline at Milang during the Millenium drought. (Bottom left and right) Google Earth images from 2009 and 2020.

Figure 22: Front page of the Milang Community News in April 2009

(a)

(b)

Figure 23: Photographs taken of Lake Alexandrina on 26th March, 2023 during the field trip when the River Murray is still in flood showing: (a) Emily Leyden pointing to the jetty with the red crane near the end of the jetty, which is also shown in Figure 21 during the Millenium drought. See also stacked sandbags adjacent to jetty and along the banks of Lake Alexandrina to prevent flooding of holiday houses/shacks and (b) close-up view of the dominant murky greyish water with pockets of back water and evidence of sporadic fish-kills on the banks / water edge. Photograph taken by Rob Fitzpatrick.

Figure 24: Photograph taken of the River Murray in flood near Murray Bridge at Long Flat on 28th January, 2023 showing: flooded fields, roads and infrastructures due to bursting of the levee banks and fish kills as the water levels recede. Photograph taken by Rob Fitzpatrick

Boggy Lake – view from Bus with discussion

Community volunteer groups / citizen science projects

Sampling protocols for monitoring changes in acid sulfate soil conditions in the Lower Lakes region were also specifically developed for community volunteers by Thomas and Fitzpatrick (2011). Seminars and field days were held to build the capacity of 85 community group volunteers to effectively monitor acid sulfate soils four times during 2009 and 2010. This resulted in a total of 486 soil profiles and 1 458 soil layers being sampled and tested for pH in the field by community groups, and in the laboratory by CSIRO. The graphs showing pH changes and trends are available (i) on the ASRIS (Australian Soil Resource Information System), which also contains the Atlas of Australian Acid Sulfate Soils (AAASS) (ii) in a technical report (Thomas & Fitzpatrick 2011) and journal publication (Thomas et al. 2016). The engagement of citizen scientists greatly raised awareness of acid sulfate soils in the Lower Lakes, and in turn helped inform more detailed follow-up work and management in some areas.

Based on soil-and water-monitoring results, warning signs were erected (Figure 25) to warn the public of the hazards present at these sites. This would not have been possible without the monitoring information to inform the risk assessment.

Figure 25: Two angles of the same notice giving public notification of risk in Boggy Lake (which is in the background) adjacent to Lake Alexandrina, because of the widespread occurrence of both Acid Sulfate Soils with sulfuric materials (pH <2.5) on beaches and ponded acidic water (pH <4). (From Fitzpatrick et al. 2011d)

Figure 26 shows aerial dosing operations in Boggy Lake, which is connected to Lake Alexandrina, to neutralise strongly acidic ponded water in May 2010 (Fitzpatrick et al. 2011, 2018; Mosley et al. 2014b,c).

Figure 26: Left: Aerial application of limestone in Boggy Lake, SA. Right: photos showing mechanism used to upload fine agricultural limestone into the aircraft in a nearby paddock. (From Fitzpatrick et al. 2011d)

ACKNOWLEDGEMENTS

We especially thank other members past and present of the Acid Sulfate Soil team in CSIRO Land and Water (Dr Gerard Grealish, Richard Merry, Mark Raven, Steve Marvanek, Warren Hicks, Stuart McClure, Dr Mark Thomas, Dr Nathan Creeper, Dr Andrew Baker, Dr Stuart Simpson, Dr Peter Self, Dr Nilmini Jayalath and Sonia Grocke), EPA (David Palmer, Ben Zammit, Eaton, Andrew Beal), University of Adelaide (Dr Patrick Michael) and University of WA (Dr Matt Hipsey) for assistance; Greg Rinder for drafting the figures.

Stop 3: Jervois - Lower Murray Reclaimed Irrigation Area.

Figure 27: Stop 3 Location – see Figure 29 for closer detail.

Text, Figures and Tables Extracted from the below publications and their Supplementary Material:

Fitzpatrick, RW, Shand P and Mosley LM (2017a). Acid sulfate soil evolution models and pedogenic pathways during drought and reflooding cycles in irrigated areas and adjacent natural wetlands. Geoderma. ***308****, 270-290. http://dx.doi.org/10.1016/j.geoderma.2017.08.016*

Fitzpatrick, RW, Mosley LM, Raven MD and Shand P (2017b) Schwertmannite formation and properties in acidic drain environments following exposure and oxidation of acid sulfate soils in irrigation areas during extreme drought. Geoderma. ***308****, 235-251. http://dx.doi.org/10.1016/j.geoderma.2017.08.012)*

Collectively, the LMRIA covers 5,200 ha between the townships of Mannum and Wellington. Most of this land was drained and developed for agriculture between 1880 and 1940 with levee banks constructed along the river's edge to control flooding (Figure 28). Before agriculture was established, the flood plains along the River Murray contained reed beds (*Phragmites Australis*) with regular flooding under natural river regime.

The levee banks along the River Murray, as well as weirs along the River and barrages at the river mouth (which prevent seawater ingress), allowed farming to thrive, as water levels became more stable and periodic flooding was controlled (Figure 28). The regulation of the river also raised the water level of the River channel to approximately 1-1.5 m above that of the flood plains. This allowed the use of flood irrigation on the now agricultural land behind the levee banks. Dairy farming was the predominant land use with a smaller area used for beef cattle, fodder production and lifestyle farming. From 2003 to 2006 a major $22 million Commonwealth funded rehabilitation project was completed with the installation

of more efficient irrigation and runoff reuse systems to reduce the pollutant return loads to the river, as well as improved on-farm management practices. This type of irrigation was generally successful due its low capital and energy costs, and effect in reducing soil salinisation.

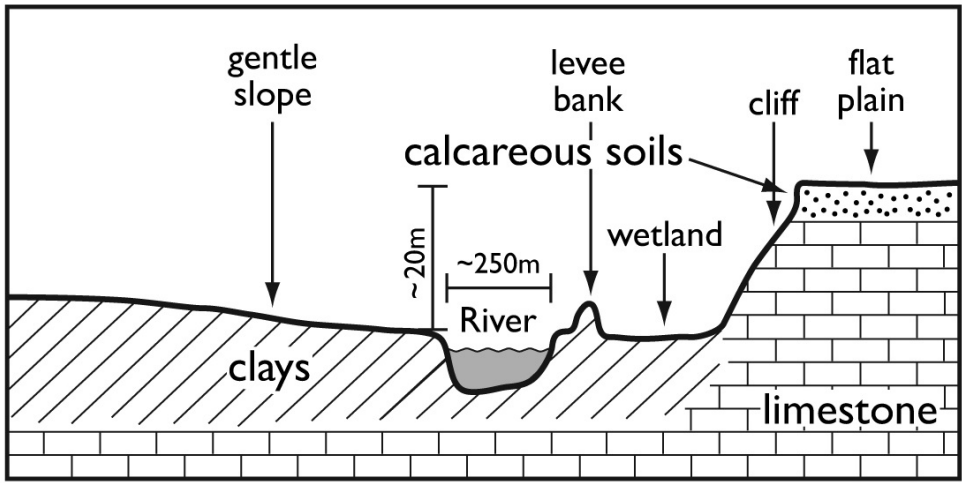

Figure 28: Stratigraphical section of the Lower Murray-Darling Basin in the LMRIA showing distribution of heavy clays, wetlands, levee banks and limestone cliffs (modified from Grealish et al., 2011).

Reduced inflows to the River Murray from approximately 2006 to early 2010, however, resulted from an extended drought and over allocation of irrigation water in the Murray-Darling Basin. In the wetlands between Lock 1 and Wellington near the entrance to Lake Alexandrina, the combination of decreasing water levels due to the extreme drought conditions during the Millennium Drought from 2007 to 2010 resulted in the water level in the Lower Murray to fall to -1.75 m AHD (Australian Height Datum), the lowest river level in over 90 years of records, and gently sloping near-shore beds caused large expanses of previously inundated sediments and subaqueous soils to be exposed. With continued lowering of water levels, pyrite-rich sediments and subaqueous acid sulfate soils (i.e. with hypersulfidic and hyposulfidic materials) became progressively oxidised to greater depths in the soil. The resultant formation of sulfuric material (pH < 4) led to water quality, ecological and public health issues from metal/metalloid mobilization, de-oxygenation, wind erosion and noxious gas release (Fitzpatrick et al., 2009).
From March 2010 to early 2011, increased rainfall within the Murray Darling Basin catchment resulted in water levels in the lower River Murray region to increase from approximately −1.75 m AHD to 0.7 m AHD (Australian Height Datum or Mean Sea Level).

In February 2011, the Environment Protection Authority (EPA) discovered acidic (pH 3) water being discharged to the River Murray from the largest irrigation area in the LMRIA, at Jervois. Subsequent screening of other drains found that 14 of the 27 salt drains within an area of approximately 3500 ha, were acidic (EPA, 2008). These iron-rich precipitates comprise mostly of schwertmannite with scavenged metals in acidic drain waters. This condition has persisted for over 7 years in most of the LMRIA drains with significant implications for short-term rehabilitation options.

The severe Millennium Drought (2007-2010) left an area of over 5,000 ha in the LMRIA dried, cracked and acidified as river and groundwater levels fell nearly 2 m. In the study by Fitzpatrick et al. (2017a), they examined both the irrigated agricultural areas and an adjacent natural wetland for comparison, which were both affected by the drought.

Approximately 3 m deep soil cores were collected along transects in three sections of the Lower Murray Reclaimed Irrigation Area (LMRIA) on multiple occasions between 2011 and 2015 and an adjacent natural wetland in 2007 Fitzpatrick et al. 2017a).

Soil properties measured included detailed soil profile descriptions (Table 4, Table 5, Table 6) pH (pH incubation after 8 & 16 weeks and pH after oxidation with hydrogen peroxide), reduced inorganic sulfur (RIS, pyrite), titratable actual acidity (TAA), retained acidity, acid neutralizing capacity (ANC) (Table 5; Figure 30) X-ray diffraction analyses and scanning electron microscopy.

The result of the formation of thick “Sulfuric clay materials” at depth and iron-rich acid drainage waters across the LMRIA is that many irrigators ceased or down-scaled their operations. Irrigation has now become “more patchy” across the region with less commercial irrigation and dairy land use. Remaining irrigators initially observed large water losses during irrigation due to lateral movement to adjacent irrigation bays and properties. This is likely due to the legacy of deep soil cracking, which provides preferential pathways for water flow and lower groundwater levels compared to pre-drought on adjacent irrigation properties. These losses increase drainage pumping costs and pollution returned to the River Murray. Due to more limited irrigation across the LMRIA and the drought, large areas of land have become strongly salinised, acidic (i.e. pH < 4; formation of acid sulfate soils with sulfuric materials), sodic and eroded. Approximately 4,200 ha of this land was rehabilitated under the LMRIA rehabilitation project with approximately 1,000 ha of land retired from farming and not rehabilitated (EPA, 2009). Dairy production has therefore reduced from approximately 5,000 ha to 1,866ha – a reduction of approximately 63%. However, the total area of ‘productive’ farms remaining in the LMRIA is estimated to be 3,192ha (Fitzpatrick et al. 2017a).

The result of the formation of thick “Sulfuric clay materials” at depth and iron-rich acid drainage waters across the LMRIA is that many irrigators ceased or down-scaled their operations. Irrigation has now become “more patchy” across the region with less commercial irrigation and dairy land use. Remaining irrigators initially observed large water losses during irrigation due to lateral movement to adjacent irrigation bays and properties. This is likely due to the legacy of deep soil cracking, which provides preferential pathways for water flow and lower groundwater levels compared to pre-drought on adjacent irrigation properties. These losses increase drainage pumping costs and pollution returned to the River Murray. Due to more limited irrigation across the LMRIA and the drought, large areas of land have become strongly salinised, acidic (i.e. pH < 4; formation of acid sulfate soils with sulfuric materials), sodic and eroded. Approximately 4,200 ha of this land was rehabilitated under the LMRIA rehabilitation project with approximately 1,000 ha of land retired from farming and not rehabilitated (EPA, 2009). Dairy production has therefore reduced from approximately 5,000 ha to 1,866ha – a reduction of approximately 63%. However, the total area of ‘productive’ farms remaining in the LMRIA is estimated to be 3,192ha (Philcox et al., 2012).

Soil profile descriptions of 3 soils along the Jervois (DS02) transect

The soil profile transect shown in Figure 29 at the Jervois irrigation site (DS02) in the LMRIA was specifically selected to be viewed during this Pre-conference field trip because the two other transects investigated by Fitzpatrick et al. (2017a) at Long Flat (DS01) and Toora (DS03) were completely flooded due to bursting of the levee banks at both Long Flat (as shown Figure 24) and Toora. Members of the Jervois community banded together to repair the 20 kilometre stretch of government-owned levee running across 30 properties, which had not been maintained appropriately.

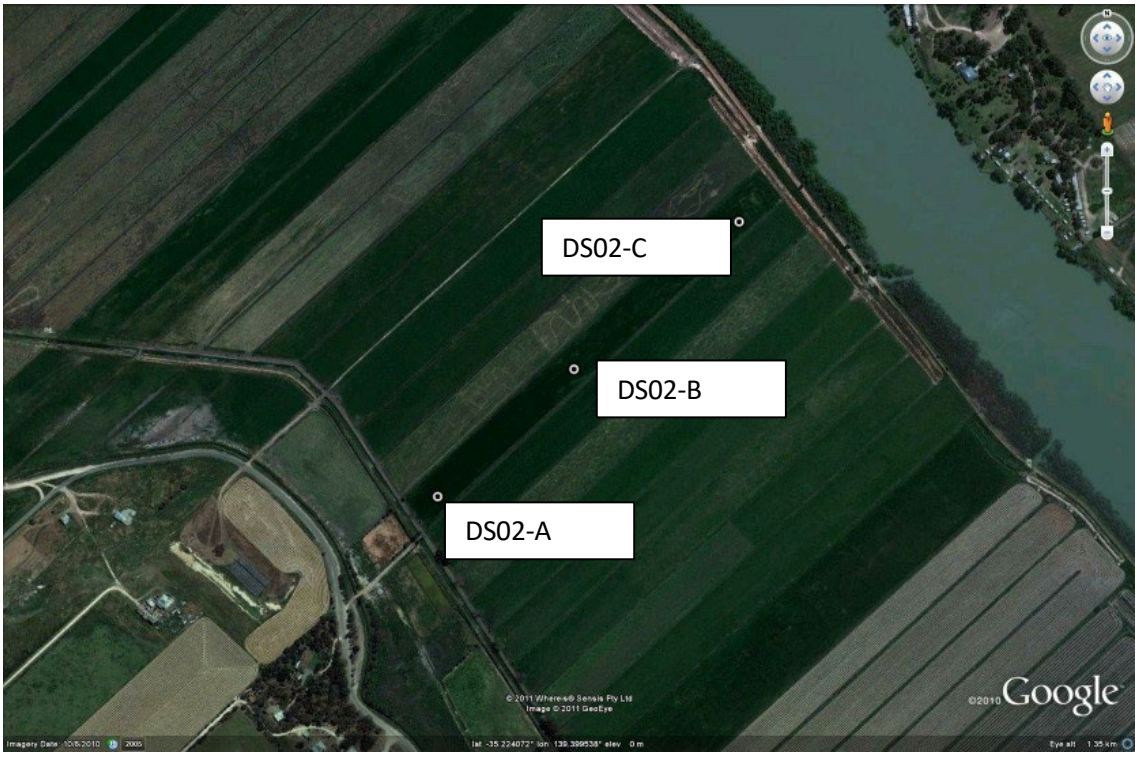

Figure 29: Aerial photograph showing the localities of the 3 sites at the Jervois irrigation site (Aerial photograph taken in March 2008) (from Fitzpatrick et al. 2017a).

Table 4: JERVOIS (DSa 02-A): Sampling on 22nd June 2011 Sulfuric organic soil (Australian ASS Key) Humose-Acidic, Sulfuric, Redoxic Hydrosol (ASC) Sulfic Endoaquept (Soil Taxonomy), Hyperthionic Gleysol (Drainic, Hypersulfidic) (WRB) (from Fitzpatrick et al. 2017a).

Sample ID Depth cm	[2]Locality description and photographs	Morphology	[1]Chip-tray photograph
DSa 02-A.1 0-40 Ap	DSa 02A Located in the field (paddock), near salt drain and road to west. Owner: Kim and Kate Bartlett  View looking from east to west towards the salt drain area (trees in background) from site DSa 02-A **Water table depth: 80 cm**	Black (10Y 2.5/1), pH 5.3; light clay; coarse sub-angular blocky breaking to fine polygonal cracks with high organic matter content throughout; many coarse roots and fine rootlets; few decomposing roots, sharp boundary.	
DSa 02-A.2 40-65 Bg1		Dark reddish brown (5YR 3/3; 70%); medium clay, strong planar vertical cracks and weaker horizontal planes/closed cracks, 20% medium prominent irregular black (10YR 2/1), moist masses of reduced iron on faces of peds, remnant organic matter and fine roots maintaining the surfaces and preserving plans of weakness, clear, wavy boundary. pH 4.5	
DSa 02-A.3 65-100 Bjgse2		Dark grayish brown (10YR 4/2; dominant); heavy clay, 10% pale yellow (2.5Y 7/4) masses of jarosite along old root channels and faces of peds (pH 3.9); very sticky; sharp, wavy boundary	
DSa 02-A.4 100-140 Bjgse3		Dark grayish brown (2.5Y 4/2; dominant); heavy clay; 10% pale yellow (2.5Y 7/4) masses of jarosite along old root channels and remnant cracks (pH 3.9) soft, very sticky clear, wavy boundary.	

1Chip-tray application (Fitzpatrick et al. 2010); 2Easting: 354171; Northing: 6100771 (based on the WGS84 datum, Zone 54H)

Table 5: JERVOIS (DSa 02-B): Sampling on 22nd June 2011 Sulfuric organic soil (Australian ASS Key) Humose-Acidic, Sulfuric, Redoxic Hydrosol (ASC) Sulfic Endoaquept (Soil Taxonomy), Hyperthionic Gleysol (Drainic, Hypersulfidic) (WRB) (from Fitzpatrick et al. 2017a).

Sample ID Depth cm	Locality description and photographs	Morphology	[1]Chip-tray photograph
DSa 02-B.1 0-40 Ap	Located in the middle of the field (paddock), between River Murray and salt drain to west. Owner: Kim and Kate Bartlett	Black (10Y 2.5/1), pH 6 to 7; light clay; coarse sub-angular blocky breaking to fine polygonal cracks with high organic matter content throughout; many coarse roots and fine rootlets; few decomposing roots, sharp boundary.	
DSa 02-B.2 40-65 Bg1	 View looking from west to east towards the River Murray (willow trees in background) from site DSa 02-B **Water table depth: 80 cm**	Black (10YR 2/1; dominant); medium clay, strong planar vertical cracks and weaker horizontal planes/closed cracks, 10% medium prominent irregular dark grey (5Y4/1),moist masses of reduced iron on faces of peds; remnant organic matter and fine roots maintaining the surfaces and preserving plans of weakness, clear, wavy boundary. pH 5;	
DSa 02-B.3 65-90 Bgse2		Dark greyish brown (10YR 4/2; dominant); heavy clay; 10% pale yellow (2.5Y 7/6) masses of jarosite along old root channels and crack faces (pH 4 to 3.5); sharp, wavy boundary	
DSa 02-B.4 90-150 Bgse3		Dark grayish brown (2.5Y 4/2; dominant) heavy clay; 10% pale yellow (2.5Y 7/4) masses of jarosite along old root channels and crack faces (pH 4 to 3.5); soft, very sticky clear, wavy boundary.	

1Chip-tray application (Fitzpatrick et al. 2010); 2Easting: 354355; Northing: 6100948 (based on the WGS84 datum, Zone 54H)

Table 6: JERVOIS (DSa 02-C): JERVOIS (DSa 02-C): Sampling on 22nd June 2011 Sulfuric organic soil (Australian ASS Key) Humose-Acidic, Sulfuric, Redoxic Hydrosol (ASC) Sulfic Endoaquept (Soil Taxonomy), Hyperthionic Gleysol (Drainic, Hypersulfidic) (WRB) (from Fitzpatrick et al. 2017a).

Sample ID Depth cm	**Locality description and photographs**	**Morphology**	**[1]Chip-tray photograph**
DSa 02-C.1 0-40 Ap	Located in the field (paddock), nearest to River Murray and drain to south. Owner: Kim and Kate Bartlett  View looking from west to east towards the River Murray (willow trees in background) from site DSa 02-C **Water table depth: 1 m**	Black (2.5Y 2.5/1, dominant), light clay; fine sub-angular blocky breaking to fine polygonal cracks with very high organic matter content throughout; many coarse roots and fine rootlets; few decomposing roots, (pH=6-5) sharp boundary.	
DSa 02-C.2 40-60 Bg1		Black (2.5Y 2.5/1; dominant), medium clay, with 5% diffuse pale yellow (2.5Y 7/6) jarosite mottles strong planar vertical cracks and weaker horizontal planes/closed cracks, with few remnant organic matter and fine roots maintaining the surfaces and preserving plans of weakness; (pH=4.7) clear, wavy boundary	
DSa 02-C.3 60-80 Bjgse2		Very dark grey (2.5Y3/1; dominant), heavy clay; strong planar vertical cracks; 40% pale yellow (2.5Y 7/4) masses of jarosite along old root channels and faces in cracks (pH3.5-4), soft and very sticky; sharp, wavy boundary	
DSa 02-C.4 80-100 Bjgse3		Dark reddish brown (5Y 3/2; dominant), mixture of heavy clay with 10% medium peaty clay with distinct layer of “black peat (90%); 10% pale yellow (2.5Y 7/4) masses of jarosite along old root channels (pH4); soft, sticky clear, wavy boundary.	
DSa 02-C.5 100-155 Bjgse4		Dark grayish brown (10YR 4/2); mixture of heavy clay (50%) and peaty clay (50%); 10% pale yellow (2.5Y 7/4) masses of jarosite along old root channels (pH4), soft, very sticky	

1Chip-tray application (Fitzpatrick et al. 2010); 2Easting: 354578; Northing: 6101153 (based on the WGS84 datum, Zone 54H)

Table 7: Jervois site: summary of ASS incubation data, ASS material classification, ASS subtype classification and Soil Taxonomy classification for DSa02-22nd June 2011 and DSb02-4th April 2012 (from Fitzpatrick et al. 2017a).

Sample	Depth (cm)	Horizon designation	pHINC t=zero	pHINC 8 weeks	Texture	ASS material	[1]ASS subtype [2]Soil Taxonomy
DSa02							
DSa 02A.1	0-40	Ap	6.04	5.88	LC	*Other soil material*	
DSa 02A.2	40-65	Bg1	4.39	4.00	MC	**Hypersulfidic**	**Sulfuric organic soil**
DSa 02A.3	65-100	Bjgse2	3.72	3.72	HC	**Sulfuric**	**Sulfic Endoaquept**
DSa 02A.4	100-140	Bjgse3	4.02	2.66	HC	**Hypersulfidic**	
DSa 02B.1	0-40	Ap	5.95	5.94	LC	*Other soil material*	
DSa 02B.2	40-65	Bg1	5.17	5.02	MC	*Other soil material*	**Sulfuric organic soil**
DSa 02B.3	65-90	Bjgse2	4.01	4.15	HC	**Sulfuric**	**Sulfic Endoaquept**
DSa 02B.4	90-150	Bjgse3	3.77	2.9	HC	**Sulfuric**	
DSa 02C1	0-40	Ap	6.23	5.92	LC	*Other soil material*	
DSa 02C2	40-60	Bg1	6.06	6.01	MC	*Other soil material*	
DSa 02C3	60-80	Bjgse2	5.51	5.01	HC	Hyposulfidic	**Sulfuric organic soil**
DSa 02C4	80-100	Bjgse3	3.90	3.16	HC	**Sulfuric**	**Sulfic Endoaquept**
DSa 02C5	100-155	Ap	3.95	2.3	HC	**Sulfuric**	
DSb02							
DSb 02A.1	0-10	Ap1	5.58	5.44	LC	*Other soil material*	
DSb 02A.2	10-40	Apjg2	3.86	3.77	LC	**Sulfuric**	
DSb 02A.3	40-75	Bjg1	3.81	3.72	MC	**Sulfuric**	**Sulfuric organic soil**
DSb 02A.4	75-125	Bjgse2	3.93	2.95	HC	**Sulfuric**	**Typic Sulfaquept**
DSb 02A.5	125-175	Bgse3	6.91	2.87	HC	**Hypersulfidic**	
DSb 02A.6	175-220	Bgse4	7.77	5.10	HC	Hyposulfidic	
DSb 02A.7	220-270	Bgse5	7.88	5.38	HC	Hyposulfidic	
DSb02B.1	0-10	Ap1	5.99	6.29	LC	*Other soil material*	
DSb02B.2	10-40	Ap2	6.10	6.03	LC	*Other soil material*	
DSb02B.3	40-75	Bg1	5.07	4.88	MC	Hyposulfidic	
DSb02B.4	75-125	Bjgse2	4.00	3.87	HC	**Sulfuric**	**Sulfuric organic soil**
DSb02B.5	125-175	Bjgse3	3.73	2.75	HC	**Sulfuric**	**Sulfic Endoaquept**
DSb02B.6	175-220	Bgse4	5.06	2.35	HC	**Hypersulfidic**	
DSb02B.7	220-270	Bgse5	7.20	4.49	HC	Hyposulfidic	
DSb 02C.1	0-10	Ap1	5.92	6.06	LC	*Other soil material*	
DSb 02C.2	10-40	Ap2	6.50	6.18	LC	*Other soil material*	
DSb 02C.3	40-60	Bg1	5.73	5.26	MC	Hyposulfidic	**Sulfuric organic soil**
DSb 02C.4	60-80	Bg2	5.73	5.21	HC	Hyposulfidic	**Sulfic Endoaquept**
DSb 02C.5	80-120	Bjgse3	3.41	2.95	HC	**Sulfuric**	
DSb 02C.6	120-170	Bjgse4	3.78	2.40	HC	**Sulfuric**	
DSb 02C.7	170-300	Bgse5	7.01	4.63	HC	Hyposulfidic	
DSb 02C.8	300-380	Bgse6	7.12	5.29	HC	Hyposulfidic	
DSb 02C.9	380-465	Bgse7	7.01	6.32	HC	Hyposulfidic	

1 ASS subtype classification: (Fitzpatrick, 2013).

2Soil Taxonomy (Soil Survey Staff ,2014): Other Sulfaquerts that do not have a sulfuric horizon within 100 cm of the mineral soil surface (Sulfic Sulfaquerts); Other Sulfaquerts: Typic Sulfaquerts

****Where acid sulfate soil material is based on the definition in the 2nd edition of the Australian Soil Classification (Isbell and National Committee on Soils & Terrain, 2016)**

****Where the soil classification is a Sulfuric soil, Sulfuric material (pH <4 at time zero incubation) has been identified in a layer or horizon (at least 15cm thick) within 150 cm of the soil surface;**
***Where the soil classification is a Hypersulfidic soil, hypersulfidic material (pH decreased to <4 after incubation of at least 16 weeks) has been identified in a layer or horizon (at least 10cm thick) within 150 cm of the soil surface.**

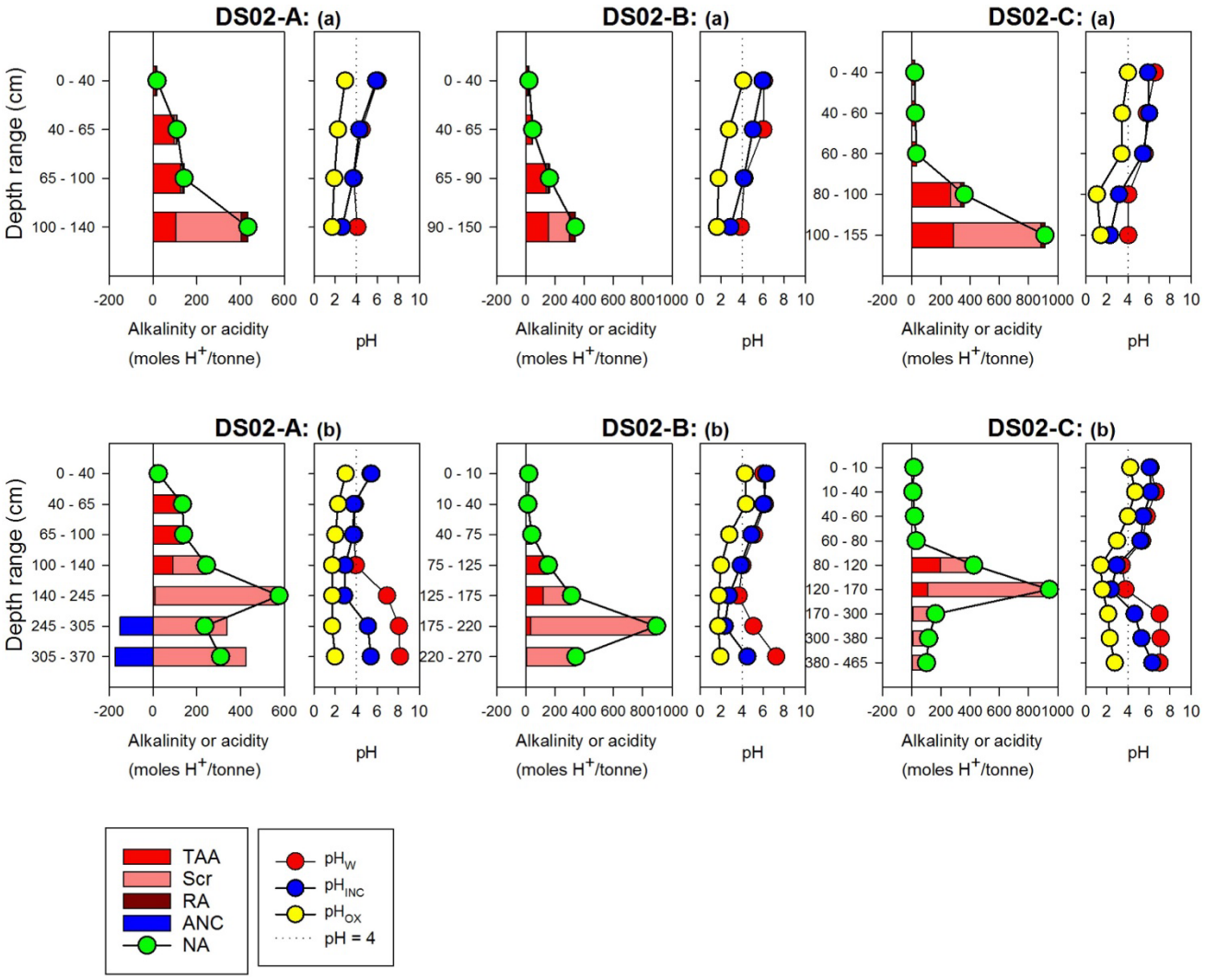

Figure 30: Acid base accounting [Titratable Actual Acidity (TAA), Reduced Inorganic Sulfur (SCr), Acid Neutralising Capacity (ANC), Retained Acidity (RA) and Net Acidity (NA)], pH measured in 1:1 soil:water ratio (pHw), incubation pH after 16 weeks (pHINC) and pH after oxidation with hydrogen peroxide (pHOX) data plotted against depth for each of the three soil profiles (A, B and C) collected along the irrigated Jervois transect (DS02) on 22nd June 2011 [DS02-A: (a), DS02-B: (a), DS02-C: (a)] and 4th April 2012 [DS02-A: (b), DS02-B: (b), DS02-C: (b)] from (from Fitzpatrick et al. 2017a).

Table 8: Jervois site: pH and ASS material classification, ASS subtype classification and Soil Taxonomy classification for DSc02-A sampled on 2nd March 2023 by Rob Fitzpatrick and Luke Mosley

Sample	Depth (cm)	Horizon designation	pH	Texture	ASS material	[1]ASS subtype [2]Soil Taxonomy
DSc 02C.1	0-5	Ap1	6.5	LC	*Other soil material*	
DSb 02C.2	30-35	Ap2	5.5	LC	*Other soil material*	
DSb 02C.3	35-50	Bg1	5.0	MC	Hyposulfidic	**Sulfuric organic soil**
DSb 02C.4	50-60	Bg2	4.7	HC	Hyposulfidic	**Sulfic Endoaquept**
DSb 02C.5	60-80	Bjgse3	4.0	HC	**Sulfuric**	
DSb 02C.6	80-100	Bjgse4	3.9	HC	**Sulfuric**	
DSb 02C.7	100-120	Bgse5	3.8	HC	**Sulfuric**	
DSb 02C.8	120-140	Bgse6	4.0	HC	**Sulfuric**	
DSb 02C.9	140-160	Bgse7	3.9	HC	**Sulfuric**	
DSb 02C.10	160-180	Bgse8	3.9	HC	**Sulfuric**	

1 ASS subtype classification: (Fitzpatrick, 2013). 2Soil Taxonomy (Soil Survey Staff ,2014): Other Sulfaquerts that do not have a sulfuric horizon within 100 cm of the mineral soil surface

This information was used to construct a series of explanatory soil-regolith hydro-toposequence models were developed during the pre-drought period, drying period, and subsequent wetting/reflooding post-drought period (Figure 31). These models indicate that prior to draining of the natural wetlands for irrigated agriculture the region cycled between wetting and flushing, and partial drying conditions in response to seasonal and climatic cycles causing the build-up of hypersulfidic material to be kept in check by oxidation of pyrite during dry periods/droughts and removal during scouring floods. As the region became managed for navigation and irrigation by installing barrages and locks, pyrite began to build-up. The extreme lowering of the water table during the Millennium Drought resulted in deep oxidation of sulfides in anaerobic hypersulfidic material to depths > 3.5 m in the previously saturated irrigated pastures and within 50 cm of the soil surface in the natural wetlands. Oxidation and acidification between 0.5 and 3.5 m of Hypersulfidic clayey soils was enhanced by the formation of large cracks up to 3.5 m deep. Rewetting and flooding after the drought caused mobilization of sulfuric acid, soluble sulfates, ferrous iron, nutrients and metals with transport into the River Murray.

Our findings highlight that irrigated areas formed deeper sulfuric materials (>3.5 m) than in adjacent natural wetlands (<1m) due to the difficulties in the management of water tables in irrigation areas because of the installation of high levee banks and deep drains. Maintaining water tables on agricultural soils via irrigation and subsequent drainage will promote the rapid formation of deep (>3.5 m) acid sulfate soils with sulfuric material containing extensive retained acidity (jarosite), which can persist for decades or longer. A soil profile was sampled at site DS02-A by Rob Fitzpatrick and Luke Mosley on 2nd March 2023 (labelled DSc02-A in Table 8), which showed evidence of pale yellow (2.5Y 7/6) masses of jarosite along old root channels and crack faces between 60-180 cm with <pH 4 indicating that this soil still contains sulfuric materials at depth (i.e. ~14 yrs since reflooding).

The explanatory soil-regolith hydro-toposequence model developed during post-drought reflooding and irrigation during 2011 (Figure 31), illustrates the spatial distribution of: (i) deep collapsed cracking patterns, (ii) sulfuric materials extending to a depth of 3.8 m along cracks with light yellow jarosite mottles, (iii) sulfuric materials extending to the soil surface with reddish-yellow surface coatings of iron-rich precipitates containing schwertmannite (see inset photograph of soil surface with reddish-yellow coatings of iron-rich precipitates and white salt efflorescences Fitzpatrick et al., (2017b), (iv) hyposulfidic materials near the soil surface, (v) hypersulfidic materials below 3.8 m and (v) surface water levels, groundwater table levels and river flow (modified from).

These soil-regolith hydro-toposequence models developed here for the irrigated pasture areas provided the framework to construct a generalized schematic cross-section diagram of the LMRIA, which displays a sequence of eleven dominant soil-water landscape features (see Fitzpatrick et al., 2017c). This generalized cross-section diagram with colour photographs of soil-water features, soils and water flow paths has been included in the Handbook for Understanding and Managing Irrigated Acid Sulfate and Salt-affected Soils in the LMRIA developed by Fitzpatrick et al., (2017c). The cross-section diagram incorporates land management options, which are targeted to specific parts of the landscape (e.g. irrigated floodplain land, drains, levee banks). The Handbook provides greatly improved knowledge of optimal irrigation and soil-water-landscape management in the LMRIA under changing land use and climate patterns and is used as an aid by farmers, land managers, agencies and service providers to provide farm property management plans that help prevent the spread of acid sulfate and salt-affected soils.

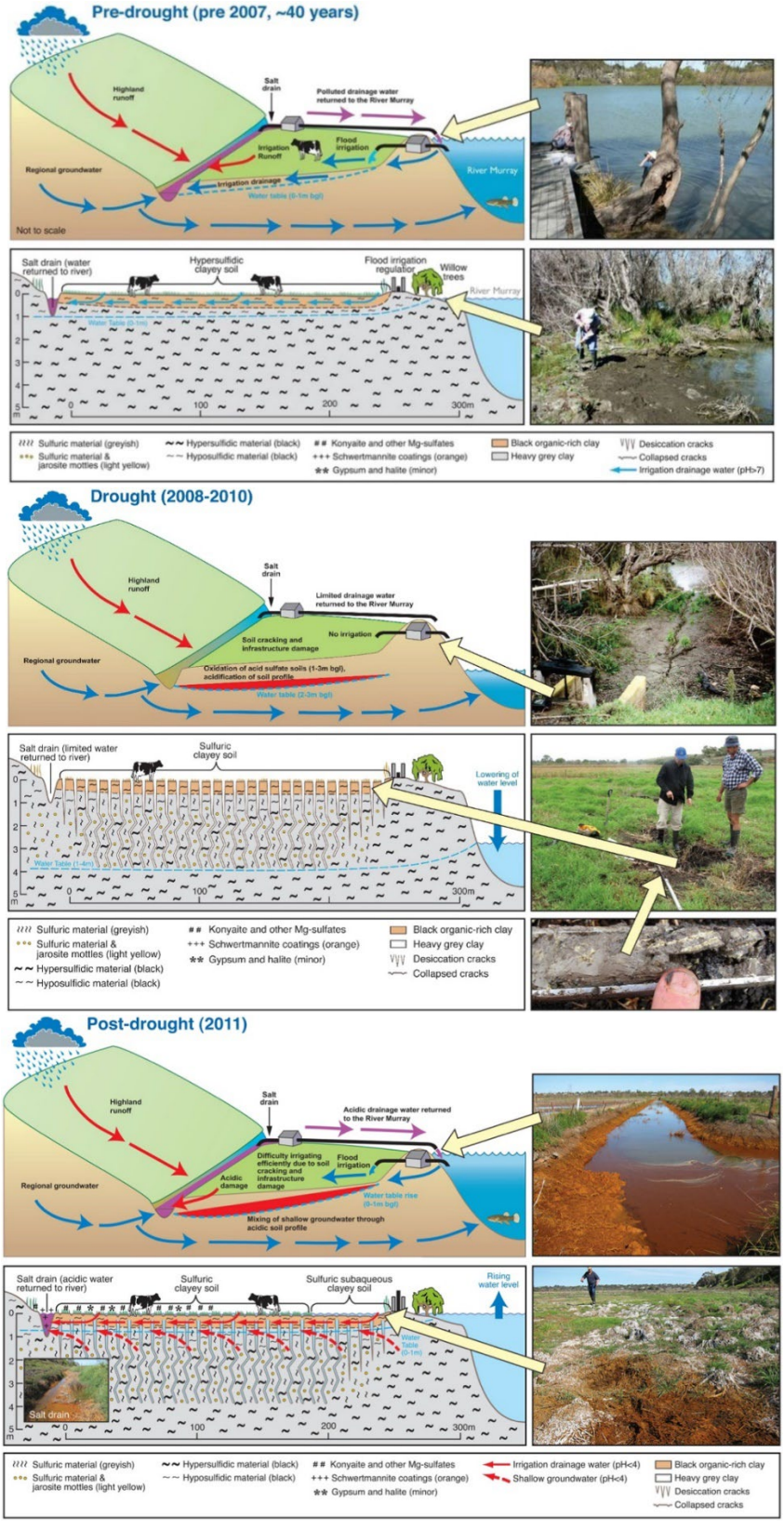

Figure 31: Explanatory soil-regolith hydro-toposequence model during pre-drought, drought and irrigation during 2011 (modified from Fitzpatrick et al., 2017a)

Suspended iron-rich precipitates in irrigation retention / reuse / evaporation pond and drains

This section summarises investigations by Fitzpatrick et al., (2017b) on the occurrences, mineralogical assemblages and environmental relevance of iron-rich precipitates derived from acidic (pH <4) waters containing dominantly schwertmannite from a diverse range of six physical settings across the Lower Murray Reclaimed Irrigation Area (LMRIA) in Australia, comprising:

(1) suspended flocculated precipitates in ponded drain water,

(2) moist coatings or pastes in drying ponds and drains,

(3) hard cemented crusts and aggregates amongst Phragmites roots and stems,

(4) dry coatings on concrete and wooden structures,

(5) dry coatings on surface soils and vegetation and

(6) suspended flocculated precipitates in the mixing zone of drain discharge into the River Murray.

Schwertmannite formed in these acid drain environments following exposure and oxidation of deep (~0.5 ->3.5m) clayey hypersulfidic material (pH >4) that dried, cracked and acidified to form deep sulfuric materials (pH<4) due to river and groundwater levels falling by nearly 2 m during the latter part of the Millennium Drought (2007 to 2010). Reflooding events occurred between 2011 and 2015. All samples displayed X-ray diffraction (XRD) patterns typical for schwertmannite and summarised in Table 9. In some samples, additional weak reflections from small amounts of jarosite, natrojarosite, gypsum, hexahydrite, konyaite and halite indicated deposition under variable pH conditions and sulfate concentrations due to different flow or evaporation stages. SEM images indicated that morphological and compositional features of schwertmannite were dominated by: (1) framboid-like spheroidal clusters with Fe/S ratio > 5 that were preserved after crystallization and likely formed by dissolution of pyrite and microbial oxidation of Fe2+ by acidophilic bacteria and (2) fibrous spheres (0.3-3 µm) with filamentous morphology and a high degree of porosity (for details see Fitzpatrick et al., (2017b)

Table 9: Mineralogical composition of the iron-rich precipitates listed in Figure 32

Ds	Qz	Kyt	Ht	Gyp	Schw	Mi	Kn	Jar	Gth
DSb02D	T		T	M	D		T		T
DSb02E	M		M	M	D	T	T	M	

Qz = quartz, Kyt = konyaite, Ht = halite; Gyp = gypsum; Schw = schwertmannite; Mi = mica; Kn = kaolin; Jar = jarosite; Gth = goethite
Where: D = Dominant (>60%), SD = Sub-dominant (20-60%), M = Minor (5-20%), T = Trace (<5%).

Speciation calculations (PHREEQC) using the dissolved metal and major ion concentrations in drain waters supported the XRD results as the saturation index (SI) exceeded zero for schwertmannite in many drains as shown in Table 10. There was also spatial variability in pH, salinity, dissolved oxygen, and concentrations of Cl, Ca, Mg, Na, K and Fe in drain waters as shown in Table 10.

Figure 32: Photograph of suspended strong brown coloured iron-rich precipitates in the Jervois site irrigation retention / reuse / evaporation pond on 2nd September 2011 (from(Fitzpatrick et al., 2017b). The following 2 sample numbers were taken from: DSb02-D: Edge of retention / evaporation pond: Soft iron precipitate: 1mm to 50mm thick (7.5 Y 5/6 Strong Brown) overlying black MBO (10 to 15cm) & grey clay (pH 3.67); DSb02-E: Middle of retention pond: Soft iron gel/ precipitate (10 YR 5/6 Yellowish Brown): saturated 20mm thick (pH 2.81)

Figure 33: Drain discharges from the LMRIA into the River Murray (from Fitzpatrick et al. 2017b).

The precipitates also contained high concentrations of metals (Al> Cu> As> Zn> Pb> Co) and nutrients (e.g. P) due to co-precipitation/scavenging of these elements during the formation of schwertmannite (Table 11, Table 10). There was also spatial variability in concentrations of metal(loids) in precipitates between drains (Table 11, Table 10).

Table 10: Measured drain water pH, salinity, dissolved oxygen (D.O.) major ions (SO4, Cl, Ca, Mg, Na, K), dissolved (<0.45 µm filtered) Fe and Schwertmannite saturation indices (SI) calculated in PHREEQC.

Site Name	pH	Salinity	D.O.	Temp	SO_4	Cl	Ca	Mg	Na	K	Fe	SI
		g/L	*mg/L*	*◦C*	*mg/L*	*mg/L*	*mg/L*	*mg/L*	*mg/L*	*mg/L*	*mg/L*	**Schwertmannite**
BURDETT	4.2	8.2	5.1	16.3	3980	2990	559	541	1720	24	231	22.04
JERVOIS	3.83	5	3.2	14.4	2500	1210	300	314	833	24	66	16.04
LONG FLAT	4.22	7.2	1.3	15.1	2670	1780	390	402	1260	60	39	18.77
POMPOOTA	4.12	9.5	2	12.9	3940	3590	564	592	2020	83	77.6	19.49
TOORA	**3.67**	**17.3**	**3.5**	**14.6**	**4080**	**7300**	**664**	**884**	**3610**	**91**	**106**	**13.85**

Table 11: Summary of highest concentrations of metals and metalloids for each site, listed in sequential order from upstream (Pompoota) to downstream (Jervois)

Site	Al	Cu	As	Zn	Pb	P	Ni	Cr	Co	B	Mn	Na
DS	**mg/kg**											
05: Pompoota	12,900	348	[1]167	41.5	[1]58.5	991	31.2	<10	23.6	31	228	38,000
03: Toora	35,900	29.6	88.4	164	20.5	3360	131	20.1	70.0	56.0	165	6,120
04: Burdett	81,900	89.1	97.2	39.6	10.9	5,890	27.6	26	19.7	<20	[1]271	31,800
01: Long Flat	2,530	15.1	[1]116	<10	<10	2,020	<10	17.2	<10	<20	20.0	1,180
02: Jervois	**14,700**	**<10**	**12.9**	**30.3**	**<10**	**824**	**11.5**	**17.4**	**<10**	**<20**	**128**	**[1]35,500**

[1]Consistently highest value for all samples taken at this site

A conceptual model was constructed (Figure 34), which explains and summarizes the morphological properties, mineralogy, geochemistry and environmental processes influencing the formation and relative stabilities of schwertmannite-rich precipitates from six diverse physical settings.

The environmental relevance, which has significant implications for rehabilitation options is shown in three perspectives:

1. the conditions for schwertmannite formation have persisted in irrigation drains for over 7 years
2. the ability for schwertmannite-rich precipitates to reveal acid sulfate conditions and therefore act as a mineralogical indicator in irrigation systems and
3. the pollution potential of metals and metalloids scavenged by schwertmannite-rich precipitates

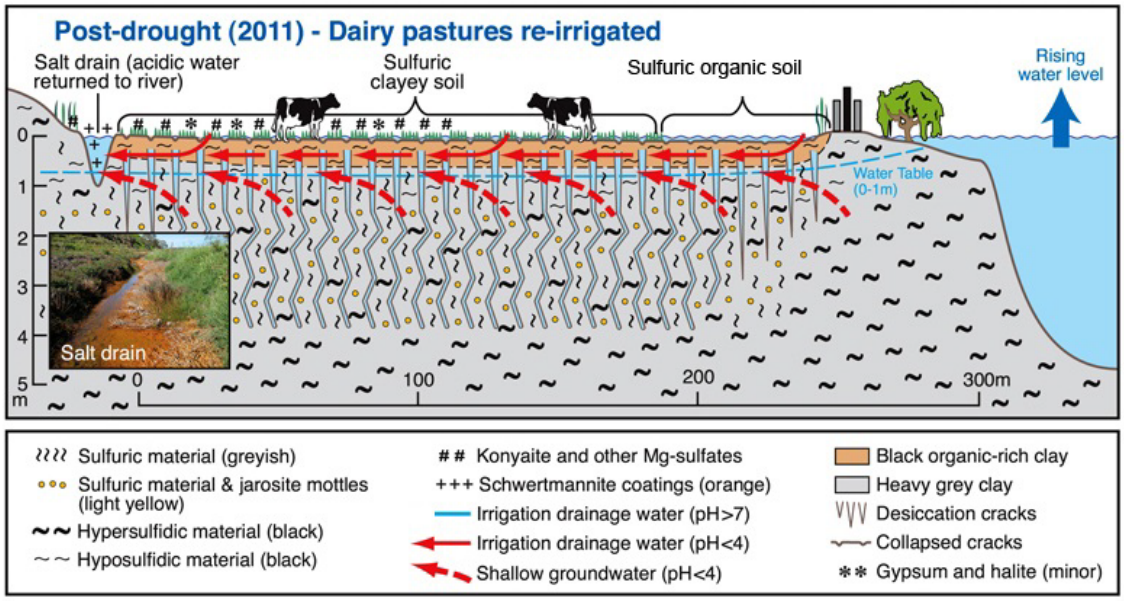

Figure 34: Explanatory soil-regolith hydro-toposequence model showing the spatial and down profile heterogeneity with inset colour photograph of a salt drain during post-drought reflooding and irrigation during 2011, illustrating: (1) distribution of sulfuric, hyposulfidic and hyposulfidic materials, (2) water flows (i.e. surface water levels, groundwater table levels and river flow) and (3) the strong brown iron-rich precipitate (comprising schwertmannite) and white salt efflorescences (from Fitzpatrick et al., 2017b).

REFERENCES

Baker A.K.M, Fitzpatrick, R.W., Shand P., Simpson S.L. et al. (2010) Temporal variations in representative acid sulfate soil environments around Lakes Alexandrina and Albert, South Australia. Client Report R-352-8-2. Available at www.clw.csiro.au/publications/science/2010/SAF-Lakes-Alexandrina-Albert-sulfate-soils-temporal.pdf.

Baker, A.K.M., Fitzpatrick, R.W., Simpson S.L. & Merry R.H. (2011) Temporal variations in re-flooded acid sulfate soil environments around Lakes Alexandrina and Albert South Australia. CSIRO Land and Water Science Report, 04/11. Available at www.clw.csiro.au/publications/science/2011/sr04-11.pdf. [Accessed 30 August 2018]

Baker, A.K.M., Shand, P. & Fitzpatrick, R.W. (2013) 'Recovery of re-flooded acid sulfate soil environments around Lakes Alexandrina and Albert, South Australia' (CSIRO: Water for a Healthy Country National Research Flagship, Canberra). https://data.environment.sa.gov.au/Content/Publications/CLLMM_15_Recovery%20of%20RE-Flooded%20Acid%20Sulfate%20Soil%20Environments_March%202013.pdf

CSIRO (2011) The Millennium Drought and 2010/11 floods. South-eastern Australian Climate Initiative Factsheet (CSIRO, Canberra.)

Dear, S.E., Moore, N.G., Dobos, S.K., Watling, K.M. et al. (2002) 'Queensland acid sulfate soil technical manual: Soil management guidelines (version 3.8)' Available at http://www.envirodevelopment.com.au/_dbase_upl/soil_mgmt_guidelines_v3_8.pdf

de Mooy, C.J. (1959) Soils and land use around Lakes Alexandrina and Albert, South Australia. CSIRO Soils and Land Use Series No. 29. (CSIRO Division of Soils, Melbourne).

DENR (2010) Acid Sulfate Soils research program summary report. Report by the Lower Lakes Acid Sulfate Soils Research Committee to SA Dept Environment and Natural Resources, Adelaide. Available at www.environment.sa.gov.au/Conservation/Rivers_Wetlands/Coorong_Lower_Lakes_Murray_Mouth/The_environment/Acid_sulfate_soils/Acid_Sulfate_Soils_Research_Program_reports. [Accessed 30 August 2018].

DWLBC (2007) ‘Regional land resource information for southern South Australia’ DVD (Soil and Land Program, Department of Water, Land and Biodiversity Conservation, Adelaide).

Drexel, J. F., and Preiss, W. V. (1995). The Geology of South Australia, The Phanerozoic (Vol. 2). Geological Survey of South Australia, Bulletin 54. Department of Primary Industries and Resources SA.

DWLBC. (2007). Regional land resource information for southern South Australia’ DVD. Soil and Land Program, Department of Water, Land and Biodiversity Conservation.

Fitzpatrick, R.W. (2013b) Demands on soil classification and soil survey strategies: Special-purpose soil classification systems for local practical use. In ‘Developments in Soil Classification, Land Use Planning and Policy Implications: Innovative Thinking of Soil Inventory for Land Use Planning and Management of Land Resources’ (Eds S.A. Shahid, F.K. Taha & M.A. Abdelfattah) pp. 51–83 (Springer Science+Business Media, Dordrecht, Netherlands).

Fitzpatrick, R.W, Baker, A.K.M, Shand, P., Merry, R.H. et al. (2012) A modern soil-landscape characterization approach to reconstructing and predicting pedogenic pathways of nland Acid Sulfate Soils. In ‘Geological Survey of Finland, Guide 56’ (Eds P. Osterholm, M. Yli-Halla & P. Eden). pp. 47–50 (Proceedings of 7th International Acid Sulfate Soil Conference, 26–30 August 2012, Vaasa, Finland).

Fitzpatrick, R.W., Grealish, G., Chappell, A., Marvanek, S. et al. (2010a) Spatial variability of subaqueous and terrestrial acid sulfate soils and their properties, for the Lower Lakes, South Australia. CSIRO Sustainable Agriculture National Research Flagship Client Report R-689-1-15’ (CSIRO, Sputh Australia).

Fitzpatrick, R.W., Grealish, G.H., Shand, P. & Creeper, N.L. (2011a) Monitoring and assessment of reflooded acid sulfate soil materials in Currency Creek and Finniss River Region, South Australia. Client Report R-325-8-6 to SA. Department of Environment and Natural Resources (DENR) (CSIRO: Sustainable Agriculture Research Flagship, Adelaide).

Fitzpatrick, R.W., Grealish, G., Shand, P., Simpson, S.L. et al. (2009a) Acid sulfate soil assessment in Finniss River, Currency Creek, Black Swamp and Goolwa Channel, South Australia. CSIRO Land and Water Science Report 26/09 (CSIRO, Adelaide).

Fitzpatrick, R.W., Marvanek, S., Powell, B. & Grealish, G. (2010b) Atlas of Australian Acid Sulfate Soils: Recent developments and future priorities. In ‘Proceedings of the 19th World Congress of Soil Science; Soil Solutions for a Changing World’ (Eds R.J. Gilkes & N. Prakongkep) pp. 24–27 (Brisbane, Australia).

Fitzpatrick, R.W., Marvanek, S., Shand, P., Merry, R.H. et al. (2008a) Acid sulfate soil maps of the River Murray below Blanchetown (Lock 1) and Lakes Alexandrina and Albert when water levels were at pre-drought and current drought conditions. CSIRO Land and Water Science Report 12/08 (CSIRO, Adelaide).

Fitzpatrick, R., Powell, B. & Marvanek, S. (2011b) ‘Atlas of Australian Acid Sulphate Soils. V2. Data Collection’ (CSIRO, Adelaide).

Fitzpatrick, R.W. & Shand, P. (2008) Inland acid sulfate soils: Overview and conceptual models. In ‘Inland Acid Sulfate Soil Systems Across Australia’ (Eds R.W. Fitzpatrick & P. Shand) CRC LEME Open File Report No. 249 (Thematic Volume) pp. 6–73 (CRC LEME, Perth).

Fitzpatrick, R.W., Shand, P., Grealish, G., Thomas M. et al. (2010c) Acid sulfate soil investigations of vertical and lateral changes with time in five managed wetlands between Lock 1 and Wellington. CSIRO Land and Water Science Report, 03/10 (CSIRO, Adelaide).

Fitzpatrick, R.W., Shand, P. & Hicks, W. (2011d) Technical guidelines for assessment and management of inland freshwater areas impacted by acid sulfate soils. CSIRO Land and Water Science Report, 05/11.

Fitzpatrick, R.W., Shand, P., Marvanek, S., Merry, R.H. et al. (2008b) Acid sulfate soils in subaqueous, waterlogged and drained soil environments in Lake Albert, Lake Alexandrina and River Murray below Blanchetown (Lock 1): Properties, distribution, genesis, risks and management. Report to Department of Environment and Heritage, Adelaide. CSIRO Land and Water Science Report 46/08 (CSIRO, Adelaide). Available at www.clw.csiro.au/publications/science/2008/sr46-08.pdf. [Accessed 30 August 2018].

Fitzpatrick, R.W., Shand, P. & Merry, R.H. (2009b) Acid sulfate soils. In ‘Natural History of the Riverland and Murraylands’ (Ed. J.T. Jennings) pp. 65–111 (Royal Society of South Australia Inc., Adelaide).

Fitzpatrick, R.W., Shand, P., Merry, R.H., Thomas, B. et al. (2008c) Acid sulfate soils in the Coorong, Lake Alexandrina and Lake Albert: Properties, distribution, genesis, risks and management of subaqueous, waterlogged and drained soil environments. Land and Water Science Report 52/08 to Department of

Water, Environment, Heritage and Arts (CSIRO, Adelaide). Available at www.clw.csiro.au/publications/science/2008/sr52-08.pdf. [Accessed 30 August 2018].

Fitzpatrick, R.W., Shand, P. and Mosley, L. M. (2018). Soils in the Coorong, Lower Lakes and Murray Mouth Region. In: Natural History of the Coorong, Lower Lakes and Murray Mouth Region. (Eds. Luke Mosely, Qifeng Ye, Scoresby Shepherd, Steve Hemming and Rob Fitzpatrick). Chapter 2.9 pp. 227-251. Royal Society of South Australia (Inc.) Adelaide, South Australia. DOI: https://doi.org/10.20851/natural-history-cllmm-2.9

Fitzpatrick, R.W., Shand, P. & Thomas, B.P. (2011c) Risk assessment of acid sulfate soil materials in Ramsar wetlands of the Murray Darling Basin: Coorong. CSIRO Land and Water Science Report 51/09 (CSIRO, Adelaide).

Fitzpatrick, R.W., Shand, P., Thomas, M., Merry, R.H. et al. (2008d) Acid sulfate soils in subaqueous, waterlogged and drained soil environments of nine wetlands below Blanchetown (Lock 1), South Australia: Properties, genesis, risks and management. CSIRO Land and Water Science Report 42/08 to SA Murray-Darling Basin Natural Resources Management Board (CSIRO, Adelaide). Available at www.clw.csiro.au/publications/science/2008/sr42-08.pdf. [Accessed 30 August 2018].

Grealish, G., Chappell, A., Marvanek, S. & Shand, P. (2010a) Spatial variability of subaqueous and terrestrial acid sulfate soils and their properties, for the Lower Lakes, South Australia. Report to SA Department of Environment and Natural Resources, Adelaide (DENR). Client Report R-689-1-15 (CSIRO Sustainable Agriculture National Research Flagship, Adelaide).

Hall, J., Maschmedt, D., & Billing, B. (2009). *The Soils of Southern Australia* (Vol. 1). Geological Survery of South Australia, Bulletin 56. Department of Water, Land and Biodviersity Conservation.

Hipsey, M. R., Salmon, S. U., & Mosley, L. M. (2014). A three-dimensional hydro-geochemical model to assess lake acidification risk | Environmental Modelling & Software. *Environmental Modelling and Software*, *61*(C), 433–457. https://doi.org/10.1016/j.envsoft.2014.02.007

Hipsey, M. R., Salmon, S. U., Mosley, L. M., Barnett, L., & Frizenschaf, J. (2011). Development of a 3-D hydro-geochemical model to assess water quality and acidification risk in the Murray Lower Lakes, South Australia. *MODSIM2011, 19th International Congress on Modelling and Simulation.* 19th International Congress on Modelling and Simulation. https://doi.org/10.36334/modsim.2011.I7.hipsey2

Hicks, W.S., Creeper, N., Hutson, J., Fitzpatrick, R.W. et al. (2009) The potential for contaminant mobilisation following acid sulfate soil rewetting: Field experiment. Report to SA Department of Environment and Natural Resources, Adelaide (CSIRO Land and Water, Adelaide).

Isbell, R.F. & National Committee on Soils and Terrain (2016) 'The Australian Soil Classification' 2nd Ed (CSIRO Publishing, Melbourne, Australia).

IUSS Working Group WRB. (2014). *World reference base for soil resources 2014: International soil classification system for naming soils and creating legends for soil maps*. FAO.

Johnson DL, Watson-Stegner D (1987) Evolution model of pedogenesis. Soil Science 143, 349-366.

Kölbl, A., Marschner, P., Fitzpatrick, R., Mosley, L. et al. (2017) Linking organic matter composition in acid sulfate soils to pH recovery after re-submerging. Geoderma 308, 350–362. https://doi.org/10.1016/j.geoderma.2017.07.031.

Kölbl, A., Marschner P., Mosley, L., Fitzpatrick, R. et al. (2018) Alteration of organic matter during remediation of acid sulfate soils. Geoderma 332, 121–134. https://doi.org/10.1016/j.geoderma.2018.06.024.

Maschmedt, D. (2009) Soils. In 'Natural History of the Riverland and Murraylands' (Ed J.T Jennings). pp. 36-50. (Royal Society of South Australia Inc., Adelaide).

Mosley, L. M., Fitzpatrick, R., & Groenenberg, B.-J. (2012). *Lower Murray Reclaimed Irrigation Area (LMRIA) Acidification Project: A biogeochemical model for assessing and managing acid sulfate soils in the Lower Murray region of South Australia*. South Australia Environment Protection Authority.

Mosley, L. M., Fitzpatrick, R. W., Palmer, D., Leyden, E., & Shand, P. (2014a). Changes in acidity and metal geochemistry in soils, groundwater, drain and river water in the Lower Murray River after a severe drought. *Sci Total Environ*, *485–486*, 281–291. https://doi.org/10.1016/j.scitotenv.2014.03.063

Mosley, L.M., Shand, P., Self, P. & Fitzpatrick, R. (2014b) The geochemistry during management of lake acidification caused by the rewetting of sulfuric (pH<4) acid sulfate soils. Applied Geochemistry 41, 49–56. https://doi.org/10.1016/j.apgeochem.2013.11.010.

Mosley, L.M., Zammit, B., Jolley, A. & Barnett, L. (2014c) Acidification of lake water due to drought. Journal of Hydrology 511, 484–493. https://doi.org/10.1016/j.jhydrol.2014.02.001.

Mosley, L.M., Zammit, B., Jolley, A., Barnett, L. et al. (2014d) Monitoring and assessment of surface water acidification following rewetting of oxidised acid sulfate soils. Environmental Monitoring and Assessment 186, 1–18. https://doi.org/10.1007/s10661-013-3350-9.

Mosley, L.M., Zammit, B., Leyden, E., Heneker, T.M. et al. (2012) The impact of extreme low flows on the water quality of the Lower Murray River and Lakes (South Australia). Water Resources Management 26, 3923–3946. https://doi.org/10.1007/s11269-012-0113-2.

Muhs DR (1984) Intrinsic thresholds in soil systems. Physical Geography 5, 99-110.

Natural Resources SA Murray-Darling Basin (2009) Goolwa Channel Flow Regulators. See: https://www.naturalresources.sa.gov.au/samurraydarlingbasin/projects/all-projects-map/goolwa-channel-flow-regulators.

Ngarrindjeri Nation (2007) Ngarrindjeri Nation Sea Country plan: Caring for Ngarrindjeri Sea Country and culture (Ngarrindjeri Tendi, Ngarrindjeri Heritage Committee and Ngarrindjeri Native Title Management Committee, Ngarrindjeri Land and Progress Association, Meningie).

Palmer, D., Mitchell, R., Powell, C., Spencer, J. et al. (2011) Air quality in the Lower Lakes during a hydrological drought (Environment Protection Authority, South Australia). Available at www.epa.sa.gov.au/xstd_files/Water/Report/lower_lakes.pdf. [Accessed 30 August 2018].

Shand, P., Self, P.G., Baker, A.K.M. & Grocke, S. (2017) Legacy of limestone dosing in Boggy Lake. CSIRO Report.

Simpson, S.L., Fitzpatrick, R.W., Shand, P., Angel, B.M. et al. (2010a) Climate-driven mobilisation of acid and metals from acid sulfate soils. Marine Freshwater Research 61, 129–138. https://doi.org/10.1071/MF09066.

Simpson, S., Jung, R., Jarolimek, C. & Hamilton, I. (2010b) The potential for contaminant mobilisation following acid sulfate soil rewetting: lab experiment. Report 40/09 (CSIRO Land and Water Science, Adelaide).

Sturt, C. (1833). Two Expeditions into the interior of southern Australia during the years 1828, 1829, 1830, 1831 with observations on the soil, climate, and general resources. Volume II, Smith, Elder & Co., London, 271pp.

Taylor, J.K. & Poole, H.G. (1931) Report on the soils of the bed of Lake Albert, South Australia. Journal for the Council for Scientific and Industrial Research 4, 83–95.

Thomas, M. & Fitzpatrick, R.W. (2011) Community monitoring of acid sulfate soils in the Lower Lakes, South Australia: Four surveys between August 2009 and June 2010. Client Report R-325-8-4 (CSIRO Sustainable Agriculture National Research Flagship, Adelaide).

Thomas, M., Richardson, C., Durbridge, R., Fitzpatrick, R. et al. (2016) Mobilising citizen scientists to monitor rapidly changing acid sulfate soils. Transactions of the Royal Society of South Australia 140(2), 186–202. https://doi.org/10.1080/03721426.2016.1203141.

MID CONFERENCE FIELD TRIP

GARDEN ISLAND, GILLMAN AND ST KILDA

WEDNESDAY 29TH MARCH 2023

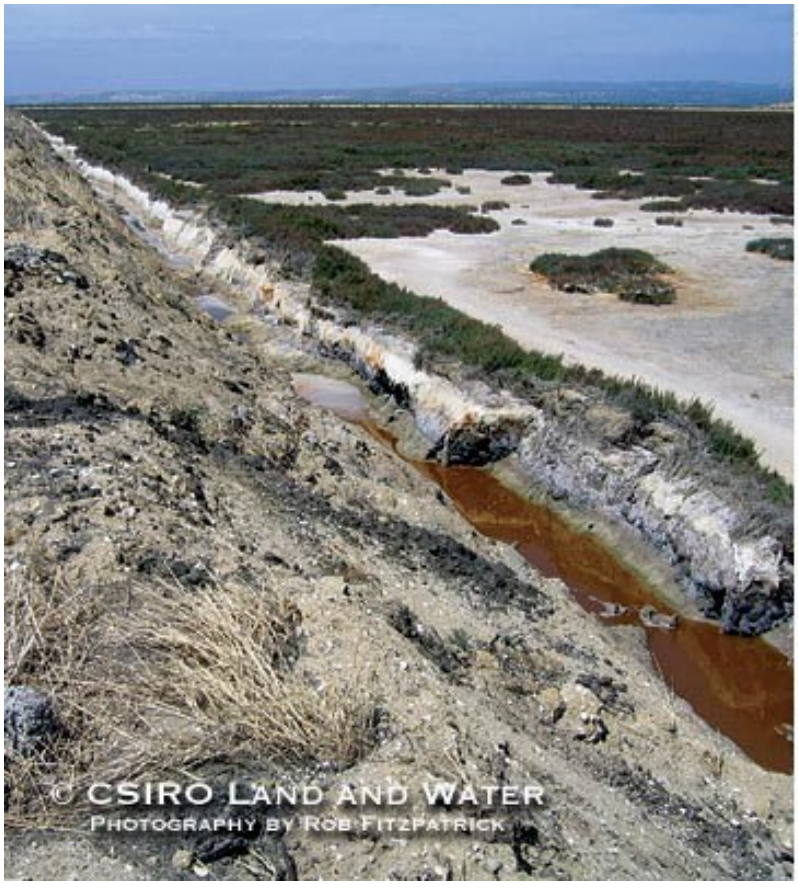

FIELD TRIP ITINERARY

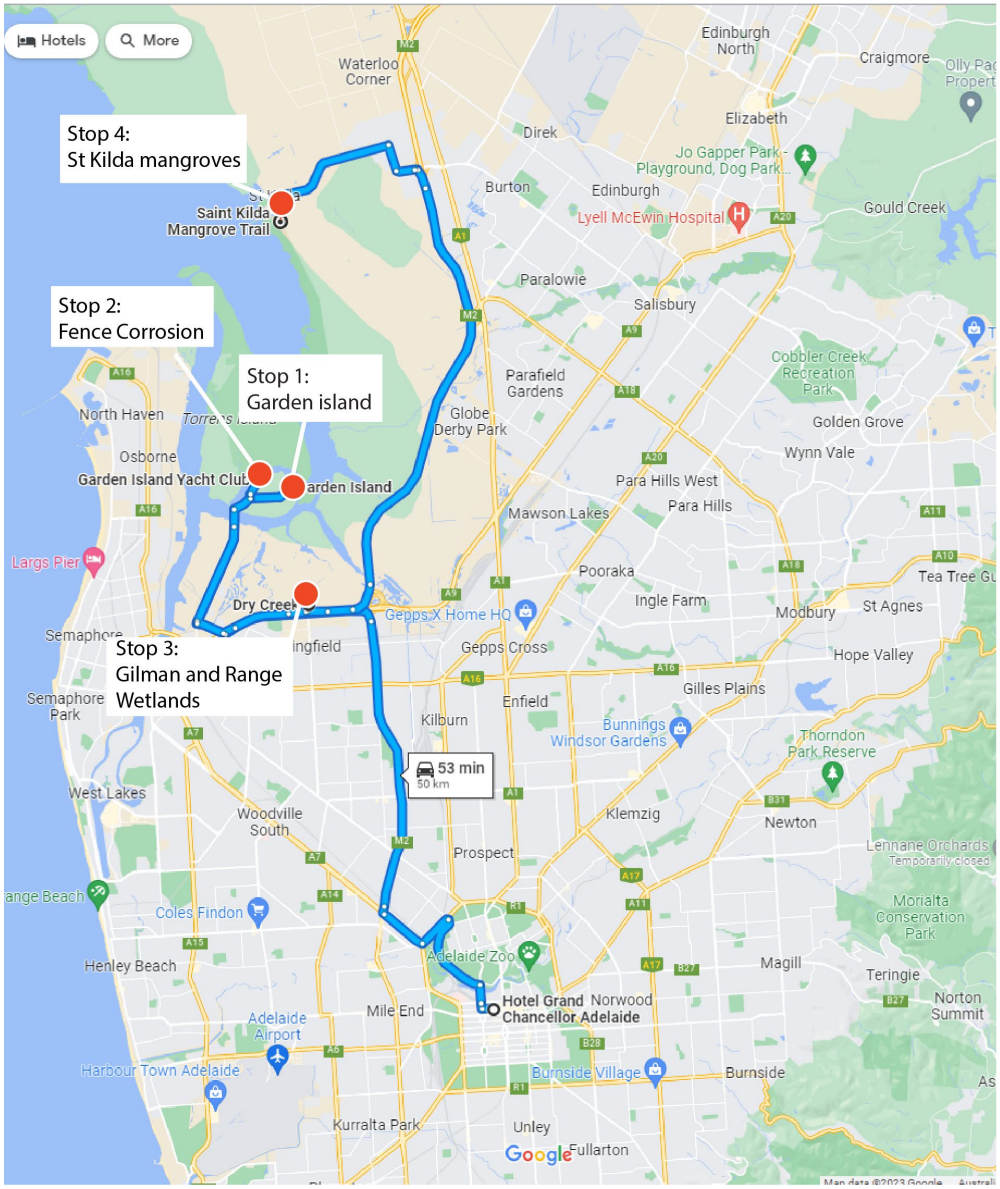

Location	Time
Meet in lobby	8:45 am
Leave Hotel Grand Chancellor	9:00 am
Arrive Stop 1: Garden Island Car park	9:30 am
Morning tea	10:00 am
Leave Stop 1	10:30 am
Arrive Stop 2: Anthropogenic sulfuric soils fence corrosion	10:35 am
Leave Stop 2	10:50 am
Arrive Stop 3: Gillman and Range Wetlands	11:00 am
Leave Stop 3	1:15 pm
Arrive Stop 4: St Kilda	1:30 pm
Lunch and presentations	1:40 pm
Explore St Kilda Mangrove Trail	2:30 pm
Leave St Kilda Mangroves	4:00 pm
Arrive at Hotel Grand Chancellor	4:30 pm

Figure 35: Google Earth Map of Field Trip sites

Follow QR Code to view aerial tour of sites on this field trip

Summary

In nature, some things are best left alone, buried well beneath the surface! But housing, marina and infrastructure developments frequently disturb coastal soil-landscape environments comprising acid sulfate soils and sediments – sometimes with disastrous consequences.

This section summarises the soil-landscapes in Barker Inlet associated with formation of pyrite and sulfuric acid in Acid Sulfate Soils (ASS). Four case study areas in Barker Inlet have been selected to illustrate the diverse properties and impacts of coastal acid sulfate soils. A wide range of ASS types containing sulfidic materials (pH > 4 with pyrites), sulfuric materials (pH < 4 with oxyhydroxysulfates of Fe and Al) and monosulfidic black ooze (pH > 4 with monosulfides) are currently developing in different physical settings, which occur mostly because of changing hydrological and biogeochemical conditions in Barker Inlet. The key physical setting are:

- Quaternary coastal marine facies and mangrove transgression since 1935
- Current tidal inundation with occurrence of mangroves and samphire marsh
- Loss of tidal inundation with mangrove deaths caused by construction of levee banks between 1890s and 1950s'

Colour photographs of key soil features, mechanistic cross-section diagrams and maps are presented to illustrate the major geomorphic stages in acid sulfate soil-landscape evolution. Also detailed here are the chemical and physical changes that occur when tidal influences are altered or excluded in these environments. Various sources of organic matter fractions (i.e. sapric and hemic materials), minerals (e.g. pyrite, jarosite/natrojarosite, sideronatrite, tamarugite and gypsum), and micro-scale weathering pathways and mechanisms occur under drained (e.g. tidal exclusion through levee bank construction) and undrained (e.g. ranging from natural tidal to intertidal, to supratidal zones) conditions.

Maps showing the distribution of the various types of Acid Sulfate Soils and their extent in hectares for Gulf St Vincent and Barker Inlet and "risk classes" are also provided.

The South Australian government has responded to the challenge of managing coastal Acid Sulfate Soils environments by introducing planning and development controls for coastal Acid Sulfate Soils through the Coast Protection Board (CPB).

The organisers of the field trip would like to acknowledge the traditional custodians of the land on which we stand, work, and travel. The traditional owners of the land we are visiting today is the of the Kaurna people. We pay our respects to their Elders past, present, and emerging, and recognize their continuing connection to the soil, land, water, and culture. We extend our respect to all Aboriginal and Torres Strait Islander people and their contributions to this country.

History and Geomorphic Setting

The recent geological evolution of Barker Inlet has largely been controlled by global sea level fluctuations (Edmonds, 1995). Two million years ago sea level was 45 m lower than at present and Gulf St Vincent was dry land. Alluvial fans formed as rivers and streams drained from the higher land inland, depositing sands, gravels and particularly the thick Hindmarsh Clay (Figure 36) that underlies Barker Inlet and Adelaide.

About 9000 years ago sea level rose. The Le Fevre peninsula was built between 6000 years ago and the present, by sand building up as a result of wave and wind action. The reworking of coastal sediments since sea level stabilisation about 7,500 BP resulted mostly in the northerly extension of sand ridges on Le Fevre Peninsula and the Port River outlet (Figure 36).

The establishment of extensive sea-grass meadows led to the rapid accumulation of marine and estuarine sediments resulting in coastal progradation throughout the late Holocene (Edmonds, 1995). Progradation led to the simultaneous back-barrier development of marshes and mangrove swamps parallel to the shoreline. The Barker Inlet embayment is now mostly in-filled except for the Port River estuary.

Seagrass banks developed in shallow water, but this gradually became enclosed and estuarine mangroves took over in the intertidal zones. Then the early settlers arrived, and the area became severely modified by human activities. The Gillman area has been progressively reclaimed from the intertidal and supratidal environments of Barker Inlet by construction of a series of bund walls that prevent tidal inundation for agriculture and industry (Figure 38 and Figure 39).

Subsidence rates of 1 mm per year have been documented in the Barker Inlet area (Belperio, 1993), and are attributed to movement along the Para Fault, ground water extraction and consolidation of inter-tidal soils after drying due to construction of levee banks. The presence of “sulfide-rich sediments” in the Gillman area was identified firstly by Harbison (1986), and observed in later investigations (Belperio, 1993; Belperio & Harbison, 1992; Belperio & Rice, 1989).

In 1991, CSIRO was contracted to conduct an urgent investigation of the Gillman area for the proposed construction of a multi-function-polis (MFP). The MFP was a concept for a high technology community comprising housing, education and leisure facilities, and high-tech industries to provide employment. Fitzpatrick (1991) alerted the promoters to the problem of acid sulfate soils, and for this and other reasons the project was eventually abandoned.

Prior to 1991, no specific soil investigations had been conducted to identify and characterise types of Acid Sulfuric Soils and their extent in the Barker Inlet area. However, based on several later investigations ((R. Fitzpatrick, 1993; R. Fitzpatrick & Self, 1997; R. W. Fitzpatrick, 1991; R. W. Fitzpatrick et al., 1992, 1996; Poch et al., 2009; Thomas, 2010; Thomas et al., 2004), the properties, formation and distribution of the following 6 major types of ASS materials that commonly occur as layers in soil profiles in the wide range of physiographical environments in Barker Inlet,:

- Contemporary tidal zones with hypersulfidic material (mangrove and samphire marshes).
- Disturbed tidal zones with sulfuric material (drained tidal, intertidal or supratidal mangrove or samphire marshes, particularly near Gillman).
- Disturbed tidal zones with hypersulfidic material (drained tidal, intertidal or supratidal mangrove or samphire marshes, particularly in disturbed salt evaporation ponds).
- Sandplains and dunes overlying relict buried layers of hypersulfidic material.

- Anthropogenic fill materials overlying buried hypersulfidic and sulfuric materials.
- Subaqueous soils below the low tidal mark with hypersulfidic and monosulfidic materials beneath shallow, stagnant water bodies (e.g. poorly flushed or blocked estuaries, rivers, river tributaries, salt evaporation seeps and seagrass mud flats associated with Barker Inlet Estuary and Port Adelaide River).

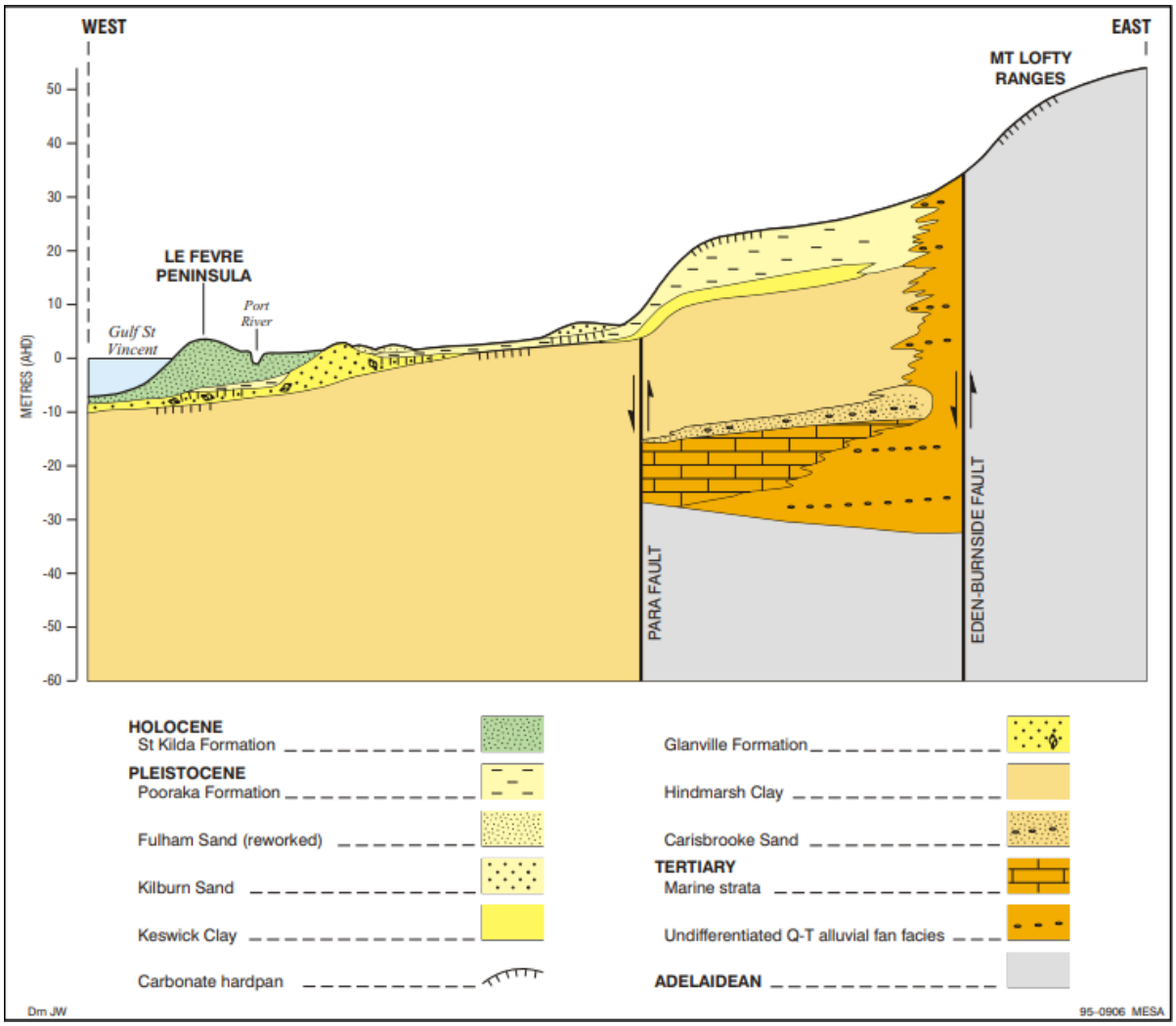

Figure 36: Schematic cross-section from Le Fevre Peninsula to the Mount Lofty Ranges, showing relationships between Quaternary coastal marine and continental facies of the St Vincent Basin. The St Kilda Formation (Holocene sands and clays) overlay the Glanville Formation (Pleistocene clays), and they together on-lap the thick alluvial Hindmarsh Clay Formation (after Belperio & Rice 1989; Belperio 1995; and Thomas 2010)

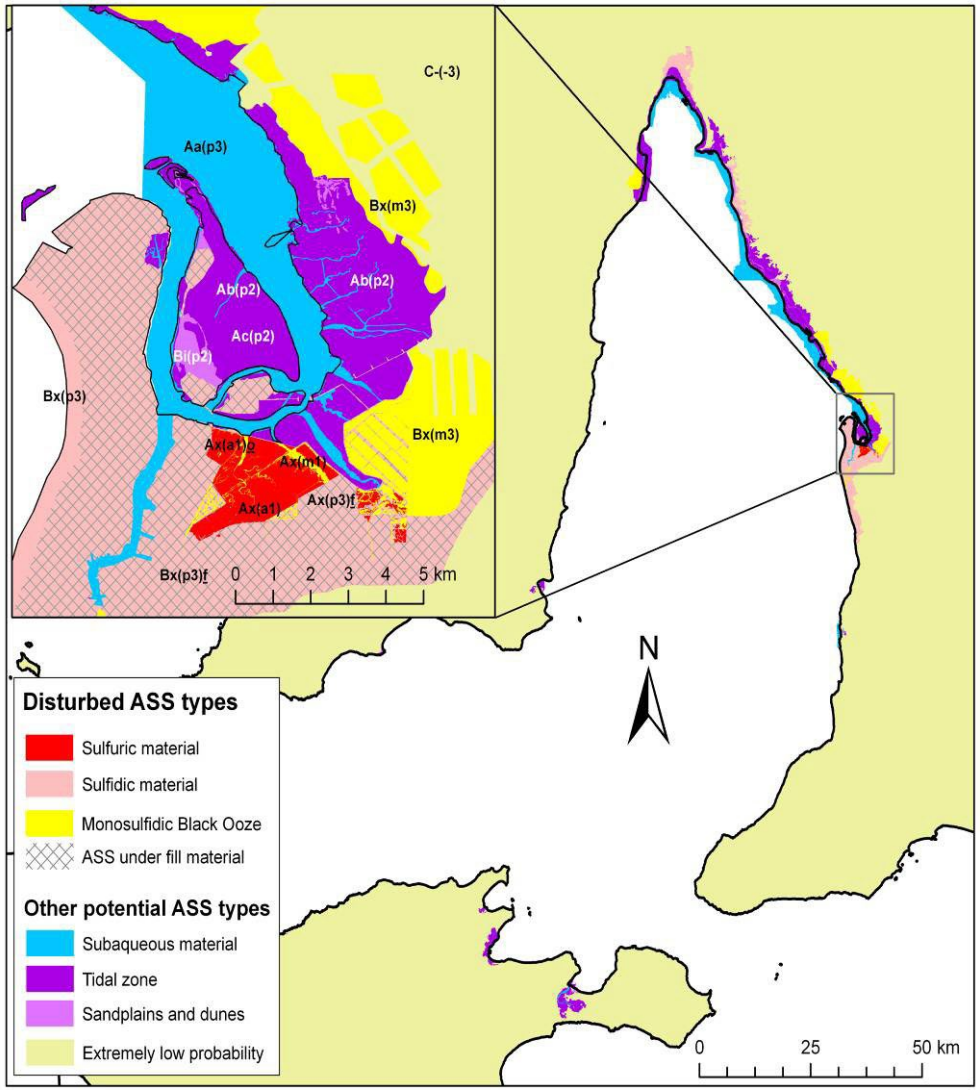

A - High probability of occurrence (> 70% of mapping unit)
B - Low probability of occurrence (< 70% of mapping unit)
C. Extreme low probability of occurrence (< 5% of mapping unit) with occurrences in small localised areas.

Codes:

x - Disturbed ASS materials such in former tidal zones inside bund wall areas (e.g. Gillman); former or contemporary salt evaporation ponds.
a - Subaqueous materials below low tide mark (Light blue colour)
b - Hypersulfidic material within upper 1 m in intertidal flats (e.g. mangroves) – Dark purple colour
c - Hypersulfidic material within upper 1 m in supratidal flats (e.g. samphire) – Dark purple colour
d - hypersulfidic material within upper 1 m in extratidal flats (salt marshes)
i - Sulfidic material below 1m from surface in sandplains and dunes 2- >10 m AHD (e.g. relict buried sulfidic material in Figure 7b). AHD = Australian Height Datum, which approximates mean sea level; (Light purple colour)

Subscripts to codes:

(a-) - Sulfuric material - (Red colour)
(m-) - Monosulfidic Black Ooze (MBO) material. (Yellow colour)
(p-) - Hypersulfidic material – (Dark and light purple and blue colours)
Confidence levels (Isbell 1996) Map polygon contains ASS, and: **(-1)** - All necessary analytical and morphological data are available
(-2) - Analytical data are incomplete but are sufficient to classify the soil with a reasonable degree of confidence.
(-3) - No necessary analytical; data are available but confidence is fair, based on a knowledge of similar soils in similar environments.

Descriptors:

o - Organic material (sapric and hemic material)
f - Fill material (dredge fill or housing) (Black cross hatching)
h –Hypersaline or gypseous horizons generally within 10 cm of surface. [1]Atlas of Australia Acid Sulfate Soils (Fitzpatrick *et al.* 2006)/ Australian Soil Resource Information System (ASRIS) site (www.asris.gov.au).

Figure 37: Map showing distribution of coastal ASS in Gulf St Vincent and Gillman-Barker Inlet (inset map). (From Fitzpatrick et al. 2008b,c)

Table 12: ASS types, map symbol[1], Australian Soil Classification[2], Soil Taxonomy[3], World Reference Base[3], Risk Class, Treatment category[4] & aerial extentulf St Vincent

ASS type	Map Code[1]	Australian Soil Classification[2]	Soil Taxonomy[3]	World Reference Base[3]	Risk Class	Treatment category[4]	Area (Ha)
Hypersulfidic material in contemporary tidal zones	Ab (p2)o	Sapric Histic-Hypersulfidic Intertidal Hydrosols	Sapric Sulfiwassists Fibric Sulfiwassists	Subaquatic/Tidalic, Histic Gleysols (Hypersulfidic, Arenic	High	H - XH	8 936
Sulfuric material in disturbed tidal zones	Ax (a1)o Ax (a1)h Ax (a1)	Sulfuric Sapric Organosol Sulfuric Hypersalic Hydrosols	Terric Sulfosaprists Terric Sulfohemists Hydraquentic Sulfaquepts, Salidic Sulfaquepts Sulfic Fluvaquents	Sapric or Hemic Histosols (Hyperthionic, Drainic) Subaquic or Salic Fluvisols (Hyperthionic, Drainic)	Very High	VH - XH	135 87 188
Hypersulfidic material in disturbed tidal zones	Bx (p3)	Hypersulfidic Hypersalic Rudosols	Haplic Sulfaquent	Haplic Gleysols (Protothionic, Arenic)	Moderate	M- H	5 273
Hypesulfidic material in disturbed tidal zones (mainly MBO)	Ax (m1) Ax (m3 Bx (m3))	Hypersulfidic Hypersalic Rudosols	Haplic Sulfaquent	Anthraquic Gleysols (Protothionic, Drainic)	Moderate	M- H	5 973
Hypersulfidic material in upper 1 m in supratidal flats often with samphires	Ac(p2)	Histic-Hypersulfidic Supratidal Hydrosols	Sapric Sulfiwassists Fibric Sulfiwassists	Subaquatic/Tidalic, Histic Gleysols (Hypersulfidic, Arenic)	High to moderate	M-H	4 244
Hypersulfidic material in upper 1 m in extratidal flats (saltbush)	Ad(p2)h	Histic-Hypersulfidic Extratidal Hydrosols	Terric Sulfisaprists Terric Sulfihemists	Histic Gleysols (Protothionic, Tidalic)	High to moderate	M-H	7 139
Hypersulfidic material in sandplains and dunes	Ai(p2)	Hypersulfidic Arenic Rudosols	Sulfic Fluvaquent Sulfaquent	Subaquic or Tidalic Fluvisols (Protothionic, Arenic)	Moderate to Low	L - M	2 751
Hypersulfidic material buried below fill materials	Ax (p3)f Bx (m3)f	Dregic or Urbic Hypersulfidic Anthroposols	Thapto-Histic Sulfaquents	Spolic or Urbic Technosols (Protothionic)	Moderate to Low	L - M	6 602
Sulfuric material buried below fill materials	Ax (a1)f -	Sulfuric Hypersalic Hydrosols	Hydraquentic Sulfaquepts	Spolic or Urbic Technosols (Orthothionic)	Very High	VH - XH	17
Subaqueous materials below the low tidal mark	Aa(p3)	Hypersulfidic [5]Subaqueous Hydrosols	Terric Sulfisaprists Terric Sulfihemists	Subaquatic, Histic Gleysol (Hypersulfidic, Arenic)	Moderate	M- H	15 964
TOTAL							57 222

[1]Map Codes from Figure 37: Atlas of Australian Acid Sulfate Soils (Fitzpatrick et al. 2006)/ Australian Soil Resource Information System (ASRIS) site (www.asris.gov.au)
[2]Australian Soil Classification (Isbell and The National Committee on Soil and Terrain 2021). [3]Soil Taxonomy (Soil Survey Staff 2022); [3]IUSS Working Group WRB (2014),
[4]Treatment category: L=Low level treatment; M = Medium level treatment, H = High level treatment, VH = Very high level treatment, XH = Extra High level treatment (from Dear et al. 2002); [5]Proposed new suborder

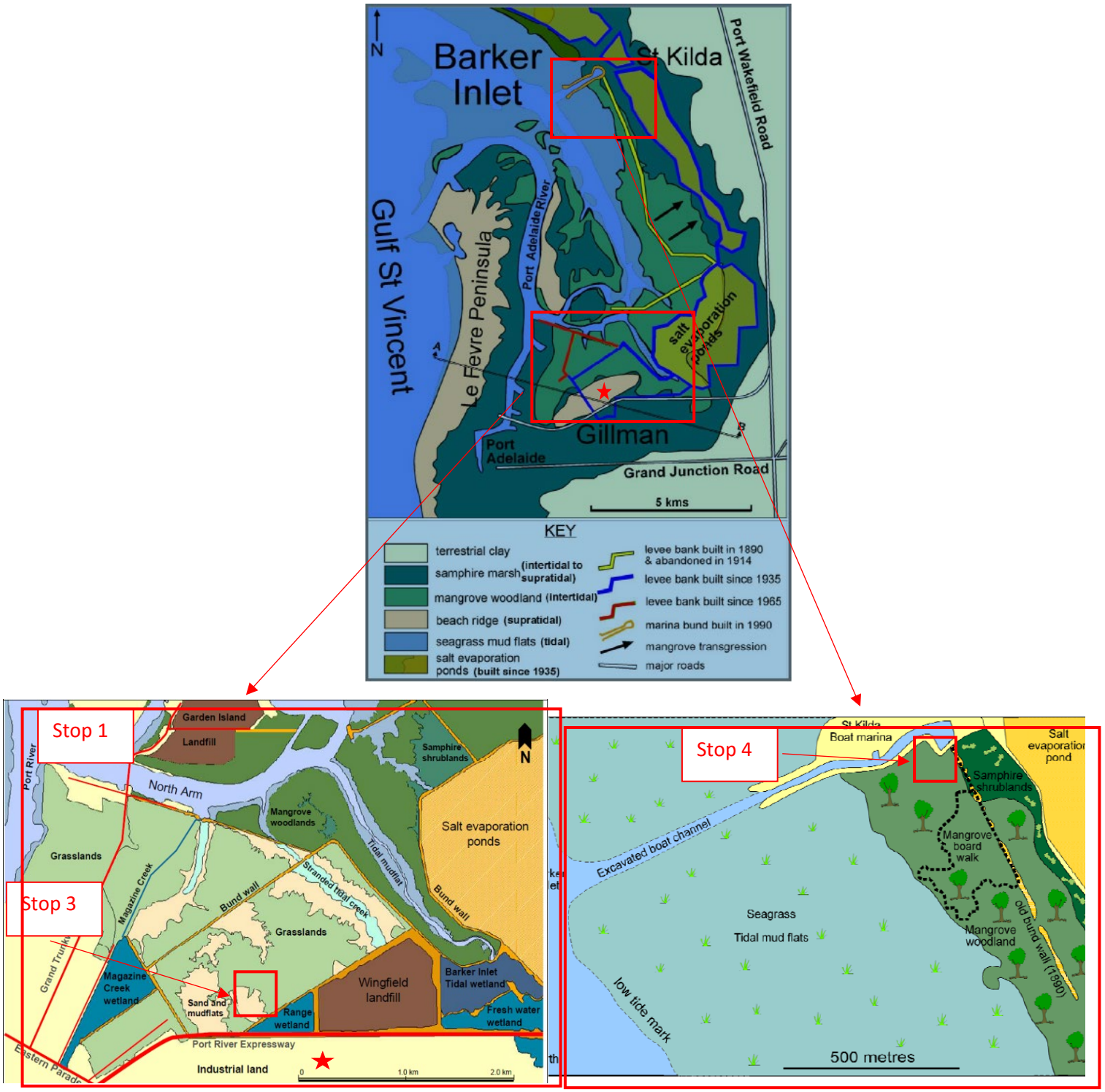

Figure 38 : Barker Inlet tidal estuary showing the major original vegetation types, physiographic settings. The Gillman site (Stop 3) is predominately vacant, consisting open grasslands, samphire shrublands and salt and sand flats. It is bordered by urban and industrial development to the south and abuts tidal mangrove woodland along North Arm. The Gillman area has been progressively reclaimed from the intertidal and supratidal environments of Barker Inlet since the 1930s by construction of a series of bund walls that prevent tidal inundation for agriculture and industry. The land at Gillman was soon abandoned due to severe acidification, salinity and stormwater ponding. The acid sulfate soil profile BG11 (red star) is located in this "reclaimed" area. (From Fitzpatrick et al. 2008b,c; Thomas 2010).

Figure 39: View of the landward (drained) side of the artificial bund wall at Gillman (left photo), which was constructed in the 1950s to prevent tidal inundation showing: dead mangrove tree stumps (background) and contaminated water in a stranded tidal creek with water containing orange iron oxyhydroxide surrounded by white salt deposits and dead mangrove. Photo on the right is the soil profile from close to the bund wall

Summary of Field Sites

Stop 1: Garden Island to view almost pristine tidal, intertidal or supratidal mangrove and samphire marshes and how they function. It provides good examples of occurrences of organic rich acid sulfate soils with high concentrations of pyrite.

Stop 2: Corrosion of zinc-aluminium and galvanised-steel fencing in Anthropogenic sulfuric soils: Visit an anthropogenic sulfuric silty soils present on Garden Island were extremely acidic (pH < 2) and highly saline (11 and 13 dS/m), and consequently were predicted to be very highly corrosive towards fencing. This is visible at stop 2.

Stop 3. Range Wetland area at Gillman (near Wingfield Dump) via a guided tour with on-site explanations and field demonstrations, provides excellent examples of:

- Drainage waters with extremely high concentrations of sulfuric acid and metals, especially Al, Mg
- Organic rich acid sulfate soils with bright yellow jarosite mottles, exposed in excavated drains: demonstrate sampling, chip-tray incubation
- Several rehabilitation experiments (Coast Protection Board, 2003). Dredge spoil overlying relict ASS materials
- Monosulfidic material in drains and wetlands

Stop 4: St Kilda Mangrove Trail at Fooks Terrace, St Kilda to view the critical role, which intertidal mangrove woodlands and samphire salt marsh play in maintaining marine environments. The Mangrove Boardwalk Trail comprises a 2km boardwalk that meanders through the mysterious mangrove forest and samphire areas of the Barker Inlet Aquatic Reserve, which provides excellent examples of:

- Occurrences of a wide range of organic rich acid sulfate soils with high concentrations of pyrite and shell fragments.
- The bund wall (levee banks) built in the 1890s from St Kilda to the south along the landward extent of mangrove woodlands (including occurrences of a Chenier ridge, seagrass and tidal mud flats and salt evaporation ponds).
- Tidal creeks filled with rotting organic matter (sapric material) formed from sea-grass and ulva causing extreme anoxic or reducing conditions.
- Hypersaline ponds adjacent the mangrove areas, which mined salt from 1950-2013, and are now in a holding pattern pending Government direction on future use.
- Examples of mangrove deaths due to hypersaline contamination events from the nearby salt evaporation ponds in 2020.

Stop 1 Garden Island Boat Ramp

View coastal acid sulfate soils with hypersulfidic material occur in modern tidal floodplains

Garden Island (and seawater areas of Stop 4) provides good examples of modern tidal floodplains with mangrove and samphire marsh environments comprising a range of organic rich acid sulfate soils with hypersulfidic, hyposulfidic and monosulfidic material.

Figure 40: Map of Garden Island (Stop 1 and 2)

Coastal acid sulfate soils with hypersulfidic material occur in modern tidal floodplains, which are <5 m above sea level where sulfate, iron and other salts are available from seawater and estuarine sediments. The examples of these coastal acid sulfate soils in somewhat 'natural' conditions are observed at Garden Island (Stop 1: see Figure 41). These can also be seen in the seawater areas at St Kilda (Stop 4).

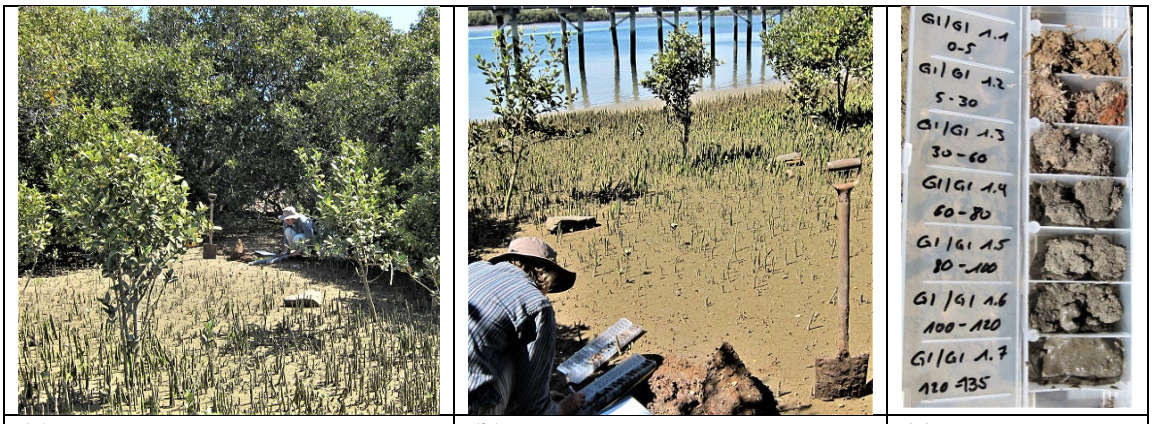

(a) (b) (c)

Figure 41: Photographs of the tidal mangrove swamp site on Garden Island (a) and samples collected from the soil profile (b) and 7 soil horizons and placed in plastic chip tray compartments 2.5 cm X 5 cm (c).

Table 13: pH incubation data and classification of acid sulfate soil material from the tidal mangrove swamp site on Garden Island

Depth (cm)	**[1]Material**	**pH_{H2O}** 1:1 soil:solution, oxic conditions **2015**			
		day 0	8 weeks	16 weeks	24 weeks
0-5	Hyposulfidic	7.5	7.04	7.15	7.20
5-30	Hyposulfidic	7.0	7.13	7.12	7.11
30-60	Hyposulfidic	6.9	6.81	6.82	6.82
60-80	**Hypersulfidic**	6.8	3.58	1.76	1.56
80-100	**Hypersulfidic**	6.8	3.64	1.87	1.50
100-120	**Hypersulfidic**	6.8	3.48	2.30	1.96
120-135	**Hypersulfidic**	6.6	3.28	2.10	1.85

[1] Acid sulfate soil material classification used in Australia (Isbell and National Committee on Soils and Terrain, 2021)

Table 14: pH incubation data, organic carbon, nitrogen, C:N ratios and dithionate- citrate-bicarbonate (DCB) extractable Fe and Mn for the mangrove swamp site on Garden Island

Depth (cm)	**pH_{H2O}** (oxic incubation) day 0	**pH_{H2O}** 16 weeks	**OC** mg g^{-1} mean	*SD*	**N_t** mg g^{-1} mean	*SD*	**C/N**	**Fe_{DCB}** mg/g mean	*SD*	**Mn_{DCB}** mg/g mean	*SD*
Barker Inlet, Garden Island											
0-5	7.5	7.2	**23.0**	*0.66*	**1.87**	*0.04*	12	**6.3**	*0.09*	**0.16**	*0.01*
5-30	7.0	7.1	**19.5**	*1.66*	**1.28**	*0.08*	15	**2.4**	*0.09*	**0.04**	*0.01*
30-60	6.9	6.8	**11.1**	*0.47*	**0.69**	*0.01*	16	**1.7**	*0.07*	**0.04**	*0.00*
60-80	6.8	1.8	**5.1**	*0.08*	**0.34**	*0.01*	15	**1.7**	*2.26*	**0.00**	*0.00*
80-100	6.8	1.9	**5.8**	*0.06*	**0.35**	*0.01*	17	**0.8**	*0.03*	**0.00**	*0.00*
100-120	6.8	2.3	**5.3**	*0.21*	**0.34**	*0.01*	16	**0.8**	*0.01*	**0.00**	*0.00*
120-135	6.6	2.1	**4.8**	*0.04*	**0.29**	*0.01*	17	**0.6**	*0.01*	**0.00**	*0.00*

Table 15: Equivalent soil classifications for the tidal mangrove swamp site on Garden Island (S 34°48′21.2″ and E 138°32′29.0″)

Sampling locations[1]	Soil Profile Depth (cm)	pH	Australian acid sulfate soil classification key[3]		Australian soil classification[4]	World Reference Base[5]	Soil Taxonomy[6]	Australian acid sulfate soil classification key[3]	Chiptray Photograph 2.5cm X 5cm)
			[2]Material						
Garden Island (mangrove swamp)	0-60		Hyposulfidic		Sapric Histic-Hypersulfidic, Intertidal Hydrosol	Subaquatic/Tidalic, Histic Gleysol (Hypersulfidic, Arenic)	Sapric Sulfiwassists *Or* Sulfic Haplowassists	-	-
	60-100	6.3	***Hypersulfidic***					**Hypersulfidic, organic soil**	
	100-135		***Hypersulfidic***					-	-

[2] Acid sulfate soil material classification used in Australia (Isbell and National Committee on Soils and Terrain, 2021); [3] Acid sulfate soil profile classification key used in Australia (Fitzpatrick, 2013); [4] Australian soil classification (Isbell and National Committee on Soils and Terrain, 2021)
[5]IUSS Working Group WRB (2014): World Reference Base for Soil Resources 2014. World Soil Res. Report 106, FAO, Rome. http://www.fao.org/3/a-i3794e.pdf
[6]Soil Survey Staff (2022) Keys to soil taxonomy, 13th edition. USDA-Natural Resources Conservation Service, Washington, DC

Table 16: Moisture content, texture and Acid Base Accounting data for the tidal mangrove swamp site on Garden Island

Sample Ident	Depth	Texture	Moisture Content		Potential Sulfidic Acidity (Chromium Reducible Sulfur CRS)-) (I		Actual Acidity(Titratable Actual Acidity - TAA)		Acid Neutralising Capacity (ANC)		Net Acidity based on S_{CR})	Lime Calculation
	m		% moisture of total wet wt	g moisture / g of oven dry soil	%S	mol H⁺/t	pH_{KCl}	mol H⁺/t	% $CaCO_3$	mol H⁺/t	mol H⁺/t	kg CaCO3/t DW
GI- 1	**0 - 0.05**	Fine	40.2	0.67	0.017	11	8.76	0	2.88	575	-373	-19
GI- 2	**0.05 - 0.3**	Fine	30.3	0.43	0.081	51	7.77	0	0.20	40	24	2
GI- 3	**0.3 - 0.6**	Medium	23.6	0.31	0.279	174	6.63	0	0.06	12	166	12
GI- 4	**0.6 - 0.8**	Medium	25.1	0.33	0.245	153	6.54	0	0.08	16	142	11
GI- 5	**0.8 - 1**	Medium	25.6	0.34	0.220	137	6.43	1	..	..	138	10
GI- 6	**1 - 1.2**	Medium	26.4	0.36	0.184	115	6.44	1	..	..	116	9
GI- 7	**1.2 - 1.35**	Medium	23.3	0.30	0.189	118	6.32	1	..	..	119	9

These soils form due to permanently waterlogged or saturated conditions from the interaction of seawater with abundant organic material. Where these organic-rich soils accumulate more than 18 % organic carbon, they classify as Histosols and Hydrosols (see Table 12; Table 15; for correlation between the three soil classification systems in common usage as well as the Acid sulfate soil profile classification key used in Australia as outlined in Fitzpatrick, 2013). In Barker Inlet organic- rich soils (see Table 14 for organic carbon and nitrogen contents) contain two different forms of organic soil materials, as defined by the amount of rubbed fibre content: namely: (i) sapric (forms <17% by volume rubbed fibre), and (ii) hemic (forms >40% rubbed fibre) ((Soil Survey Staff, 2010)). Hence horizons that contain predominantly sapric material contain a high proportion of decomposed organic matter whereas hemic materials contain a moderate proportion of decomposed organic matter. These organic rich soils contain either sulfidic material (Isbell, 2021; Soil Survey Staff, 2010) or Hypersulfidic (Sullivan et al., 2010) because when incubated as a layer 1 cm thick under moist conditions and while maintaining contact with the air at room temperature, they show a reduction in pH to 4 or less within 8 weeks as shown in Table 13. Based on the pH_{water}, and $pH_{incubation}$ analyse, the Acid Sulfate Soil qualifies as having hypersulfidic material (pH > 4) with high Acid Sulfate Soil Hazard Rating. Based on the titratable actual acidity (TAA), chromium reducible sulfur (Crs) and acid neutralising capacity (ANC) analyses, net acidity values were derived to assess the potential to produce acidity as shown in Table 16. For coastal and inland acid sulfate soils in Australia, the action criteria or trigger values for the preparation of an ASS management plan for sands to loamy sands and peaty soils is 0.03 % S, which equates to approximately 19 mole H+/tonne (Dear et al. 2002). The following "net acidity thresholds' are currently being applied for reporting purposes by the Murray Darling Basin Authority (2010):

- low net acidity (<19 mole H+/tonne)
- moderate net acidity (19 - 100 mole H+/tonne)
- high net acidity (> 100 mole H+/tonne)

All the hypersulfidic material samples contained positive net acidity values > 19 mole H+/tonne, which is the trigger or net acidity threshold for >1000 tons of disturbed peat as shown in Table 16.

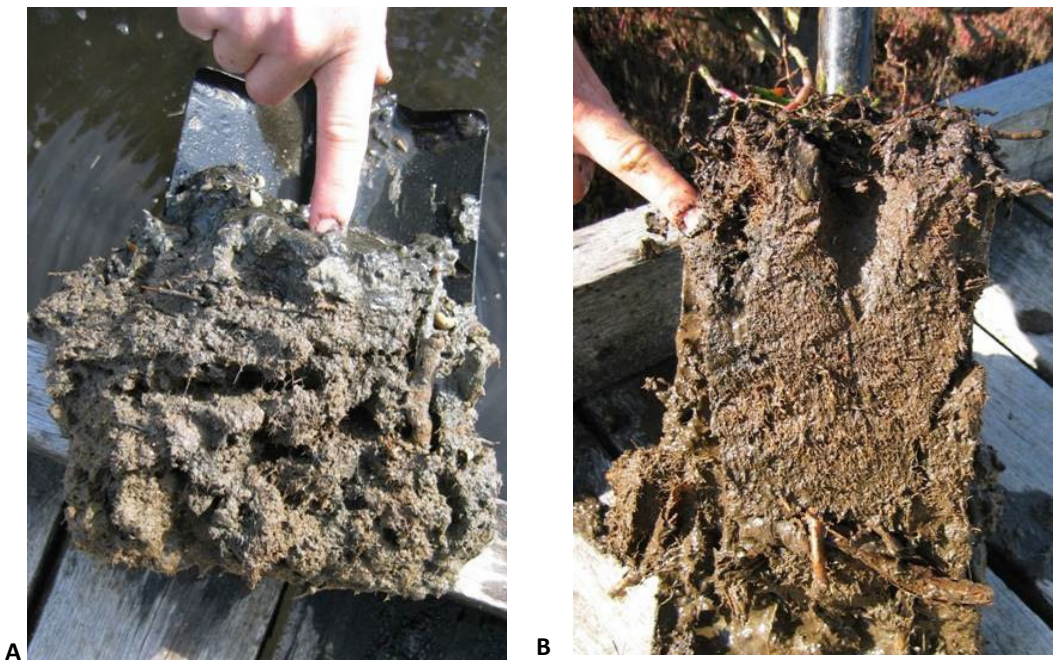

Figure 42: Photographs of hypersulfidic material in permanently saturated contemporary tidal zones featuring layers with dominant: A (left) sapric material (Terric Sulfisaprist), highly decomposed roots from mangrove trees and samphire vegetation, and B (right) hemic material (Terric Sulfihemist), moderately decomposed mangrove roots and pneumatophores from mangrove trees (width of each photograph is ~ 20 cm). (from Fitzpatrick et al. 2008b,c).

Acid sulfate soils in Barker Inlet commonly have thin layers of hemic materials at the near surface with dominant sapric materials at depth (Figure 42 A). The sapric material identified in these soils is more finely divided and reactive than the coarser, “fibric” materials commonly observed in tropical areas, where organic carbon decomposition rates are much faster. The sapric materials in temperate climate soils form from the detritus of seagrass (*Posidonia* sp.), sea lettuce (*Ulva* sp.) and mangroves. The dominant sapric material contributes strongly to the intense reducing conditions (i.e. low redox potential, or Eh values to -600 mV SHE), especially where mangrove dieback is present in the St Kilda area (see discussion below). A dominant hemic-rich soil is shown in Figure 42 B (above).

The fragmentation of pyrite framboids in sapric material, observed in Figure 43 is possibly due to wave and tidal action (Fitzpatrick et al. 1993), and bioturbation. Secondary sulfide minerals were associated with organic matter and were likely bio-mineralised with Pb and V. The source of these contaminants is likely to be related to the quality of ‘fill’ used to develop the land, that has included industrial wastes.

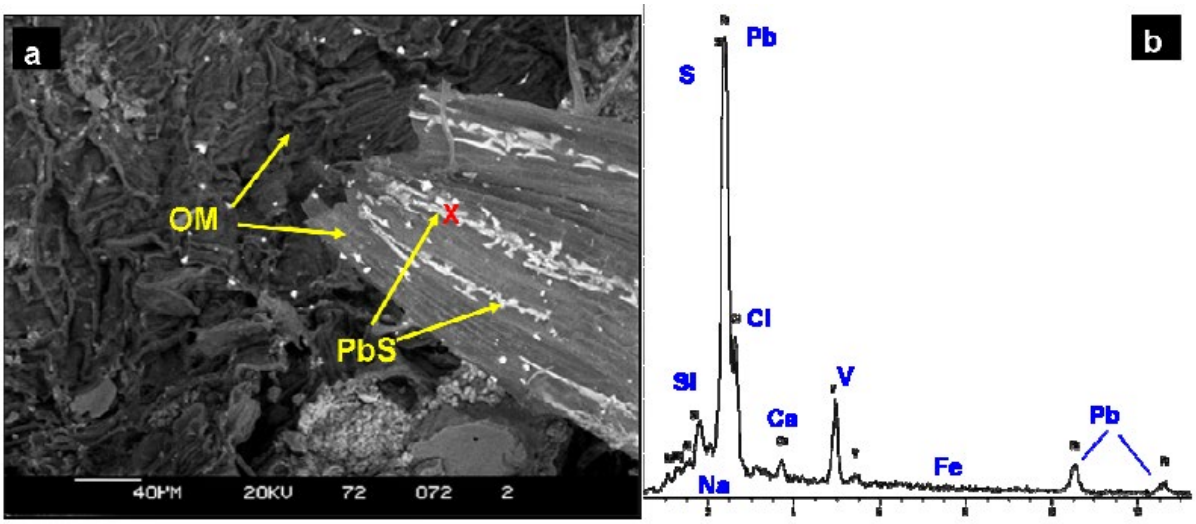

Figure 43: SEM (a) (SE) and (b) BSE showing lead bearing secondary sulfide minerals (PbS) formed on organic matter (OM) in an intertidal mangrove sediment from Garden Island, Barker Inlet (Fitzpatrick 1996). (c) EDX of the light grey coloured mineral occurring in (b) indicated with the red cross (Thomas 2011).

Stop 2 Garden Island near Boat Club:

Anthropogenic sulfuric soils and associated fence corrosion

This site illustrates anthropogenic sulfuric silty soils, which originated from a sulfuric acid manufacturing plant. The material was dumped along a section of fencing on Garden Island in South Australia.

Waste from a sulfuric acid manufacturing plant was dumped along a section of fencing on Garden Island in South Australia. There is wide scale fence corrosion is visible at this site (Figure X). A nine month study was initiated by Stiglingh (2022) to quantify the corrosion processes occurring in this anthropogenic sulfuric soil.

There are two soil profiles at this site, which were classified as Anthropogenic sulfuric silty soils in the Australian ASS classification key Fitzpatrick (2013).

Hyperthionic Spolic Technosol (according to the World Reference Base for Soil Resources, (IUSS Working Group WRB, 2014) and

Sulfuric Spolic Anthroposol (in accordance with the Australian soil classification (Isbell, 2021).

Figure 44: Photographs showing the condition of fencing on Garden Island (South Australia). The section of the fence, which is heavily impacted by corrosion damage is located above Anthropogenic sulfuric silty soils, which originated from a sulfuric acid manufacturing plant.

Both of the anthropogenic sulfuric silty soils present on Garden Island were extremely acidic (pH < 2) and highly saline (11 and 13 dS/m) (see Table 17).

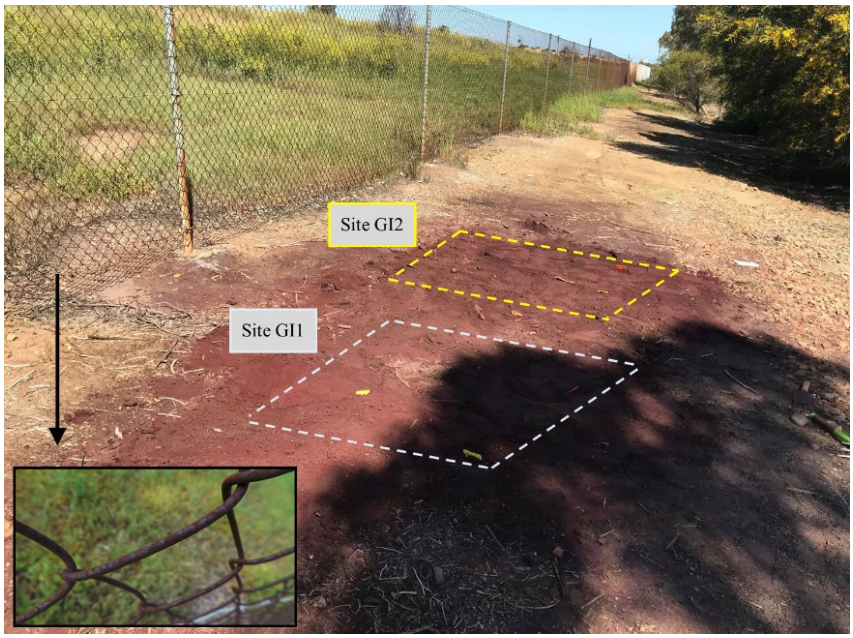

Figure 45: Photograph of the Anthropogenic acid sulfate soil site on Garden Island. Two field sites (GI1 and GI2) were used for a nine-month fencing trial. The condition of the nearby fence is shown as an inset

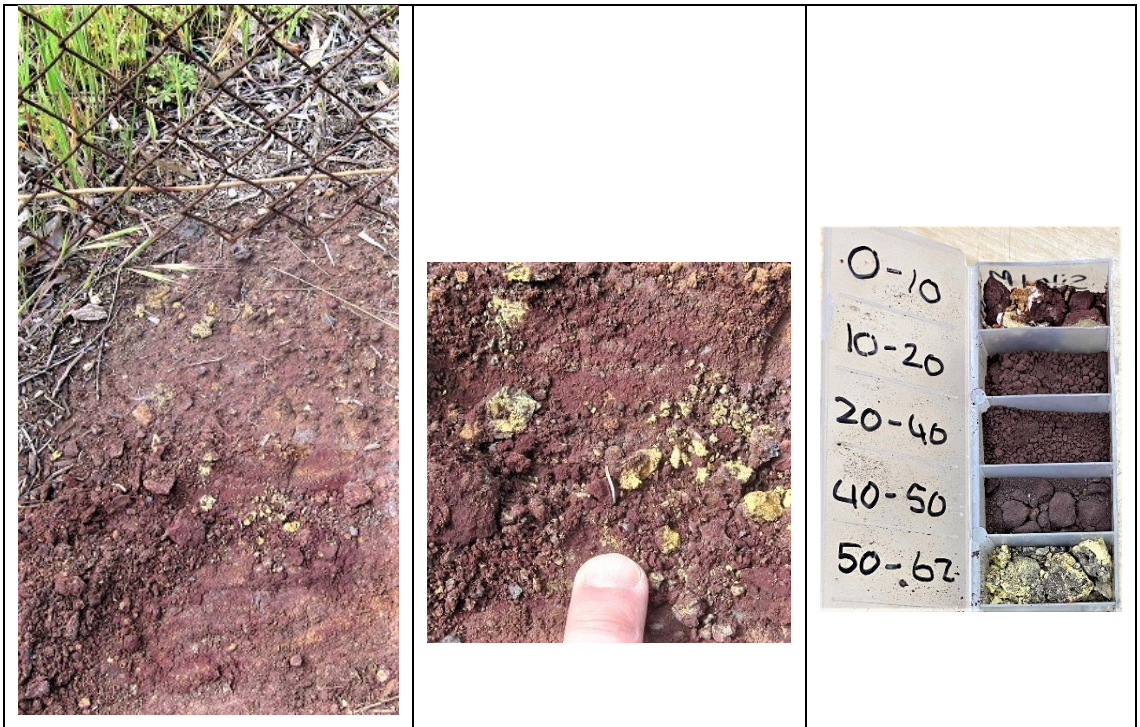

(a) (b) (c)

Figure 46: Photographs of Site GI 1 on Garden Island showing (a) Anthropogenic Sulfuric silty soil profile with dusty red (5R3/3) silty matrix and bright yellow jarosite mottles/fragments underlying a highly corroded fence, (b) close view of the dusty red (5R3/3) silty matrix and bright yellow jarosite mottles/fragments and (c) five samples collected from soil horizons at 5 depths and placed in plastic chip tray compartments 2.5 cm X 5 cm.

Table 17: Soil profile morphology, pHf, pHinc, ECe and equivalent soil classifications of site GI 1 on Garden Island (34°48'19.88"S and 138°31'50.37"E)

Soil Profile Depth (cm)	Chiptray Photograph (5cm x 2.5cm)	Description	pH Field	pH 8 Wks	ECe (dS/m)	[2]Material	Australian acid sulfate soil classification key[3]	Australian soil classification[4]	World Reference Base[5]
0-10		Dusty red (5R3/3) matrix, silty with 30% bright yellow jarosite fragments	2.1	1.1	13.5	Sulfuric	Anthropogenic silty sulfuric soil	Sulfuric Spolic Anthroposol	Hyperthionic Spolic Technosol
10-20		Dusty red (5R3/3) matrix, silty with 10% bright yellow jarosite fragments	2.2	0.9	7.8	Sulfuric			
20-40		Dusty red (5R3/3) matrix, silty with 10% bright yellow jarosite fragments	1.9	0.6	8.1	Sulfuric			
40-50	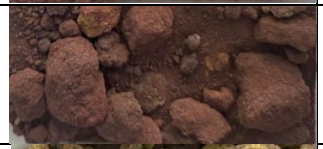	Dusty red (5R3/3) matrix, silty with 20% bright yellow jarosite fragments	1.7	0.5	4.1	Sulfuric			
50-62		Dusty red (5R3/3) matrix, silty with 70% bright yellow jarosite fragments	1.5	0.2	3.4	Sulfuric			

[1] Sampling location see Figures 3, 4 and 5
[2] Acid sulfate soil material classification used in Australia (Isbell and National Committee on Soils and Terrain, 2021)
[3] Acid sulfate soil profile classification key used in Australia (Fitzpatrick, 2013)
[4] Australian soil classification (Isbell and National Committee on Soils and Terrain, 2021)
[5]IUSS Working Group WRB (2015): World Reference Base for Soil Resources 2014. World Soil Res. Report 106, FAO, Rome. http://www.fao.org/3/a-i3794e.pdf

During the nine-month study standard zinc-aluminium fence netting and galvanised-steel fence wires were buried at two replicate field sites as shown in **Error! Reference source not found.** for three and nine months, to assess their suitability for use in this region. Standard zinc-aluminium netting samples lost 98-100% of their protective wire coatings after only three months buried in highly acidic (pH < 2) and highly saline (11-13 dS/m) soils. Standard zinc-aluminium netting samples were completely disintegrated after nine months in contact with the Anthropogenic sulfuric silty soil. Likewise, galvanised-steel samples lost 96-97% of their zinc coatings after only three months. These results show that neither of the fencing products tested are suitable for use in these very highly corrosive soils. Further research is recommended to assess the suitability of more corrosion-resistant materials such as stainless-steel or wires with a polymer coating. Corrosion products identified on fence samples using scanning electron microscopy (SEM) and energy dispersive X-ray (EDX) spectroscopy predominantly consisted of iron (up to 37%), chloride (up to 5%) and sodium (up to 21%). XRD analyses of corrosion products formed on wire surfaces are currently being processed.

Stop 3 Gillman and Range Wetlands

Sulfuric materials in disturbed tidal zones

The Gillman site was bunded and isolated from tides exposing large areas of sulfidic material to oxygen, oxidising sulfides to produce sulfuric acid. The 2 m thick soil profile with has substantial sulfuric material, very low pH (<4), jarosite mottles and limited neutralising material. This site is in the process of being capped for industrial development.

Figure 47: Map of Gillman and Range Wetlands (Stop 3), with bund wall in red and Profile BG 11(Table 18 and Table 19) and profile BG 15 (Table 20) location in the red star

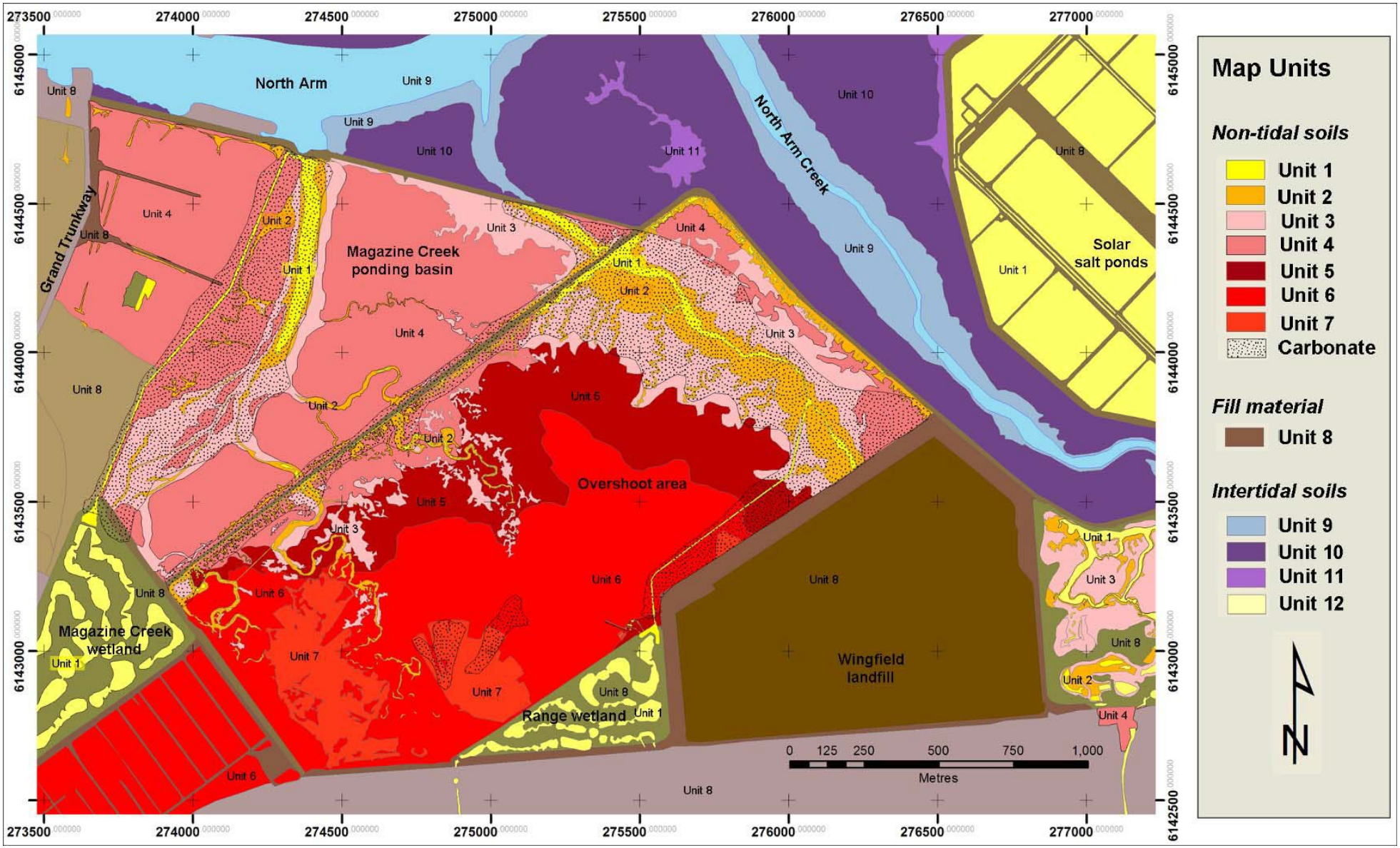

Figure 48: Soil-landscape map for the Gillman study site. Refer to Table 18 for a detailed map legend and descriptions of Map units. The Dean Rifle Range was located at coordinates E 73500, N 6142500 (at the bottom left corner of the map). From Thomas (2010).

Table 18: Map units located within Gillman Focus areas A, B, C and D combined with soil profiles classified according to Soil Taxonomy (Soil Survey Staff 2010), the Australian Soil Classification (Isbell 2002) and acid sulfate soil material terminology from Sullivan et al. (2010) (From Thomas 2010)

Map unit no. (unit colour)	Soil profile no.	Australian Soil Classification (Isbell 2002)	Soil Taxonomy (Soil Survey Staff 2010)	Acid Sulfate Soil materials
Disturbed former intertidal to supratidal areas (Gillman study site)				
1. Water	**BG 30** **BG P 5**	Sodosolic Salic Hydrosol Sodosolic Salic Hydrosol	Typic Hydrowassents	Hyposulfidic, monosulfidic
2. Benthic mat, bare salt scald, mud flats	**BG 4, 28, 31**	Sulfuric, Hypersalic Hydrosol Epicalcareous, Hypersalic Hydrosol Haplic, Hypersalic Hydrosol	Salidic Sulfaquepts Typic Haloquepts Aeric Haloquepts	Hypersulfidic, hyposulfidic, monosulfidic
3. Bare salt scalded mud flats	**BG 17, 32**	Sulfuric, Salic Hydrosol Haplic, Hypersalic Hydrosol	Salidic Sulfaquepts Aeric Haloquepts	Sulfuric, hypersulfidic, hyposulfidic, monosulfidic
4. Dense low heath - samphire shrublands	**BG 22, GGT 5**	Haplic, Hypersalic Hydrosol Sulfuric, Salic Hydrosol	Aeric Haloquepts Typic Sulfaquepts	Sulfuric, hyposulfidic
5. Open low scrub - grasses	**BG 15**	Sulfuric, Salic Hydrosol	Typic Sulfaquepts	Sulfuric, hypersulfidic
6. Open grass plain and scrub	**BG 11, 5**	Sulfuric, Salic Hydrosol	Typic Sulfaquepts	Sulfuric, hypersulfidic, hyposulfidic
7. Bare, scalped, salt scalds, sand flat	**MFP 14**	Sulfuric, Salic Hydrosol	Typic Sulfaquepts	Sulfuric, hypersulfidic, hyposulfidic
8. Artificially filled areas and embankments	**GGT 2**	Sulfidic, Dredgic Anthroposol	Haplic Xerarents	Hypersulfidic, hyposulfidic, monosulfidic
9. Water	**BG 24**	Hemic, Epicalcareous, Intertidal Hydrosol	Typic Hydrowassents	Hyposulfidic, monosulfidic
10. Mangrove woodlands	**BG 21**	Hemic, Sulfidic, Intertidal Hydrosol	Sulfic Hydrowassents	Hypersulfidic, hyposulfidic, monosulfidic
11. Low growing salt marsh plants	**BG 20**	Hemic, Sulfidic, Intertidal Hydrosol	Sulfic Hydrowassents	Hypersulfidic, hyposulfidic, monosulfidic

Table 19: Map units in Gillman area combined with soil profiles classified and net acidity (Thomas 2010)

Soil profile number	Map unit	Aust. Soil Classification (Isbell 2002)	Soil Taxonomy (Soil Survey Staff 2010)	Acid Sulfate Soil materials present	Significant net acidity occurrence
BG 11	**6.** Open grass plain and scrub	Sulfuric Salic Hydrosol	Typic Sulfaquepts	Sulfuric, hypersulfidic hyposulfidic	190 cm @ 203 mole H^+/t from 50 cm depth
BG 15	**5.** Open low scrub and grasses	Sulfuric Salic Hydrosol	Typic Sulfaquepts	Sulfuric, hypersulfidic	105 cm @ 1903 mole H^+/t from 65 cm depth
BG 17	**3.** Bare salt scalded mud flats	Sulfuric Salic Hydrosol	Salidic Sulfaquepts	Sulfuric, hypersulfidic	95 cm @ 1491 mole H^+/t from 25 cm depth, including an AVS content of 0.03%
BG P 5	**1.** Water	Sodosolic Salic Hydrosol	Typic Hydrowassents	Hyposulfidic, monosulfidic	5 cm @ 456 mole H^+/t from 0 cm depth, including an AVS content of 1.1%

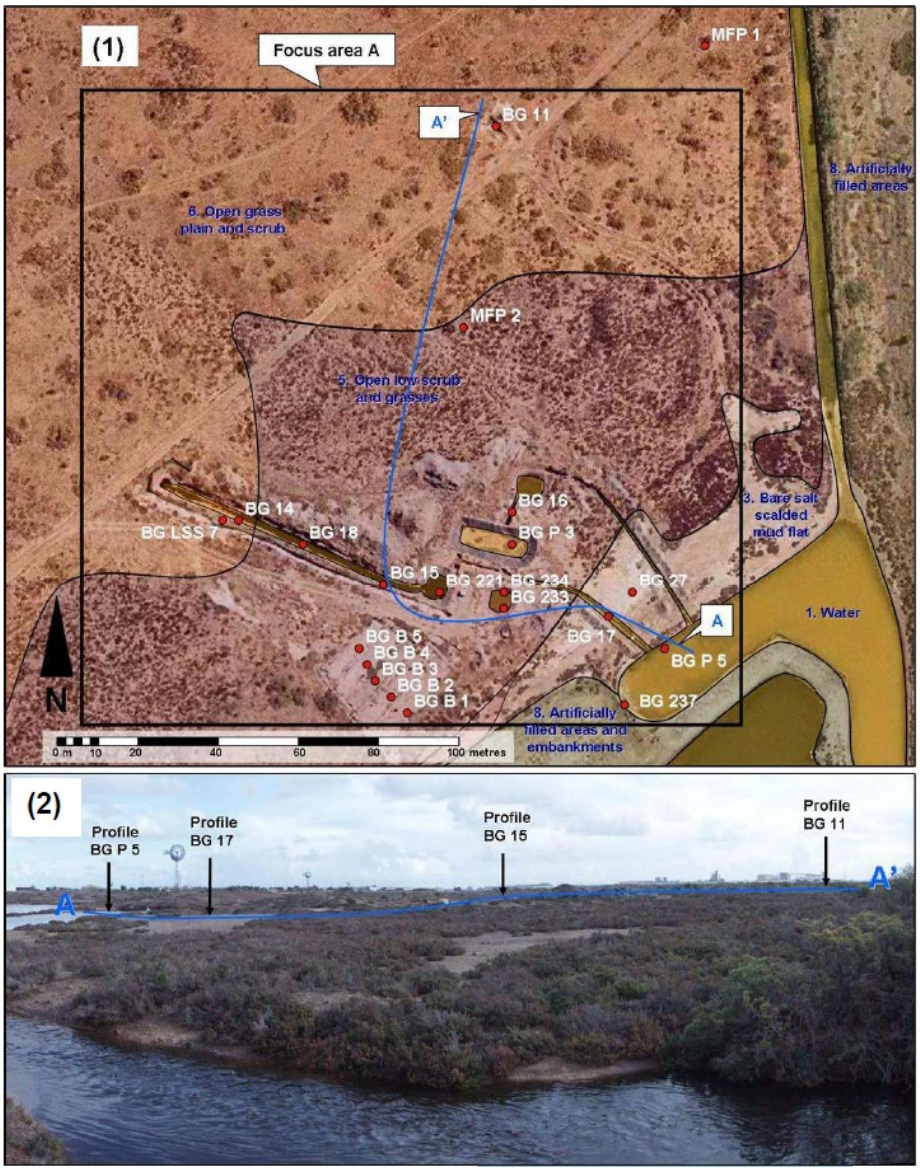

Figure 49: Map (1) and photograph (2) showing locations of sites listed in Table 19

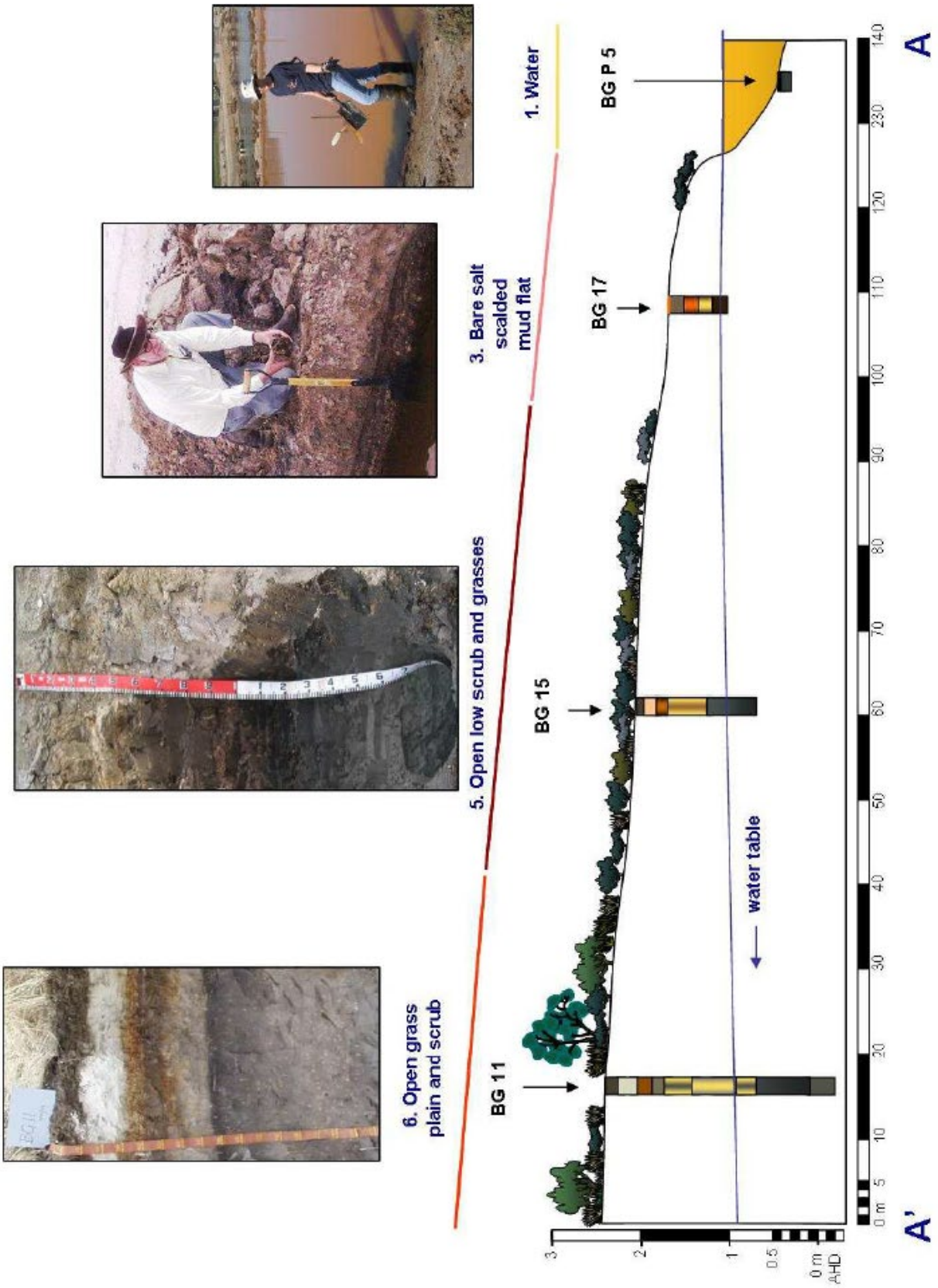

Figure 50: CSM showing the relative position of representative soil profiles with colour photographs and average water table depth and groundwater flow direction. Detailed descriptions for the four profiles (BG 11, BG 15, BG 17 and BG P 5. Profile descriptions are provided below.

In several parts of Barker Inlet, bund walls were constructed across tidal zones (e.g. mangrove and samphire swamps) nearly 50 years ago to cut off tidal flushing, which effectively disturbed (drained) these areas causing mangrove trees and samphire vegetation to die (Figure 38, Figure 39, Figure 48, Figure 52, Figure 53, Figure 54).

Excluding seawater from the original sulfidic material caused the surface to dry and oxidise sulfide to produce sulfuric acid (pH commonly between 2.5-3.5) and bright yellow mottles of jarosite [$KFe^3(SO_4)2(OH)_6$] (Figure 48, Figure 52, Figure 53, Figure 54). This process transforms sulfidic material to sulfuric material. Sulfuric material in this area is composed of either organic (i.e. Histosols) or mineral material (15 cm or more thick), and has both pH less than 4 and bright yellow jarosite mottles. See Table 12 for correlation between the three soil classification systems in common usage.

The schematic cross-sections in Figure 52 and Figure 53 illustrate how the former back barrier sand ridge at Gillman has developed a 2 m thick soil profile with sulfuric material because pyrite framboids in and surrounding decomposed mangrove pneumatophores have oxidised to form yellow jarosite mottles (4Bj horizons) and acidity where neutralising by alkaline materials is limited (Figure 55). Coatings of jarosite and iron oxides form rapidly along large root channels during periods of drying. Some small, unoxidised pyrite framboids still occur in the underlying sandy, sulfuric horizons (horizons 4Bj3, 4Bj4) (Figure 55). In the upper horizons (0-58 cm), the oxidation of pyrite in organic residues caused precipitation of iron oxides and lenticular gypsum crystals, which are now being leached out of the profile.

At Gillman, it has been estimated that about 85 % of sulfides above the oxidation front of these ASS have oxidised over the past 60 years, with an estimated 520 000 t of H_2SO_4 being produced (Thomas et al., 2004). The back barrier sands have limited acid neutralising capacity and the pH of soil solution is generally less than 2.5. Long term, in situ redox monitoring (Thomas unpublished) indicated that the large seasonal variation in watertable height (>1 m) may contribute to the reformation of pyrite and consumption of acidity near the base of the profile during the wetter months, where soil organic matter content is still adequate for reducing conditions to return. This pyrite oxidises during successive dryer months. Most of the sulfuric acid that has been produced is still contained within the soil profile due to the low hydraulic gradient of the area. However, when a drain is excavated and the soils are further drained, salt efflorescences precipitate on the soil surface along the drain walls. These soluble salts dissolve during subsequent rain events and contribute to acidity and metal content in the drainage waters.

According to Belperio & Harbison (1992), at Gillman, 0.7 m of ground subsidence, coincides with an area of about 400 ha of exposed mangrove peat that has been subjected to meteoric infiltration and aeration since the bund wall was constructed in the 1950s. The sulfuric acid produced from pyrite oxidation has resulted in acidic interstitial waters. The highly acid waters with pH values < 3.5 at Gillman have released large amounts of ferric iron that continue to oxidise pyrite and decalcify surrounding sediments to a depth of >2 m (Belperio & Harbison, 1992; Thomas et al., 2004) . Decalcification is greatest in the earliest reclaimed areas, and gypsum is locally present along the sharp redox front between decalcified and the unaltered marine sediments.

Most of the sulfuric acid that has been produced is still contained within the soil profile due to the low hydraulic gradient of the area. However, when a drain is excavated (Figure 53, Figure 54) and the soils are further drained, salt efflorescences precipitate rapidly on the soil surface along the drain walls (Figure 54). These soluble salts dissolve during subsequent rain events and contribute to acidity and metal content in the drainage waters.

In the last 5 years, the site is being progressively infilled with up to 3 meters of fill to allow industrial development. You will see this progress on the trip today.

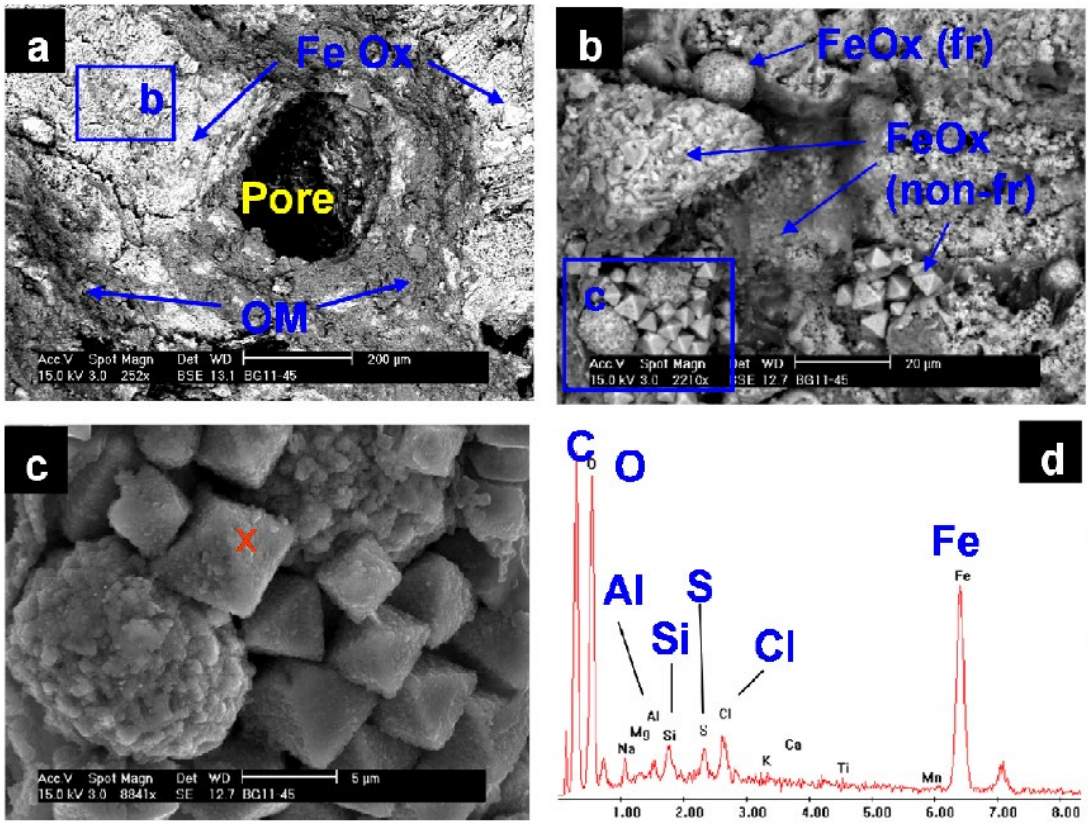

Figure 51: SEM photomicrographs of rough-surfaced soil samples (a-c) and EDX spectra (d) from profile BG 11. (a) horizon 2Ey2 showing a root channel surrounded by organic matter and Fe oxide. (b) enlargement of area (b) in image (a) showing framboidal Fe oxides and non-framboidal Fe oxides occurring as pseudomorphs after pyrite. (c) enlargement of area (c) in image (b) showing clay coating on large octahedral Fe oxide pseudomorphs and smaller framboidal pseudomorphs. (d) EDX spectra of large octahedral crystals (at site "X" in image (c)) indicating that they are composed of Fe oxide with clay coatings. The field of view indicates scale and is 1.2mm across in (a); 110µm across in (b); 25µm across in (c).

Extremely acidic environments that occur in open drains where soluble Fe and sulfate-salt efflorescences precipitate provides a vector for the movement of trace metals to pore water and surface water. The efflorescences are also a store of acidity, Na, Ca, Mg, Cl, Sr and SO_4 and metals (e.g., Al, Fe, Zn, Ni) to precipitate in oxic-acidic conditions and may present an environmental hazard to connected water bodies following rainfall. The salts (containing Fe and S) also contribute to the formation of monosulfidic material in water bodies lower in the landscape where soil conditions were reducing with neutral pH. Metal concentrations (Cu, Ni, Pb and Zn) were elevated in topsoil of profile BG 15 (Table 20; (Thomas, 2010). The source of metals was likely anthropogenic. Potential sulfidic acidity was highest between 95 cm and 120 cm, with chromium reducible sulfur (SCR) concentrations up to 6.88%, contributing to a positive net acidity of 5700 mol H+/t. Sulfuric materials occurring between 60 cm and 120 cm depth contained significant acidity, in the form of titratable actual acidity (TAA) and retained acidity, at the level where the dominant salt efflorescence mineral was sideronatrite [$Na2Fe(SO_4)2(OH).3H_2O$] (Fig 7). Metals (Zn, Ni, Fe, and Al) were enriched in soil pore water collected in the top 5 cm of peeper P1 (Figure 54), located in the oxic-acidic drain wall. Salt crusts in Areas c2 and c3 had a field pH < 1 (Figure 54), indicating ASS weathering. Trace element concentrations in soil layers were similar to concentrations in juxtaposed salt crusts. In summary, acidic drain waters contained elevated Al, Fe and other major cations and anions, but did not contain detectible concentrations of trace elements. Nearby circum-neutral stream waters only contained elevated concentrations of Fe, where hyposulfidic and monosulfidic materials occurred, with an Acid Volatile Sulfur content of 1.15 % (AVS).

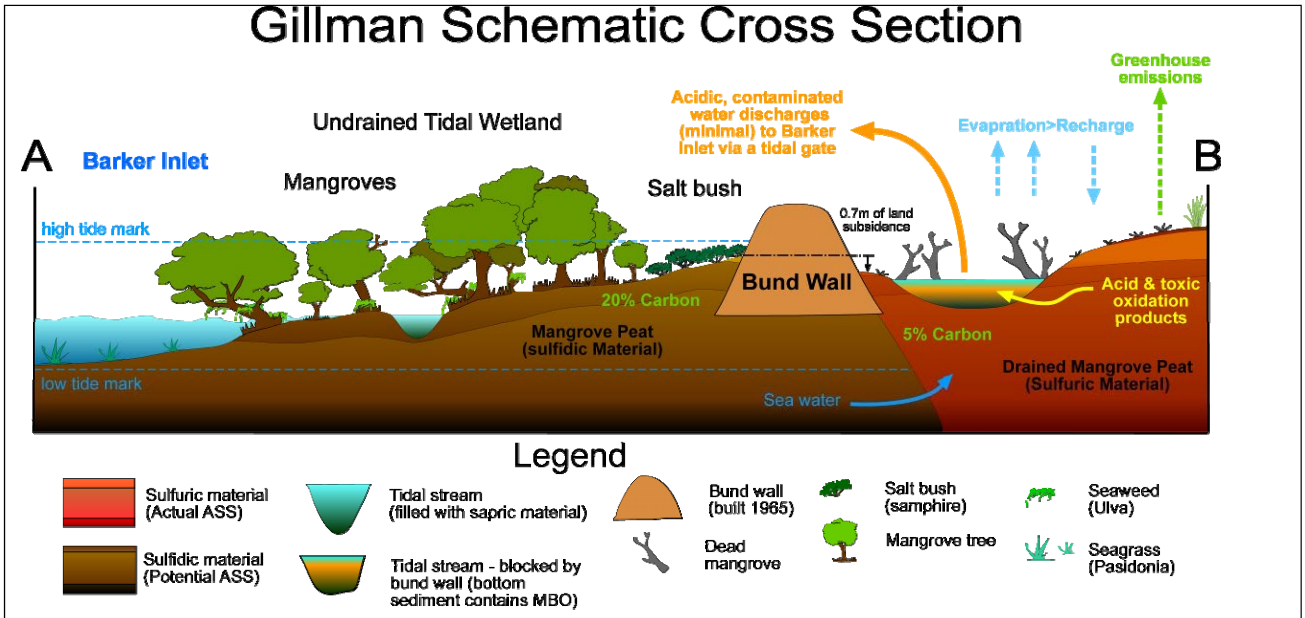

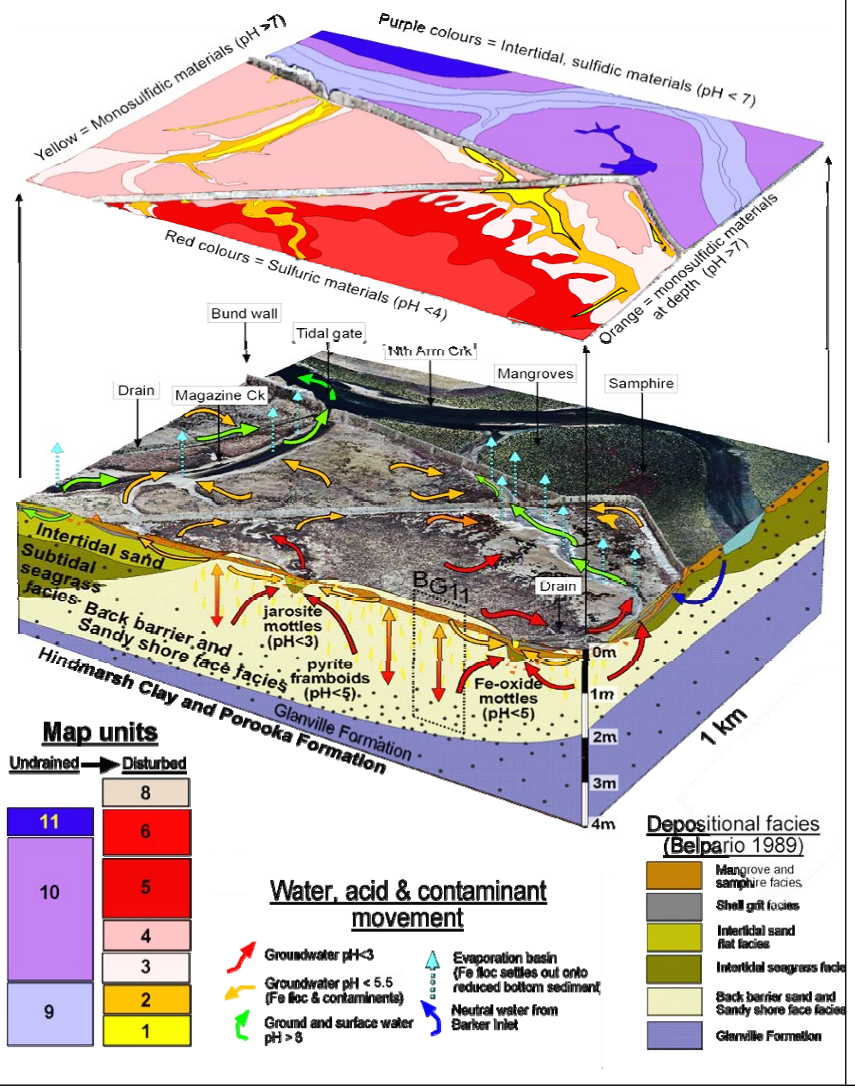

Figure 52: Schematic soil-landscape cross sections at Gillman in Barker Inlet. Normal tidal dynamics are interrupted by a bund wall (levee bank) causing oxidation of hypersulfidic and monosulfidic materials to occur, which contributes to degraded acidic saline land, denuded vegetation, reduction of wetland biodiversity, poor estuarine and stream water quality, ground subsidence, increase in greenhouse emissions and loss of amenity.

The 3D-soil-regolith explanatory model also shows the following contrasts between tidal and drained coastal landscapes:

(i) the top layer sulfuric (Red), sulfidic materials (purple) and monosulfidic (yellow) materials are displayed and (ii) in bottom layer the depositional facies, location of pyrite oxidation and movement of acidic groundwater and contaminants within the site; and arrows indicate surface and groundwater water flow paths (Fitzpatrick et al. 2008b; Thomas 2010).

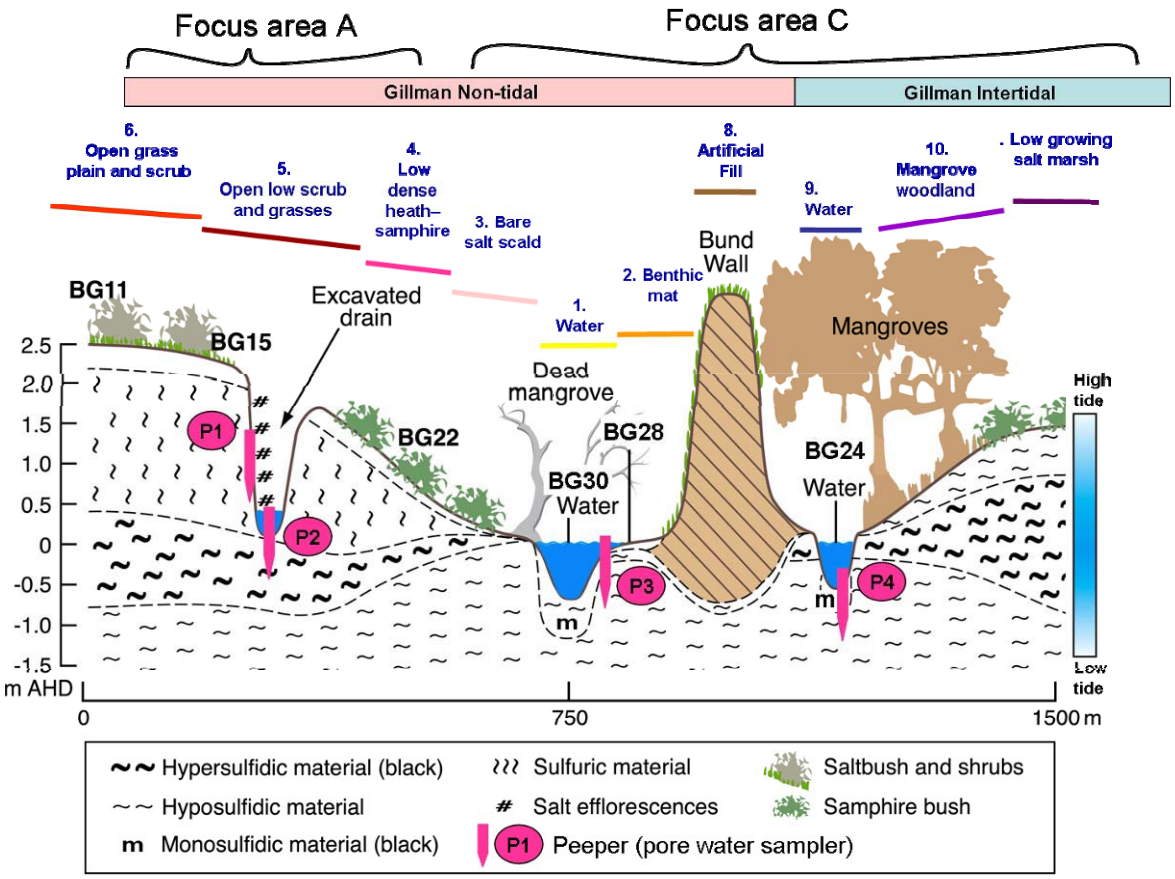

Figure 53: Detailed schematic soil-landscape cross section at Gillman in Barker Inlet illustrating the distribution of the various acid sulfate soil materials (from Thomas 2010).

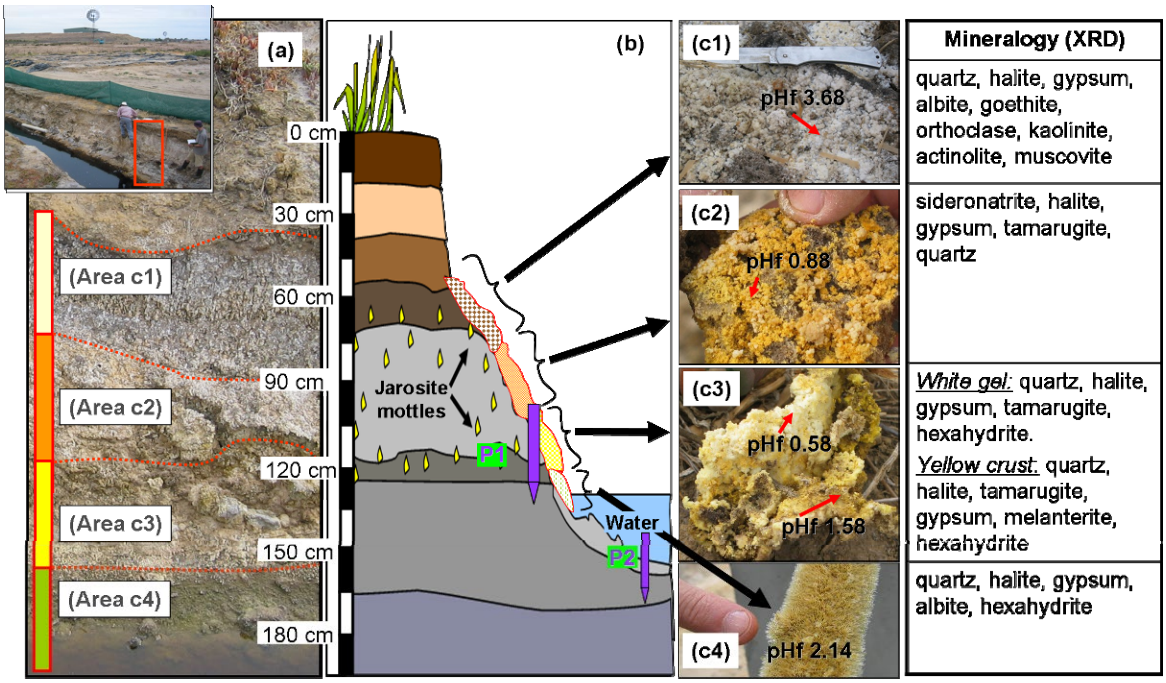

Figure 54: (a) Salt efflorescences precipitated on the exposed wall of soil profile BG 15 in a drain at Gillman, near Adelaide. (b) Schematic cross section of the drain showing position of peeper P1 within the drain wall and peeper P2 in the bottom of the drain. (c) Mineralogy of salt efflorescences from each of the areas (c1-c4). (From: Thomas *et al.* 2010).

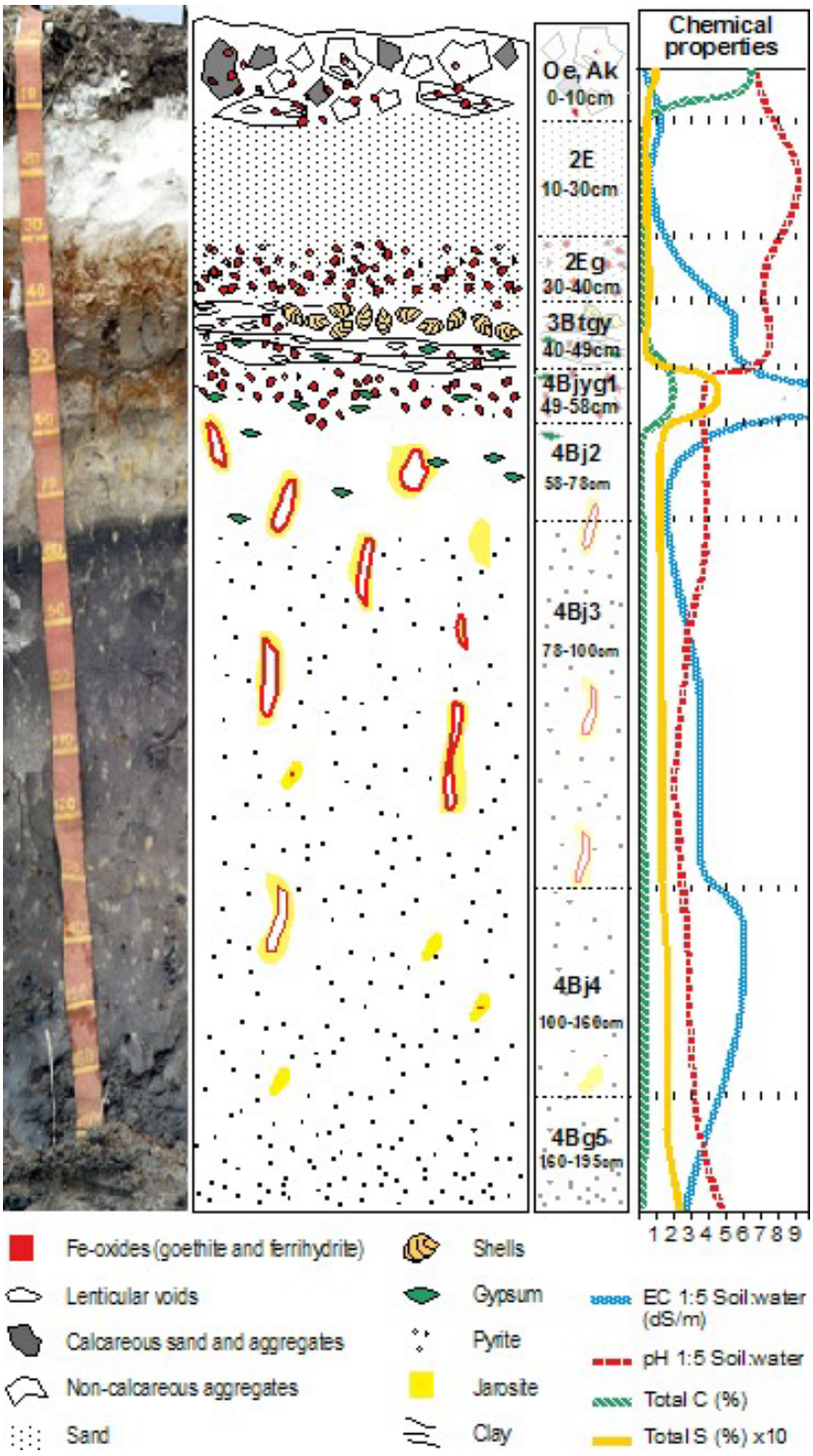

Oe, Ak: Crumb structure, calcareous, siliceous, lenticular voids, sand-size iron nodules, not related to pores. Ferrihydrite-goethite nodules are pseudomorphs after pyrite framboids.

2E: Sand, little organic residue. Very fine clay coatings on sands.

2Eg: Sand, goethite pseudomorphs after pyrite associated with blackened organic matter. Shell lenses with gypsum on surfaces.

3Btgy: Layered clay, lenticular voids with gypsum crystal infillings. Few jarosite coatings.

4Bjyg1: Sulfuric material, sand, jarosite and gypsum coatings around roots, iron coatings on jarosite. Infillings of lenticular gypsum, decreasing with depth. Horizontal intercalations of blackened organic matter and black pseudomorphs of pyrite. Coarse lenticular pores (mangrove pneumatophores).

4Bj2, 4Bj3 and **4Bj4:** Sulfuric material and pyrite. Jarosite coatings around large root channels. Fe-oxide coatings on jarosite. Few scattered pyrite framboids in groundmass.

4Bg5, 4Bg6: Hypersulfidic material (pyrite framboids).

Figure 55: Main macro- and micromorphological features and chemical properties of an ASS soil with sulfuric material in disturbed tidal zones (Hydraquentic Sulfaquept) from Gillman showing horizons with five lithological discontinuities, which includes sulfuric material (58 to 160 cm) and hypersulfidic material (160 to >195 cm). Groundwater height fluctuates seasonally between 140 cm and 180 cm. (modified from Poch et al. 2009).

Profile BG 11

Photograph and soil profile description of the Sulfuric clayey peat soil in the Gillman wetlands, South Australia in the disturbed supratidal zone showing horizons with six lithological discontinuities, which includes sulfuric material with prominent masses of jarosite (20 to 160 cm) and hypersulfidic material (160 to >195 cm).

Described by: Rob Fitzpatrick 25th April, 2018

Locality: Gillman wetlands Gillman (34°49'47.21"S 138°32'39.77"E) (see Figure 1; Fitzpatrick et al. 2012)

Landform: flat plain – former supratidal zone

Elevation: 2.5 m AHD

Groundwater height: fluctuates seasonally between 140 cm and 180 cm.

Soil Classification:

- *Sulfuric clayey peat soil (Australian acid sulfate soil classification: Fitzpatrick et al., 2008; Fitzpatrick, 2013).*
- *Salic Fluvisol (Hyperthionic, Drainic) (World Reference Base: IUSS Working Group WRB., 2014)*
- *Peaty, Sulfuric, Hypersalic Hydrosol (Australian Soil Classification: Isbell and National Committee on Soils & Terrain, 2021).*
- *Hydraquentic Sulfaquept (Soil Taxonomy: Soil Survey Staff, 2022).*

References: published reports and papers: (Poch et al., 2009) (Kölbl et al., 2019, 2021), (Thomas, 2010; Trueman et al., 2020, 2021)

*Description: The Gillman site in the Barker Inlet estuary is a former tidal wetland, which was covered with mangrove woodland. The area has been progressively reclaimed from the intertidal and supratidal environments since the 1930s by construction of a series of bund walls that prevent tidal inundation to develop agriculture and industry. The loss of tidal inundation has resulted in lowering of the water table, enabling oxygen to diffuse into the hypersulfidic material. Exposure results in the oxidation of pyrite, with each mole of pyrite yielding 2 moles of sulfuric acid and the formation of sulfuric material (pH <4) (*Table 20,Table 21*).*

Table 20: Soil profile (BG 11) Photograph and soil profile description of the Sulfuric clayey peat soil in the Gillman wetlands, South Australia in the disturbed supratidal zone showing horizons with six lithological discontinuities, which includes sulfuric material with prominent masses of jarosite (20 to 160 cm) and hypersulfidic material (160 to >195 cm).

Oe 0-5cm;	Very dark greyish brown (10YR3/2) silt loam; moderate fine granular structure; very friable, moderately alkaline, abundant fine roots; gradual, smooth boundary
A1 5-20 cm;	Dark greyish brown (10YR4/2) silt loam; common fine, very faint, yellow (10YR7/8) masses of oxidised iron on faces of peds and inside peds; strong fine subangular blocky structure; firm; common fine roots; moderately alkaline; sharp and wavy boundary.
2Ey1 20-30 cm;	Pale yellow (5Y7/3) silty clay with 10 percent medium prominent strong brown (7.5YR5/6) masses of oxidised iron faces of peds; strong fine subangular blocky; few gypsum crystals; few fine roots; gradual and irregular boundary. (sulfuric material)
3Btyg1 30-60 cm;	Greyish brown (10YR5/2); sandy clay loam with 20 percent medium prominent pale yellow (2.5Y7/4) masses of jarosite infilling old mangrove root channels / pneumatophores; and some prominent, 2 mm thick, brown (7.5YR5/4) mottles of Fe-oxide coating or infilling root channels; structureless massive, some gypsum coatings; few living roots; abrupt and smooth boundary. (sulfuric material)
4Btg1 60-80 cm;	Dark greyish brown (10YR3/2) clayey peat with 30 percent medium prominent pale yellow (2.5Y7/4) masses of jarosite infilling old mangrove root channels / pneumatophores; prominent, 2 mm thick, brown (7.5YR5/4) concentrations of oxidised iron coating and infilling mangrove root / pneumatophores channels; structureless massive, few living roots, common dead roots; abrupt and smooth boundary. (sulfuric material)
5Bjg1 80-100 cm;	Very dark grey (10YR3/1) sandy clay loam in organic matrix; 20 percent prominent (up to 5 mm thick) light yellowish brown (2.5Y6/4) masses of jarosite infilling old mangrove root channels / pneumatophores; single grain structure; no roots; gradual and smooth boundary. (sulfuric material)
6Bjg1 100 – 160 cm;	Light brownish grey (10YR6/2); medium sand with 5 percent prominent (up to 5 mm thick) light brownish grey (2.5Y6/2) masses of jarosite infilling old mangrove root channels / pneumatophores, single grain structure; no roots; diffuse and irregular boundary (sulfuric material)
7Bseg1/ W1 60-200 cm;	Dark greyish brown (10YR4/2) medium sand with 10 percent abundant black (10YR2.5/1) concentrations due to charcoal residues and charcoal fragments; single grain structure; no roots and diffuse boundary. (hypersulfidic material)

Table 21: Summary of ASS incubation data, shown for day 0 and after 16 weeks (measured by Rob Fitzpatrick). Organic Carbon (OC), nitrogen (N), Fe (DCB) and Mn (DCB) data are published in Kölbl et al. (2019).

Depth (cm)	pH_{H2O}	pH_{H2O}	OC		N_t		C/N	Fe_{DCB}		Mn_{DCB}	
	(oxic incubation)		mg g^{-1}		mg g^{-1}			mg/g		mg/g	
	day 0	16 weeks	mean	*SD*	mean	*SD*		mean	*SD*	mean	*SD*
Barker Inlet, Gillman											
0-5	7.4	6.4	**47.1**	*0.58*	**4.56**	*0.01*	10	**30.5**	*0.67*	**1.01**	*0.05*
5-20	7.1	6.2	**10.7**	*0.08*	**1.10**	*0.01*	10	**41.8**	*0.69*	**0.46**	*0.00*
20-30	3.7	3.9	**3.9**	*0.05*	**0.25**	*0.01*	16	**6.0**	*0.37*	**0.00**	*0.00*
30-60	2.9	2.8	**6.4**	*0.04*	**0.41**	*0.01*	16	**10.4**	*0.10*	**0.00**	*0.00*
60-80	2.8	1.9	**25.9**	*0.64*	**1.21**	*0.01*	22	**69.1**	*1.12*	**0.05**	*0.02*
80-145	2.5	2.6	**2.9**	*0.13*	**0.18**	*0.01*	17	**5.7**	*0.06*	**0.00**	*0.00*
145-160	3.4	1.5	**1.0**	*0.01*	**0.10**	*0.00*	10	**1.0**	*0.03*	**0.00**	*0.00*
160-180	4.7	2.6	**1.5**	*0.02*	**0.27**	*0.01*	5	**2.6**	*0.06*	**0.02**	*0.00*
180-200	5.1	2.6	**1.6**	*0.05*	**0.29**	*0.02*	6	**4.1**	*0.02*	**0.02**	*0.00*

Highlighted in red = sulfuric material (pH <4) anoxic incubation experiments).

Highlighted in blue = hypersulfidic material (pH >4) or acidifies following oxidation

Figure 56: Photograph of the Sulfuric clayey peat soil profile in an excavated drain in the Gillman wetlands displaying: (i) soils horizons with six lithological discontinuities, which includes sulfuric material with prominent masses of jarosite (20 to 160 cm) and hypersulfidic material (160 to >195 cm), (ii) white and yellow salt efflorescences precipitated on the exposed and dry wall of the drain comprising gypsum, tamarugite, hexahydrite, halite and sideronatrite and (iii) suspended strong brown coloured schwertmannite-rich precipitates at the water-air interface in the drain

Table 22: Profile BG 15: Moist (winter) moderately well drained, open low scrub and grasses; classifies as: Typic Sulfaquepts (Soil Survey Staff 2010); Peaty, Sulfuric, Hypersalic Hydrosol (Isbell and National Committee on Soils & Terrain, 2021).

Horizon (ID)	Depth (cm)	Soil morphology	Sample (frame size: 5 x 2.5 cm)
Oe (BG 15-188)	0-5	Brown to greyish brown (10YR3/2) silty loam without mottles; moderate coarse subangular blocky structure; strong consistency; some fine roots; gradual and diffuse boundary	
A (BG 15-189)	5-15	Greyish brown (10YR4/2) clay loam with common fine, very faint, yellow (10YR7/8) mottles penetrating peds; strong subangular blocky structure; strong consistency; few fine roots; diffuse boundary	
E (BG 15-190)	15-25	Pale yellow (5Y7/3) silty clay with strong brown (7.5YR5/6) mottles (10% volume) impregnating matrix of peds. Strong, subangular blocky structure; very few living roots, diffuse boundary	
2Ey1 (BG 15-191)	25-30	Pale yellow (5Y7/3) silty clay with strong brown (7.5YR5/6) mottles (15% volume) impregnating matrix of peds. Strong, subangular blocky structure; very few living roots, diffuse boundary. Few gypsum crystals	
2Ey2 (BG 15-192)	30-40	Pale yellow (5Y7/3) silty clay with strong brown (7.5YR5/6) mottles (20% volume) impregnating matrix of peds. Strong, subangular blocky structure; very few living roots, diffuse boundary. Some gypsum crystals	
3Bty (BG 15-193)	40-65	Greyish brown (10YR5/2) medium sandy clay with few brown (7.5YR5/4) mottles of Fe-ox coating or infilling root channels (mangrove pneumatophores and seagrass); weak, medium subangular blocky structure; very few living roots, graded, sharp boundary	
4Bjy (BG 15-194)	65-95	Dark greyish brown (10YR3/2) clayey peat with many pale brown (10YR6/3) mottles (25% volume) of jarosite around root channels, up to 5 mm thick, and some distinct dark brown (7.5YR4/4) mottles of Fe-ox coating root channels; weak, subangular blocky structure; non calcareous; no living roots, common dead roots; sharp and smooth boundary	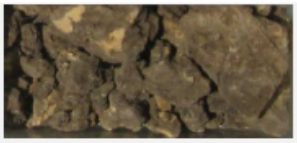
5Oijg (BG 15-250)	95-110	Dark greyish brown (10YR3/2) organic sandy peat with many pale beown (10YR6/3) mottles (20% volume) of jarosite impregnating matrix; weak; layered mat structure (dominated seagrass fragments); non calcareous; no living roots; sharp and smooth boundary	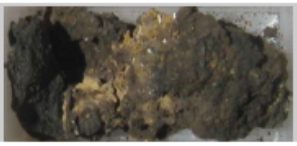
6Bijg/W1 (BG 15-196)	110-120	Light brownish grey (10YR6/2) medium sand with prominent light brownish grey (2.5Y6/2) jarosite mottles (5% volume) along root channels and seagrass fibres up to 5 mm thick; sand texture; weak single grain structure; non calcareous; no roots; diffuse boundary	
6Bg/W2 (BG 15-251	120-150	Dark greyish brown (10YR4/2) medium sand with no mottles; weak single grain structure; non calcareous; no roots and diffuse boundary	
7Bg/W1 (BG 15-252)	150-170	Dark greyish brown (10YR4/2) (gleyed) sandy clay no mottles; strong blocky structure; non calcareous; no roots	

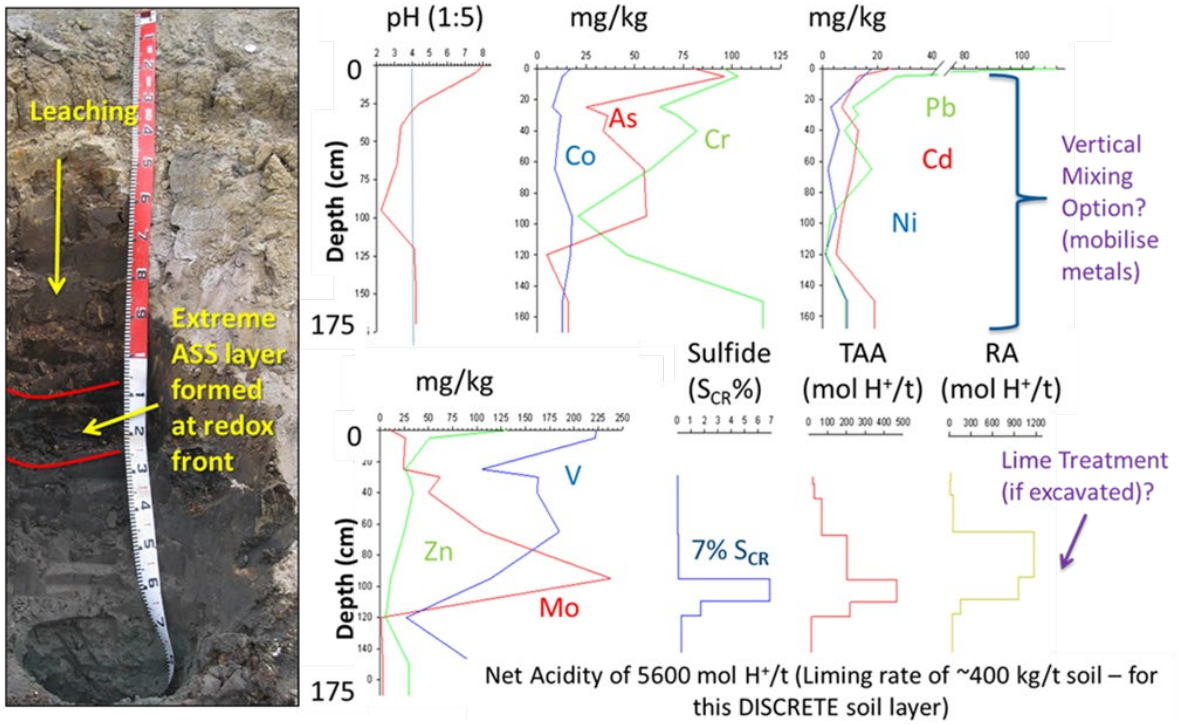

Figure 57: Profile BG15 - down profile characteristics for Acid Base Accounting and metal contaminants

Soil profile BG 15 (Table 23) is located at a lower position in the landscape. Although the profile looks similar BG 11, it was deposited in a calmer setting with a slower rate of deposition and fewer episodes of exposure (tidal and seasonal). This 'back barrier' depositional environment allowed more organic matter to accumulate and also concentrated heavy minerals (such as pyrite) in sandy layers. In profile BG 15 a thick layer (30 to 160 cm depth) of sulfuric material contains high amounts of existing acidity and extremely high Potential Sulfidic Acidity (PSA). The reduced inorganic sulfide content if this Sulfuric material measured up to 6.88% SCR remaining in the profile. Below the acidic water table, sulfuric material also contains minor amounts of AVS in black mottles.

The very high SCR levels measured in profile BG 15 may be natural (historically high in sediments of the 'back barrier' formation, however the down profile leaching and nutrient rich hypersaline groundwater water is probably contributing constituents for the formation of FeS and FeS2 in the saturated soils. Soil profile near other stranded tidal creeks at Gillman have similarly elevated SCR values (maximum of 7.05%) and are also influenced by hypersaline waters.

The Gillman area has a long and complex history of contaminating landuses, that includes 100 years as a firing range overshoot area, contributing high metal contents to the surface soils. Acidification has contributed to the mobilisation of oxidation products and metals within the landscape. In profile BG 15, metals such as Pb, As, Cr, Ni and Zn have leached DOWN the profile to accumulate at the present day oxidation front to re-form at the layer of Extreme Potential and Existing Acidity. These processes occur laterally at the landscape scale. The distribution of metals and acidity within a profile has implications for Vertical MIXING of ASS as a management technique. Filling over the sulfuric profiles at Gillman has potential to raise the acidic groundwater table and bring it into contact with the metal contaminated topsoils. Acidification and salinization of fill may also occur through capillary rise, resulting in corrosion of infrastructure.

Profile BG 17 on salt scalded mud flats – PROFILE OF FIELD VISIT STOP 3

Table 23: Summary of soil morphology for profile BG 17: Moist, poorly drained, bare salt scalded mud flat. Salidic Sulfaquepts (Soil Survey Staff 2022); Peaty, Sulfuric, Hypersalic Hydrosol (Isbell and National Committee on Soils & Terrain, 2021)

Horizon (ID)	Depth (cm)	Soil morphology	Sample (frame size: 5 x 2.5 cm)
AE (BG 17-236)	0-10	Very dark greyish brown (10YR3/2) sandy loam with some dark yellowish brown (10YR4/4) mottles; friable structure; weak consistency without coarse fragments; abundant fine roots; gradual and smooth boundary	
2Bjg1 (BG 17-238)	10-25	Dark greyish brown (10YR4/2) sandy loam some diffuse light yellowish brown (2.5Y6/4) mottles (5%:volume) penetrating peds; weak consistency without coarse fragments; no roots; diffuse wavy boundary	
2Bjg2 (BG 17-239)	25-40	Dark greyish brown (10YR4/2) loamy sand with common prominent light yellowish brown (2.5Y6/4) mottles (20%:volume) penetrating peds; weak consistency without coarse fragments; no roots; diffuse wavy boundary	
3Bjg1 (BG 17-240)	40-60	Very dark greyish brown (10YR3/2) loamy sand with common prominent light yellowish brown (2.5Y6/4) mottles (20%:volume) penetrating peds and forming along macropores up to 5 mm thick (mangrove pneumatophores) and organic matter and some distinct dark brown (7.5YR4/4) mottles of Fe-ox in the centre of root channels; weak consistency without coarse fragments; no roots; diffuse wavy boundary	
3Bg/W2 (BG 17-241)	60-100	Very dark grey (10YR3/1) medium organic rich sand with no mottles; weak single grain structure; non calcareous; no roots; gradual and smooth boundary	
4Bg/W1 (BG 17-242)	100-120	Dark greyish brown (10YR4/2) medium sand with no mottles; weak single grain structure; non calcareous; no roots	

Acid Sulfate Soil Characteristics

Soil pH testing (pHW, pHOX and pHIncubation) see Figure 58

Soil-water pH (pHW) indicated all soil layers were acidic, ranging from 2.4 to 3.4 (mean pHW of 2.5). The pHOX results suggest that although the samples are already acidic, one soil sample contains enough sulfidic material to further significantly drop the pH. After incubating soil samples for at least 19 weeks, only the surface sample showed a further drop in pH. The vast majority of samples showed a slight rise in pH of between 0.5 and 1 pH unit. The pH of soil horizon 4Bg/W1 (the deepest layer) rose substantially following incubation, from pHw 3.06 to pHIncubation 4.74. This rise may be

attributed to incubation samples being too moist, allowing reformation of sulfides to occur, and/or the soil carbonate present to react.

Existing acidity (Titratable actual acidity (TAA) and Retained acidity)

All six samples analysed had a pHKCl of <6.5 (Figure 58), indicating they contain Existing Acidity as TAA, which ranged between zero (in the surface layer) and 140 mole H+/tonne of soil in the 3Bjg1 layer (at 40 to 60 cm depth). The mean TAA value was 38 mole H+/tonne) (Figure 6-6). Retained acidity was measured on all 6 samples and ranged between 87 mole H+/tonne at the base of the profile to 524 mole H+/tonne in the 2Bjg2 layer (25 to 40 cm depth) (Figure 58). The mean retained acidity value for the profile was 240 mole H+/tonne.

Chromium Reducible Sulfur (SCR)

Reduced inorganic sulfur was detected in all 6 horizons sampled indicating that they all contain potential sulfidic acidity. SCR values ranged form 0.01% for the two upper soil layers to 4.41% SCR in a gleyed, very dark grey sandy soil layer 3Bg/W2 (from 60 to 100 cm). The profile had a mean SCR value of 1.22%. The bottom three soil horizons were analysed for AVS due to the presence of dark grey to black mottles. AVS contents were low and ranged from 0.01 to 0.03% AVS.

Acid Neutralising Capacity (ANC)

All samples had a pHKCl below 6.5 indicating they contain zero effective ANC.

Net Acidity

Net Acidity values were positive for all soil layers assessed and range between 110 mole H+/tonne at the surface to 2798 mole H+/tonne at between 60 and 100 cm depth. The soil layer above (40 to 60 cm depth) had a similarly elevated net acidity of 2056 mole H+/tonne. The mean net acidity value for profile BG 17 was 1037 mole H+/tonne. The majority of the acidity in profile BG 17 is in the form of Potential Sulfidic Acidity.

Acid sulfate soil classification: According to the acid sulfate soil terminology adopted (refer to Table 22; Table 23), soil profile BG 17 classifies as an acid sulfate soil, containing; sulfuric material, hypersulfidic material and monosulfidic material.

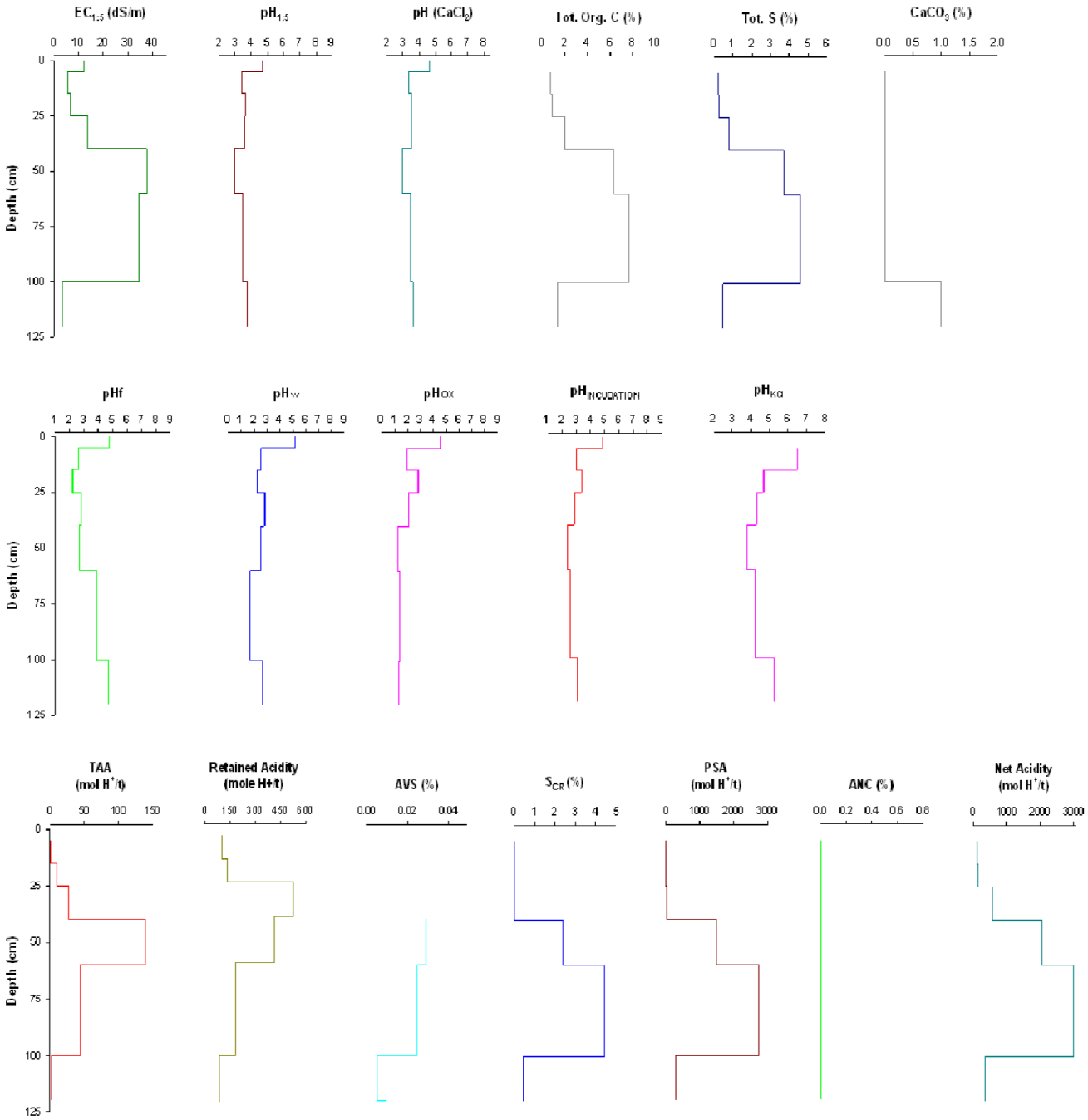

Figure 58: Down profile soil chemistry and acid sulfate soil characteristics of profile BG 17

Wet (subaqueous): poorly drained, erosional channel – water

Profile BG P 5 (Table 24) originally developed in an intertidal to supratidal regime. Profile BG P 5 occurs in a pond that was excavated during the construction of the Range Wetland in 1992 and has since been filled with saline and iron-rich groundwater being pumped via windmills (Figure 49, Figure 50, Figure 59). The black surface Oa/W1 and Ag/W1 horizons (from 0 to 10 cm) comprises wet, organic matter rich, light clay with a gel-like or ooze consistency. The black colour and ooze-like consistency is a good indicator of strongly reduced redoximorphic conditions and indicates the likely

presence of monosulfidic material (i.e. AVS). Underlying B horizons (from 10 to 60 cm) consist of gleyed, dark olive grey clays with abundant black mottles. Clay content increased with depth.

Table 24: Soil profile BG P 5 classifies as: Sapric Sulfiwassists (Soil Survey Staff 2022) and Sapric Monohypersulfidic Intertidal Hydrosol (Isbell and National Committee on Soils & Terrain, 2021)

Horizon (ID)	Depth (cm)	Soil morphology	Sample (frame size: 5 x 2.5 cm)
Oa/W1 (BG P 5-310)	0-5	Black (5Y2.5/1) without mottles; massive structure; weak (gel-like when wet) consistency without coarse fragments; no roots; gradual and smooth boundary	
Ag/W1 (BG P 5-307)	5-10	Very dark grey (5Y3/1) without mottles; massive structure; weak (gel-like when wet) consistency without coarse fragments; no roots; gradual and diffuse boundary	
2Bg/W1 (BG P 5-308)	10-25	Dark olive grey (5Y3/2) medium clay without mottles; massive structure; weak consistency without coarse fragments; non calcareous; no roots; diffuse boundary	
3Bg/W1 (BG P 5-309)	25-60	Olive grey (5Y4/2) heavy clay with some pale olive (5Y6/4) mottles (10% volume); massive structure; firm consistency without coarse fragments; non calcareous; no roots	

Soil profile BG P 5 contains hyposulfidic material and monosulfidic material (with up to 1.14% AVS) in ear surface layers.

The extent of the inter-tidal areas is being constrained by existing water levels in the Range wetland, which is a freshwater system from stormwater runoff, to ensure that it does do not compromise the function of a freshwater wetland through salt-water intrusion. As such, groundwater interception is required in this area as the normal level of the shallow hypersaline groundwater is above the intended water level of the freshwater Range wetland ponds. The construction of interception drains are laid beneath the area using a system of windmills as shown in Figure 59 (a), which are connected to these drains and continuously pump saline groundwater allowing a freshwater lens to develop beneath the Freshwater Range wetland ponds. The groundwater table also lowers the zone affected by capillary rise in the adjacent mound shown in Figure 59. Flows from windmills are gravity discharged into a saline discharge pond shown in Figure 59 (a) and (b).

However, the saline groundwater is saturated with ferrous iron, which precipitates when exposed to air as reddish-brown sludge comprising of bacterial cells and the mineral ferrihydrite as determined by X-ray diffraction in 2002. This slimy residue then sticks to the pipes and windmill pumps causing clogging of the pipes. The iron oxidising bacteria (mostly *Gallionella* spp. and *Lepothrix* spp) in the shallow groundwater get their energy from decomposing organic matter and from oxidizing dissolved ferrous iron or manganese in groundwater. Once a month a "pig" tool (see Figure 59) is sent down the windmill pipelines and is propelled by the pressure of the windmill pump flow in the pipeline to remove the iron precipitates that have accumulated in the pipes.

(a)	(b)	(c)

Figure 59: Photographs showing: (a) the windmill in background and black pipeline in foreground, (b) reddish-brown iron-rich precipitate/ sludge and saline groundwater being discharged from the black pipe connected to windmills, which are linked to interception drains beneath the area to continuously pump saline groundwater allowing a freshwater lens to develop beneath the Freshwater Range wetland ponds and (c) a so called "pig" tool, which was sent down the pipeline site by council workers during our field visit to the to the site. The pig tool is propelled by the pressures from the windmill pump flow in the pipeline to remove the iron precipitates that have accumulated in the plastic pipes shown in all three photographs. A sample was taken of the reddish-brown iron-rich precipitate from the "pig" tool for X-ray diffraction analyses.

Disturbed tidal zones with hypersulfidic material

In several parts of Barker Inlet, bund walls were also constructed across tidal zones nearly 50 years ago to cut off tidal flushing for construction of numerous salt evaporation ponds for commercial salt extraction. In most of these contemporary and abandoned evaporation pond mixtures of hypersulfidic materials and MBO occur to produce a wide range of soil types (Table 12).

Figure 60: A (left) Soil pit in an abandoned commercial salt evaporation pond showing about 25 cm of black hypersulfidic and mainly MBO materials overlying >50 cm of gleyed clay, B (centre) Deep excavation at Barcoo Outlet (connecting the Patawolonga with the sea) and construction site through a sand ridge showing a relict hypersulfidic material buried under beach dunes (from a former mangrove swamp). C (right) Soil pit near Gillman, Port Adelaide showing about 70 cm of calcareous clayey dredge spoil, used to raise the land surface, overlying 80 cm of relict sapric hypersulfidic material (derived from a former mangrove swamp) and underlain at 140 cm by coarse shelly material. (from Fitzpatrick et al. 2008b,c).

Sandplains and dunes overlying hypersulfidic material

There is evidence of relict, buried, hypersulfidic material formed in mangrove soils below sand dunes in the Adelaide and Port Adelaide areas, but these layers are likely to be maintained below the water table. Excavation through sand dunes is expected to be uncommon. It is common to see iron oxide materials staining beaches. We have observed oxidation of iron sulfides leaving iron oxide staining on beaches; however neutralising capacity is provided through tidal flushing and carbonate minerals within the sand. Consequently, these deep, sandy, relict ASS types fall into the treatment category "Low" (Table 12).

Relict, buried hypersulfidic material formed in mangrove soils has also been found below calcareous clays (probably with significant terrestrial input) at Price on upper GSV (Merry et al., 2003). The peaty hypersulfidic material usually has both high organic carbon and total sulfur contents, with a strong H_2S smell. Although the overlying clay (upper 40 cm) is often significantly calcareous, the relict hypersulfidic material contains insufficient buffering to neutralise the acid potentially produced, should the material be exposed to the air. The presence of these peaty hypersulfidic layers being about 80-100 cm thick also presents a high risk of de-watering under load with consequent consolidation. Indicator shells (Anadara) confirm that at least some of the buried mangrove sediments observed in GSV are older than 120 000 years.

Anthropogenic fill materials overlying buried hypersulfidic and sulfuric materials

Much of the land surrounding Barker Inlet has been progressively filled since the early 1900s to raise the land surface above the high tide mark. The fill material has been sourced from all over the Adelaide region and includes a mixture of clays, sands, building rubble and industrial by-products such as slag. Dredged sediments from the Port River were commonly disposed of on land to produce a range of hypersulfidic and sulfuric Anthroposols (Table 12). Here and elsewhere, these buried materials lie below road fill and constructions in coastal areas.

It is likely that some of this fill material was hypersulfidic when it was dredged, and has since oxidised. In most cases sufficient carbonate would have been present in the sediment to neutralise the acid generated as the pyrite oxidised, but this may not always be the case. Disposing of hypersulfidic sediments on land always presents some risk to the environment.

Stop 4: St Kilda Mangroves

Contemporary tidal zones with sulfidic materials and site of hypersaline contamination event in 2020.

St Kilda illustrates a modern tidal floodplain with mangrove and samphire marsh environments comprising a range of organic rich acid sulfate soils with hypersulfidic, hyposulfidic and monosulfidic materials. In 2020, the South Australian Government became aware of the death of saltmarsh and mangrove vegetation near St Kilda, adjacent Section 2 of the Dry Creek Salt Fields. Extreme hypersaline water leakage from the adjacent retired salt evaporation pond was the likely cause.

Figure 61: Google maps of the St Kilda mangroves. The boundary between the salt ponds and the mangroves can be seen.

The St Kilda Mangroves are owned by the Crown, under the care and control of Salisbury Council. There is strong community interest from City Councils and community groups.

Constructed in 1984, the St Kilda Mangrove Trail and Interpretive Centre includes a two kilometre boardwalk showcasing the mangrove forest of the Barker Inlet Aquatic Reserve. The grey mangroves of St Kilda are part of the largest mangrove estuary, and the most significant nursery for recreational and commercial fish species in Gulf St Vincent. The mangroves are low lying land with elevation ranging from -1.0 m AHD on the tidal mudflats to 1.5 m AHD on the intertidal chenier ridges (Figure 62). Networks of tidal creeks run in an east to west direction through the saltmarsh and mangrove areas. These creeks adjoin remnant creek channels in the adjancent salt ponds. The mangrove zone is flooded and drained twice daily with the tides. This tidal movement assists the oxygenation of the soils that the trees grow in. Over 200 species of birds have been recorded in the coastal wetlands of the Barker Inlet. Within sight of the boardwalk there are many bird habitats. The vegetation type and species in the intertidal zone is directly related to the topography and consequent degree of tidal inundation. The shrubby samphires (small red or green shrubs belonging to the same family as saltbushes) offer shelter and food for insect and seed eating birds such as fairy wrens, chats and thornbills. Wading birds survey the shallow samphire pools for tiny crustaceans and worms. At low tide the seagrass beds become feeding grounds for many birds including black swans.

The bund walls of the saltfield, which run north/north-west to south, are the highest land features in the area, between 1.5 and 2.75 m AHD high. The old bund wall (the current St Kilda Mangrove boardwalk) is lower at 1.5 m to 2.0 m AHD high. It was built in the 1890s by scouring sediment from either side of the levee to form the embankment. There are several breached sections along its length which allow tidal flushing through creek lines into the intertidal area east of the boardwalk bund. The boardwalk bund joins a 3 m AHD high embankment that runs east-west beside the St Kilda marina channel. The new bund wall ('Section 2 bund') separating Section 2 and the intertidal zone runs is 2.75 m AHD high and runs parallel to the boardwalk bund.

Comprehensive work on the soils in the St Kilda Mangoves was completed by (Thomas, 2010). This work was subdivided into three main focus areas (Figure 63). Focus area A was located close to open water and strongly influenced by tidal waves. The area has open water and mangrove vegetation. Focus area B is slighly elevated, noth south striking shell grit (chenier) ridgeline that was intermittently traversed by meandering tidal creeks. The area has bare shell grit ridges and mangrove vegetation Focus area C is located landward of the two other areas, and has supratidal samphire vegetation, mangrove vegetation and a permanently flooded tidal creek depression.

Soil Profiles and cross sections from each of these focus areas are shown below and can be located on Figure 64.

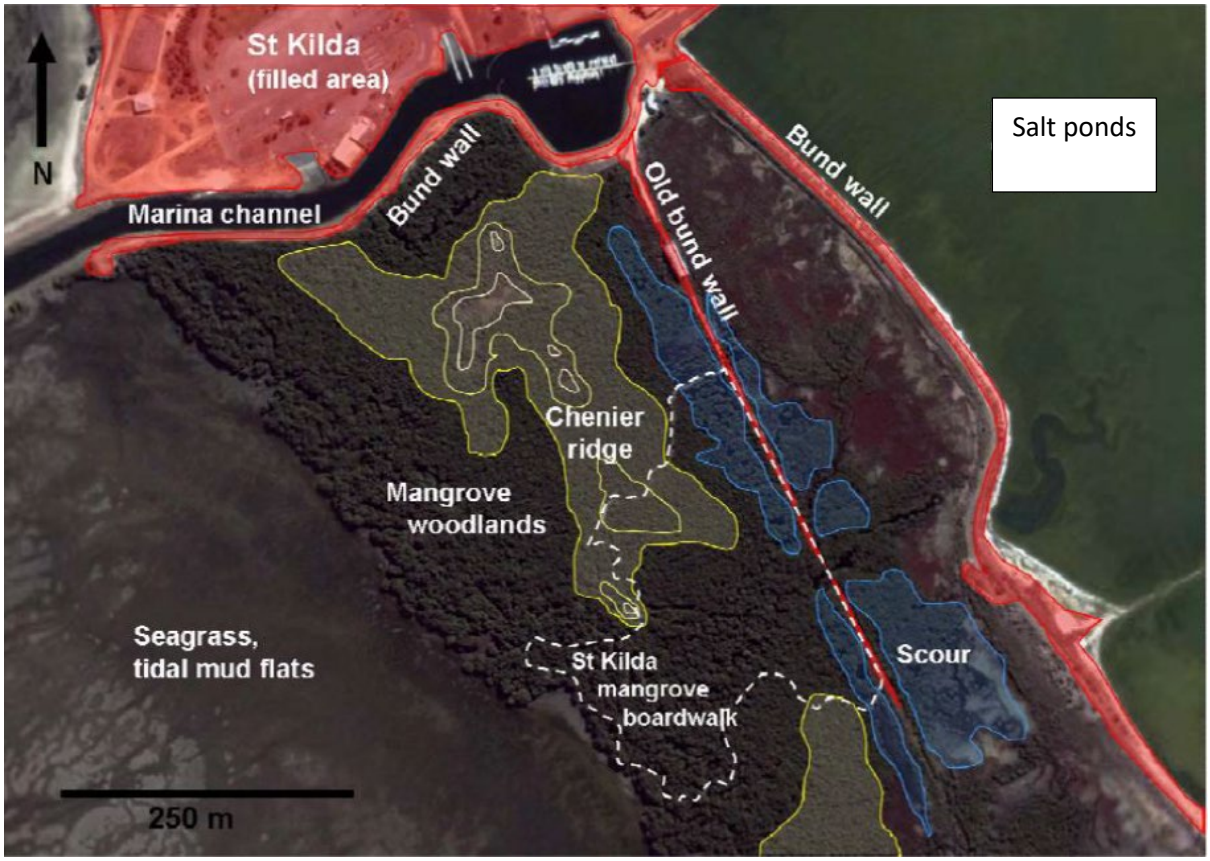

Figure 62: Aerial photograph of the St Kilda study site with major topographic features highlighted. The topography of the site is very much related to vegetation type, corresponding to tidal influence. Seagrass and mudflats occur in the lowest lying areas to the west of the site and are generally between -1.0 and 0.0 m AHD, mangrove trees cover the majority of the site where elevation ranges between 0.0 and 1.0 m AHD, while samphire vegetation occurs along shell-grit mounds that have less tidal influence, ranging 1.0 to 1.5 m AHD (Thomas, 2010).

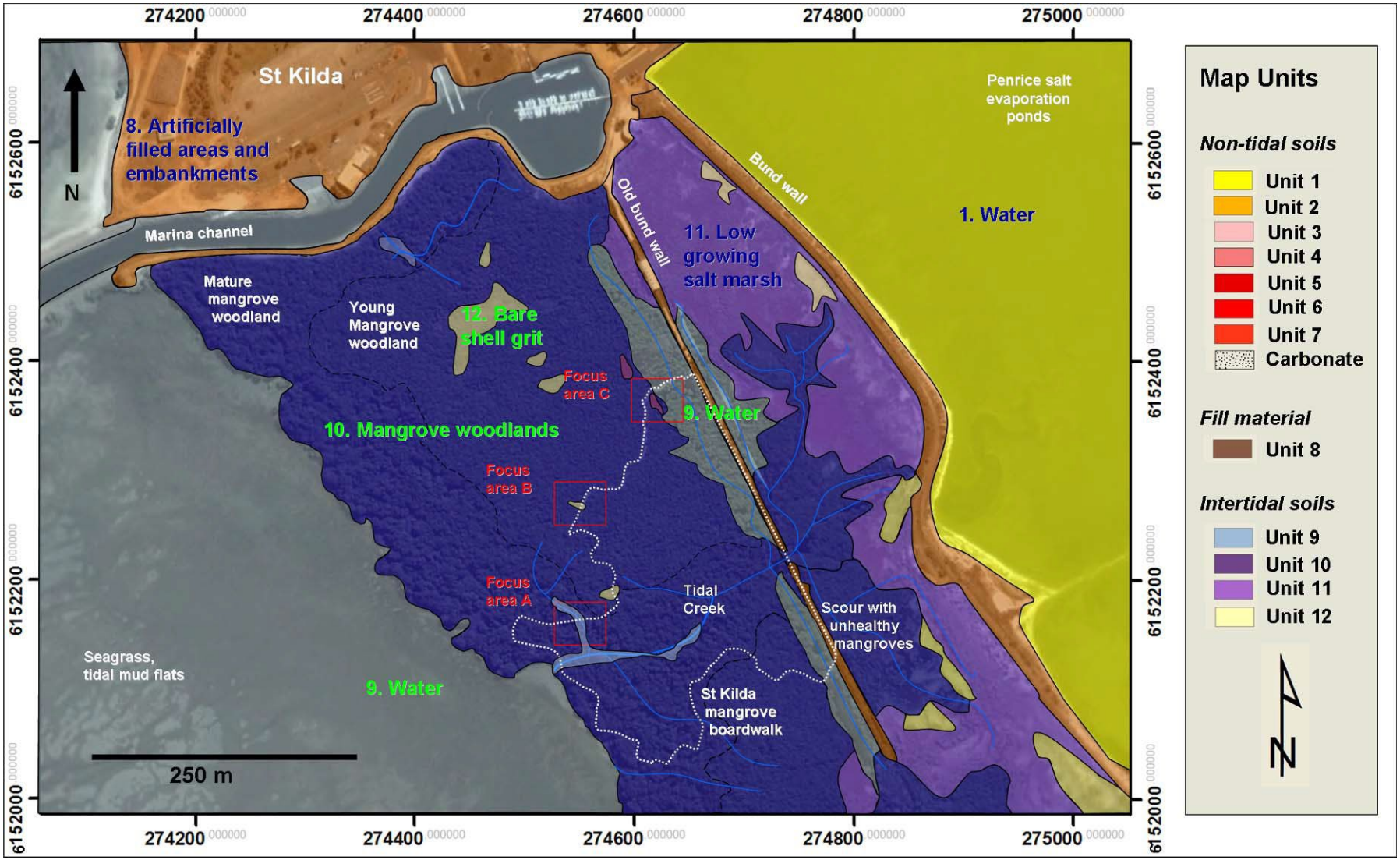

Figure 63: Soil-landscape map for the St Kilda study site. Refer to Table 18 for a detailed map legend and descriptions of Map units (From Thomas, 2010).

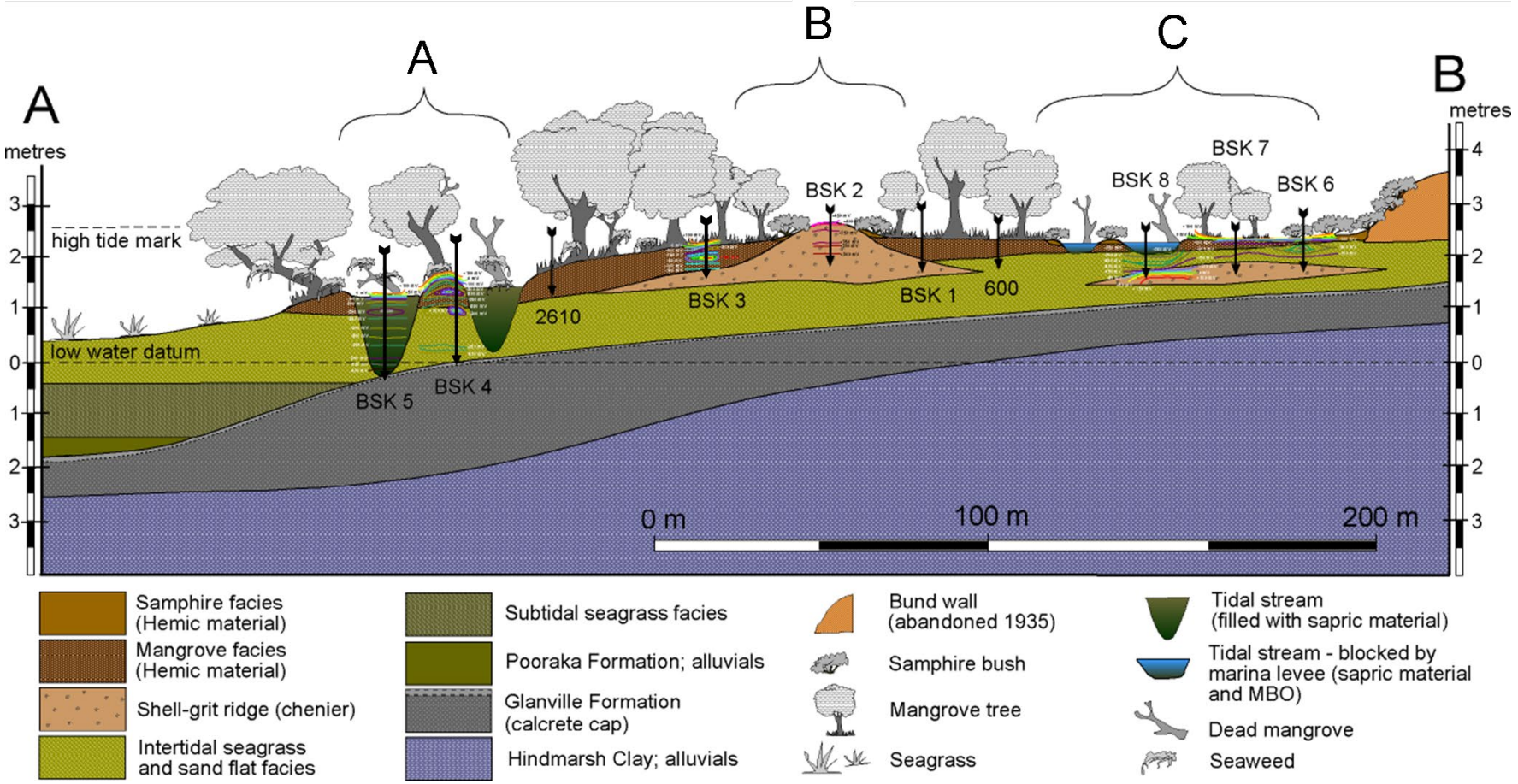

Figure 64: In the 1890s a levee bank was built from St Kilda to the south along the landward extent of mangrove vegetation. The bund wall was breached and abandoned in 1935 and there is now little evidence of soil acidification in the re-flooded area, but there is evidence of soil consolidation from drying and loss of organic matter. In some areas healthy mangrove soil is slowly being eroded away by outward flowing water through the tidal creeks. The creeks are filled with rotting organic matter such as sea-grass and ulva (sapric material) and causing extremely reducing conditions (Eh values down to –410mV). These soil conditions are "toxic" to the mangrove pneumatophores, which have to retreat to "higher ground" (less reducing soils). This leaves the creek banks very susceptible to erosion, further restricting the area in which pneumatophores can survive. When these areas become too small, the trees are unstable and easily knocked down during storms, killing them (From Fitzpatrick et al., 2008; Thomas, 2010).

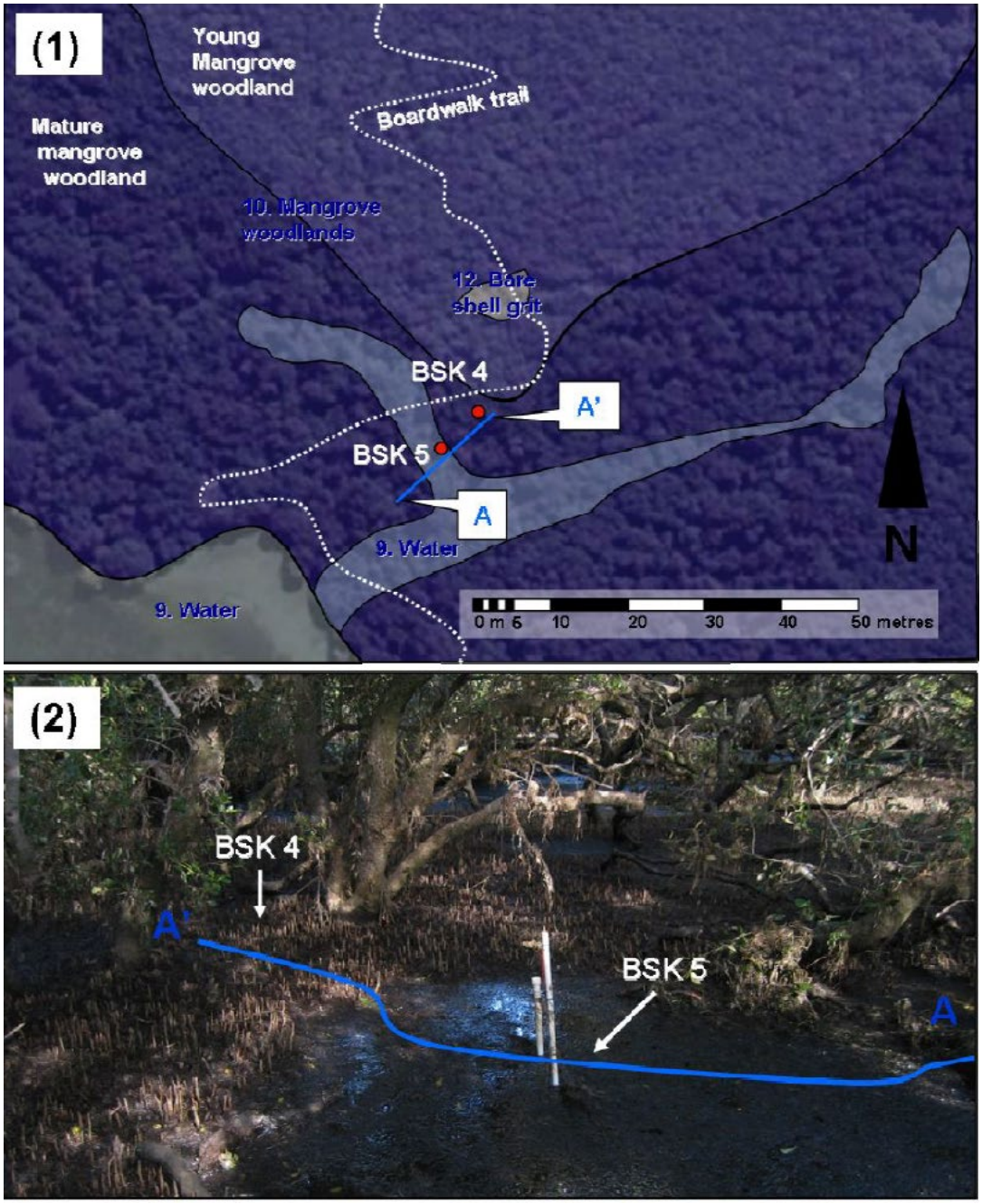

Figure 65: (1) Focus area C (2) landscape photo of when profiles were taken (Thomas, 2010).

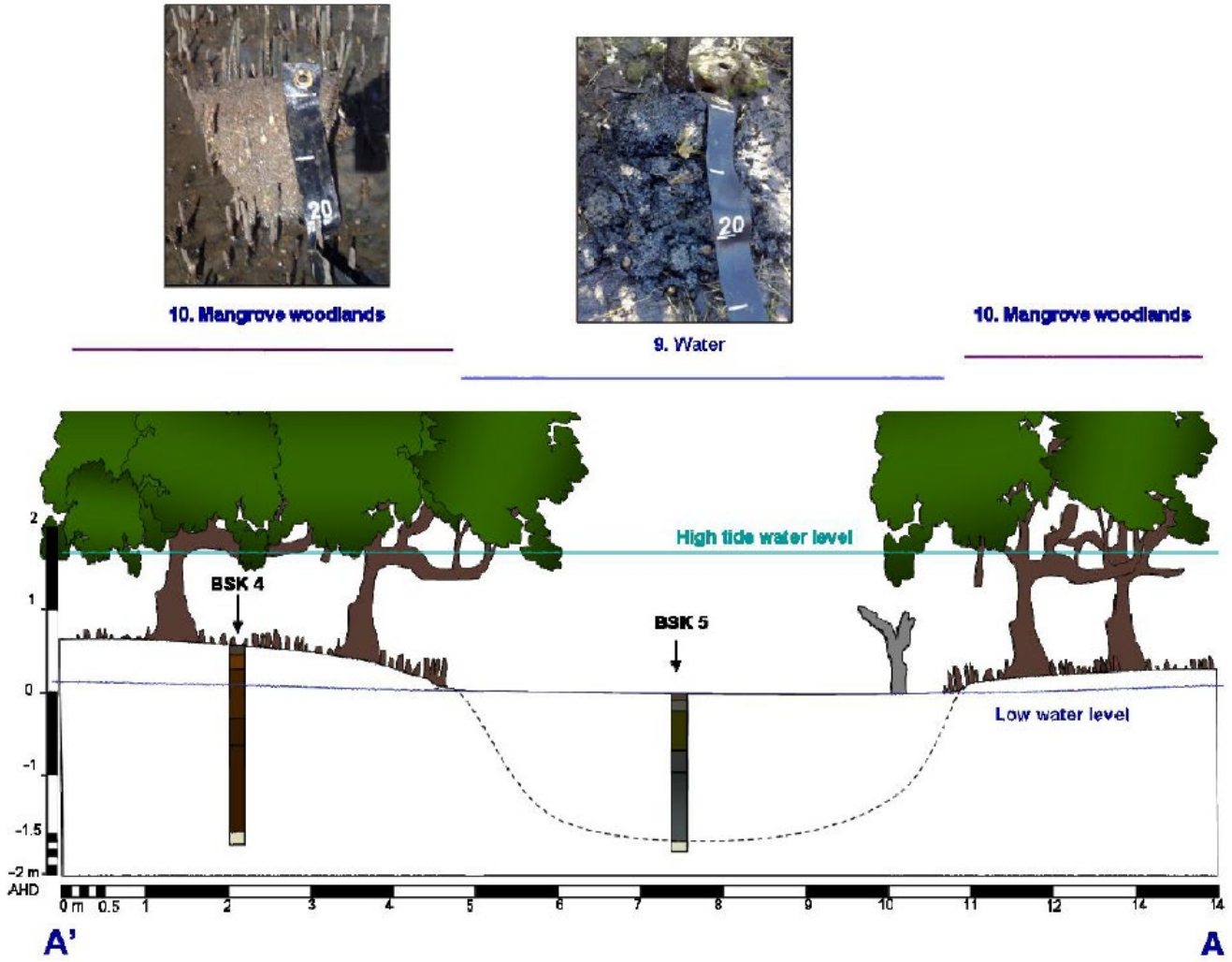

Figure 66: Cross section of Focus area C with position of BSK4 and BSK 5 (Thomas, 2010)

Table 25: Soil profile BSK 4 classifies as: Sapric Sulfiwassists (Soil Survey Staff 2014) and a Sapric, Histic-Hypersulfidic, Intertidal Hydrosol (Isbell and National Committee on Soils & Terrain, 2021) (modified from Thomas, 2010)

Horizon (ID)	Depth	Soil morphology	Sample (5 x 2.5 cm)
Oe/W1 (BSK 4-68)	0-5 cm	Very dark brown (10YR2/2) peat (5% mineral, 95% fibric and hemic material); abundant coarse live roots; diffuse boundary	
Oe/W2 (BSK 4-69)	5-10 cm	Very dark brown (10YR2/2) peat (5% mineral, 95% hemic material); abundant coarse live roots; diffuse boundary	
Oe/W3 (BSK 4-70)	10-20 cm	Very dark brown (10YR2/2) peat (5% mineral, 95% sapric and hemic material); abundant coarse live roots; diffuse boundary	
Oe/W4 (BSK 4-71)	20-50 cm	Black (5Y2.5/1) peat (5% mineral, 95% sapric and hemic material); some coarse live roots; diffuse boundary	
Oe/W5 (BSK 4-72)	50-90 cm	Black (5Y2.5/1) peat (5% mineral, 95% sapric and hemic material); no roots; diffuse boundary	
Oe/W6 (BSK 4-73)	90-110 cm	Very dark brown (10YR2/2) clayey peat (10% mineral, 90% sapric and hemic material); no roots; diffuse boundary	
Oe/W7 (BSK 4-74)	110-130 cm	Very dark brown (10YR2/2) clayey peat (10% mineral, 90% sapric material); no roots; diffuse boundary	
Oe/W8 (BSK 4-75)	130-150 cm	Very dark brown (10YR2/2) clayey peat (10% mineral, 90% sapric material); no roots; diffuse boundary	
Oe/W9 (BSK 4-76)	150-170 cm	Very dark brown (10YR2/2) peaty clay (15% mineral, 85% sapric material); no roots; diffuse boundary	
Oe/W10 (BSK 4-77)	170-190 cm	Very dark grey (10YR3/1) peaty clay (20% mineral, 80% sapric material); no roots; slight H_2S smell; clear wavy boundary	
Oek/W11 (BSK 4-78)	190-210 cm	Grey (10YR5/1) peaty clay (40% mineral, 60% sapric material); no roots; slight H_2S smell; some medium to coarse broken shell fragments.	

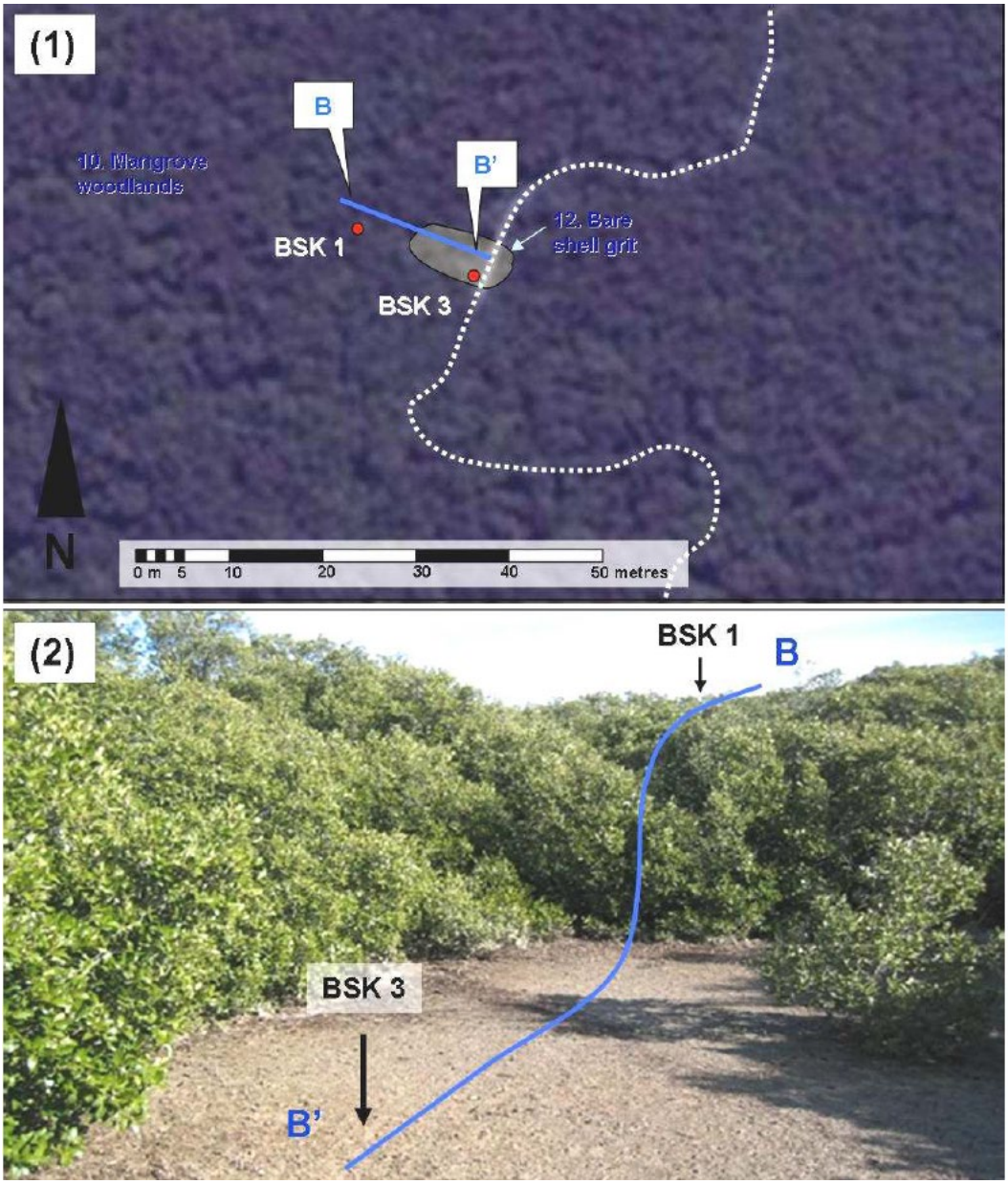

Figure 67 (1) Focus area C (2) landscape photo of when profiles were taken (Thomas, 2010).

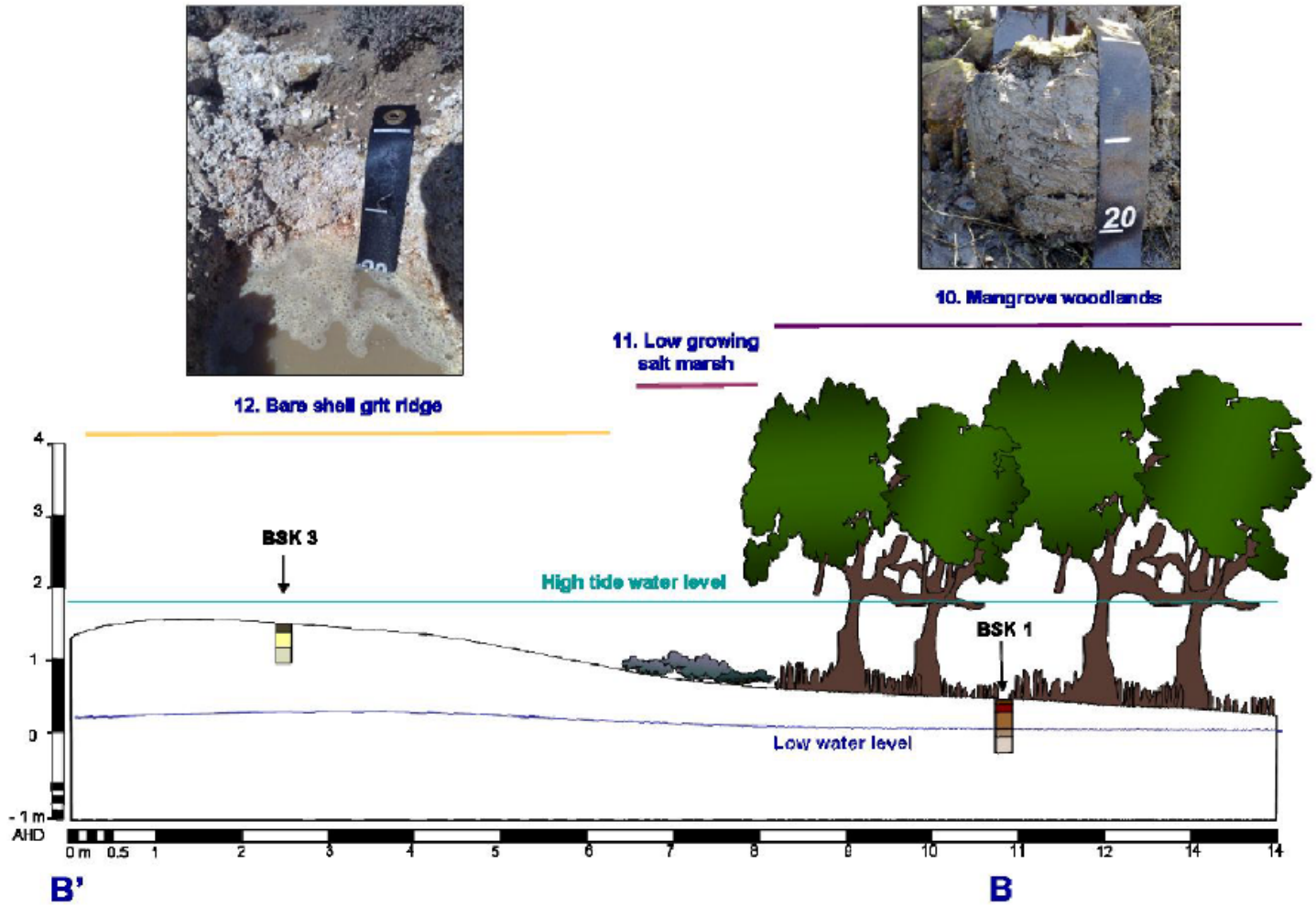

Figure 68: Cross section of Focus area B with position of BSK3 and BSK 1 (Thomas, 2010).

Table 26: Soil profile BSK 3 classifies as: Terric Sulfiwassents (Soil Survey Staff 2014) and a Hemic, Epicalcareous, Intertidal Hydrosol (Isbell and National Committee on Soils & Terrain, 2021)

Horizon (ID)	Depth	Soil morphology	Sample (5 x 2.5 cm)
Oa1 (BSK3-63)	0-5 cm	Very dark brown (10YR2/2) clay (10% mineral, 50% hemic material); many coarse and medium live roots; material; some coarse carbonate fragments with strong brown coatings (<5% volume); clear smooth, wavy boundary	
Oa2 (BSK3-64)	5-15 cm	Very dark greyish brown (10YR3/2) clay (30% mineral, 70% sapric material); many coarse and medium roots; minor H_2S smell; gradual wavy boundary. Some shell surfaces have strong brown coatings (<5% volume)	
B/W1 (BSK3-65)	15-30 cm	Light grey (10YR7/1) shell hash with some sapric material and some live roots. Minor strong brown (7.5YR 5/8) mottles on shell surfaces (5% volume). Carbonate shell fragments are coarse; diffuse boundary	
B/W2 (BSK3-66)	30-55 cm	White (10YR8/1) shell hash with abundant coarse broken shells. Few strong brown (7.5YR 5/8) mottles on shell surfaces (2% volume). Diffuse boundary	
B/W3 (BSK3-67)	55-70 cm	White (10YR8/1) shell hash with abundant very coarse broken shells.	

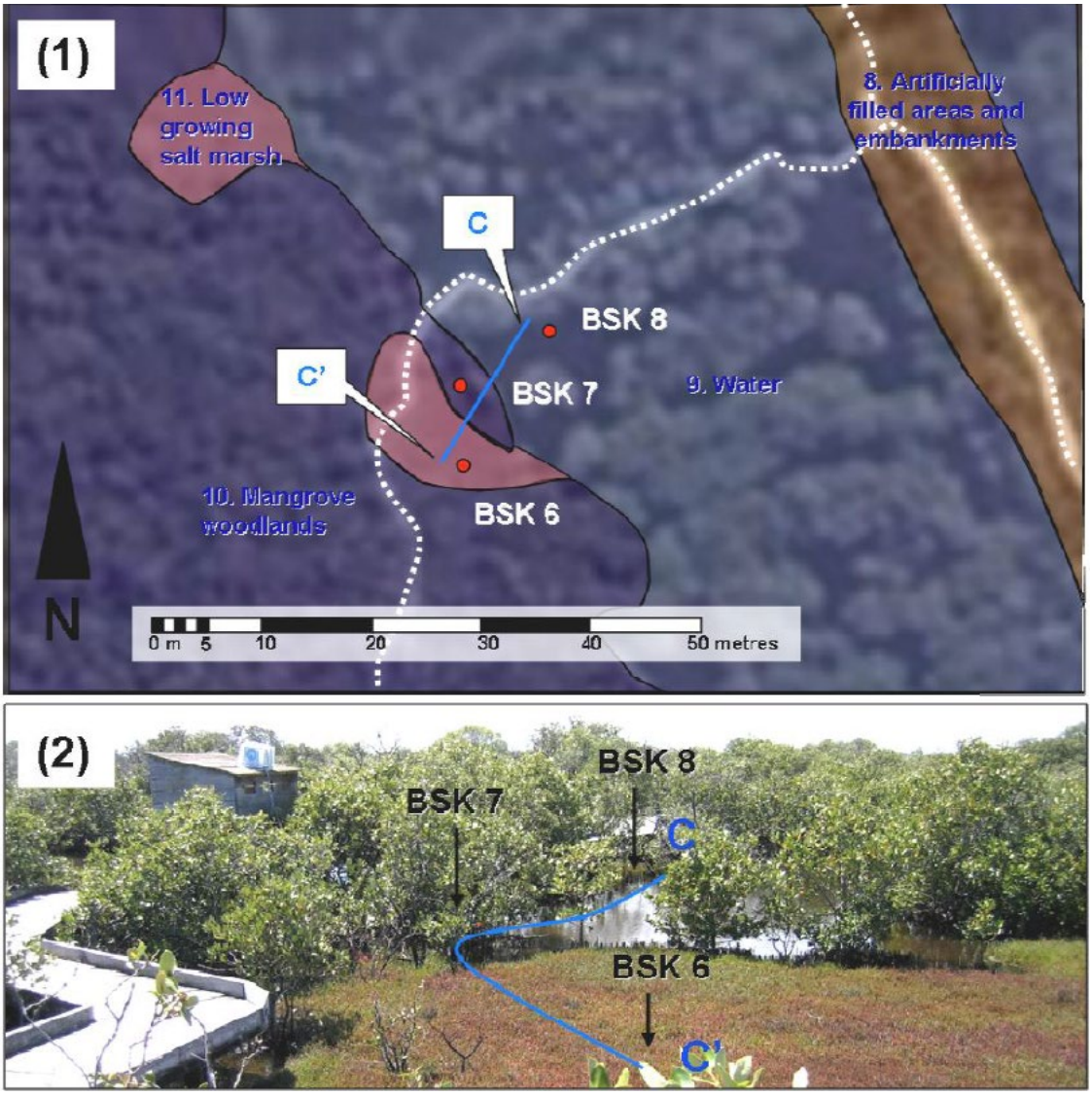

Figure 69 (1) Focus area C with profile below (2) landscape photo of when profiles were taken (Thomas, 2010).

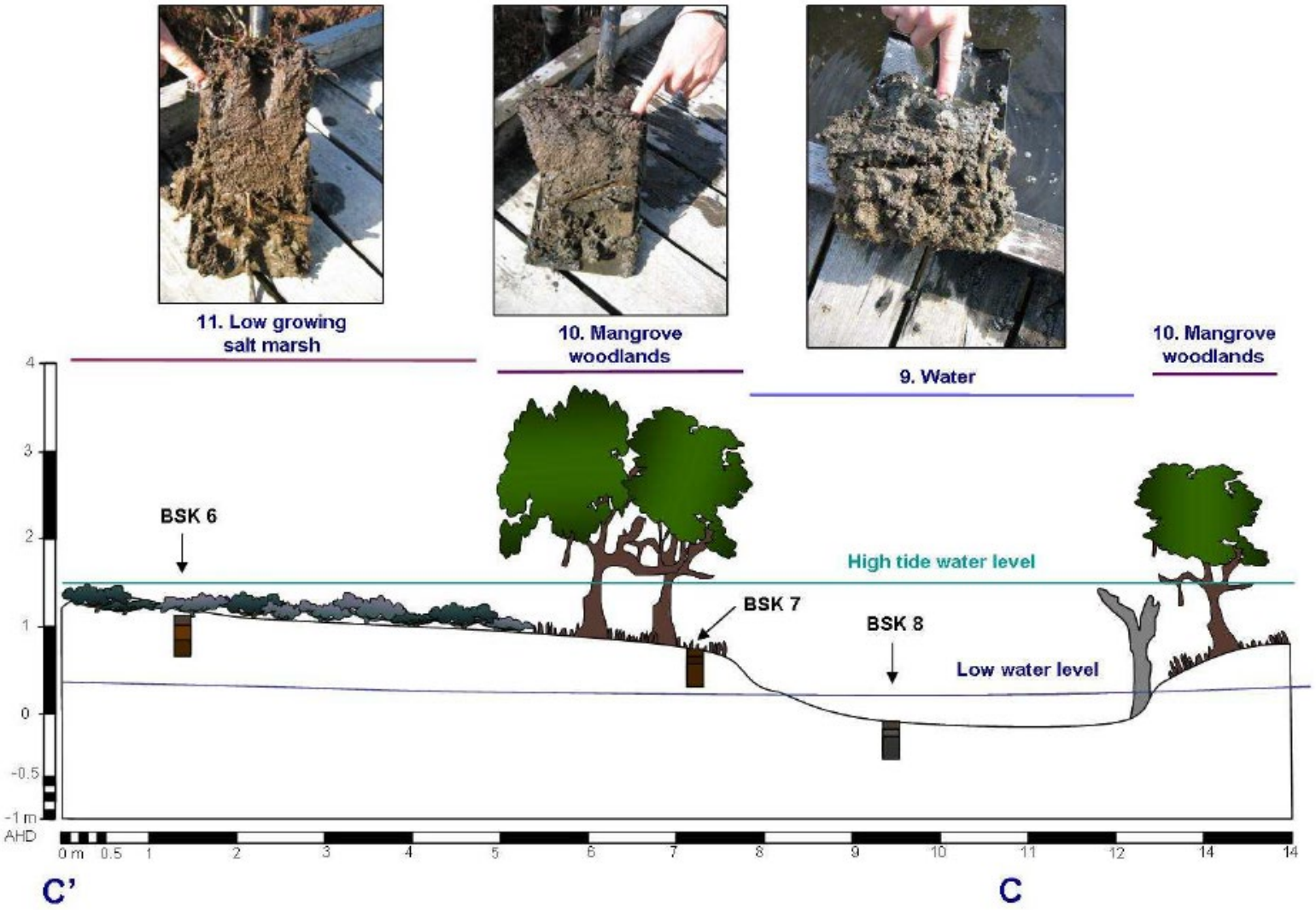

Figure 70: Cross section of Focus area A with position of BSK6, BSK 7 and BSK 8 (Thomas, 2010)

Table 27: Soil profile BSK 3 classifies as: Fibric Sulfiwassists (Soil Survey Staff 2010) and a Histic-Hypersulfidic, Intertidal Hydrosol (Isbell and National Committee on Soils & Terrain, 2021)

Horizon (ID)	Depth (cm)	Soil morphology	Sample (5 x 2.5 cm)
Oe/W1 (BSK 6-86)	0-5 cm	Very dark brown (10YR2/2) clayey peat (5% mineral, 95% fibric and hemic material); abundant coarse and medium live roots; minor strong brown (7.5YR5/8) mottles coating live root channels (<5% volume); diffuse boundary	
Oe/W2 (BSK 6-87)	5-15 cm	Very dark brown (10YR2/2) clayey peat (10% mineral, 90% fibric and hemic material); abundant coarse and medium live roots; few strong brown (7.5YR5/8) mottles coating live root channels (<2% volume); gradual wavy boundary	
Oe/W3 (BSK 6-88)	15-30 cm	Very dark grey brown (10YR2/3) peaty clay (20% mineral, 80% hemic material); many medium live roots; slight H_2S smell.	

Redox equipment was also installed by (Thomas, 2010) to see what impact oxidising and reducing conditions, tidal conditions, vegetation type and underlying geology had on acid sulfate soils.

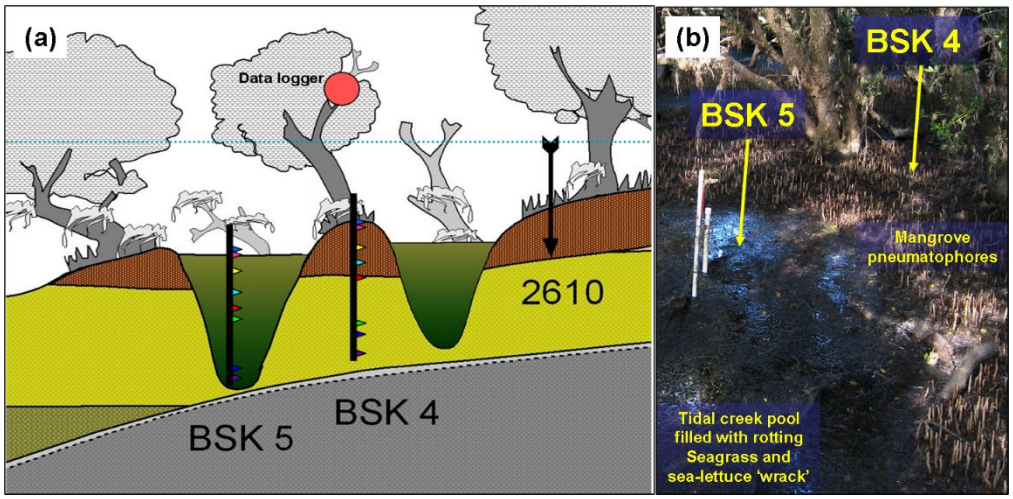

Figure 71: position of redox probes at BSK 5 and BSK 4 (Thomas, 2010)

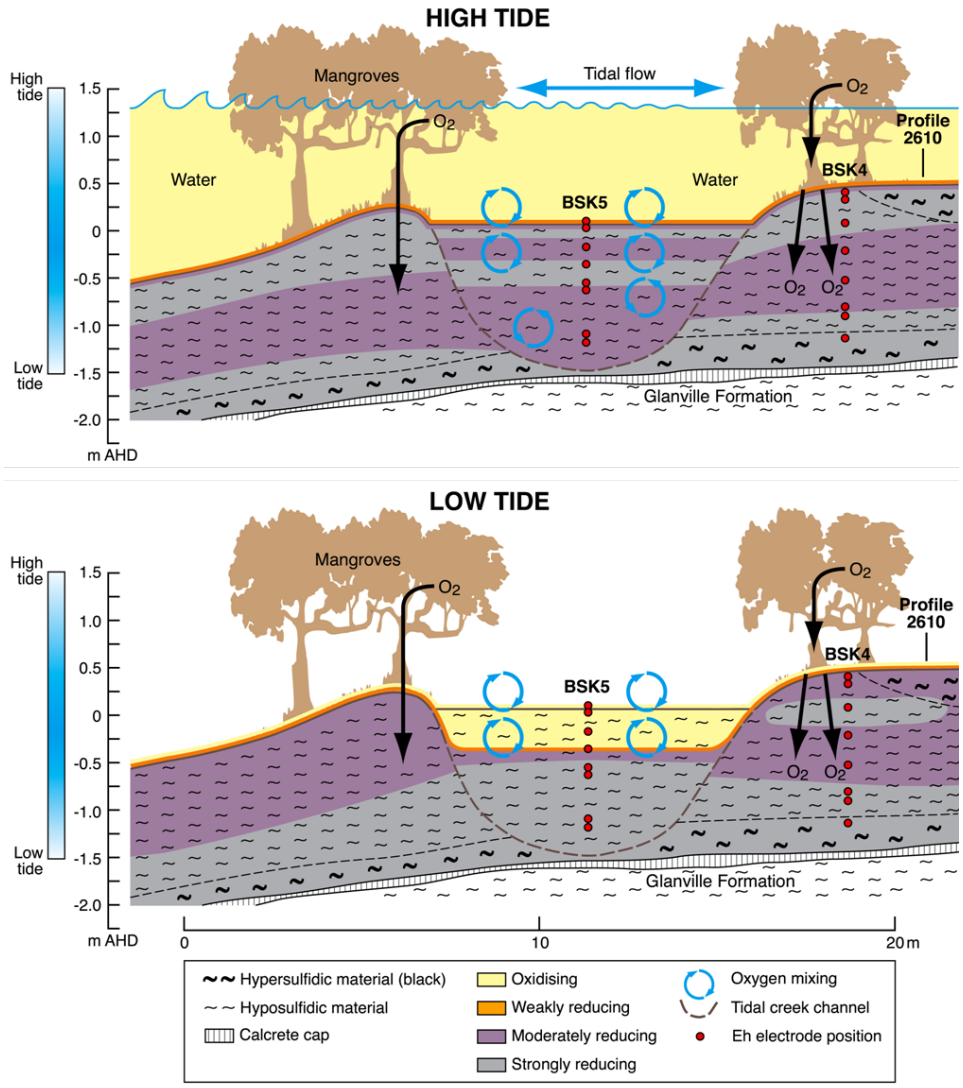

Figure 72: High and low tide redox condition in Focus area C from (Thomas, 2010)

2020 Hypersaline Brine Contamination:

In 2020, the South Australian Government became aware of over 24 hectares of saltmarsh and mangrove vegetation near death St Kilda, adjacent Section 2 of the Dry Creek Salt Fields.

Background:

The Dry Creek salt fields (4,000 ha) extend about 35 km from Dry Creek (Section 1) to St Kilda (Section 2) to Port Gawler (Section 3) to Middle Beach (Section 4) (Figure 73). Salt was produced at the site from the late 1930's by evaporating seawater pumped into a series of concentrating ponds to the point where common salt (NaCl or halite) precipitates. The less soluble salts, iron oxide (e.g. Fe(OH)3) and calcite (CaCO3), followed by gypsum (CaSO4.2H2O), were precipitated out during passage and evaporation of seawater along the chain of ponds. Salt production operation ceased in 2013. Since this time, a temporary 'holding pattern' was established at the site. The holding pattern allows seawater to be pumped into the northern section (Sections 4 and 3) with the intention of maintaining the salinity gradient and pond habitat for invertebrates and wading shorebirds. Currently brine exits Section 3 (from pond PA 5) and is pumped into the Bolivar channel where it is diluted with discharges from the SA Water waste treatment plant (to a target salinity of 45 g/L Total Dissolved Salts (TDS) – set by the South Australia Environment Protection Authority). The diluted water returns to Gulf St. Vincent. During the holding pattern, the ponds in Section 3 both increased in salinity and depth. Data suggests salinities were highly variable compared to that recorded during salt production operation phases (EPA data). This was due to more variable movement and control of salt through the system, compared to the salt production operation phase.

The southern sections (Sections 2 – adjacent the St Kilda Mangroves and 1) (Figure 73) were drained and dried from late 2013 onward. Various infilling activities have occurred in Section 1, while Section 2 has remained mostly dry between 2014 and 2019, except for pooling on the ponds following winter rainfall. During the time when the pond level was dry or very low, intertidal vegetation began to recolonise (evidenced from aerial images) in previously salt scalded areas directly west of the bund wall. The drying of the ponds, and subsequent pooling of winter rainfall followed by evaporation in summer between 2014-2019, altered the surface minerology and chemistry of the pond surface in Section 2, with the surface becoming dominant in both gypsum (CaSO4) and halite (NaCl). Cracking was also observed in the gypsum crust during this time. A part of Section 2 (PA 8, 9 and 10) was used for a wastewater trial in between 2015 and 2018. A low surface water level and low salinity was maintained during this trial and little evidence for impact of vegetation in the intertidal zone was observed during this time (from aerial images).

Over time, the availability of water from the SA Water waste treatment plant has declined, as water diversions to the Northern Irrigation Scheme increased. Consequently, there has been less wastewater available to dilute the brine from PA 5 in the Bolivar Channel and lower volumes of brine has been able to be discharged. In late 2019 and during 2020, to prevent build-up of water in Section 3, the brine was instead discharged in the ponds of Section 2 (adjacent the St Kilda Mangroves) and then moved south to Section 1. The pond level in Section 2 (PA 6,7, 8, 9 and 10) increased substantially during this time, to the highest level since the drying of the ponds when salt production ceased.

In September 2020, over 24 hectares of vegetation death in the intertidal zone adjacent Section 2 was observed, including 9 hectares of mangrove (see **Error! Reference source not found.**), 10

hectares of saltmarsh, and nearly 5 hectares of bare, sparsely vegetated, or aquatic ecosystems DEW (2021). A larger area of vegetation stress was identified by (Dittmann et al., 2022). Extremely hypersaline water (> 100-200 g/L TDS, **8 x seawater**) was observed in surface water, monitoring piezometers along the bund wall and intertidal zone, and extremely hypersaline sediments were recorded in transects affected by vegetation death.

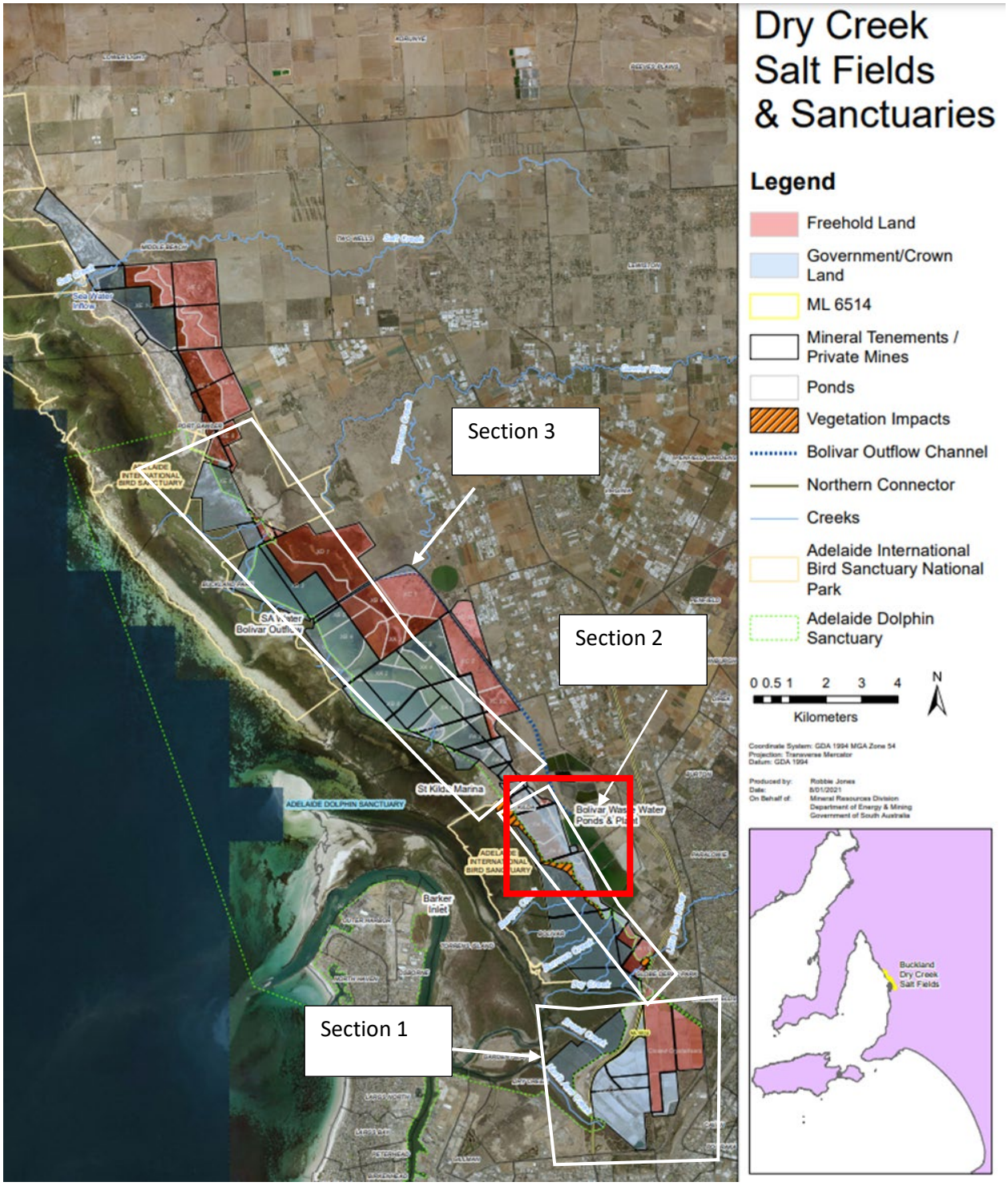

Figure 73: Salt field sections and land parcels, red square is the St Kilda area from Stop 4.

Figure 74: Photograph taken of Mangrove deaths along the St Kilda Mangrove boardwalk with Peri Colman (Principal Consultant, Delta Environmental Consulting) providing explanations of estuarine chemistry, mangrove ecology and entomology.

Key Findings:

At comprehensive report can be read with the below QR Code. Below is a summary of the findings from the report and the two conceptual models (Figure 75, Figure 76) developed by (Leyden et al., 2022).

The increase in the surface water level in Section 2 ponds of the saltfield from December 2019 to October 2020, due to discharge from Section 3, increased the recharge to the groundwater mound under the ponds. Surface cracking of the gypsum crust in the ponds further enhanced transport of surface water to the groundwater mound. The elevated groundwater mound under the ponds in Section 2 increased the hydraulic gradient towards the intertidal zone.

- Upon refill, the pond surface water became extremely hypersaline due to a combination of highly saline input water and dissolution of surface salts from the surface of Section 2 ponds.
- Due to hydraulic connectivity with the pond surface water, the groundwater underneath the ponds also became extremely hypersaline. This groundwater moved towards the intertidal zone under the increased hydraulic gradient.
- There are numerous hydraulic pathways of groundwater flow from the ponds to the intertidal zone, including remnant creek lines and transmissive sediments under the bund wall.
- As sediments became hypersaline and waterlogged in the intertidal zone, vegetation (saltmarsh, mangrove) death occurred rapidly. This was observed from mid to late 2020.
- Spatial satellite analysis determined retrospectively that 24 hectares of vegetation death was recorded in the intertidal zone adjacent Section 2, including 9 hectares of mangrove (see **Error! Reference source not found.**), 10 hectares of saltmarsh, and nearly 5 hectares of bare, sparsely vegetated, and aquatic ecosystems. It is likely there is a greater area which recorded vegetation stress following impact between the recorded dead vegetation zone and the healthy vegetation zone.
- It is probable that other ecosystem impacts occurred, like stress or acute toxicity to benthic invertebrates and fish communities, as well as changes in sediment/soil physical characteristics, however, there is currently no available ecosystem data to quantitatively assess these impacts.
- Once the surface water level reduced in Section 2, the recharge to the groundwater mound underneath the ponds in Section 2 decreased and the hydraulic gradient to the adjacent intertidal zone reduced. Less hypersaline groundwater was moving towards the intertidal area and tidal flushing diluted surficial sediment salinity in the intertidal zone.
- Sediments and tidal flushing are highly heterogenous and spatially variable across the intertidal zone of the affected area. Barriers (bunds, chenier ridges, sea wrack) to tidal flushing limit some sediments from benefiting from dilution by tidal water. This also reduce the ability of vegetation in these areas to recover from hypersalinity impact.
- Fine grained sediments (muds/clays), sediments in low elevation areas, deeper sediments and those close to the Section 2 bund remain higher in salinity than higher elevation, surface and coarser sediments further away from the Section 2 bund, some of which have returned to pre-impact salinity.
- Hypersaline water has been flushed from some surficial sediments, however, there is no recent data on the salinity of deeper sediments.
- Seedling emergence and regeneration has been observed in some limited areas (high saltmarsh), and propagules have been observed in the mangrove area since spring 2021, but the lack of recent vegetation survey data makes the quantitative analysis of vegetation recovery trends impossible. It is also unclear whether saltmarsh and mangrove species can survive once roots extend into deeper sediment layers (due to residual hypersalinity in the subsurface sediments).

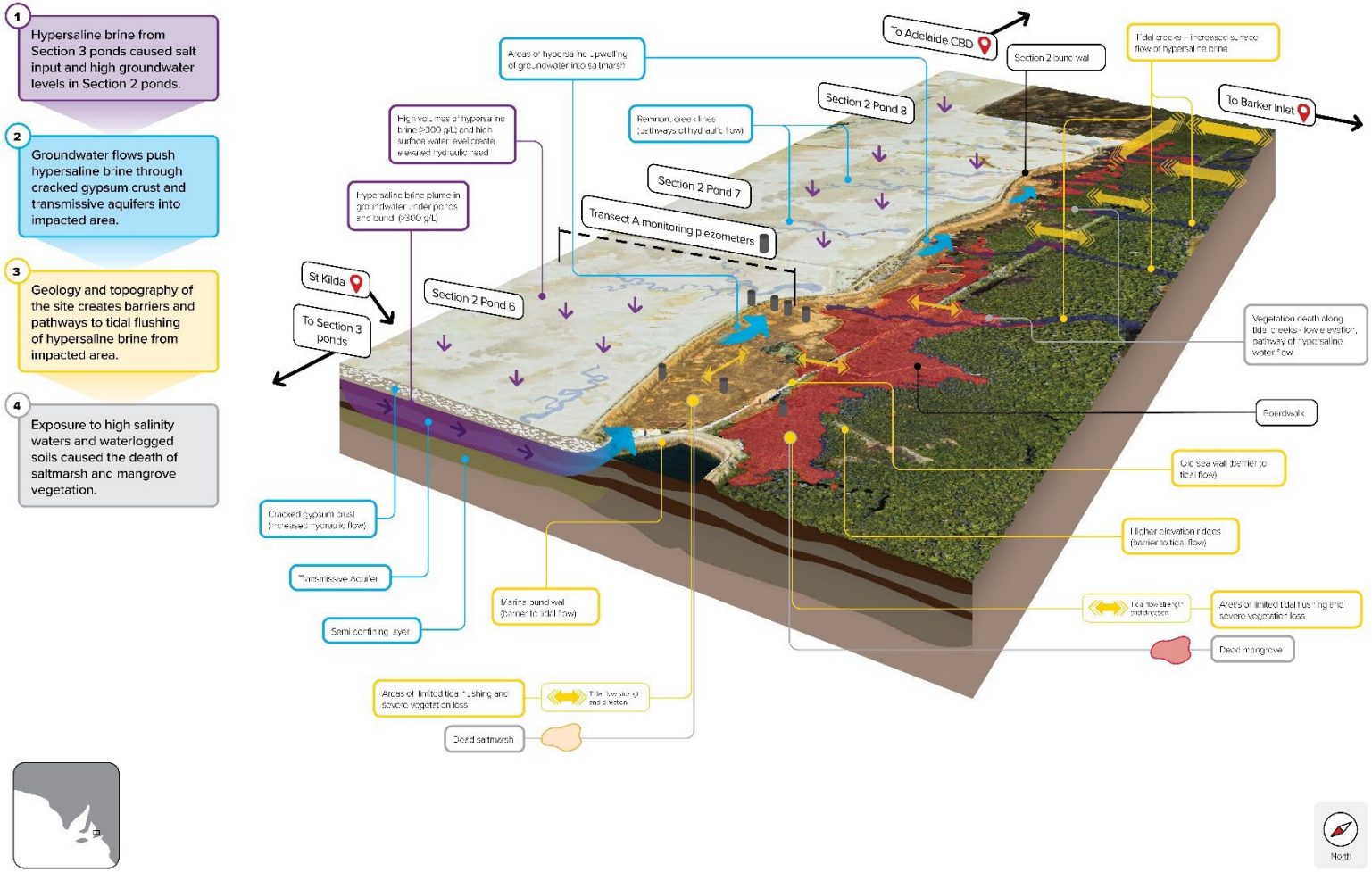

Figure 75: Conceptual site model developed by The University of Adelaide and Department for Environment and Water

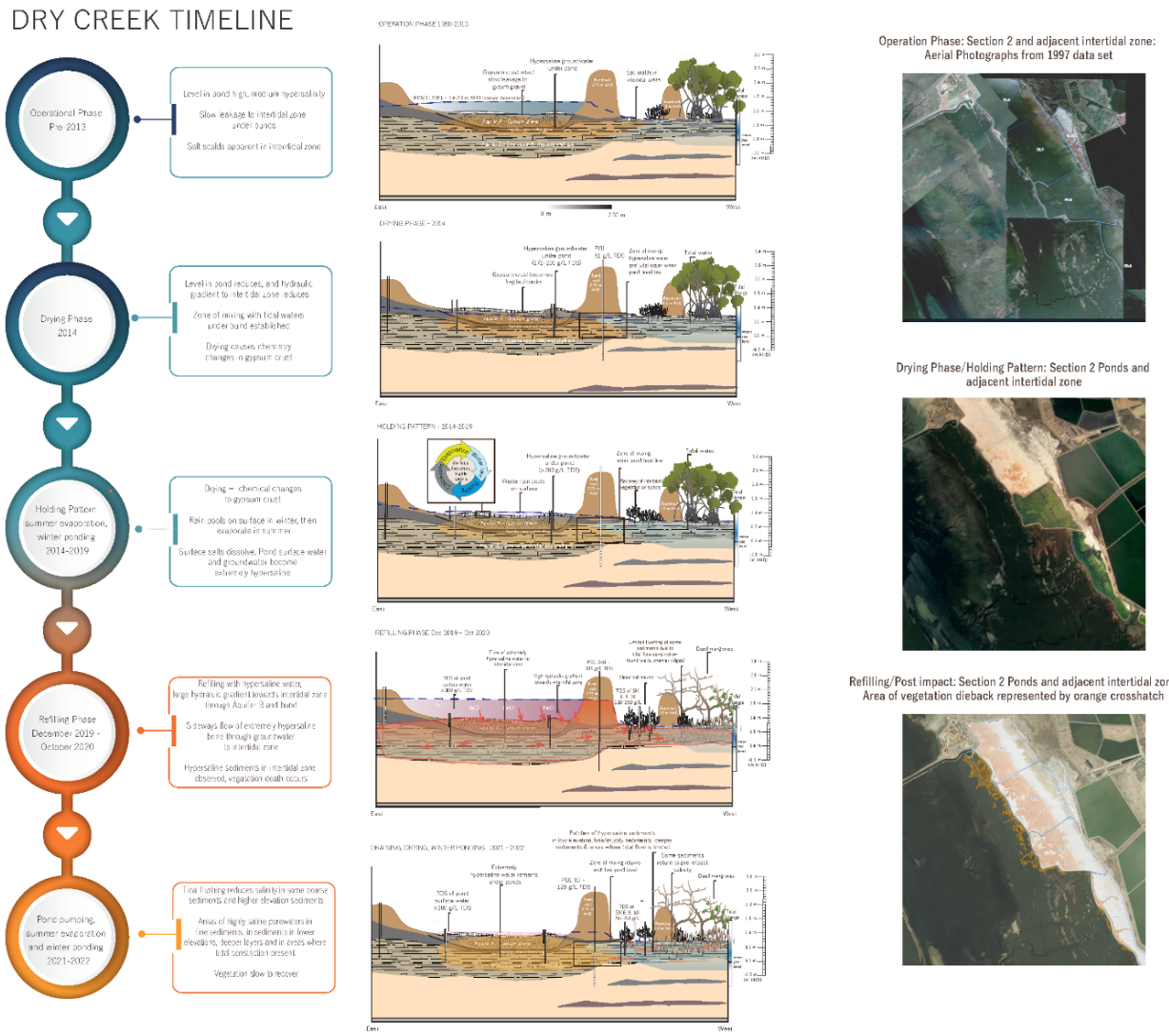

Figure 76: Conceptual model of the timeline of events from the hypersaline contamination

Pond Geochemistry:

Work done by (Fitzpatrick et al., 2014), showed high amounts iron monosulfides in the sediments in the ponds as shown in Figure 77. This work also showed that the acidification hazard was medium for western segments of ponds and low for eastern segments of ponds.

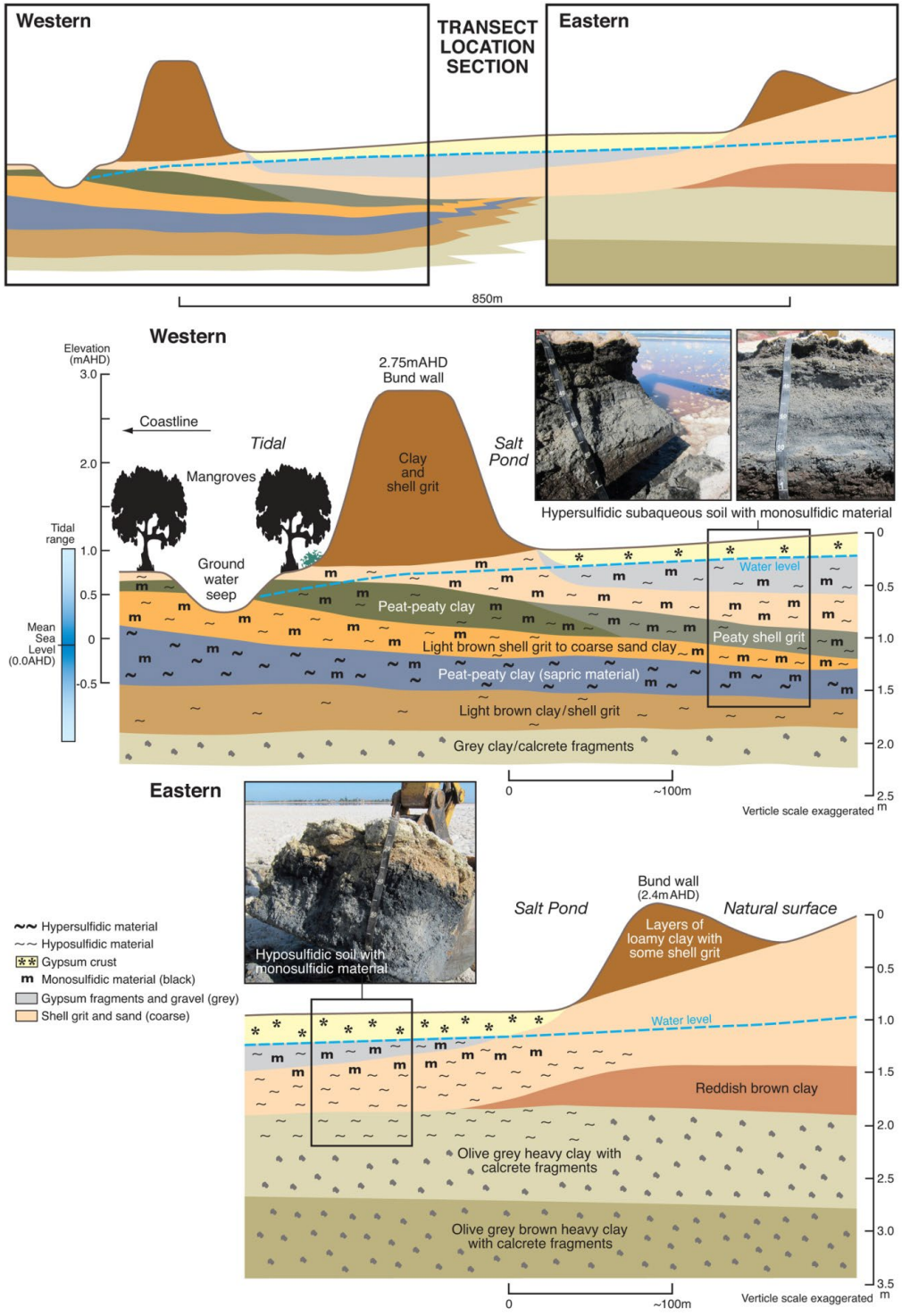

Figure 77: Cross section of the salt ponds illustrating the geology. Hypersulfic subaqueous soils with monosulfidic material dominate the western side of the ponds and Hyposulfidic soils with monosulfidic material dominate the eastern side of the ponds (from Fitzpatrick et al. 2014).

Case Study in South Australia – Dry Creek salt field, tidal reconnection trial

The tidal reconnection of a former salt pond XB8A commenced in July 2017, following the cessation of salt production in 2013. The pond is part of the Dry Creek salt field which extends over 25 km along the coast north of Adelaide and encompasses an area of 4,224 ha of ponds (3,598 ha excluding the crystalliser ponds) (Figure 1a). Operation of the solar evaporation ponds commenced in 1937, with water intake occurring initially at pond XB8A, before being relocated north as the salt field expanded (Mosley et al. 2019, 2020). Seaward ponds in the middle (St Kilda to Gawler River) section of the salt field were considered more suitable for restoration to tidal wetlands than those near the former crystalliser ponds, where salt harvesting took place. Ceasing of salt production also offered the opportunity to achieve carbon sequestration through tidal reconnecting of large sections of the salt field (Dittmann et al. 2019a, 2020).

Pond XB8A was reconnected to the Gulf of St Vincent with a tidal gate infrastructure that allowed control of water entering and exiting the pond, as required by regulatory authorities (Figure 1 b, c). Introducing tidal cycling was also a trial to remediate hypersaline and monosulfidic conditions which had developed during decades of salt field operation (Mosley et al. 2015). The infrastructure consists of 4 x 1.2 m diameter x 10 m long polyethylene pipes and controllable tidal gates (AWMA i-gate), powered by solar panels. Engineering design calculations provided the pipe sizing, orientation, and elevation for suitable water exchange within the typical tidal ranges (Mosley et al. 2020). A multi-parameter water quality sensor (YSI EXO2) was installed on the pond side of the gate, with level sensors also installed on both sides of the gate. No adverse effects on water quality were recorded since reintroduction of tidal flow (Mosley et al. 2020).

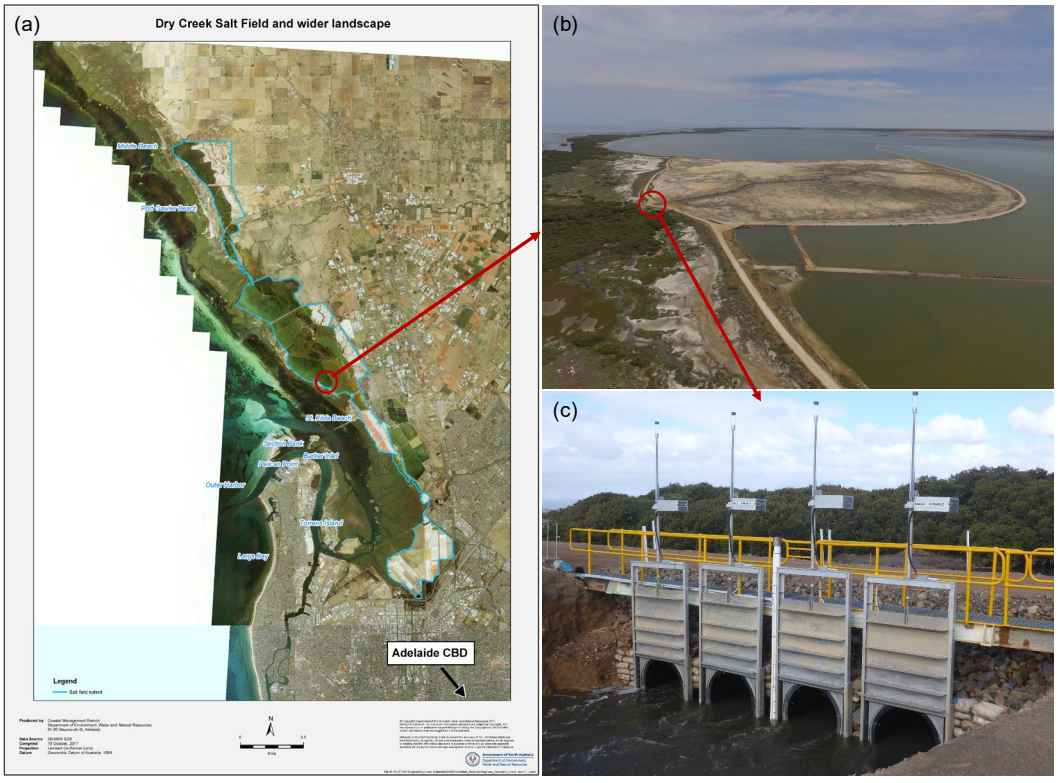

Figure 78: Location of the Dry Creek salt field, South Australia, encircled by blue line. Red circle indicates trial pond XB8A. (b) Trial pond XB8A a few months after tidal reconnection. (c) controllable tidal gates allowing regular cycling of tides in and out of the trial pond.

Sub-Bottom profiling and sediment core sampling had been undertaken across Sections 3 and 4 by CSIRO Land and Water to assess the occurrence and thickness of monosulfidic black oozes and also acidification risks via incubation experiments (Baker and Fairbrother 2016). Only two layers were assessed as hypersulfidic and these were at depth >60 cm in the soil profile which was likely to remain saturated and unlikely to pose any significant risk. Hence the potential acid sulfate soil risks in Pond XB8A were assessed as low which supported further progression with the trial scoping and implementation.

Key findings of monitoring and assessment post tidal restoration were (Mosley et al. 2020):

- Tidal restoration resulted in major decreases in salinity in Pond XB8A from the hypersaline conditions present before the trial. When it receives reasonable tidal inflow, the trial pond now has salinities approaching seawater values (35-40 Practical Salinity Units, psu) while the control pond, as expected, remained hypersaline (approx. 2-3x seawater salinity). There is an apparent seasonal trend of lower salinities in winter and higher salinities in summer, likely due to lower tidal and storm surge influences in summer and higher evaporation rates.
- pH, dissolved oxygen, dissolved metals, chlorophyll a and nutrients are variable but are being maintained at satisfactory levels during tidal exchange
- The general characteristics of the soil before commencement of the trial were a black (presumed monosulfide-rich) layer in the top 10−20 cm, a green-grey clay layer extending from about 20−45 cm, and a red-brown (presumed old mangrove root zone) peaty layer at >45 cm. Following tidal restoration, there has been an apparent shift to more oxidised conditions in the top sediment layer, with lighter coloration present at many sites, see Figure 2) and substantial reductions in Acid Volatile Sulfide (AVS, measure of iron monosulfide material content) due to introduction of wetting and drying cycles. This demonstrates that monosulfidic hazards can be remediated in situ via wetting and drying with little environmental risk, providing large-scale resuspension does not occur. The regular drying cycles are conducive to oxygen penetration into the soil to enable oxidation reactions to occur. The soils at the site appear, in general, to be transitioning to normal salt marsh soils with low hazards.
- Soil pH has showed only minor decreases but remained circum-neutral with no acidification (pH<5) occurring inn any soil layers following drainage. This was anticipated due to mostly hyposulfidic materials present in the initial surveys (Baker and Fairbrother 2016). There were some hypersuldific materials at depth in the profile but these either did not oxidise (regular tidal wetting and drying cycles enabled sub-soil saturation to be retained) or there was sufficient neutralizing capacity in the soil and water to prevent any acidification.
- Reduction in soil salinity from the conditions in the hypersaline salt ponds prior to tidal restoration due to dilution and salt export. Saline minerals deposited on the pond surface (mostly gypsum, but also aragonite and halite) have also showed some apparent dissolution over time.
- Soil organic carbon has shown a net increase over time
- Salt marsh vegetation rapidly recolonised the pond with the first vegetation observed in November 2017, approximately 4 months after tidal reconnection commenced. Vegetation is now well established over most of the pond (Figure 2), with the exception of some areas still receiving seepage from adjacent ponds
- There was increased tidal channel definition over time as tidal flow restored natural flow paths.
- A significant increase in macroinvertebrate diversity has occurred following tidal reconnection. The ecology has shifted from a simple (yet productive) hypersaline assemblage, to a diverse marine assemblage.

- Local and migratory wader bird activity has been observed (nesting and feeding). Particularly high feeding activity was observed during early morning high tides when water flowed over the mudflats.
- There is potential for wider application of tidal restoration strategies at the Dry Creek salt field to reduce environmental hazards, including acid sulfate soil materials, and restore coastal ecosystems.

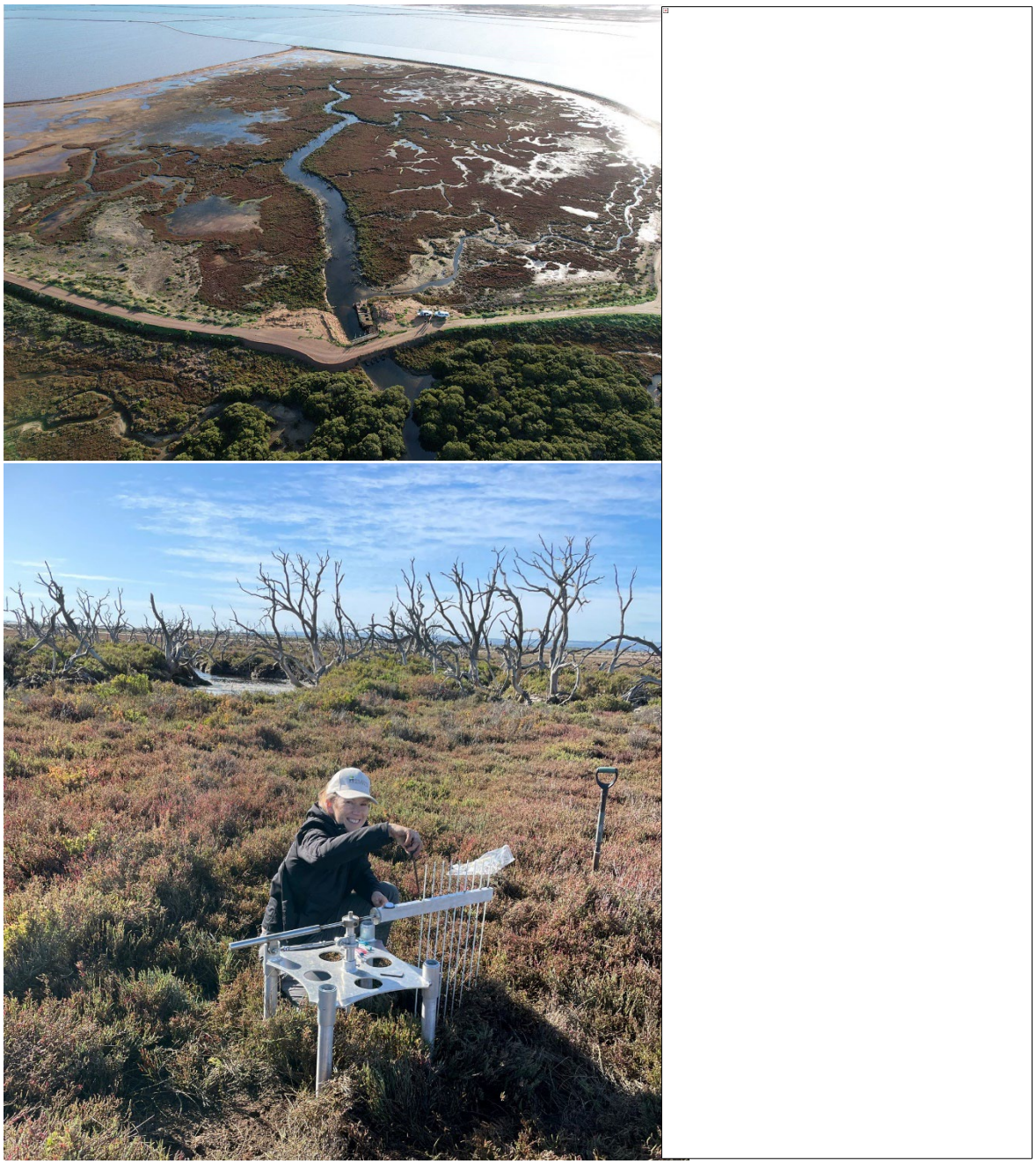

Figure 79: Photos in June 2022 of (top) overview of vegetation recovery after tidal restoration (credit Emily Leyden), (bottom) vegetation at Sediment Elevation Table site (credit Luke Mosley), and (right) soil profile (hyposulfidic hydrosol) following tidal restoration (credit Luke Mosley).

Photograph of Prof Del Fanning taken during the Mid-conference field trip demonstrating the “index of squishiness” or “n-value” test, which was developed by Pons and Zonneveld (1965) to define the degree of physical ripening of soft sediments. The soil used to conduct the test was hypersulfidic material from Soil profile BSK 4 (see Table 25), which classifies as a Sapric Sulfiwassists (Soil Survey Staff 2022) and Sapric, Histic-Hypersulfidic, Intertidal Hydrosol (Isbell and National Committee on Soils & Terrain, 2021).

Figure 80: Photograph of Prof Del Fanning during the Mid-conference field trip demonstrating the “index of squishiness” or “n-value” test (developed by Pons and Zonneveld, 1965 to define the degree of physical ripening of soft sediments) on hypersulfidic material from Soil profile BSK 4 (see Table 25), which classifies as a Sapric Sulfiwassists (Soil Survey Staff 2022) and Sapric, Histic-Hypersulfidic, Intertidal Hydrosol (Isbell and National Committee on Soils & Terrain, 2021) (photograph credit Luke Mosley).

REFERENCES

Baker AKM, Fairbrother LG (2016) Sub-Bottom Profiling data ground truthing and ASS hazard assessment at the Dry Creek Saltfield, South Australia. CSIRO, Australia.

Belperio, A. P. (1993). Land subsidence and sea level rise in the Port Adelaide Estuary: Implications for monitoring the greenhouse effect. *Australian Journal of Earth Sciences*, *40*, 359–368.

Belperio, A. P., & Harbison, P. (1992). *St Kilda Greenfields and the MFP - Australia Site: A geological excursion guide to natural, artificial and reclaimed wetlands* (Report Book 85/54). Geological Survey Department of Mines and Energy South Australia.

Belperio, A. P., & Rice, R. L. (1989). *Stratigraphic investigation of the Gillman investigation site, Port Adelaide estuary. Geological Survey, Department of Mines and Energy South Australia.* Geological Survey, Department of Mines and Energy South Australia.

Bowler, J. M., Hope, G. S., Jennings, J. N., & Singh, G. (1976). Late Quaternary climates of Australia and New Guinea. *Quaternary Research*, *6*, 359–394. https://doi.org/10.1016/0033-5894(67)90003-8.

Coast Protection Board. (2003). *A strategy for implementing CPB policies on coastal acid sulfate soils in South Australia* (Coastline No. 33; pp. 1-11.). https://cdn.environment.sa.gov.au/environment/docs/january_2003_strategy_for_implementing_cpb_policies_on_acid_sulphate_soils.pdf

Cox, R., Grindley, P., Taylor, J., & Pape, S. (2006). *Successfully lowering the risks and costs associated with the legacy of the abandoned Brukunga Pyrite Mine, South Australia*. 365–377. https://doi.org/10.21000/JASMR06020365

de Mooy, C. J. (1959). *Soils and land use around Lakes Alexandrina and Albert, South Australia* (CSIRO Soils and Land Use Series No. 29.). CSIRO Division of Soils.

Dear, S. E., Moore, N. G., Dobos, S. K., & Watling, K. M. (2002). *Queensland acid sulfate soil technical manual: Soil management guidelines (version 3.8)*. Available at http://www.envirodevelopment.com.au/_ dbase_upl/soil_mgmt_guidelines_v3_8.pdf

Department for Energy and Mining. (2017). *Brukunga mine site water monitoring report 2017* (2018/00020,). Mineral Resources Division. Department for Energy and Mining,.

Dittmann, S., Mosley, L., Stangoulis, J., Nguyen, V. L., Beaumont, K., Dang, T., Guan, H., Gutierrez-Jurado, K., Lam-Gordillo, O., & McGrath, A. (2022). Effects of Extreme Salinity Stress on a Temperate Mangrove Ecosystem. *Frontiers in Forests and Global Change*, *5*. https://doi.org/10.3389/ffgc.2022.859283

Dittmann, S., L. Mosley, M. Clanahan, J. Quinn, S. Crooks, et al. 2019b. Proof of concept for tidal re-connection as a blue carbon offset project. Goyder Institute for Water Research Technical Report Series No. 19/29.

Dittmann, S., Beaumont, K., Mosley, L., Leyden, E., Jones, A., et al. 2020. A Blue Carbon future through introducing tidal flow to salt ponds and stranded samphire for Dry Creek and the Samphire Coast. Report for the Adelaide and Mt Lofty Ranges NRM Board and Green Adelaide.

Drexel, J. F., & Preiss, W. V. (1995). *The Geology of South Australia, The Phanerozoic* (Vol. 2). Geological Survery of South Australia, Bulletin 54. Department of Primary Industries and Resrouces SA.

DWLBC. (2007). *Regional land resource information for southern South Australia' DVD*. Soil and Land Program, Department of Water, Land and Biodiversity Conservation,.

Edmonds, V. (1995). An Archaeological Survey of Range Creek Wetlands site, Adelaide. *Archaeological Consulting Services. Prepared for CMPS and F (Unpublished)*.

Fitzpatrick, R. (1993). Origin and properties of inland and tidal saline acid sulfate soils in South Australia. In *Selected papers of the Ho Chi Minh City Symposium on Acid Sulfate Soils* (Vol. 53, pp. 71–80). International Institute for Land Reclamation and Improvement.

Fitzpatrick, R., Grealish, G., Shand, P., & Simpson, S. (2009). *Fitzpatrick, R.W., Grealish, G., Shand, P., Simpson, S.L. et al. (2009a) Acid sulfate soil assessment in Finniss River, Currency Creek, Black*

Swamp and Goolwa Channel, South Australia. (CSIRO Land and Water Science Report 26/09). CSIRO.

Fitzpatrick, R., Marvanek, S., Shand, P., Merry, R., & Thomas, M. (2008). *Acid sulfate soil maps of the River Murray below Blanchetown (Lock 1) and Lakes Alexandrina and Albert when water levels were at pre-drought and current drought conditions. Adelaide, SA* (No. 2008-02.). CSIRO Land and Water.

Fitzpatrick, R., & Self, P. G. (1997). Iron oxyhydroxides, sulfides and oxyhydroxysulfates as indicators of acid sulfate weathering environments. *Advances in GeoEcology*, *30*, 227–240.

Fitzpatrick, R., Shand, P., & Mosley, L. (2018). Soils in the Coorong, Lower Lakes and Murray Mouth Region. In *Natural History of the Coorong, Lower Lakes, and Murray Mouth region (Yarluwar-Ruwe)*. Royal Society of South Australia. https://doi.org/10.20851/natural-history-cllmm-2.9

Fitzpatrick, R. W. (1991). *Preliminary assessment of the properties and development of saline acid sulphate soils at the Gillman MFP Australia Site. Consulting Report to PPK Consultants.* (No. 11/1991). CSIRO Division of Soils Technical Report.

Fitzpatrick, R. W., Cass, A., & Davies, P. J. (1996). *Assessment of soils and fill materials for landscaping Phase 1 of the Gillman Urban Development Site (Project No. V002-94-522M)* (Tech Report No. 36/1996; p. 62). CSIRO Division of Soils.

Fitzpatrick, R. W., Grealish, G., Chappell, A., & Marvanek, S. (2010). *Spatial variability of subaqueous and terrestrial acid sulfate soils and their properties, for the Lower Lakes, South Australia. CSIRO Sustainable Agriculture National Research Flagship Client Report R-689-1-15 (CSIRO, South Australia).* (CSIRO Sustainable Agriculture National Research Flagship Client Report R-689-1-15). CSIRO.

Fitzpatrick, R. W., Hudnall, W. H., Lowe, D. J., Maschmedt, D. J., & Merry, R. H. (1992). *Proposed changes in the classification of Histosols, Alfisols, Andisols, Aridisols, Inceptisols, Mollisols, Entisols, and Spodosols in South Australia* (pp. 1–17) [Report]. CSIRO Division of Soils.

Fitzpatrick, R. W., Shand, P., Baker, A. K. M., Grocke, S., & Thomas, B. T. (2014). *Dry Creek Salt Fields: Assessment of Acid Sulfate Soil environments in Section 2 for ponds (PA3 to PA12) and drains* (Acid Sulfate Soils Report No ASSC_067). The University of Adelaide.

Fitzpatrick, R. W., Shand, P., & Mosley, L. M. (2017). Acid sulfate soil evolution models and pedogenic pathways during drought and reflooding cycles in irrigated areas and adjacent natural wetlands. *Geoderma*, *308*, 270–290. https://doi.org/10.1016/j.geoderma.2017.08.016

Fitzpatrick, R. W., Thomas, B. P., Merry, R. H., & Marvanek, S. (2008). *Acid Sulfate Soils In Barker Inlet And Gulf St. Vincent Priority Region* (No. 1834–6618; CSIRO Land and Water Science Report Series). CSIRO Land and Water.

Hall, J., Maschmedt, D., & Billing, B. (2009). *The Soils of Southern Australia* (Vol. 1). Geological Survery of South Australia, Bulletin 56. Department of Water, Land and Biodviersity Conservation.

Hipsey, M. R., Salmon, S. U., & Mosley, L. M. (2014). A three-dimensional hydro-geochemical model to assess lake acidification risk | Environmental Modelling & Software. *Environmental Modelling and Software*, *61*(C), 433–457. https://doi.org/10.1016/j.envsoft.2014.02.007

Hipsey, M. R., Salmon, S. U., Mosley, L. M., Barnett, L., & Frizenschaf, J. (2011). Development of a 3-D hydro-geochemical model to assess water quality and acidification risk in the Murray Lower Lakes, South Australia. *MODSIM2011, 19th International Congress on Modelling and Simulation.* 19th International Congress on Modelling and Simulation. https://doi.org/10.36334/modsim.2011.I7.hipsey2

Isbell, R. F. and Isbell and National Committee on Soils & Terrain (2021). *The Australian Soil Classification: 3rd Edition*. CSIRO.

IUSS Working Group WRB. (2014). *World reference base for soil resources 2014: International soil classification system for naming soils and creating legends for soil maps*. FAO.

Kölbl, A., Bucka, F., Marschner, P., Mosley, L., Fitzpatrick, R., Schulz, S., Lueders, T., & Kögel-Knabner, I. (2019). Consumption and alteration of different organic matter sources during remediation of a sandy sulfuric soil. *Geoderma*, *347*, 220–232. https://doi.org/10.1016/j.geoderma.2019.04.006

Kölbl, A., Kaiser, K., Winkler, P., Mosley, L., Fitzpatrick, R., Marschner, P., Wagner, F. E., Hausler, W., & Mikutta, R. (2021). Transformation of jarosite during simulated remediation of a sandy sulfuric soil. *Sci Total Environ*, *773*, 145546. https://doi.org/10.1016/j.scitotenv.2021.145546

Kölbl, A., Marschner, P., Fitzpatrick, R., Mosley, L., & Kögel-Knabner, I. (2017). Linking organic matter composition in acid sulfate soils to pH recovery after re-submerging. *Geoderma*, *308*, 350–362. https://doi.org/10.1016/j.geoderma.2017.07.031

Leyden, Thomas, B. P., & Mosley, L. M. (2022). *St Kilda Mangrove and Saltmarsh Hypersaline Brine Contamination 2020*.

Maschmedt, D. J. (2009). Soils. In *Natural History of the Riverland and Murraylands* (pp. 36–50). Royal Society of South Australia Inc., Adelaide.

Merry, R. H., Fitzpatrick, R. W., Barnett, E. J., Davies, P. J., Fotheringham, D. G., Thomas, B. P., & Hicks, W. S. (2003). *South Australian Inventory of Acid Sulfate Soil Risk (Atlas)*.

Mosley, L.M., P. Marschner, & R.W. Fitzpatrick. 2015. Research to inform a tidal cycling trial at the Dry Creek salt ponds. Report to the Department for Environment Water and Natural Resources. University of Adelaide Acid Sulfate Soil Centre.

Mosley, L., B. Thomas, R. Fitzpatrick, & Quinn J. 2019. Pathways to tidal restoration of the Dry Creek salt field. Report to the Department for Environment and Water. https://www.energymining.sa.gov.au/__data/assets/pdf_file/0008/672551/Mosley_et_al_2019_Pathways_to_~the_Dry_Creek_salt_field_Final.PDF

Mosley, L., T. Dang, P. Marschner, R. Fitzpatrick, & Quinn J. 2020. Environmental outcomes from a tidal restoration trial at the Dry Creek salt field. Report to the Department for Environment and Water and Adelaide-Mt Lofty Ranges Natural Resources Management Board. The University of Adelaide.

Poch, R. M., Thomas, B. P., Fitzpatrick, R. W., & Merry, R. H. (2009). Micromorphological evidence for mineral weathering pathways in a coastal acid sulfate soil sequence with Mediterranean-type climate, South Australia. *Australian Journal of Soil Research,, 47*, 403–422.

Pons J.L. and Zonneveld, I.S. (1965). Soil ripening and soil classification. Initial soil formation in alluvial deposits and classification of the resulting soils. Inst. Land Reclam. and Impr. Pub. 13. Wageningen, The Netherlands. 128pp.

Soil Survey Staff. (2010). *Keys to Soil Taxonomy*. Natural Resources Conservation Service. http://www.nrcs.usda.gov/resources/guides-and-instructions/keys-to-soil-taxonomy

Sullivan, L., Fitzpatrick, R., Bush, R. T., Burton, E., Shand, P., & Ward, N. (2010). *The classification of acid sulfate soil materials: Further modifications* (Southern Cross GeoScience Technical Report No. 310).

Thomas, B. P. (2010). *Coastal acid sulfate soil processes in Barker Inlet, South Australia*. The University of Adelaide.

Thomas, B. P., Fitzpatrick, R.W., Merry, R., Poch, R.M., Hicks, W.S., & Raven, M. D. (2004). *Contemporary and relict processes in a coastal acid sulfate soil sequence: Macroscopic and geomorphic features*. 3rd Australian New Zealand Soils Conference, University of Sydney, Australia. www.regional.org.au/au/asssi/supersoil2004

Trueman, A. M., Fitzpatrick, R. W., Mosley, L. M., & McLaughlin, M. J. (2021). Exploring passivation-based treatments for jarosite from an acid sulfate soil. *Chemical Geology*, *561*, 120034. https://doi.org/10.1016/j.chemgeo.2020.120034

Trueman, A. M., McLaughlin, M. J., Mosley, L. M., & Fitzpatrick, R. W. (2020). Composition and dissolution kinetics of jarosite-rich segregations extracted from an acid sulfate soil with sulfuric material. *Chemical Geology*, *543*. https://doi.org/10.1016/j.chemgeo.2020.119606

POST-CONFERENCE FIELD TRIP

MOUNT LOFTY RANGES: GUTHRIES WETLAND AND BRUKUNGA MINE

FRIDAY 31ST MARCH 2023

FIELD TRIP ITINERARY

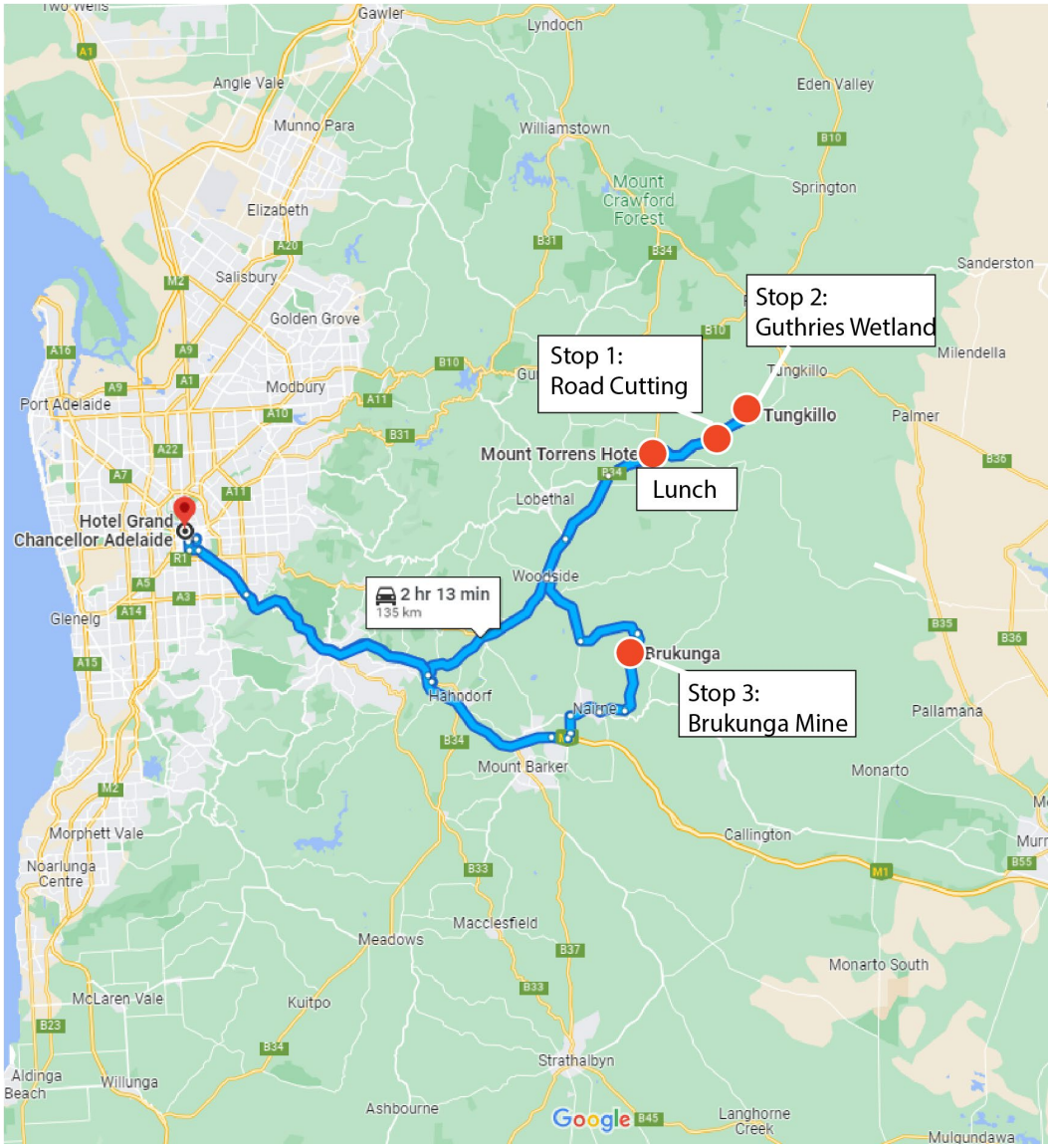

Location	Time
Meet in lobby	8:45 am
Leave Hotel Grand Chancellor	9:00 am
Arrive Stop 1: Regolithic profile at road cutting	10:20 am
Arrive Stop 2: Guthries Wetland	10:40 am
Morning tea at Guthries wetland	10:45 am
Leave Stop 2	12:30 pm
Arrive Mount Torrens Hotel for lunch	12:45 pm
Leave Mount Torrens Hotel	1:30 pm
Arrive Stop 3: Brukunga Mine	2:00 pm
Visit Acid Treatment Plant	2:10 pm
Visit Acid Dam	3:00 pm
Visit Mine spoil heaps	3.15 pm
Leave Stop 2	3.45 pm
Arrive Hotel Grand Chancellor	5:00 pm

Figure 81: Google Earth Map of the Post conference field trip

Summary:

This field trip will take participants to three sites to view naturally occurring acid sulfate soils and rock in the Mount Loft Ranges, South Australia. These sites have been altered by human activities allowing the oxidation of pyrite material and the generation of acidity, metals and metalloids and associated environmental impacts.

The organisers of the field trip would like to acknowledge the traditional custodians of the land on which we stand, work, and travel. The traditional owners of the land we are visiting on this field trip is the of the Kaurna people. We pay our respects to their Elders past, present, and emerging, and recognize their continuing connection to the soil, land, water, and culture. We extend our respect to all Aboriginal and Torres Strait Islander people and their contributions to this country.

Geological History of Mount Lofty Ranges

The Mount Lofty Ranges stretch to the east of the Adelaide metropolitan area to Cape Jervis on the Fleurieu Peninsula. The geological history of the Mount Lofty Ranges spans over 500 million years and is characterized by a complex history of sedimentation, tectonics, and erosion. The story of the Mount Lofty Ranges began in the late Precambrian period, around 650 million years ago, when the region was covered by a shallow sea. Sediments deposited in this sea eventually formed the Adelaide Geosyncline, a large basin that extended from the Eyre Peninsula in the west to the Flinders Ranges in the north. During the Cambrian period, around 500 million years ago, the Adelaide Geosyncline began to fill with sedimentary rocks, including sandstones, shales, and limestones. These rocks were subsequently deformed and uplifted during the Paleozoic era, around 300 million years ago, as a result of tectonic activity along the Delamerian Orogen. The tectonic activity during this period caused the sedimentary rocks to be folded and faulted, forming the complex geological structures that are visible in the Mount Lofty Ranges today. Over the following hundreds of millions of years, the Mount Lofty Ranges were subjected to several cycles of uplift and erosion, which sculpted the landscape into the range of mountains and hills that we see today. The erosion also exposed the rocks that were once buried deep underground, revealing a rich mineral deposit of copper, gold, and silver. Mining of these resources started in the 19th century and continued until the 20th century.

Summary of Field Trip Sites:

Stop 1: Regolithic Road Cutting

The first stop will be a regolithic road cutting at the top of the catchment to demonstrate the hilltop soils (fine, kaolinitic, mesic, Typic Palexeralfs), which are capped with deeply weathered soils and saprolite (pallid zone) rich in kaolin and associated ferricrete comprising large purple, red and yellow mottles.

Weathering has occurred from the Mesozoic to the present. Over many thousands of years, salt has been accumulating in this relatively old landscape from the large (i.e. usually 20 to 200 kg/ha/yr) quantities of salt blown from the ocean by wind and rain. In addition, salts have been generated by weathering of rocks during soil formation, especially from pyrite-rich and scapolite-rich rocks as well as leaching of connate salts trapped in the original sediments.

Stop 2: Guthrie's Wetland

The second stop will be in the Guthrie wetland site where acid sulfate soils have formed as a response to land clearing and rising water tables. We will illustrate and explain the soil morphological and biogeochemical changes that have recently (20 to 50 years) taken place in the degraded wetland that has resulted in:

Degradation of wetland vegetation

Wetland expansion and erosion upslope due to the rapid formation of saline-sulfidic characteristics in surface soil layers

Formation accumulation of reddish-brown gelatinous precipitates in surface ponds during wet periods

Formation of Fe-rich cemented crust (2 to 5 mm) during dry or summer periods.

First ever discovery of schwertmannite in soils, which justified it being named as a new mineral

Development of a series of comprehensive soil-regolith models to explain the complex pedological, hydrological and biogeochemical interactions that occur in saline-sulfidic soil-regolith environments.

Development and application of the use of sulfidic/sulfuric material as a sampling medium for mineral exploration to locate the presence of blind or concealed ore deposits

Development and application of lead isotopes from sulfidic wetlands for Base Metal Exploration

Development and application of easy-to-follow pictorial manuals for identifying soil indicators for improved land use options and best management practices.

Stop 3: Brukunga Mine

The Brukunga pyrite mine is located 40 km east of Adelaide in the Mount Lofty Ranges. Iron sulfide (pyrite and pyrrhotite) was mined at the site between 1955 and 1972. During mining operations, two large waste rock piles were generated from approximately 8 million tonnes of sulfidic overburden material and a valley-fill tailings facility adjacent to the mine was filled with 3.5 million tonnes of sulfidic sand tailings. There have been significant issues with Acid and Metalliferous Drainage (AMD) entering the surrounding environment (Dawsley Creek) as a result of the oxidation of pyrite and pyrrhotite minerals. Substantial quantities of acidic water (pH 2.5-2.9) with elevated sulfate and heavy metals concentrations lead to the isolation and treatment of the acidic water.

Stop 1 and 2: Regolithic Road Cutting and Guthries Wetland

Figure 82: Google maps of Site 1 – Road Cutting (Right-Top) and Site 2 – Wetland (Right-Bottom)

Environmental Setting

The Guthries catchment and wetland is located E of Adelaide in the eastern Mount Lofty Ranges, South Australia. Landscapes in this region host deeply weathered soil-regolith profiles with high concentrations of stored salts, and base metal mineralization (Figure 83) that contributes to degraded saline seepages and poor stream water quality.

Vegetation and Land use

Since European settlement, the native vegetation of South Australia has been extensively modified. Little data exist on the extent of pre-European forest and woodland cover. However, anecdotal reports from the Adelaide Hills suggest that, prior to clearing, native vegetation consisted of river red gum (Eucalyptus camaldulensis) woodland. These trees remain prominent adjacent to water courses and roadways in the Eastern Mt Lofty Ranges.

The river red gum is a perennial, single stemmed, large-bole, medium-sized to tall tree (30-40 m tall). It may reach ages of 500 to 1000 years. The river red gum is commonly found growing on riverine sites with permanent or seasonal water. They are often associated with gleyed heavy clay soil along river banks and on floodplains subject to frequent or periodic flooding, preferring deep moist subsoils with high clay content. These trees obtain water from rainfall, groundwater and river flooding. They posses deep sinker roots that grow down towards zones of higher water supply and are effective in conducting water, hence, the high water use of the river red gums contributes to maintaining the watertable at lower depths.

Post land clearing (to allow grazing), a mix of pasture species now dominate the local vegetation including subterranean clover (*Trifolium subterraneum* L.) and cocksfoot (*Dactylis glomerata* L.) with invasions of salvation jane (*Echium plantagineum* L.), storksbill (*Erodium moschatum* L.) and soursob (*Oxalis pes-caprae* L.) that are now grazed by sheep and cattle.

Wetland vegetation is associated with wet soils in areas of groundwater discharge, through water and surface water discharges on lower slopes, terraces and valley floors. Species include: (i) cumbungi (*Typha* sp.) associated with permanently saturated soils of inner wetlands, (ii) rush (*Juncus* spp.) associated with permanently and seasonally saturated soil of inner wetlands and erosional channels, (iii) streaked arrowgrass (*Triglochin striata*) and creeping monkey flower (*Mimulus repens*) – associated with seasonally saturated soil in transitional zones around wetlands. Tall wheat grass (*Agropyron elongatum*) and puccinellia (*Puccinellia ciliata*) is often found surrounding saline wetlands.

Land use is predominantly sheep or cattle grazing on pasture that, in places, has resulted in significant erosion and land degradation. Increasingly, land is being used for more intensive purposes such as viticulture and cereal cropping. Commercial pine plantations have been established in areas of the Torrens River catchment, which is an important source of urban water supply.

Geology and geomorphology (from Baker and Fitzpatrick 2010)

The Normanville Group was deposited in the Early Cambrian during an initial phase of stable platform carbonate-dominated sedimentation (Figure 83). The Kanmantoo Trough then formed, due to extensional faulting, along the south eastern flank of the Neoproteozoic Adelaide Geosyncline.

The Kanmantoo Trough filled rapidly with mainly immature clastics and some carbonates (Kanmantoo Group) in a dominantly marine environment. Sedimentation of the Kanmantoo Trough ceased in the Mid to Late Cambrian in response to the initial compression associated with the Delamerian Orogeny. Deformation continued through to the Early Ordovician and resulted in complex structural and metamorphic zoning along the fold belt over 300 km in length in the eastern and southern Mount Lofty Ranges. At least two main phases of deformation have been recognised. Metamorphism at low pressure and high temperature locally attained amphibolite facies and appears to have coincided with a major period of granite emplacement (Foden et al. 1990).

The maximum thickness of the Kanmantoo Group is 15 km. The main rock types include sandstone, siltstone and phyllite, with intercalated pelite and minor carbonate. Deposition commenced with the muddy sandstone and siltstone of the Carrickalinga Head Formation, which grades into the cross-bedded feldspathic sandstone of the Backstairs Passage Formation. A disconformity separates the Backstairs Passage Formation from the overlying upper parts of the sequence, which comprise interbedded muddy sandstone and siltstone (Tapanappa and Balquhidder Formations), and dominantly fine-grained clastic rocks of the Talisker Calc-siltstone and Tunkalilla Formation.

The landscape of much of the eastern Mount Lofty Ranges region comprises undulating low hills. Altitude varies from 400 to 500 m with local relief between 30 and 50m. Small catchments to the west drain into the Onkaparinga and Torrens catchment systems, whilst catchments to the east form part of the Murray–Darling Basin system.

Regional Mineralisation

The Kanmantoo Group hosts a number of different styles of mineralisation. Most significant mineralisation has been historically confined to the Tapanappa Formation and the Talisker Calc-Siltstone. There is a sequence boundary at the base of the Talisker Calc-Siltstone that is associated with Pb-Zn mineralisation in the Karinya Syncline (Figure 83) (Dyson et al. 1994). Exploration has focussed on the pyritic silt/mudstone of the Talisker Calc-Siltstone and Tapanappa Formation because of the occurrence of ore bodies spatially coincident with these units (Flottmann et al. 1996).

The wide variety of mineralisation styles occurring within the sediments of the Kanmantoo Trough formed during basin most likely development either below the basin floor in discordant deposits (e.g. Kanmantoo, Bremer) or close to the sediment-seawater interface as concordant deposits (e.g. Aclare, Wheal Ellen) (Seccombe et al. 1985).

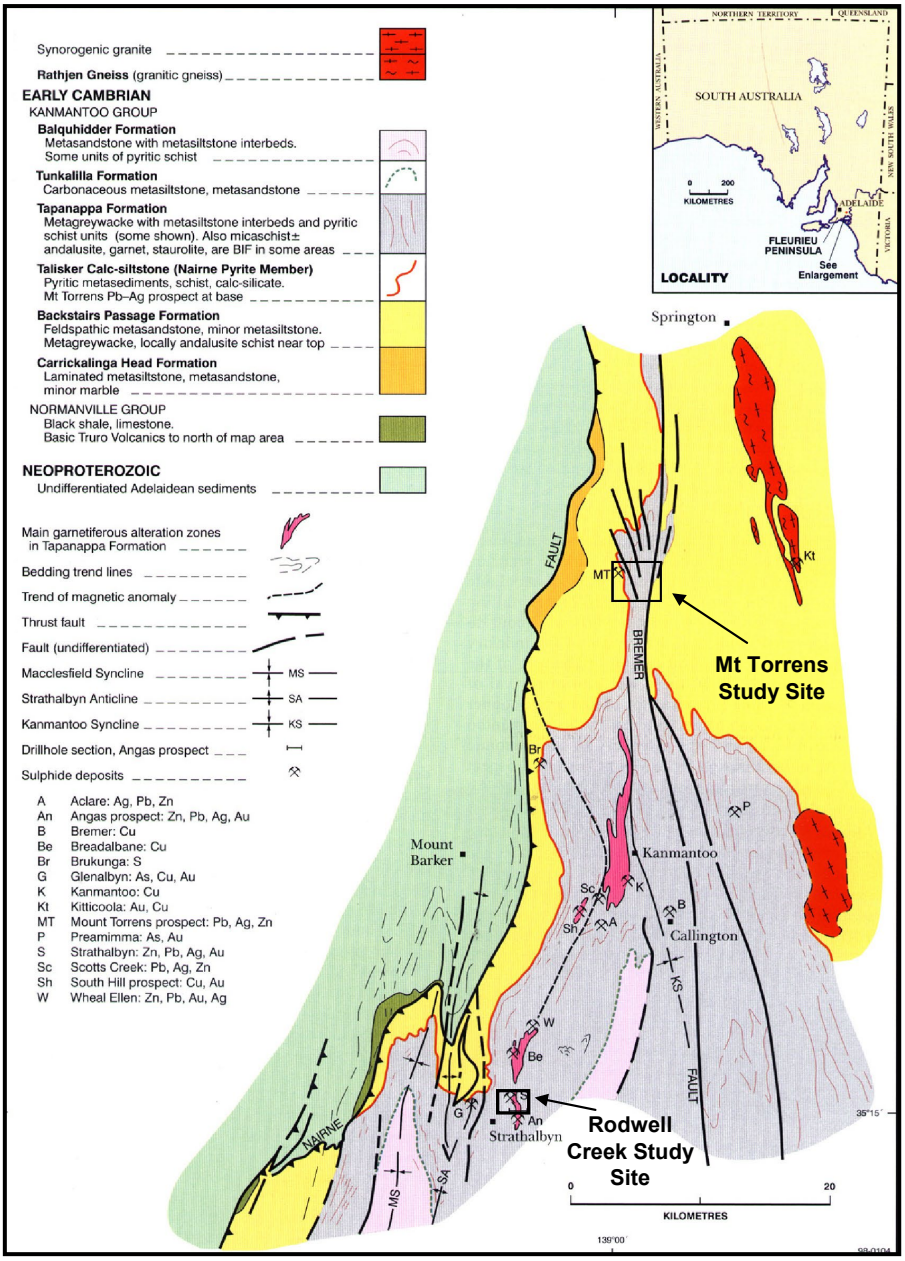

Figure 83. Regional geologic setting of the mineral deposits in the in the Kanmantoo Group (from Toteff, 1999).

In summary, the Mt Lofty Ranges represent a landscape of great antiquity with its physiography having undergone cyclic periods of weathering ranging from substantial landscape stability extending over several geological periods to tectonic instability that has given rise to erosion and the exposure of rock types bearing weatherable minerals containing salts and sulfur.

Soil landscape and land use in the Guthrie catchment

The Guthrie sub-catchment consists of a valley floor surrounded by rolling hills. It may be subdivided into three geomorphic units: hilltops, side slopes and stream terraces. The hilltops are capped by lateritic saprolite (weathered zones rich in kaolin and associated ferricrete) that have resulted from strong *in situ* weathering of very fine-grained feldspar and biotite rich metasediments. This weathering has occurred from the Mesozoic to the present. The side slopes are cut in less weathered fine-grained metasediments of interbedded siltstones and sandstones containing sulfide and pegmatite rich zones.

The stream terraces consist of Quaternary (Holocene and Recent) colluvial-alluvial deposits of gravels and fine grained materials.

The dominant feature of the soil-landscape is a wide range of soils with an abrupt textural boundary between E (A2) and B horizons and associated colluvial ferruginous gravel layers (stonelines). The soil pattern down the slope is:

i. hilltops; outcropping ferricrete and associated soils (Palexeralfs),
ii. upper side slopes; red duplex soils that have either uniform red or red-yellow mottled B horizons (Palexeralfs),
iii. lower side slopes; weakly developed bleached E (A2) horizons and B horizons exhibiting redoximorphic features and aquic conditions below 0.5 m (Aquic Palexeralfs) and well developed bleached E (A2) and B horizons exhibiting redoximorphic features and aquic conditions between the soil surface and 0.5 m (Albic Glossic Natraqualfs),
iv. footslopes and stream terraces; soils with ochric and natric horizons (Typic Natraqualfs) and recently developed wetland soils with saline-sulfidic materials overlying a natric horizon (Alfic Sodic Sulfaquents) and eroded soils.

A detailed soil description and analytical data for the hilltop soil are given in Table 28 and Table 29.

Mica schist weathering, pallid zone formation, iron oxide mottling, ferricretes and salt accumulations

The two types of weathered materials will be viewed during the stop at a road cut at the top of the catchment. X-ray diffraction patterns indicates that kaolin is the dominant layer silicate throughout the profile to a depth of 5 m.

In the ***purple and red mottles***, hematite and goethite occurs as the dominant and trace iron oxide minerals respectively.

In the ***yellow mottles***, Al-substituted goethite was the only iron oxide detected. Redox conditions have variously changed the red colours by dissolving hematite and/or goethite via:

- Complete dissolution of hematite and goethite causing bleaching because of prolonged reducing conditions;
- Partial or selective dissolution of fine-grained hematite in Bt horizons, causing fading or yellowing because of moderate reducing conditions.
- Dissolution of coarse rosettes of hematite, in the purple-red saprolite, and recrystallization as yellow fine needle-like goethite.

Table 28: Description of a fine, kaolinitic, mesic, Typic Palexeralf' at the hilltop site

Depth (cm). **Description**

0 -10: A1. Dark brown. Dark brown (7.5YR3/2, 10YR4.5/2d) matrix. Loamy sand (15% clay). Dry. Weakly water repellent. Granular to massive. Many macropores related to random packing of quartz and peds. High fauna!activity (macrotubular pores of 3 to 4mm, micropeds). Many very fine roots. Clear and smooth boundary.

10 - 15: E. Reddish brown. Reddish brown (5YR3.5/4, 7.5YR5/4d) matrix with very few and small (2mm) light red (2.5YR6/6, 5YR7/6d) remnant mottles from the top of the B layer. Loamy sand (10% clay). Dry. Massive. Many macropores related to random packing of quartz, some macrotubular pores (3 to 4mm) infilled with A matrix and very fine roots. Common very fine roots. Clear and weakly wavy boundary.

15 - 25: **En**. Reddish brown with gravels. Reddish brown (5YR4.5/4, 7.5YR6/4d) matrix with some small (2 to 5mm) red (2.5YR5/6, 5YR6/6d) remnant mottles from the top of the B layer. Loamy sand (10% clay). Dry. Massive. Many macropores related to random packing of quartz and gravels, some macrotubular pores. Gravels (40 to 50%) of platy rounded ferricrete nodules (10 to 30mm) and quartz. Few very fine roots. Abrupt and weakly wavy boundary.

25 - 35: Bt1-E. Top of the red Bt weakly bleached with infill of E matrix in small vertical cracks. Red (2.5YR4/6, 5YR5/6d) matrix surrounded near the cracks by lighter red (2.5YR5/6, 5YR6/6d) matrix. Light - medium clay (45% clay). Dry. Infill in the vertical cracks of reddish brown (5YR4.5/4, 7.5YR6/4d) E matrix. Moderate columnar (50mm) peds breaking to smaller subangular blocky (10mm). Vertical cracks (spaced every 20 to 60mm, 50mm depth, less than 1mm wide when dry) and macrotubular pores (3 to 4mm) infilled with E matrix and very fine roots. Gradual and weakly wavy boundary.

35 - 65: Bt2 (r). Red Bt with rare platy ferricrete nodules. Red (2.5YR4/6, 5YR5/6d) matrix. Heavy clay (60% clay). Moderately moist. Strong and fine (10mm) subangular blocky peds. Fine cracks (less than 1mm wide when dry) and macrotubular pores (3 to 4mm) infilled with E matrix and very fine roots. Rare very hard cemented platy ferricrete nodules in places weakly aligned to the bedding plane of the underlying weatered rock. Gradual and wavy boundary.

65 - 100: Bt3 (r-y). Red-yellow mottled Bt with some aligned (dip 70°) platy ferricrete nodules or baoulders (Ft). Red (2.5YR4/6) to yellowish red (5YR5/6) matrix, with yellowish brown (10YR5/8) then brownish yellow (10YR6/6) mottles (30%). Medium clay with some shiny micaceous particles (50% clay, 10% silt). Moderately moist. Moderate subangular blocky peds (10 to 20mm). Fine cracks (less than 1mm wide when dry) and macrotubular pores. Some platy ferricrete nodules with internal purple and red matrices surrounded by thin discontinuous yellow matrix (internal hypo-coating), better aligned to the bedding plane of the underlying weathered rock. Gradual and wavy boundary.

100 - 135: Btn4-C (r-y-w). Red-yellow-white mottled BC and locally numerous aligned (dip 80°) platy ferricrete nodules and boulders (Ft).

Dark red (10R3/6) mottles (40%) following roughly the dip of the underlying weathered rock, surrounded sharply by yellowish brown (10YR5/8) then brownish yellow (10YR6/6) matrix (50%) with some white mottles (10%). Light clay with a light silty and micaceous feel (40% clay, 20% silt). Moderately moist. Very coarse subangular blocky peds (50 to 100mm) breaking to smaller subangular blocky ones (10 to 20mm). Gradual and irregular boundary that follows the dip of the weathered rock in places.

Alignment of ferricrete nodules (Ft) are discordant on this boundary: platy nodules (20 to 30mm) with internal purple (5R2.5/3: dusky red) matrix surrounded in places by red (2.5YR4/6) and then yellow (10YR7/6) matrices.

135 - 170: C (w). White loose saprolite matrix with red-yellow sparse mottles (30%). White (10YR8/2) moist saprolite matrix. Red (10R4/6) mottles surrounded by yellow (10YR7/6) then faint yellow (10YR8/4: very pale brown) matrix. Silty clay loam with a smooth silty and micaceous feel (40% clay, 25% silt). Massive when wet. Some fine cracks when dry demarcating in localized parts large polyhedral to prismatic peds (20-50mm) with oriented light grey (2.5Y7/2) clay on their surface. Very few root channels without roots. Abrupt and irregular boundary following the dip of the weathered rock in places.

170 - 190: Cn (1>-r-y). Massive and dense bands of purple, red and yellow saprolite matrix, dipping near vertical (dip 80°, strike 153°), with micaceous particles aligned with dip.

Alignments of purple (5R2.5/3: very dusky red) to dark red (5R3/6) matrix (bands of 20-80mm thick), moderately cemented. Zones (40%) of vesicules or interlayer-bands of brownish yellow (10YR6/6) to faint yellow (10YR8/4 : very pale brown) matrix aligned with dip, weakly cemented. Some white mottles (5%, < 30mm) are nested in the latter faint yellow matrix.

Where: p = purple, r = red, y = yellow and w = white.

Table 29: Chemical and particle size distribution of the fine, kaolinitic, mesic, Typic Palexeralf

Depth	Horizon	E.C. Sat. Extract	E.C. (1:5 soil:H_2O)	pH (0.01M $CaCl_2$)	Cl	Org. C	CO_3 as $CaCO_3$	Clay	Silt	Fine Sand	Coarse Sand	Total
cm		dS/m	dS/m		mg/kg	%	%	%	%	%	%	%
0-10	A1	0.55	0.10	5.1	4.7	20	2.8	tr	16	7	51	26	100
10 - 20	E	0.34	0.05	5.8	5.2	12	0.7	tr	7	7	46	40	100
20 - 25	Bt1-E	0.31	0.07	5.7	5.1	10	0.9	tr	45	7	28	20	100
25 - 42	Bt2 (r)*	0.14	0.07	6.5	6.2	10	0.3	tr	60	14	18	12	104
75 -87	Bt3 (r-y)*	0.15	0.09	6.3	6.1	10	0.2	tr	49	20	23	12	104
120 - 132	Btn4-C (r-y-w)*	0.13	0.08	6.5	5.9	9	0.1	0.1	39	24	28	11	102
145 - 150	Ctn1(w)*	0.17	0.08	6.3	5.4	19	0.2	tr	35	28	28	10	101

Depth	Horizon	Saturation Extract Na	K	Ca	Mg	Sodium Absorpn Ratio	Exch. Sodium %	Exchangeable Cations Na	K	Ca	Mg	Total	C.E.C. (NH_4)-Cl
cm		mmol(+)/L						cmol/kg					
0-10	A1	1.4	0.39	2.8	1.2	1	3.2	0.13	0.40	4.72	0.94	6.2	4.1
10 - 20	E	1.8	0.15	0.6		3	7.5	0.14	0.15	1.09	0.48	1.9	1.9
20 - 25	Bt1-E	1.1	0.15	1.2	0.7	1	5.7	0.22	0.35	4.08	2.14	6.8	4.0
25 - 42	Bt2 (r)*	1.0	0.04	0.1	0.1	3	9.9	0.45	0.55	5.55	5.00	11.6	4.6
75 -87	Bt3(r-y)*	1.4	0.01	0.1	0.1	5	13.9	0.59	0.13	3.83	4.40	9.0	4.2
120 - 132	Btn4-C (r-y-w)*	1.2	0.01	0.0	0.0	10	19.1	0.71	0.09	2.56	4.37	7.7	3.7
145 - 150	Cn1 (w)*	1.9	0.04	0.1	0.1	6	16.6	1.15	0.09	3.06	6.83	11.1	6.9

*Where: (r) = red, (y) = yellow and (w) = white coloured soil features.(e.g. matrices or mottles).

Nature and properties of saline-sulfidic soils in the Guthrie wetland

The soil profile description in Table 30 together with the vertical and lateral distribution of saline-sulfidic soil features in the Guthrie wetland (Figure 84; Figure 88) showed that physical disturbance of soil and water features (e.g. caused from pugging by cattle and localised rising in groundwater in tree cleared landscapes) initiated biogeochemical processes (accumulation and oxidation of pyrite) that resulted in:

- Initial degradation of wetland vegetation as shown in Figure 84 and Figure 88.
- Recent (20 to 50 years) progressive transformation in the thick topsoils of undisturbed/unfarmed Mollic Natraqualfs (Soil Survey Staff, 1999) to degraded saline-sulfidic materials (i.e. pyrite as shown in Figure 86) in as shown in Figure 84. As such, Fitzpatrick et al. (1992) proposed that the recently formed saline-sulfidic characteristics of these soils meant that the newly formed degraded soil profile be classified as Alfic Sodic Sulfaquents (Table 30).
- Subsequent, soil surface disturbance by animal pugging results in the oxidation of pyrite to produce sulfuric acid in these surface horizons (Figure 87; Figure 85) and the formation if sulfuric material (i.e. pH < 4) with jarosites (Figure 87).
- Dissolution of soil minerals and the precipitation and accumulation of: (i) reddish-brown gelatinous precipitates in surface ponds during wet periods or mostly in winter as shown in Figure 84 and (ii) reddish/orange-brown thin weakly cemented crusts (2 to 5 mm) as shown in Figure 84 and Figure 91 during dry or summer periods. These Fe-rich accumulations contain mixtures of dominantly schwertmannite with minor/trace amounts of ferrihydrite and goethite. The soil profile (Table 30) in the Guthrie wetland was where schwertmannite was first identified in a natural soil environment (i.e. Alfic Sodic Sulfaquent: see Fitzpatrick and Self, 1997) as opposed to an unnatural Acid Mine Drainage (AMD) environment and hence was used to assist Professor Jerry Bigham (Figure 90) as justification to register the "AMD mineral" as a new mineral named schwertmannite by the IMA (Bigham et al. 1996).

Table 30: Description and soil classification[1] of soil profile in the Guthrie wetland (20th May 1990).

Horizon	Depth (cm)	Soil description
Apyz1	0-2	Cattle pugging evident with abundant yellowish-brown Iron-rich precipitates in ponded water and on the soil surface and coating dead plant materials comprising mostly schwertmannite (pH 3.3); sporadic occurrences of salt efflorescence's (gypsum and halite); soft; many fine roots
Apse2	2-10	Very dark grey brown (10 YR 3/2) loam; strong granular; soft; many fine roots (pH 5.7)
Ase3	10-25	Very dark brown (10 YR 2/2), dark grey (10 YR 4/1) mottles, sandy clay loam; weak granular; firm; few very fine roots (pH 5.8).
Eng1	25-35	Grey (5 Y 6/1) sandy loam; massive; hard (dispersed clay layer) (pH 5.8)
Eng2	35-45	Grey (5 Y 6/1) sandy loam; massive; soft. (pH 5.9)
Btng1/W	45-80	Brownish yellow (10 YR 6/6), with greyish brown (2.5 Y 5.5/2) primary and olive grey (5 Y 5/2) secondary mottles, heavy clay; strong medium prismatic structure; very hard (pH 6.2)
Btng2/W	80-94+	Brownish yellow (10 YR 6/6), with greyish brown (2.5 Y 5.5/2) primary and olive grey (5 Y 3/2) secondary mottles, medium clay with micaceous flecks; strong medium prismatic structure; very hard (pH 6.2)

[1]Soil classification in accordance with: (i) the Australian Classification (Isbell, 1996): Melanic-Bleached, Sulfidic, Salic, Hydrosol; thin, non-gravely, loamy, loamy, very deep and (ii) Soil Taxonomy (Soil Survey Staff, 1999): Typic Sulfaquents or Alfic Sodic Sulfaquents (proposed new subgroup see Fitzpatrick et al. 1992). Electrical conductivity was elevated (> 3 dS/m) throughout the profile.

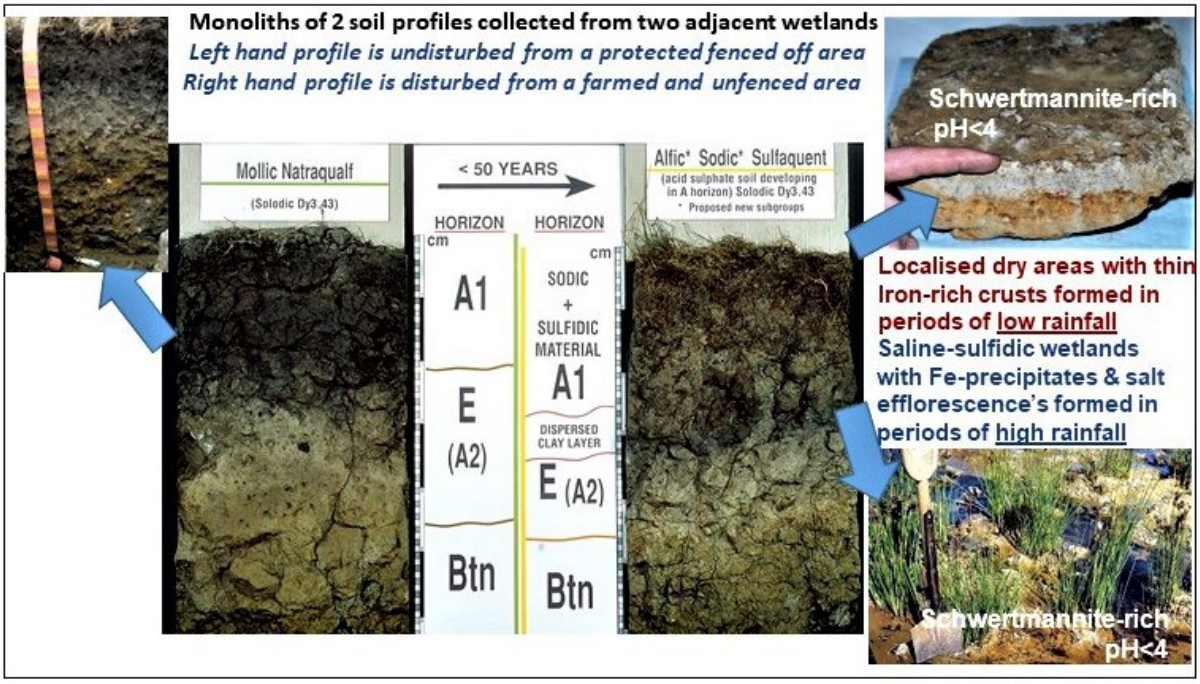

Figure 84: Conceptual pictorial model showing the rapid (< 50 years) transformation of pristine non-saline surface soil features to degraded saline-sulfidic soils in the Guthrie catchment. Photographs of two soil monoliths collected in 1990 from two adjacent wetlands show the: (i) relatively undisturbed thick and friable surface soil with uniform black colours - from a protected fenced off area for a long period of time (Left Hand Side soil profiles) and (ii) strongly disturbed surface soil with prominent redoximorphic features, ponded water with gelatinous Fe-rich precipitates in winter and iron-rich crusts in summer – from continuously farmed and unfenced off areas for long periods of time (Right Hand side soil profile)

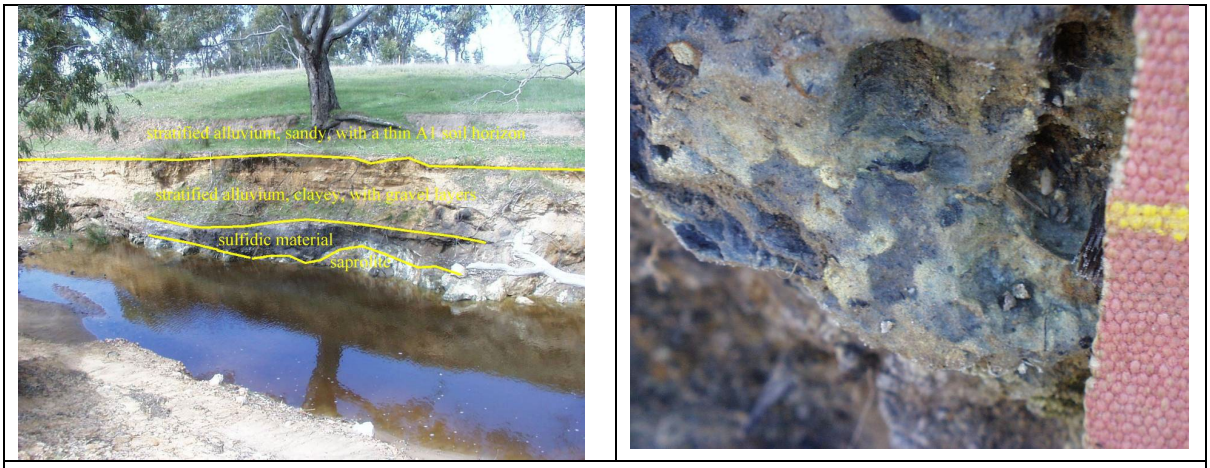

Figure 85: An exposure of buried black sulfidic material in a bank section in Dairy Creek. The regolith sequence comprises relatively young sandy alluvium (with a thin soil horizon) overlying older relatively-clay-rich alluvium with thin gravel layers. which may contain fragments of bright yellow oxidised sulfidic materials containing sideronatrite and jarosite (pH <3.5). The sulfuric material with pale yellow jarosite mottling (see Right Hand photo) and bright yellow sideronatrite developed from the oxidation of pyrite in the underlying black sulfidic material and saprolite (derived from Tapanappa Formation lithologies). Note the white salt efflorescences (halite, gypsum) just above the water surface (from Skwarnecki and Fitzpatrick 2003).

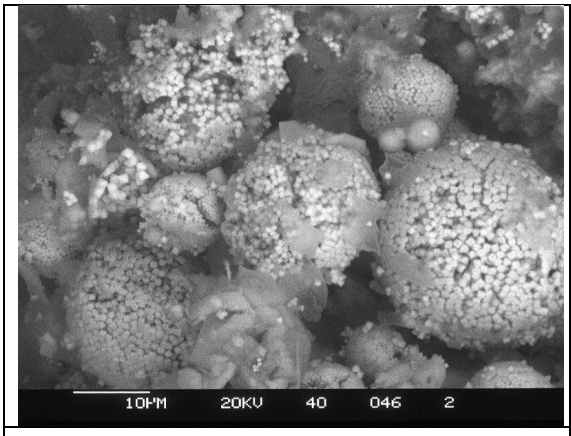

Figure 86. Back-scattered Scanning electron microscope (SEM) image of sulfide framboids (spheroidal aggregates of pyrite crystals) in sulfidic material (i.e. pH 7-8) in the southern bank of Dairy Creek shown in Figure 85 (from Skwarnecki and Fitzpatrick 2003).

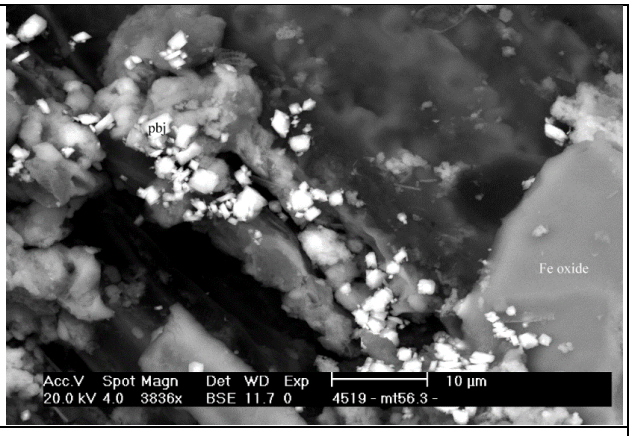

Figure 87. Back-scattered SEM image of Plumbojarosite (pbj) crystals associated with Fe oxides in partially oxidised sulfidic material (sulfuric material) (from Skwarnecki and Fitzpatrick 2003)

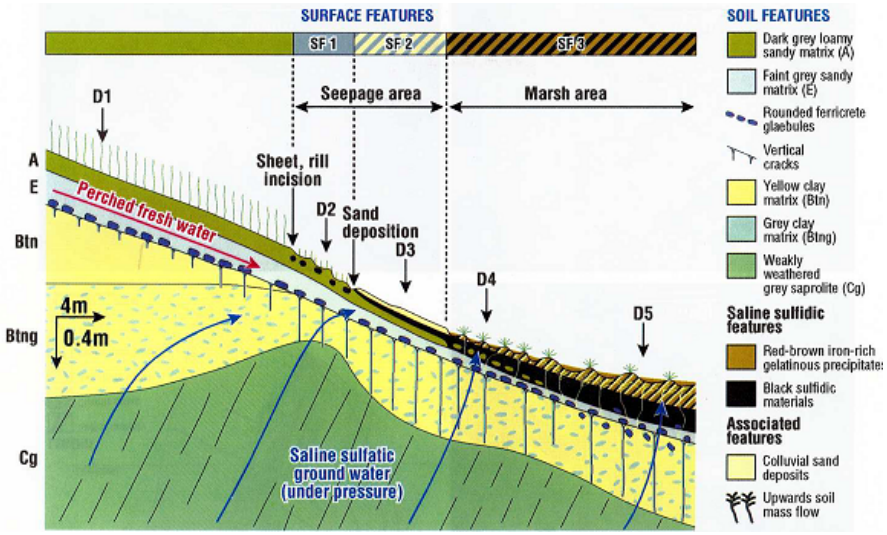

Figure 88. Cross section of a typical soil toposequence through a saline seepage and marsh area showing surface features (SF 1: Seepage areas with stunted halophytic grass with eroded and sealed soil surface; SF2: Seepage areas with flat & almost bare surface covered by sand deposits; SF 3: Marsh areas of mostly permanent wet & soft surfaces comprising tufts of halophytic grass and ponded water with Fe-rich gelatinous precipitates), soil features and water-flow (red and blue arrows) (From Fitzpatrick et al. 1996)

Vertical and lateral distribution of saline-sulfidic features (from Fitzpatrick et al. 1996)

Figure 88 depicts a typical hydro-toposequence through a seepage and marsh area and shows how the position of the black sulfidic material and red-brown iron-rich gelatinous precipitates relates to the soil horizons (A, E, Btn, Btng and Cg) and waterflow paths (throughflow for the perched water and upwards flow for the semi-confined groundwater aquifer as indicated by arrows). Figure 88 also shows the spatial extent of these saline-sulfidic features in relation to the three surface features SF 1, SF 2 and SF 3.

In SF 1 (Upper seepage areas with stunted halophytic grass, erosion and sealed soil surfaces) black sulfidic mottles form in winter when the groundwater is at the surface . The black colour changes to dark grey in summer when the groundwater drops. As the topsoil dries, vertical cracks and white salt crystals of halite with small amounts of gypsum form at the surface (Figure 88).

In SF 2 (Lower seepage area) the black sulfidic material form a thin layer (I to 3 cm thick). This black sulfidic layer is generally covered by a thin layer of colluvial sand. In winter, water containing dark-reddish-brown Fe-rich precipitates oozes to the surface through tubular pores. These precipitates consist of almost pure two line ferrihydrite and, therefore, do not contain entrapped clay particles. In summer, the black colour of the sulfidic layer changes to a dark-grey colour and small scattered white salt crystals of halite and gypsum form at the surface.

In SF 3 (Marsh area) the black sulfidic materials occur in the form of a thick soft layer (5 to 30 cm thick). In Figure 88 the black sulfidic layer is shown to increase in thickness downslope and completely replaces the organic-rich A horizon as shown in Figure 84. At the surface, a yellowish brown gelatinous precipitate, consisting of mostly schwertmannite with minor ferrihydrite and layer silicates, is abundant in micro-depressions where water is ponded. Between the surface gelatinous precipitate and the black sulfidic layer an extremely heterogeneous layer generally occurs (layer with oblique stripes in Figure 88) with a distinctive flow-like pattern due to upward flow of soil with n - value of > 1.

Iron-rich crusts: thin (2 to 5 mm) iron-rich crusts form during dry periods (Figure 86 and Figure 89) with white salt efflorescence's encrusted on the surfaces of iron-rich crusts. The salts consist mainly of sulfate minerals, in particular gypsum, and a small amount of halite and barite. The thin and friable iron crust has a dark-yellowish-brown colour (10YR 4/ 4) when moist and a yellowish-brown colour (10YR 5/8) when dry. The various iron minerals coat and weakly cement clay particles and sand grains. XRD and TEM examinations indicated that the iron minerals were dominantly the iron oxyhydroxysulfate, schwertmannite (Bigham et al., 1990, 1992) with traces of poorly crystalline goethite and ferrihydrite. The goethite content is higher in the iron crusts than in the gelatinous precipitates. Desiccation of the iron-rich gelatinous precipitates appears to contribute to the formation of these salt-iron crusts. Compared to background soils, these crusts have higher concentrations of Fe, S, P, As, Ba, Na, Pb, Zn (locally) and REE as shown in Figure 91 and Figure 92.

In summary, the physical and biogeochemical processes described above have caused the formation of less permeable: (i) Fe-rich surface layers and (ii) dispersed subsoil layers in discharge areas, which has led to degraded soils, erosion and poor stream water quality.

Sulfuric materials in the Guthrie catchment (Figure 85) generally have bright yellow or straw-coloured mottles of jarosite/natrojarosite (Figure 85) and sideronatrite (Skwarnecki and Fitzpatrick 2003). In rare instances, e.g. associated with Pb-bearing mineral deposits, minerals such as plumbojarosite (Figure 87) and plumbogummite occur where they overlie mineralized zones in bedrock (e.g Skwarnecki and Fitzpatrick 2003).

(a)

(b)

Figure 89. Photographs of the Guthrie wetland in the Mt. Lofty Ranges, South Australia taken in:
(a) July 1990 showing Drs Peter Self (left) and Rob Fitzpatrick (right) when the perched and ground water table levels were relatively high with a gelatinous reddish-brown precipitate layer, which overlies black sulfidic material (see Fitzpatrick 1991). The site was also sampled in January 1991 when the perched and ground water table levels were relatively low leaving an essentially moist to almost dry surface with a thin friable reddish/orange-brown crust (2 to 5 mm) that is weakly cemented as shown in Figure 84 and Figure 91. The reddish/orange-brown thin weakly cemented crust (2 to 5 mm) was found to contain the so-called "acid mine drainage mineral" (Fitzpatrick et al. 1992; Fitzpatrick et al. 1996; Fitzpatrick and Self 1997), which was originally identified by Bigham et al. (1990) in acid mine drainage (AMD) waters.
(b) August 1993 showing Professor Udo Schwertmann (right – after whom the mineral schwertmannite is named) and Rob Fitzpatrick (left) both pointing to the thin friable crust where schwertmannite was first identified in a natural soil environment (i.e. Alfic Sodic Sulfaquent: see Fitzpatrick and Self, 1997) as opposed to an unnatural AMD environment and hence used as part of the comprehensive justification by Prof Bigham to register the "AMD mineral" as a new mineral named schwertmannite by the IMA (Bigham et al. 1996)

Professor Jerry Bigham shown in Figure 90 headed a group of international scientists (including Professor Udo Schwertmann), who first comprehensively described the formation, properties and structure, of the mineral "schwertmannite", which is named after Prof Schwertmann by the International Mineralogical Association or IMA (Bigham et al. 1990, 1996). Schwertmannite ($Fe_8O_8(OH)_{8-2x}(SO_4)_x$ with $1 \leq x \leq 1.75$) is a poorly crystalline iron oxyhydroxysulfate mineral, which is indicative of rapidly changing local environments and variations in redox, pH and rates of availability of S and other elements. As such, the presence of schwertmannite has been included as an acceptable indicator of acidity (pH <4) for sulfuric materials or the sulfuric horizon in several international (e.g. Soil Taxonomy and WRB) and national (e.g. Australian) soil classification systems.

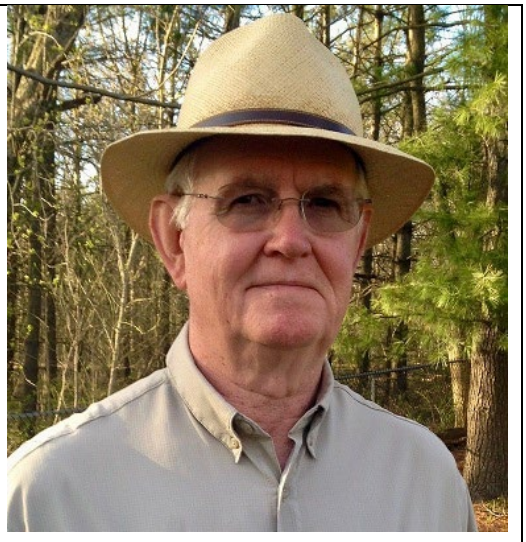

Figure 90. Photograph of Professor Jerry Bigham who headed the proposal and publications (Bigham et al. 1990, 1996) to justify registering schwertmannite as new mineral via the IMA.

Figure 91. Photograph of the Iron-rich crust formed in the Guthrie wetland (Figure 84 ;Figure 89) composed of dominantly schwertmannite and traces of ferrihydrite and goethite with layers described in Figure 92

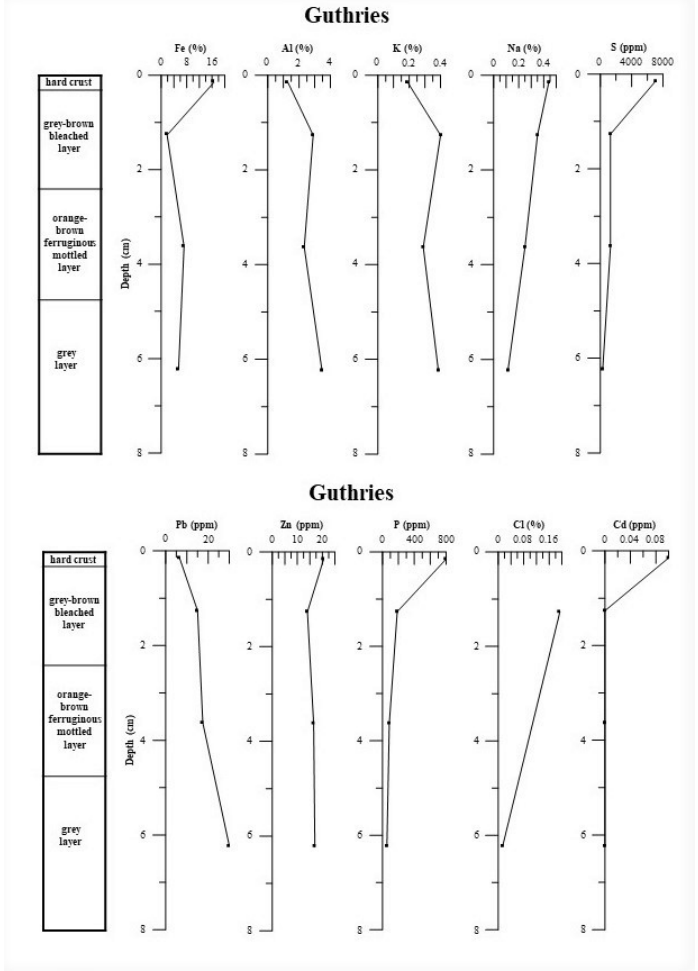

Figure 92. Vertical variations in the distribution of selected elements through the iron-rich crust formed in the Guthrie wetland shown in Figure 85 and Figure 89 (from Skwarnecki and Fitzpatrick, 2003)

Samples of two reddish-yellow Fe-rich precipitates that coated surfaces of *Eucalyptus* leaves and decomposed organic matter on soils in the Guthrie wetland were collected by Rob Fitzpatrick, Luke Mosley and Brett Thomas on the 24th February 2023 for chemical and X-ray diffraction (XRD) analyses. These types of samples are considered to be relatively pure (i.e. free of adjacent soil materials). The pH measured in both samples was 3.66. Prior to XRD analyses the reddish-yellow Fe-rich precipitates were concentrated by carefully sieving the dried samples through a 50 micron sieve. Mineralogical analysis by XRD of both Fe-rich precipitates was used to confirm the dominant occurrence of the iron oxyhydroxysulfate mineral schwertmannite, which is an indicator of acidic (pH 2.8 to 4.5) geochemical water/soil conditions (Bigham et al., 1996). X-ray patterns generally displayed 7 of the 8 broad peaks typical for schwertmannite, with the reflections at 2.55 Å, 3.5 and 1.5 Å, being most pronounced (Bigham et al. 1994).

Based on the current acidic conditions (pH 3.66) and widespread occurrence of schwertmannite in the Guthrie wetland, recommendations have been made in the below Section entitled: *Pictorial manuals for land management planning* (see Figure 103) to ameliorate the current extreme acidity across the Guthrie wetland.

Soil-regolith process models

Conceptual process models enable researchers to develop, refine and present mechanistic understanding of complex soil-regolith environments (Fritsch and Fitzpatrick, 1994). These models are graphic, cross-sectional representations of soil-regolith-bedrock profiles that illustrate vertical and lateral changes, which occur down toposequences. They are used to explain the complex pedological, hydrological and biogeochemical interactions that occur in the regolith environment (Fitzpatrick and Merry, 2002). Three categories of conceptual toposequence models have been described (Fitzpatrick and Merry, 2002; Fitzpatrick and Skwarnecki, 2003), which are:

- Descriptive soil-regolith models.
- Explanatory soil-regolith models.
- Predictive soil-regolith models.

Descriptive soil-regolith models

(from Fitzpatrick et al. 1996b; Fritsch and Fitzpatrick, 1994)

Fitzpatrick et al. (1996) and Fritsch and Fitzpatrick (1994) used a 2D toposequence (cross-section) (Figure 93) to summarise soil-regolith characteristics and key soil morphological and physio-chemical features in the Guthrie and Herrmann catchments. Fritsch and Fitzpatrick (1994) used a systematic structural approach to form relationships between soil profile features down landscape slopes. This was achieved by describing, by depth interval, all similar soil features (i.e. soil components with similar consistency, colour, textural and structural patterns, and physio-chemical and mineralogical properties). Thus, they were able to group similar soil features into fewer soil layers, which were linked down the toposequence and mapped in cross section (Figure 93). Each of these soil layers were linked to hydrological processes (e.g. water flow paths, salinity and sodicity) by using soil colour (together with other morphological, chemical and mineralogical indicators) and hydrology measurements (Cox et al., 1996; Fitzpatrick et al., 1996). This enabled the construction of **2D** linkages that described water flow paths and the development of salinity in both the Guthrie and Herrmann catchments (Figure 93).

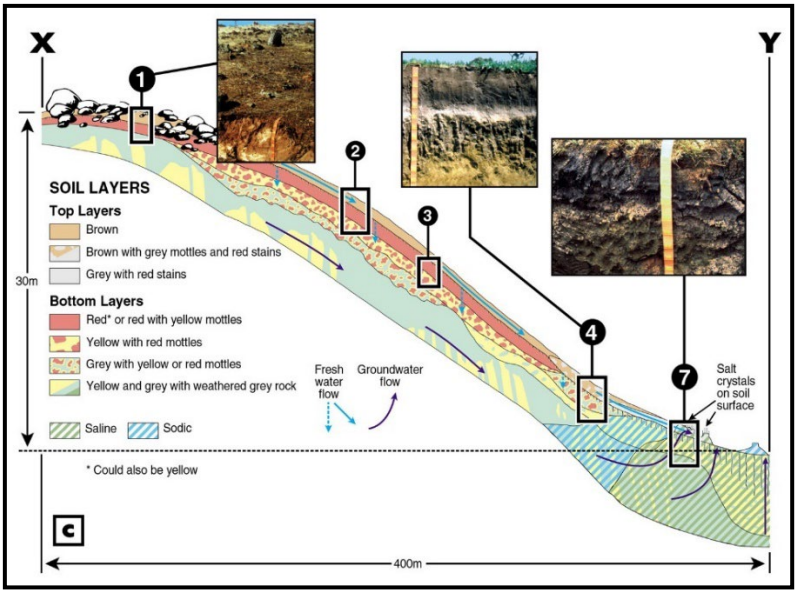

Figure 93. Descriptive soil-regolith model showing toposequences with three selected profiles, soil features (e.g. relict purple mottles and current very poorly drained saline soils with grey and red stains) and direction of perched fresh water flow and groundwater flow (Modified from Fitzpatrick et al., 1996b; Fritsch and Fitzpatrick, 1994).

Fitzpatrick and Skwarnecki (2003) extended the use of descriptive process models to characterise catchment-scale variability of relict (past geomorphological processes in development of deep weathering and erosion) and current (saline, sodic and acid sulfate soils) soil forming processes in order to help develop practical solutions for: (i) possible use in mineral exploration and (ii) ameliorating soils at farm scale.

Explanatory soil-regolith models

(from Fitzpatrick et al. 1996; Skwarnecki and Fitzpatrick 2003)

Fitzpatrick et al. (1996) used the descriptive soil-regolith toposequence model (Figure 93) to construct an explanatory soil-landscape process model to explain contemporary geochemical dispersion and erosion processes present in the lower parts of the toposequence (Figure 94 and Figure 95). These models explain the formation and degradation of ASS in a single diagram that illustrates the pedological, geological, biogeochemical, mineralogical and hydrological processes occurring in the eastern Mt Lofty Ranges. Fitzpatrick et al. (1996) illustrate that a combination of: (i) saline groundwaters enriched in sulfate (with other elements sourced from mineralised zones e.g. Pb and Zn) seeping up through soils, (ii) anaerobic conditions and (iii) organic carbon in saturated soils yield sulfidic material containing pyrite framboids through anaerobic bacterial reduction of sulfate. Thus, when these sulfidic materials are eroded and exposed to air, pyrite is oxidised producing sulfuric acid, which dissolves soil minerals and leads to precipitation of mineral combinations:

- sideronatrite, tamarugite, copiapite, halite and gypsum in sandy sulfuric soils with pH < 2.5,
- natrojarosite, jarosite and plumbojarosite in clay-rich sulfuric horizons with pH 3.5-4,
- schwertmannite (orange; pH 4); ferrihydrite (reddish-brown; pH >6), akaganéite (reddish-orange) and colloidal (nanoparticulate) poorly crystalline /pseudoboehmite-like (white) precipitates.

The formation of these complex sulfate salts (of Fe, Al, Na, Pb, Ca, As, Zn), jarosites, oxyhydroxysulfates and oxyhydroxides of Fe are indicative of rapidly changing local environments and variations in Eh (redox), pH and rates of availability of Fe, S and other elements (Skwarnecki and Fitzpatrick, 2003).

Regional sampling by Skwarnecki and Fitzpatrick (2003) has shown that a range of materials associated with sulfidic and sulfidic material (e.g. sulfidic materials, sulfuric horizons, salt efflorescences, and Fe- and Al-rich precipitates) are anomalous in elements such as As, Bi, Cd, Cu, Pb, Tl and Zn, especially where they are spatially related to sulfide mineralization. Thus, the evolution of sulfidic/sulfuric material may carry indications of the presence of blind or concealed ore deposits making these sediments a potential sampling medium for mineral exploration (Figure 94 and Figure 95).

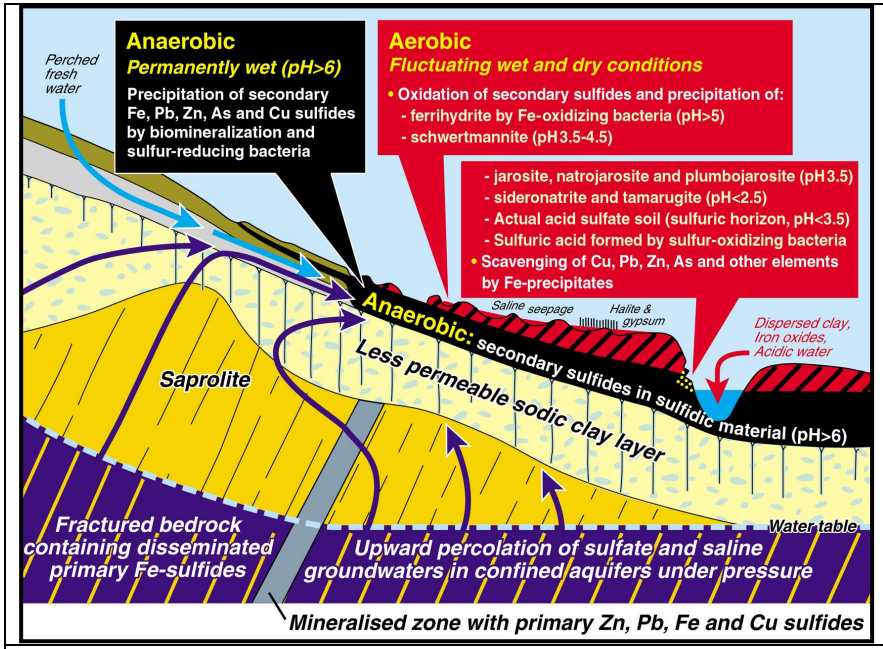

Figure 94. Explanatory soil-regolith model showing geochemical dispersion and erosion processes in saline seepages and formation of secondary sulfides in sulfidic material in a perched wetland and sulfuric materials along eroded drainage lines (From Fitzpatrick et al., 1996; 2008).

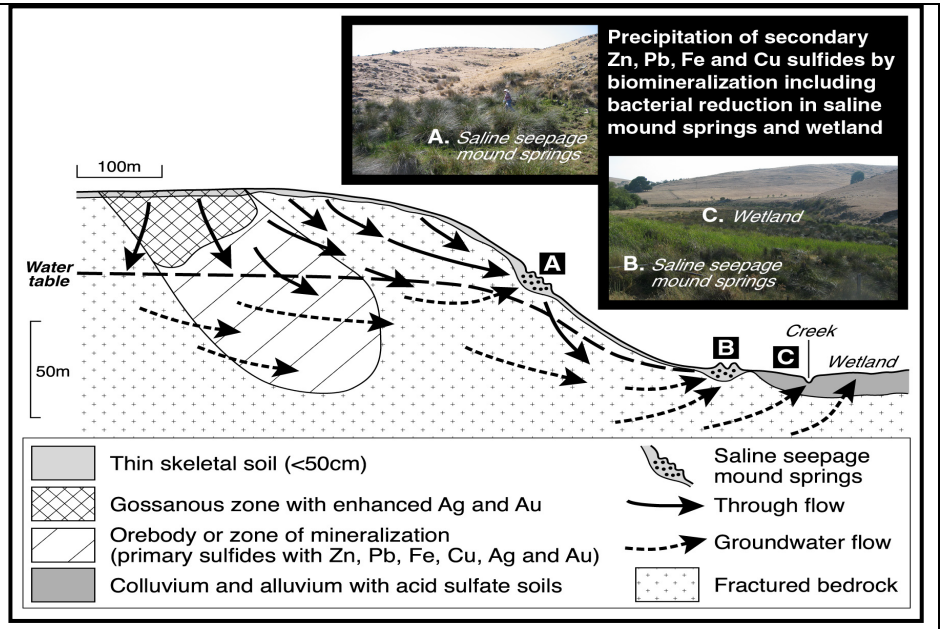

Figure 95. Explanatory soil-regolith model showing geochemical dispersion from mineralized zones in sulfidic/sulfuric materials from seeps, springs and wetlands, eastern Mount Lofty Ranges zone (Modified from Skwarnecki and Fitzpatrick, 2003).

Predictive soil-regolith models: landscape evolutionary processes

(from Fitzpatrick et al 2000a)

Fitzpatrick *et al.* (2000a) used the information contained in Figure 88, Figure 93, Figure 94 and Figure 95 to construct a predictive soil model showing the hydrogeochemical processes, which transform sulfidic material in a perched wetland to highly sulfuric material (Figure 96).

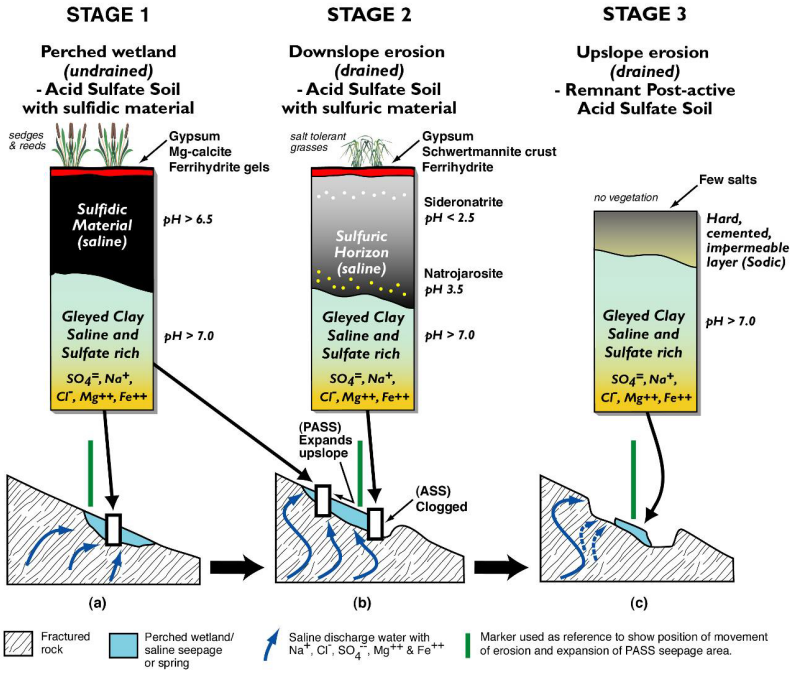

Figure 96. Predictive soil-regolith model showing the hydrogeochemical processes, which transform sulfidic material in a perched wetland to highly saline sulfuric material (after Fitzpatrick et al., 2000a).

Stage 1: Saline groundwater enriched in sulfate (SO_4^{2-}) seeps up through the soil, along with other ions in solution such as Na^+, Ca^{2+}, Mg^{2+}, AsO_4^{2-}, I^- and Cl^-, and concentrates by evaporation to form various mineral precipitates within and on top of the soil surface (Figure 96a). The combination of: (i) rising sulfatic groundwater, (ii) anaerobic conditions associated with saturated soils, (iii) agricultural activity and (iv) fractured rocks relatively enriched in Fe, S, Pb, Zn, etc., can lead to the formation of sulfidic material and precipitation of anomalous concentrations of Pb and Zn. If the soil is wet and contains sufficient organic carbon, anaerobic bacteria use the oxygen associated with the sulfate (SO_4^{2-}) ions during the assimilation of carbon from organic matter. This process produces pyrite (FeS_2) and forms sulfidic materials (Figure 96a).

Stage 2: sulfuric materials result when pugging from animals, drainage works or other disruptions expose the pyrite in previously saturated soils to oxygen in the air. Thus pyrite is oxidised to sulfuric acid and various iron sulfate-rich minerals, and sulfuric material forms (Figure 1-4b). When sulfuric acid forms, the soil pH can drop from neutral (pH 7) to below 4; locally pH may attain values as low as 2.5 to form a sulfuric horizon (Figure 96b). The sulfuric acid dissolves the clay particles in soil, causing basic cations and associated anions (e.g. Na^+, Mg^{2+}, Ca^{2+}, Ba^{2+}, Cl^-, SO_4^{2-}, SiO_4^{4-}), trace elements, and metal ions such as Fe^{3+} and Al^{3+} to be released onto the soil surface and into stream waters. As the regolith structure degrades due to the accompanying sodicity, soils become clogged with dispersed clay and iron precipitates and they lose their permeability and groundcover. This prevents the groundwater below from discharging and forces it to move sideways or upslope (Figure 96b). Soil around the clogged area eventually erodes, sending acid, metal ions and salts into waterways and dams, and a new area with sulfidic material develops upslope or adjacent to the

original area with sulfidic material. If cattle or other activities continue to disturb the soil around the newly created sulfidic material, the area affected continues to expand upslope (Figure 96b).

***Stage 3*:** If these processes express on the surface of the soil, bare eroded saline scalds surrounding a core of slowly permeable, highly saline, eroded sulfuric material result (Figure 96c). These saline landscapes are characterised by slimy red or white ooze and scalds with impermeable iron-rich crusts. As shown in Figure 96a & b, when the potential acid sulfate soils undergo changes, different salt and iron minerals form because of differences in pH and salt concentrations. In the final stage of formation, a hard soil layer remains, with only few salts (Figure 96c). The acidification process accelerates the decomposition and formation of minerals in the soils and underlying rocks and can cause an increase in salinity and carbonate formation.

Hydropedology / water-flow models

(from Fritsch and Fitzpatrick 1994)

A number of studies have been carried out in the Mt Torrens study area that focussed on the hydropedology (hydrology and soil-water flow interactions) occurring within the Herrmann catchment (Figure 97) (Cox et al., 1996; Fitzpatrick et al., 1996; Fritsch and Fitzpatrick, 1994). Fritsch and Fitzpatrick (1994) inferred water movement patterns in the Herrmann catchment from the spatial distribution of soil features and soil systems in the landscape. They found that superimposed soil features or nesting of soil features were the result of particular water flow. Vertical flow was linked to superimposed soil features (i.e. layered) whilst lateral flow was linked to nested soil features. Thus, Fritsch and Fitzpatrick (1994) were able to identify three soil-water flow systems in the Herrmann catchment. These systems consisted of: (i) a well drained red soil system with vertical flow, (ii) above this was a perched water flow system and (iii) below a, ground water flow system (Figure 5 1).

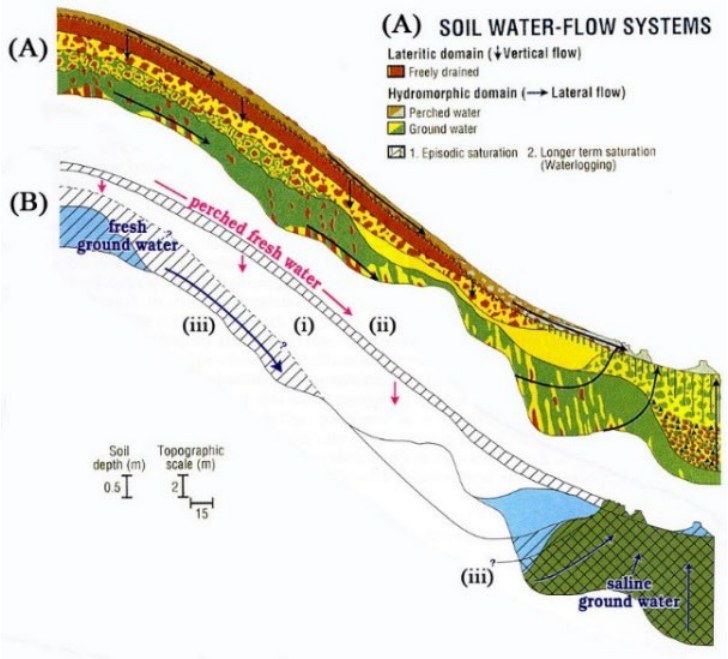

Figure 97. Three soil-water flow systems based on data from the nearby Herrmann catchment in catchment. Systems consisted of: (i) a well drained red soil system with vertical flow, (ii) above this was a perched water flow system and (iii) below a ground water flow system (From Fritsch and Fitzpatrick, 1994).

They also found that waterlogging and lateral throughflow towards downslope was common to both the ground and perched water flow systems. Fritsch and Fitzpatrick (1994) explain that the water in

the perched system was fresh and fluctuated rapidly in the permeable topsoil. In contrast, the groundwater system contained saline-sulfatic water, because of weathering of rock minerals, with much slower rates of recharge and discharge. Also as groundwater was under pressure in valleys, saline-sulfatic water oozed to the soil surface through macropores to form seepage areas, contained highly degraded saline-sulfidic soils.

Lead isotopes from sulfidic wetlands for Base Metal Exploration

(from Baker and Fitzpatrick, 2010)

Geochemistry: Skwarnecki and Fitzpatrick (2003) carried out a regional geochemical survey of sulfidic seeps and wetlands in the Kanmantoo region, which covered an area of 1000 km^2. This survey was based on the premise that black sulfidic, sulfuric and sulfide-containing materials and Fe-rich gels associated with saline wetlands and seeps concentrate elements (As, Ba, Bi, Cd, Cu, P, Pb, Sn, Tl and Zn) indicative of underlying sulfide mineralisation (Skwarnecki et al. 2002). Scavenging of elements in sulfides has occurred because of co-precipitation of these elements from groundwater with Fe sulfides/oxides. Skwarnecki et al. (2002) found that, at a prospect scale in the Mount Lofty Region, sulfidic seeps and wetland (when present) may capture geochemical dispersion halos of up to 750 m in width around the mineralised zones, compared to up to 200 m for soils and up to 700 m for stream sediments.

Skwarnecki and Fitzpatrick (2003) collected 150 samples from saline-sulfidic wetlands throughout the Kanmantoo geological province. Five sulfidic material samples were chosen for follow up work (**Error! Reference source not found.**) based on bulk geochemical analysis (Table 31). Four samples were chosen because they contained one or more elements, associated with sulfide mineralisation, which exceeded predetermined thresholds [90th percentile - as determined by Skwarnecki et al. (2002)]. Samples were ranked according to prospectivity (1 = most prospective) based on the number of elements, associated with sulfide mineralisation that exceeded threshold (Table 1). Sample KRS_22 from Rodwell Creek, which was considered most prospective and contained the highest concentrations of Pb and Zn.

Table 31. Selected geochemical results from sulfidic soil-regolith samples collected as part of a regional geochemical survey of sulfidic seeps and wetlands in the Kanmantoo geologic province by Skwarnecki and Fitzpatrick (2003). Background element concentrations were calculated as the 50th percentile and the threshold concentrations at the 90th percentile [as determined by Skwarnecki et al. (2002)]. Red values exceed threshold concentrations and are considered anomalous.

	As ppm	Ba ppm	Bi ppm	Cd ppm	Cu ppm	P ppm	Pb ppm	Sn ppm	Tl ppm	Zn ppm	
Detection	0.5	5	0.1	0.1	2	5	0.5	0.1	0.1	0.5	
Background (50th percentile)	7.75	410	0.23	< 0.1	11	165	30	1.7	0.5	19	
Threshold (90th percentile)	20.5	590	0.55	0.24	24	370	95	4	0.76	54	
Sample	**As ppm**	**Ba ppm**	**Bi ppm**	**Cd ppm**	**Cu ppm**	**P ppm**	**Pb ppm**	**Sn ppm**	**Tl ppm**	**Zn ppm**	**Prospectivity Ranking**
KRS_22 Rodwell Creek	13	430	**2**	**14**	**75**	280	**2850**	**4**	0.7	**2600**	**1**
KRS_147 Guthrie wetland	17	220	0.4	0.1	**33**	**600**	78	1	**1**	**120**	**2**
KRS_8	4.5	280	**11**	0.1	**650**	270	30	3.8	0.7	**110**	**3**
KRS_143	12	290	0.2	0.3	B.D.	**1300**	22	1.4	0.3	**600**	**4**
KRS_142	1.5	420	0.2	B.D.	4	125	14	0.9	0.5	22	**5**

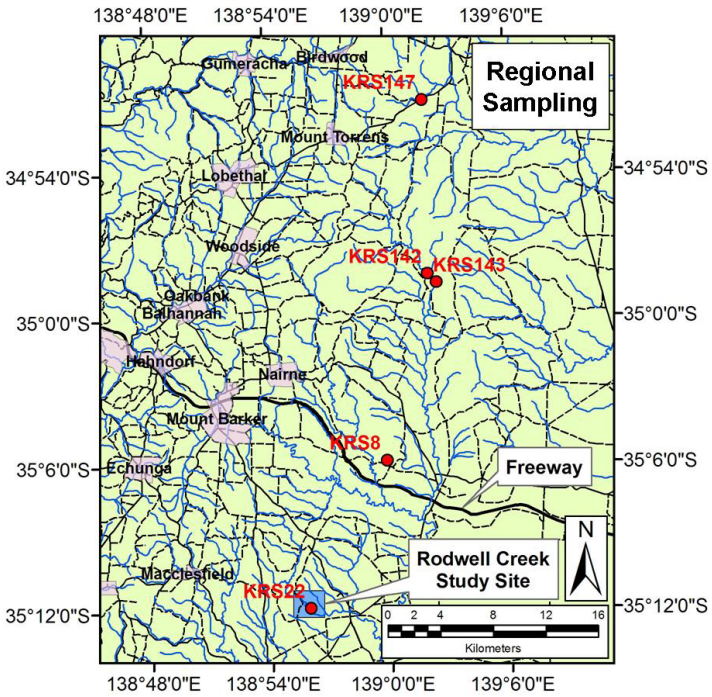

Figure 98. Map showing the 5 selected sample locations from the regional geochemical survey of sulfidic seeps and wetlands, in the Kanmantoo geologic province, carried out by Skwarnecki and Fitzpatrick (2003). Drainage is marked in blue, roadways in black and populated areas in purple. The Rodwell Creek site is marked as blue square and Guthrie wetland is marked at the red dot adjacent to KRS_147.

Pb Isotopes: The Pb isotope compositions of the sulfidic soil samples were measured to further differentiate between chemical anomalies, which were derived from sulfide mineralisation, country rock and anthropogenic contamination. Soil-regolith samples were analysed according to the methods outlined in Baker and Fitzpatrick (2010). Lead isotope ratios are presented in Table 32.

Lead isotope ratio plots for sulfidic soil-regolith samples, relative to Kanmantoo sulfide mineralisation, country rock and anthropogenic contamination, are presented in Figure 99. The Pb signature for Kanmantoo sulfide mineralisation was obtained by measuring the isotope composition of samples from zones of Pb/Zn sulfide enrichment within the Kanmantoo geological province. Twenty one samples were measured for Pb isotope composition, from the Angus, Mt Torrens, Aclare and Wheal Ellen prospects and included: (i) galena derived from the mineralised zone, (ii) gossans, and (iii) laterites proximal to mineralisation (Baker and Fitzpatrick 2010). The country rock Pb signature was defined by the isotope composition of nine samples of unmineralised Talisker Calc-Siltstone and three unmineralised soil samples from the Kanmantoo region. Mt Isa and Broken Hill Pb signatures were used to define anthropogenic contamination in the Kanmantoo geological province.

Estimates of country rock Pb and Kanmantoo sulfide mineralisation Pb in sulfidic soil-regolith samples are displayed in Table 33 Sulfidic soil-regolith samples were ranked according to prospectivity based on the percentage and concentration (ppm) of Pb derived from Kanmantoo sulfide mineralisation (1 = most prospective).

Table 32. Lead isotope results from sulfidic soil-regolith samples selected from the regional geochemical survey of sulfidic seeps and wetlands in the Kanmantoo geologic province by Skwarnecki and Fitzpatrick (2003). Isotope analysis from Fitzpatrick and Baker (2010).

Sample	$^{206}Pb/^{204}Pb$	$^{207}Pb/^{204}Pb$	$^{208}Pb/^{204}Pb$	Pb Conc (ppm)
KRS_22 Rodwell Creek	17.776	15.593	38.072	2850
KRS_147 Guthrie wetland	17.828	15.576	38.072	78
KRS_8	18.31	15.622	38.505	30
KRS_143	17.094	15.548	37.221	22
KRS_142	18.794	15.643	39.784	14

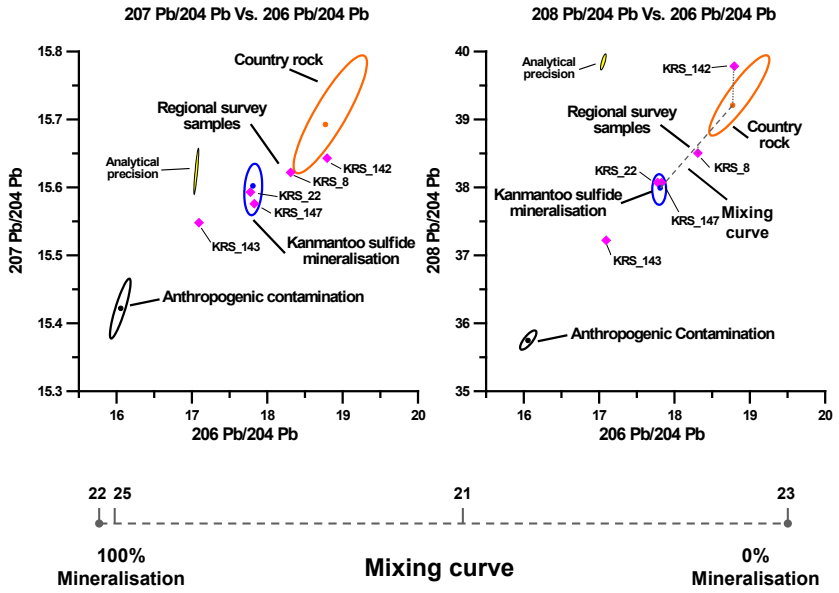

Figure 99. Ratio plots indicating the Pb isotope composition of sulfidic soil-regolith samples, from regional geochemical surveying, relative to Kanmantoo sulfide mineralisation, country rock and anthropogenic contamination. Ellipses define the spread of data and the point within each ellipse represents average Pb isotope composition. The mixing curve estimates the relative contribution of Pb from mineralisation and country rock in each sample. The Rodwell Creek sample is marked as KRS_22 and Guthrie wetland sample is marked as KRS_147.

Table 33. Estimation of Pb contributions from country rock and Kanmantoo sulfide mineralisation in samples (AC – refers to samples with anthropogenic Pb contamination). Sulfidic soil-regolith samples are ranked according to prospectivity based on the percentage and concentration (ppm) of Pb derived from Kanmantoo sulfide mineralisation (1 = most prospective).

Sample	Total Pb (ppm)	Mineralisation %	Country Rock %	Mineralisation Pb (ppm)	Country Rock Pb (ppm)	Prospectivity Ranking
KRS_22 Rodwell Creek	2850	100	0	2850	0	1
KRS_147 Guthrie wetland	78	98	2	76	2	2
KRS_8	30	47	53	14	16	3
KRS_143	22	AC	AC	AC	AC	4
KRS_142	14	0	100	0	14	5

In summary, sample KRS_22 from Rodwell Creek was identified as the most prospective sulfidic sample based on both geochemical and Pb isotope analyses (Table 33). This sample was collected from a saline-sulfidic seep on the banks of Rodwell Creek (**Error! Reference source not found.**) and hence selected as an area for further field and laboratory investigations by Baker and Fitzpatrick (2010). Sample KRS_147 from the Guthrie wetland was identified as having the second most anomalous Pb isotope (i.e. shown in Figure 99 associated with Kanmantoo sulfide mineralisation) geochemical signature (Table 33).

The Pb isotopic analysis of wetland sediments has also enabled the construction of a geochemical dispersion model by Baker and Fitzpatrick (2003) that describes the interaction of base metal mineralisation and sulfidic wetlands at the Mt Torrens Prospect region as shown in **Error! Reference source not found.**. This model provides an insight into the seasonal fluctuations observed in the wetlands and helps to explain the hydro-geochemistry and geochemistry of the area.

3D Predictive process models in response to seasonal changes

(from Baker, 2006)

The predictive conceptual process model presented in Figure 100 and Figure 101 helps to explain the mineralogical and geochemical patterns identified in and around the hydromorphic zone at the Mt Torrens study site. This model is based on geochemical and mineralogical data as well as geochemical modelling using PHREEQC 2.12.5.

Figure 100 and Figure 101 both represent the saline-sulfidic wetlands situated within the Herrmann catchment (focus area A). Each 3D block diagram describes biogeochemical processes, which occur in response to seasonal changes (e.g. rainfall and temperature), within the hydromorphic zone. Numbers within text (e.g. (1)) refer to different sections of the block diagram being discussed. Some of the processes illustrated by these models are also thought to be applicable other the saline-sulfidic seeps in adjacent catchments such as in the Guthrie catchment.

Block diagram (i) – During periods of low rainfall (summer) shown in Figure 100 indicates that there was limited fresh surface and throughflow (W1) into the wetland zone. The sandy loam (1) A and B horizons upslope of the wetland remained drained except during periods of heavy rainfall. It is probable that, even during summer, minor amounts of fresh water entered the wetland zone via the C horizon (2) as a result of infrequent rainfall events. A permanent saline groundwater table (3) was present at depth throughout the study site. Where saline groundwater came in contact with zones of sulfide enrichment (4) (e.g. Mt Torrens mineralisation), it became enriched in sulfate and other mineralisation related elements (e.g. Ba, Cu, Pb and Zn). Wetlands formed where saline groundwater reached the soil surface in mid and lower slope landscape positions. In focus area A, saline-sulfatic, metal rich groundwater (W2) seeped to the soil surface through rock fractures and quartz veining (5). Mixing of waters W1 and W2 occurred within the wetland zone (5) and (6). During summer, there was only minor fresh water input, which meant that the water entering the wetland zone was enriched in sulfate and mineralisation related elements. This resulted in vigorous bacterial reduction of sulfate to sulfide (6), which utilised organic matter as a powerful reductant within the inner wetland zone. Reducing (< -150 mV) soil Eh conditions developed, which resulted in the precipitation of mineral phases including pyrite, galena, sphalerite and chlorite. Cation exchange (6), on clay minerals (e.g. kaolinite) and organic matter also occurred within the inner wetland zone. Modelling indicated that cation exchange sites were dominated by Na+, Mg2+ and Ca2+ when minimal fresh near-surface and surface water entered the inner wetland zone. This meant that only very small concentrations of mineralisation related cations were involved in exchange (e.g. PbX2,

ZnX2 and CuX2) with clay minerals and organic matter. Saline-sulfatic, metal rich waters then seeped to the soil surface through macropores (7). Evaporation occurred and more oxidising conditions (> 200 mV) were encountered at the soil/air interface. This resulted in the precipitation of mineral phases including barite, calcite, goethite, gypsum and halite. Where oxidation of pyrite took place near the soil surface, pH dropped to less than 6 and calcite no longer precipitated. Surface complexation (7) of mineralisation related elements (e.g. As, Ba, Cu, Pb and Zn) on hydrous Fe-oxides (e.g. goethite, ferrihydrite and schwertmannite) took place at the soil surface. Thus, during low rainfall periods, elements associated with zones of sulfide enrichment at depth were likely to accumulate: (i) within the inner wetland zone because of mineral precipitation and the formation of exchange complexes and (ii) on the soil surface of the inner wetland because of complexation on hydrous Fe-oxides.

Block diagram (ii-a) – During periods of elevated rainfall (winter) shown in Figure 101 indicates increased fresh surface and throughflow water (W1) entered the wetland zone. The sandy loam (1) A and B horizons, upslope of focus area A acted as a conduit, which funnelled this fresher water into the wetland. This and greater throughflow in the C horizon (2) would have increased dilution of saline-sulfatic, metal rich groundwater in the semi-confined aquifer beneath the wetland. Thus, mixed ground and near-surface and surface water entered the wetland zone (5) through rock fractures and quartz veining. The ratio of fresh near-surface and surface water to saline-sulfatic water that entered the inner wetland (6) increased relative to winter months. As a result, concentrations of elements including Ca, Mg, Na, K, Cl, Cu, Pb and Zn, decreased in mixed waters. Greater amounts of hydraulic recharge by oxidised (> 200 mV) mixed water with increased Eh (from < -150 mV to > -50 mV) within wetland zone (6). The zone of reduction spread from the inner to the outer wetland zone (6). Pyrite remained stable under these geochemical conditions but the amount that precipitated decreased with increasing dilution. Increased dilution and changing geochemical conditions (e.g. increased Eh) caused the dissolution of minerals such as galena and sphalerite and the precipitation of plumbogummite. Cation exchange (6), on clay minerals (e.g. kaolinite) and organic matter, involving mineralisation related elements (e.g. Ba, Cu, Pb and Zn) increased as dilution of saline-sulfatic water resulted in decreased competition for exchange sites by Na+, Mg2+ and Ca2+. This was additionally enhanced by the dissolution of any galena and sphalerite present, which increased the concentration of Pb and Zn in solution. Modelling indicated that within the inner wetland zone, the net effect of mineral dissolution and cation exchange was increased concentrations of Pb and Zn (and possibly Ba and Cu) in solution. This resulted in subsurface solution transport of mineralisation related elements, from the inner to the outer wetland zone. An oxidation front was encountered at the external margin of the outer wetland (8), which resulted in an accumulation of mineralisation related elements. Surface complexation (7) of mineralisation related elements on hydrous Fe-oxides (e.g. goethite, ferrihydrite and schwertmannite) took place at the soil surface. Following rainfall events, positive Eh conditions (> 200 mV) were maintained at the soil surface (7) because of the oxidising nature of rainwater (> 500 mV). Rainfall and groundwater related surface flow resulted in physical dispersion of hydrous Fe-oxides (e.g. goethite, ferrihydrite and schwertmannite) from the surface of the inner to the surface of the outer wetland zone. This resulted in accumulations of mineralisation related elements at the surface of the outer wetland (8), sorbed to the surface of hydrous Fe-oxides. Thus, during high rainfall periods, elements associated with zones of sulfide enrichment at depth accumulated: (i) within the inner wetland zone because of the formation of exchange complexes, (ii) on the soil surface of the inner wetland zone because of complexation on hydrous Fe-oxides, (iii) on the soil surface of the outer wetland zone because of physical dispersion of hydrous Fe-oxides and (iv) at the external margin of the outer wetland zone because of solution transport of Pb and Zn following dissolution of galena and sphalerite.

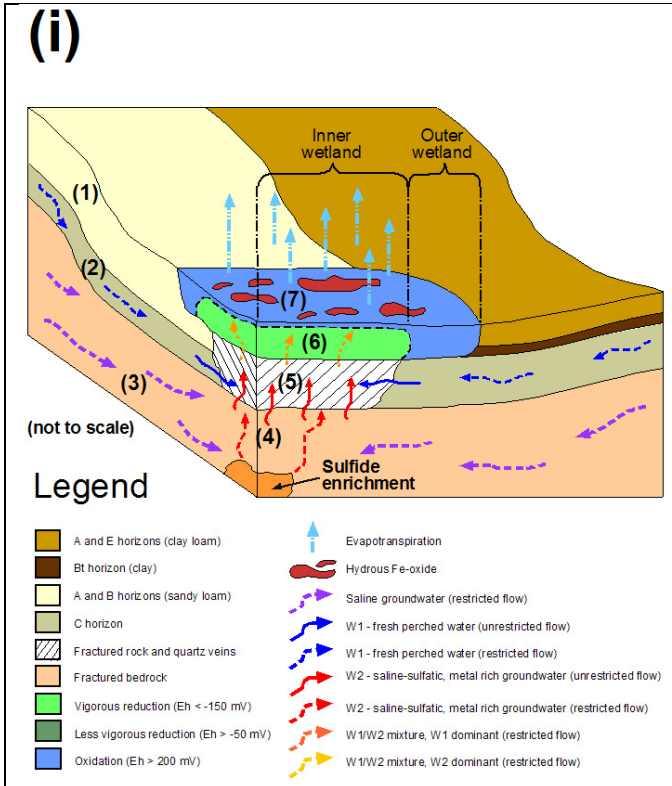

Figure 100. (i) Block diagram of the saline-sulfidic wetland, which summarises the biogeochemical processes that occurred during periods of low rainfall. Saline groundwater (restricted flow) depicted by the purple arrows represents regional groundwater and not localised upward flow of near surface groundwater. The sulfide enrichment represents any zone of sulfide enrichment that is hydraulically connected to the wetland or seep, independent of depth.

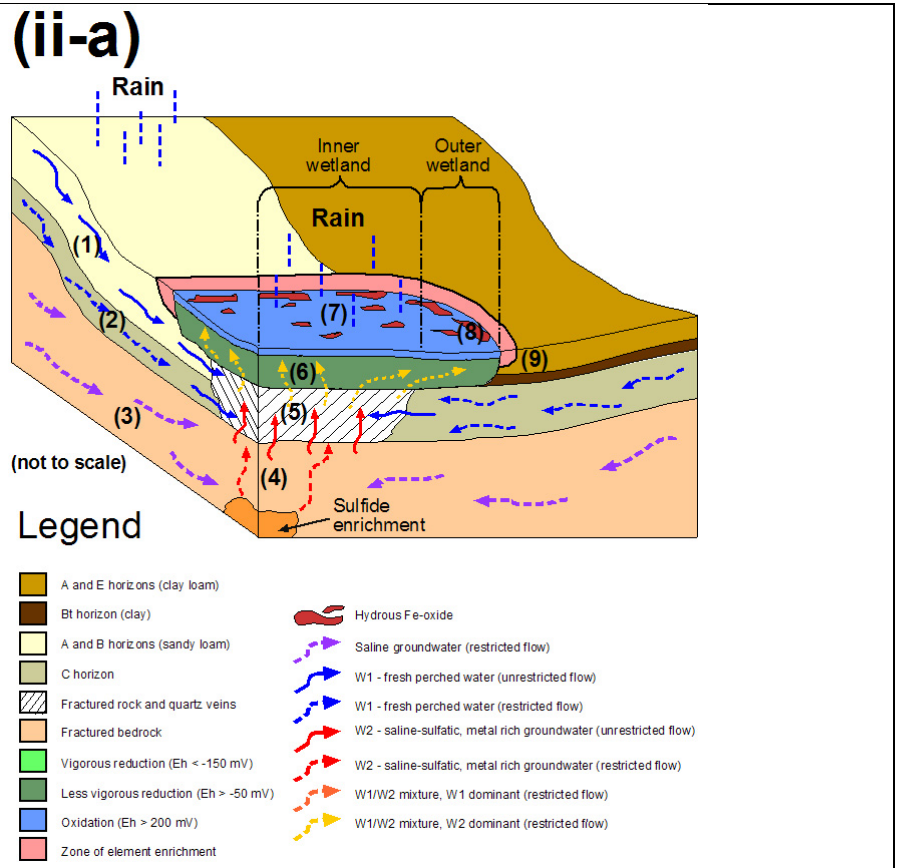

Figure 101. (ii-a) Block diagram of the saline-sulfidic wetland, which summarises the biogeochemical processes that occurred during periods of high rainfall. Saline groundwater (restricted flow) depicted by the purple arrows represents regional groundwater and not localised upward flow of near surface groundwater. The sulfide enrichment represents any zone of sulfide enrichment that is hydraulically connected to the wetland or seep, independent of depth.

Pictorial manuals for land management planning

A sequence of steps used by Fitzpatrick et al. (1997 and 2003) to develop an easy-to-follow pictorial manual for identifying soil indicators, improved land use options and best management practices is shown in Figure 102. Steps 1-5 describe soil layers and construct them in toposequences (descriptive, explanatory or predictive models), which have been used to help map soil types in the Mount Lofty Ranges areas with variable geochemistry (Fitzpatrick et al. 1997; 2003).

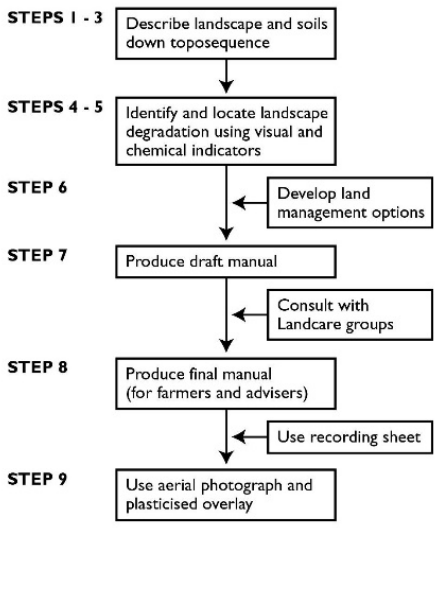

Figure 102. Flow diagram showing steps involved in developing manuals for land management (after Fitzpatrick et al. 2003).

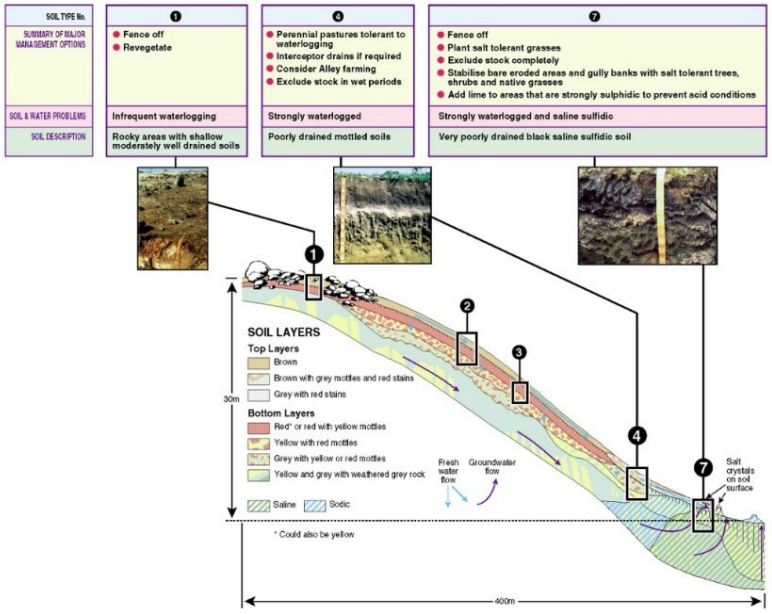

Figure 103 Sequence of soils down a slope (thee of the seven soils are illustrated) linked to a 3D mechanistic model of soil and water processes with summaries of management options associated with each soil type from Mount Lofty Ranges (after Fitzpatrick et al. 1997; 2003).

Steps 6-9 involve the participation of local communities in developing the manual by integration and adoption, where knowledge of the hydrological and soil-regolith processes models (bottom half of Figure 103) and production systems are bought together in recommendations for appropriate best management practices (top half of Figure 103). For example, in the Mount Lofty Ranges (Fitzpatrick et al. 1997; 2003) fencing protected saline-sulfidic wetlands from physical disturbance (e.g. pugging by cattle) and has:

- Allowed rapid recovery of wetland vegetation
- Prevented physical erosion of the A horizon
- Facilitated the reestablishment of more reducing soil conditions in the A horizon
- Decreased the amount of pyrite oxidation
- Allowed a return to neutral pH (pH = 6.5 to 7)

Based on the occurrence and formation of saline-sulfidic soil conditions and schwertmannite in the Guthrie wetland in 1992, recommendations were made to the landholder to urgently apply the above-mentioned best management practices. The landholder quickly responded in late 1992 by fencing the entire saline-sulfidic wetland to protect it from further physical disturbance (e.g. pugging by cattle) and also applied agricultural lime to ameliorate the extreme acidic conditions. The fencing surrounding the wetland has remained intact and protected the wetland for over 3 decades from being eroded and becoming degraded. However, based on the existing acidic conditions (pH 3.66) and the widespread occurrence of schwertmannite in the wetland a recent recommendation would be for the current landholder to apply agricultural lime to the wetland to ameliorate acidity.

Stop 3: Brukunga Pyrite Mine

Figure 104: Map of Brukunga Mine sites with each location (acid treatment plant, acid dam and mine soil heaps) with red stars. QR code take you to a video tour of the site.

The following section is Adapted from (Cox et al., 2006; Department for Energy and Mining, 2017)

The Brukunga mine operated from 1955 to 1972, extracting iron sulfide (pyrite and pyrrhotite) from an open pit quarry near the township of Brukunga. The mine commenced production in June 1955 and continued for 17 years, closing on the 31st May 1972. The mine produced 5.5 million tonnes of Fe sulfide (pyrite and pyrrhotite) ore at ~380,000 tonnes per annum. The ore had a grade of 11% S and was crushed and processed on site to produce a 40% S concentrate.

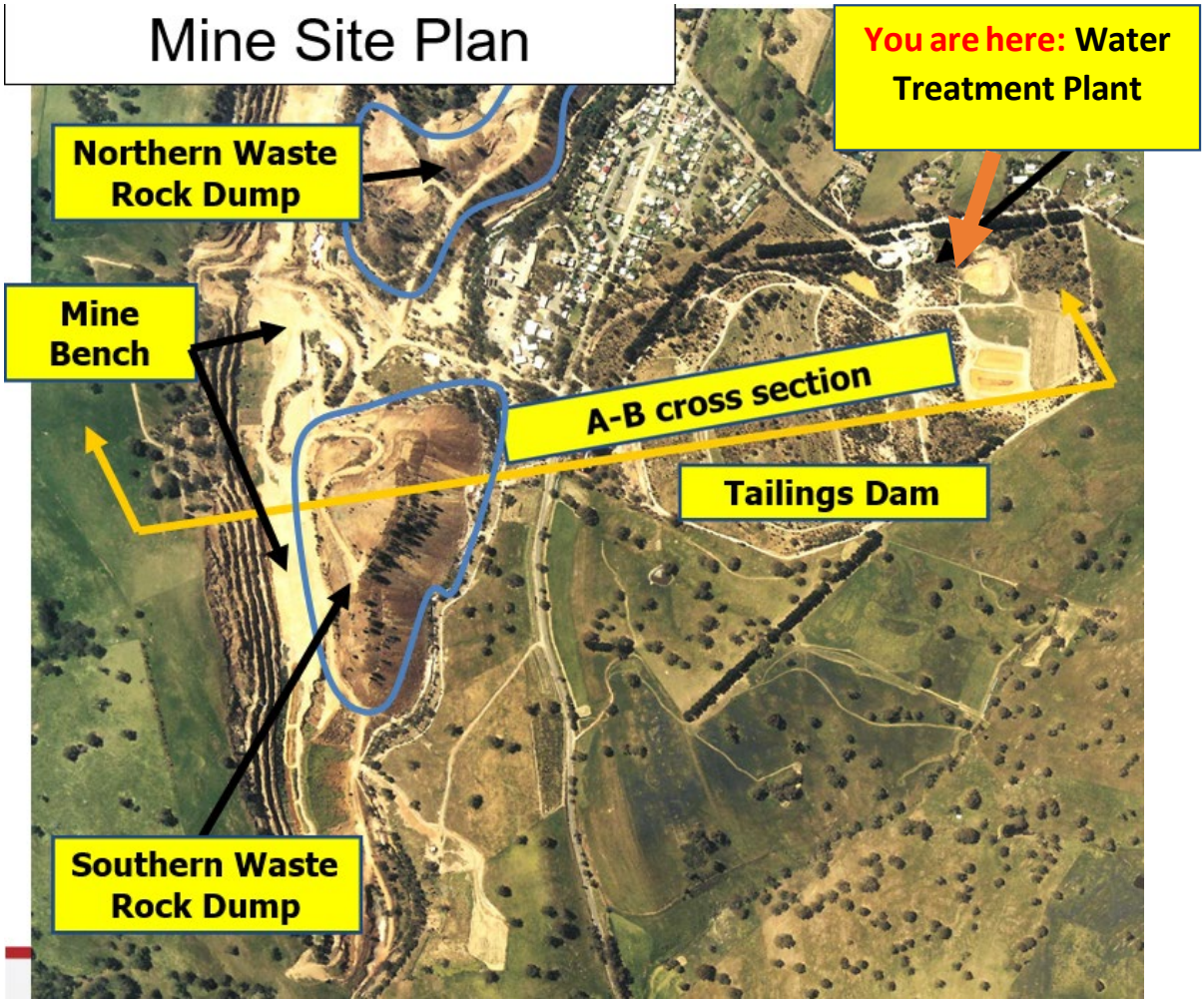

Figure 105: Location of the Brukunga Pyrite Mine and key site features (from (Cox et al., 2006))

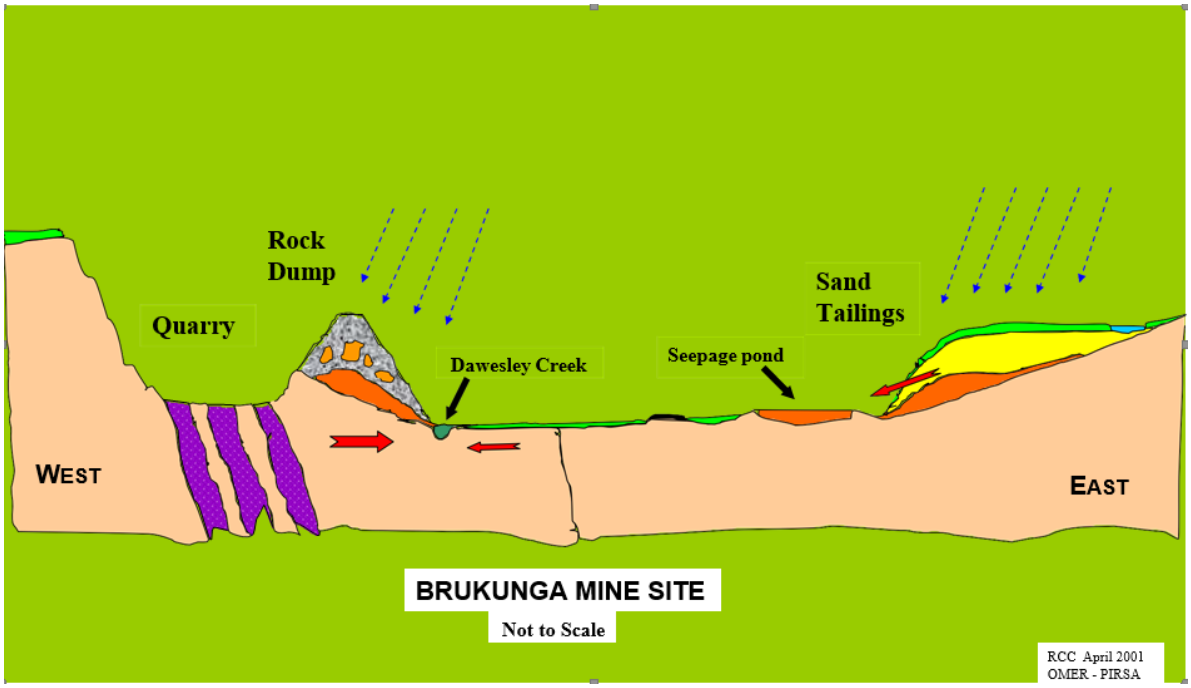

Figure 106: A-B cross section from Figure 105

Iron sulfide was quarried from the side of two steep hills using a power shovel and trucks. The mine concentrate was trucked to a rail siding at Nairne and then railed to Snowdens Beach, Port Adelaide where it was converted to H_2SO_4. Imported phosphate rock was treated with the acid to produce superphosphate fertilizer to sustain South Australian agriculture. To encourage mining of pyrite for production of sulphuric acid, the Commonwealth paid a bounty via the Sulphuric Acid Bounty Act, 1954 and the Pyrites Bounty Act, 1960. Only two mines were established in Australia specifically to mine pyrite ore, ie. Brukunga and the King Mine at Norseman, Western Australia. In the late 1960's cheaper sources of sulfur became available mainly due to Canada's refining of 'sour natural gas'. The government withdrew the pyrite subsidy on 31st May 1972 and both pyrite mines ceased mining operations on the same day.

Following mine closure, the crushers and metallurgical plant were dismantled and the mine office and workshops later became the start of the Country Fire Service (CFS) State Training Headquarters. The remaining quarry bench is 1.8 km long with 2 high walls 70 and 85 m laid back at 45° and 50°. The 8 Mt of rock removed to access the pyrite was discarded to form the north and south waste rock piles. A small rock pile, south-east of the open cut, has been rehabilitated. Concentration of the sulfide ore on site involved crushing and grinding the ore to a fine sand, with 80% passing a 75 µm sieve. This produced a total of 3.5 Mt of mill tailings that was pumped to the eastern side of Nairne Road to fill a shallow farm valley. The tailings at the front edge are 30 metres above the valley floor and covers an area of 28 hectares.

After closure in 1972, Nairne Pyrites Pty Ltd employed two caretakers to collect and pump acid drainage to a large evaporation lake on the tailings facility. In February 1974, a summer storm caused the lake to overflow and it was soon realised that water levels could not be controlled solely by evaporation. The Department of Mines and Australian Mineral Development Laboratories (AMDEL) began to investigate site water quality issues. In August 1977, the State Government accepted responsibility for rehabilitation of the site.

In September 1980, the government commissioned a lime treatment plant to treat the acid water. The Department of Engineering and Water Supply (EWS) were appointed the operators and within 5 years of successful treatment a 10 ha lake of acid water was removed from the tailings facility. The plant was then used to treat acidic seepage percolating through the tailings embankment and acid drainage transferred by 12 float-activated pumps from various locations around the quarry bench and waste rock piles. The collected water is held in two ponds located at the base of the tailings embankment. Polluted water from the holding ponds is pumped to the plant by a range of six varying capacity screw-pumps mounted in parallel. Feed to the plant (from 17 kL/hour to a peak of 50+ kL/hour) is controlled by operating one or more of these pumps.

Prior to 2003, where possible, contaminated water from Dawesley Creek was diverted, via the collection ponds, through the lime treatment plant before being discharged back into the creek. However, the capacity of the treatment plant was frequently exceeded due to high flows in Dawesley Creek, especially during the wetter winter months.

Despite all the work done from 1980 to 2003 to intercept and treat acid drainage, only approximately half the pollution from the site was treated. The remnant 50% or ~600 tonnes/year of SO_4^{-2} escaped to pollute the flow in Dawesley Creek (PIRSA, 2003b).

Government Rehabilitation Program for Brukunga Mine

(Adapted from (Cox et al., 2006; Department for Energy and Mining, 2017)

In March 1999, the Brukunga Mine Site Remediation Board (BMSRB) replaced the technically based 'Brukunga Taskforce' placing emphasis on local community involvement in developing new management solutions to lower the risks associated with the acid drainage. The BMSRB advises the State Government Minister for Primary Industries and Resources on strategies for environmental improvement and has representatives from the Dawesley Creek Catchment Landcare Group, the District Council of Mount Barker, a local community representative, and members from PIRSA (Minerals and Energy Division). In 2001, after considering various studies, the BMSRB recommended a $26M (AUD) 10 year program of new initiatives to the Minister and government (PIRSA, 2002). The government accepted the program involving:

1) creek diversion and containment of site acid drainage,
2) doubling the peak acid treatment capacity
3) decreasing the acid seepage by relocating / capping waste rock piles.

As a priority of the remediation program, acid drainage produced on site had to be contained and the amounts entering the local waterways substantially reduced. The key to this was the diversion of Dawesley Creek, and containment of acid runoff and seepage on site.

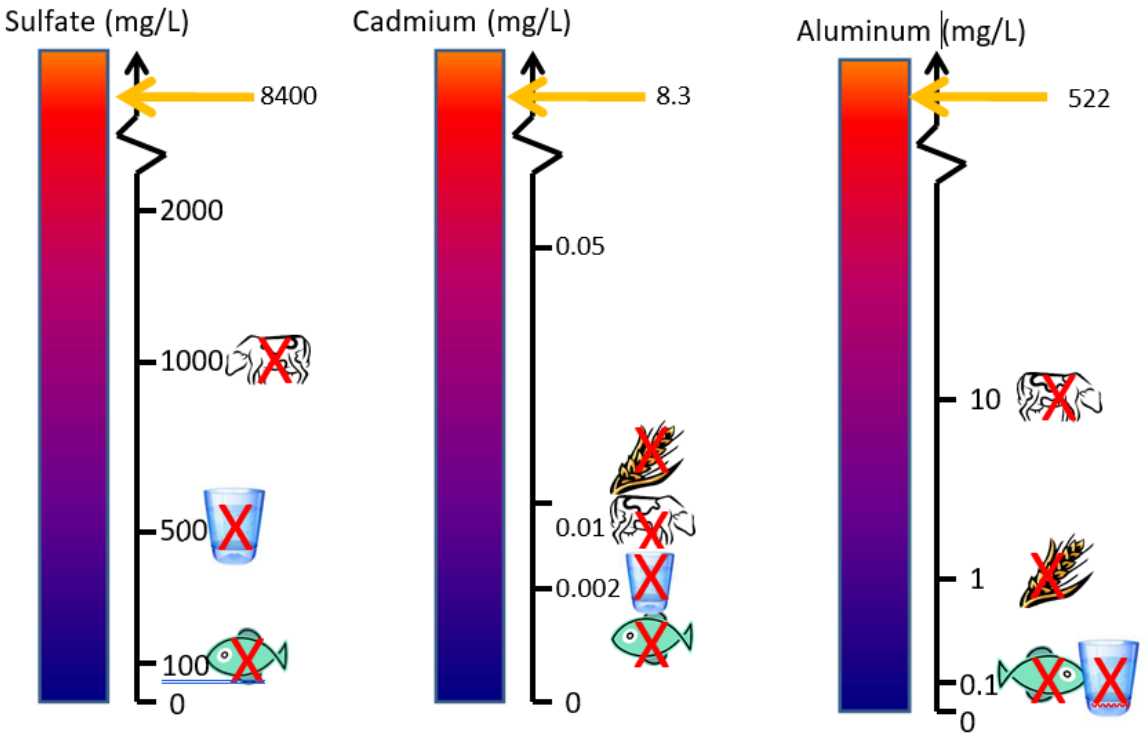

Figure 107: Pre-treatment water quality discharged into Dawesley Creek

In 2003 a major improvement in water quality in the creek downstream of the mine site was achieved primarily due to the construction of a 1.7 km creek diversion drain.

The diversion isolates Dawesley Creek from the pollution generated at the mine site. The 1.7 km diversion includes 780 metres of 1.5 metre diameter reinforced concrete pipes, 175 metres of High-

Density Polyethylene (HDPE) plastic pipe and 750 metres of drilled and blasted open channel (Fig. 2). The original section of creek, adjacent to the waste rock piles, now provides a sink for the collection of acid drainage that previously flowed directly into the creek. Construction of the drain resulted in an immediate improvement in water quality in Dawesley Creek downstream of the mine for the first time in 50 years.

In 2005 upgrading of the lime treatment plant was completed, effectively doubling its capacity to treat AMD from the sites.

These two initiatives have resulted in a marked improvement in downstream water quality, compared to levels measured prior to 2003. In June 2014 the Dawesley Creek diversion drain was extended by a further 300 m. An additional AMD collection weir was constructed and further improved water quality downstream of the mine. In 2016, a new retention pond was constructed and pumps commissioned (June 2016) that increased storage capacity by 7.6 ML and helped mitigate potential downstream AMD impacts. Water quality downstream of the mine has primarily been determined by seasonal fluctuations in rainfall and the treatment's capacity to capture and treat all AMD generated on site.

Figure 108: Dawesley Creek diversion drain. Laying pipe for the underground segments of the drain (right) and open channels (left). Photos from Cox et al., 2006

On completion of the Dawesley Creek diversion it became possible to intercept 90-95% of the pollution, with most of the loss occurring during high rainfall events. During these high rainfall events, any loss of acid drainage off site was substantially diluted.

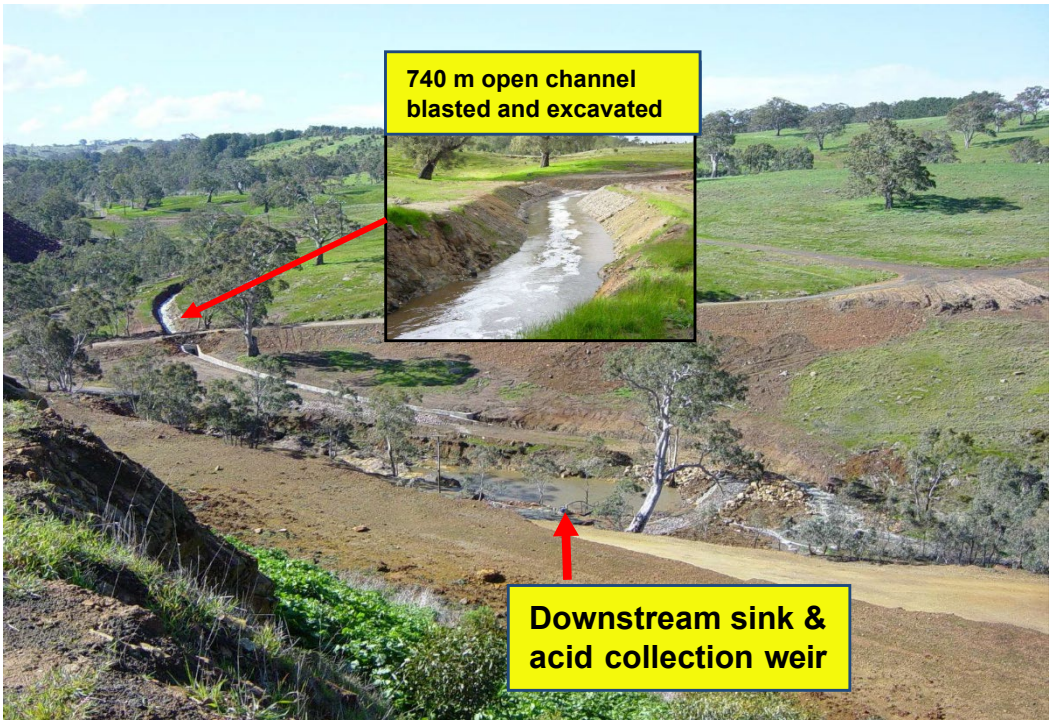

Figure 109: Dawesley Creek diversion drain

Stage 3 of the rehabilitation (relocation and treatment of the water rock dumps) was abandoned.

Lime base acid treatment facility

The originally treatment plant was designed to treat 20 kL of acid drainage per hour, but has dealt with flow rates between 10 and 35 kL per hour. Treatment requirements are greatly affected by seasonal and local rainfall events. During summer the plant was often shut down, but during the wet winter months (June through September) the plant operates 24 hours/day and 7 days/week to maintain water levels in the North and South AMD holding ponds.

In May 2005, a second parallel series of 3 larger reaction vessels was installed to effectively double the treatment capacity of the plant. The installation of the new plant and upgrade to the existing plant was completed at a cost of $750,000 (AUD). Improvements in sludge density and settling characteristics enabled the existing thickener to accommodate the sludge output of both plants.

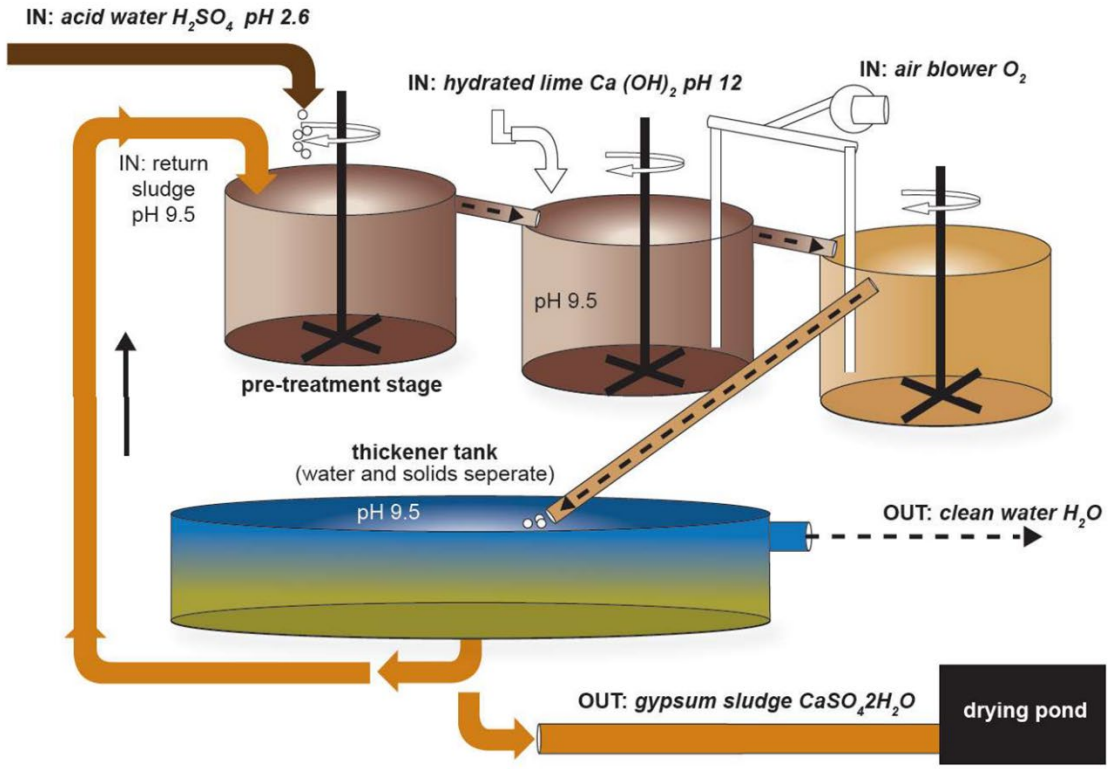

Figure 110: Schematic of the lime-based treatment facility

- Hydrated lime and Slaked lime (a waste product) mixed with acid to achieve a pH 9.5 in the thickener tank.
- Flocculate and oxygen added.
- Gypsum $CaSO_4$ precipitate settles to the bottom, clean water overflow from the top.
- Upgraded to a High Density Return Sludge System in 2005, tripled treatment capacity. Upgraded again in 2014 up to 100kL/hour.

Tailing Storage Facility Rehabilitation

Rehabilitation and revegetation of the tailings facility commenced in 1987 with trials using a thin (30 to 50 cm) soil and rubble layer spread over the tailings. Each year several thousand native tube-stock seedlings have been planted. The vegetation has reduced surface erosion, improved the visual appearance, and provided habitat for native fauna. In addition to this the capping and revegetation of the tailings facility has acted as a store and release cover, forming an evapo-transpiration layer that serves to reduce the deep percolation of rain into the tailing sand. Moisture is temporarily held in the root zone of the plants and from there it evaporates or is drawn up into the vegetation. This has greatly reduced deep percolation and hence the quantity of acid seeping from the toe of the tailings embankment. Measurements of depth to ground water in boreholes recorded each year indicate that the tailings facility is continuing to dry internally. This is also confirmed by decreasing quantities of seepage measured at a v-notch weir below the tailings embankment.

Following the ongoing efforts of PIRSA staff to lower seepage from the tailings embankment, the seepage contributed only 50 wt.% (28,031 kL) and 25 wt.% (25,169 kL) of the total acidity load to the existing treatment plant in 2002 and 2003 respectively. Tailings embankment seepage is likely to have contributed the majority of the acidity load arriving at the plant prior to decommissioning of ponds on top of the tailings facility and revegetation of its surface.

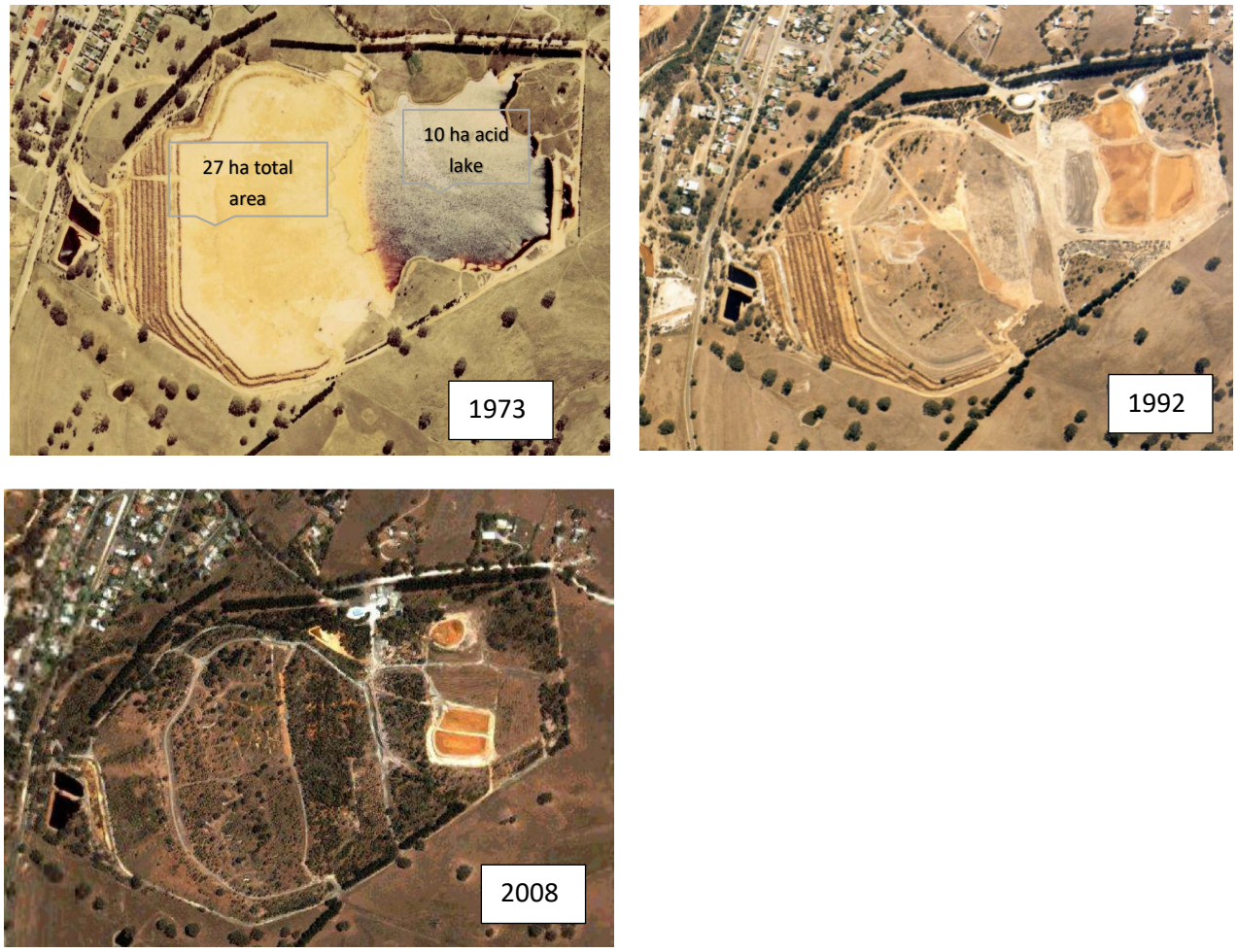

Figure 111 Aerial view of the progressive rehabilitation of the tailings storage facility

Figure 112: Aerial view of the progressive vegetation around the tailings storage facility

Mine soils on waste rock dump/mine bench cut and Iron-rich precipitates from acid mine drainage waters (from Fitzpatrick and Self 1997)

Selected properties of two mine-spoil soils sampled from the waste rock dump (Figure 113) and mine bench cut at the abandoned Brukunga pyrite mine are presented in Table 34. These soils classify as Sulfuric Spolic Anthroposols in accordance with the Australian Soil Classification (2021) and are giving rise to extensive problems through acid mine drainage seeping into local surface waters. The underlying and mined bedrock is Cambrian Kanmantoo Group Metasediments consisting of interbedded micaceous sand tones and schists with numerous sulfide-rich lenses or bands (e.g. pyrite, chalcopyrite) (Daily et al ., 1976). The acid drainage water seeping through the rehabilitated pyrite-rich tailings dam and waste-rock dump carry a range of bright red, yellow and orange coloured iron-rich precipitates as shown in Figure 113. The Fe-rich precipitates contain dominantly schwertmannite and jarosite with minor amounts of goethite and gypsum as shown in the X-ray diffraction pattern, transmission electron micrographs and energy-dispersive x-ray spectrum in Figure 114.

Jarosite and schwertmannite were also identified in drainage waters at Brukunga because the concentration of SO_4^{2+} was >3000 µg/mL and the pH between 3.5 to 4.5. According to Bigham et al. (1992), jarosite was rarely detected in their mine drainage sediments when SO_4^{2+} concentrations in associated waters were less than 3000 µg/mL. They also conclude that schwertmannite forms most readily within a narrow pH range of 3.0 to 4.0.

Table 34. Selected chemical and physical data of mine soils from the waste rock dump and mine bench cut, which classify as Sulfuric Spolic Anthroposols in accordance with the Australian Soil Classification 3rd edition (2021).

Location	Horizon	Depth (cm)	pH	Organic carbon	Total S	ESP	n-value	EC 1:5 dS/M
Waste rock	A1	0-15	3.4	0.34	3.4	3.1	<0.7	0.27
Bench cut	A1	0-15	3.4	0.54	2.7	2.7	<0.7	0.95

Figure 113: Photograph of iron-rich precipitates on the sides of the settling pond at the abandoned Brukunga pyrite min (sampled in 1992)

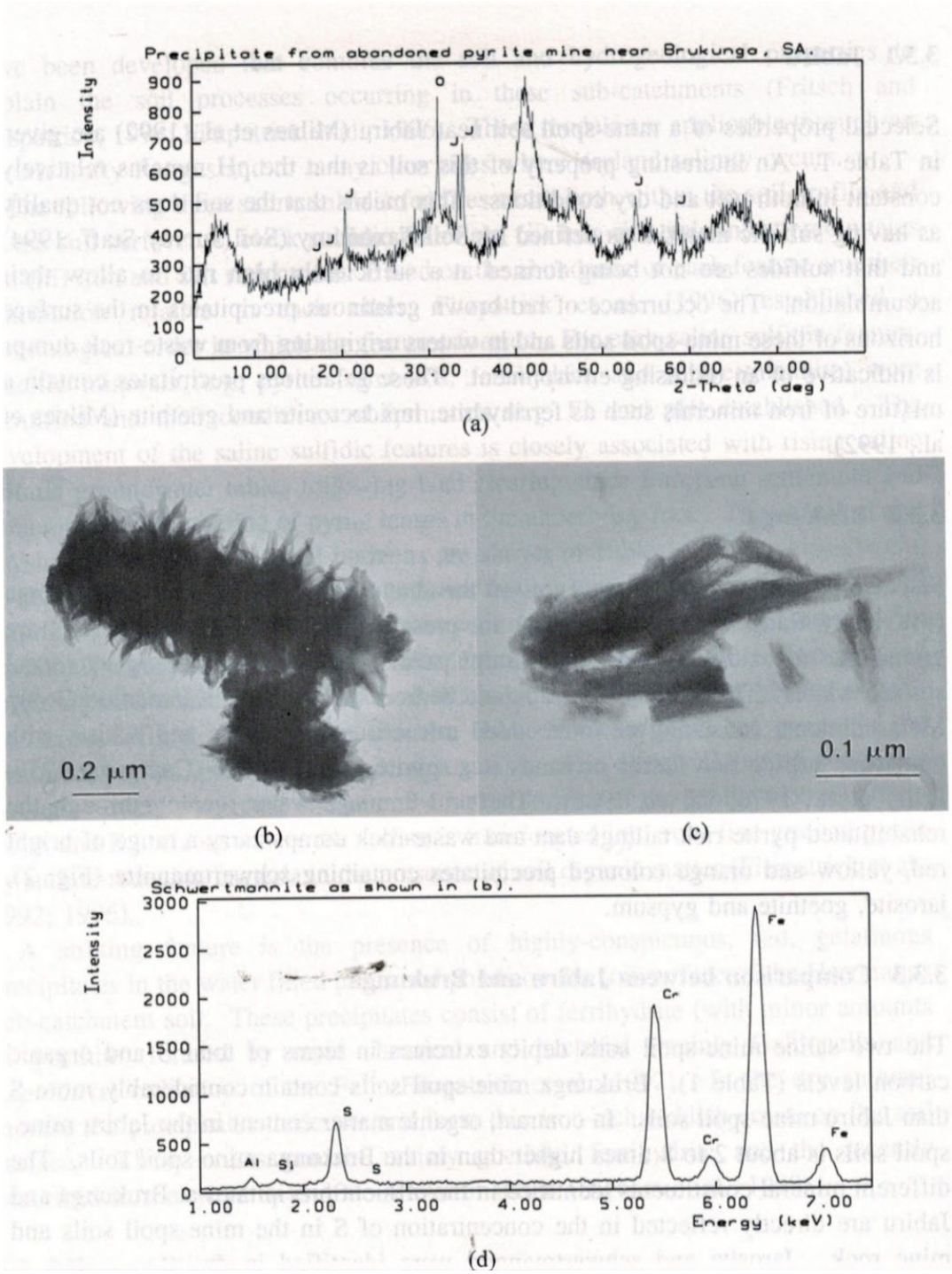

Figure 114 Mineralogy, electron microscopy and EDX of Fe-rich surface precipitates from the abandoned Brukunga pyrite mine: (a) XRD (Co Ka radiation) showing quartz (Q), jarosite (J) and schwertmannite; (b)& (c) Transmission electron micrographs of schwertmannite from the surface precipitate and (d) Energy-dispersive x-ray spectrum (EDX) of schwertmannite particle shown in (b). The dominant elements are Fe and S. Elements lighter than F cannot be detected and the Cr is from the specimen chamber and not the specimen itself (From Fitzpatrick and Self 1997).

During this Post-conference field trip photographs were taken of the mine bench cuts and adjacent waste rock dumps [Figure 115 (a)] and recently precipitated mixtures of yellow and reddish-yellow Fe-rich surface precipitates in a low lying valley within the waste rock dump [Figure 115 (a) and (b)]. Samples were taken of the yellow and reddish-yellow Fe-rich surface precipitates for X-ray diffraction and chemical analyses to determine the mineralogy of surface precipitates and to answer questions posed by field trip delegates relating to the likely geochemical processes of formation.

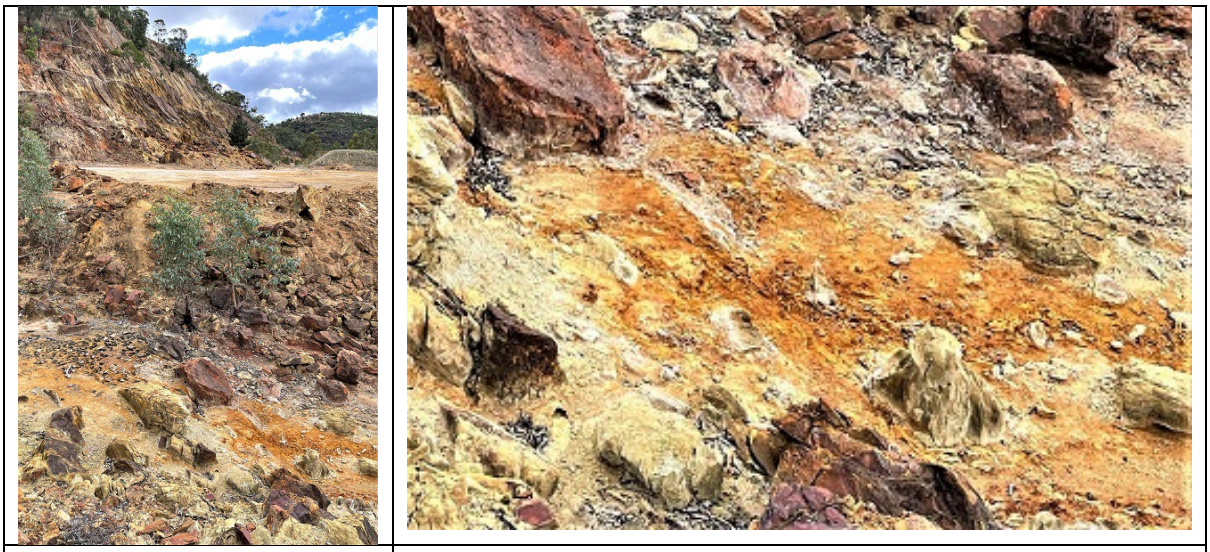

(a) (b)

Figure 115 Photographs of the waste rock dump taken during this Post-conference field trip showing: (a) the mine bench cuts and waste rock dump in the background; and recently precipitated mixture of yellow and reddish-yellow Fe-rich surface precipitates in a low lying valley within the waste rock dump and (b) close-up view of the recently precipitated mixtures of yellow and reddish-yellow Fe-rich surface precipitates, which was sampled during the field trip for future X-ray diffraction and chemical analyses. The yellow precipitate is likely a mixture of jarosite and goethite; and the reddish-yellow Fe-rich surface precipitates likely schwertmannite.

Dawesley Creek Water Monitoring Program

Required as a condition of the EPA licence for the site:

- Flow and cumulative sampling to calculate the load of contaminants leaving the site (the extent of contamination).
- Monthly grab samples of water at 11 locations down to Bremer River and analysed for sulfate and heavy metals (the range of contamination).
- Macroinvertebrate net sampling to count species and richness (the impact of contamination)

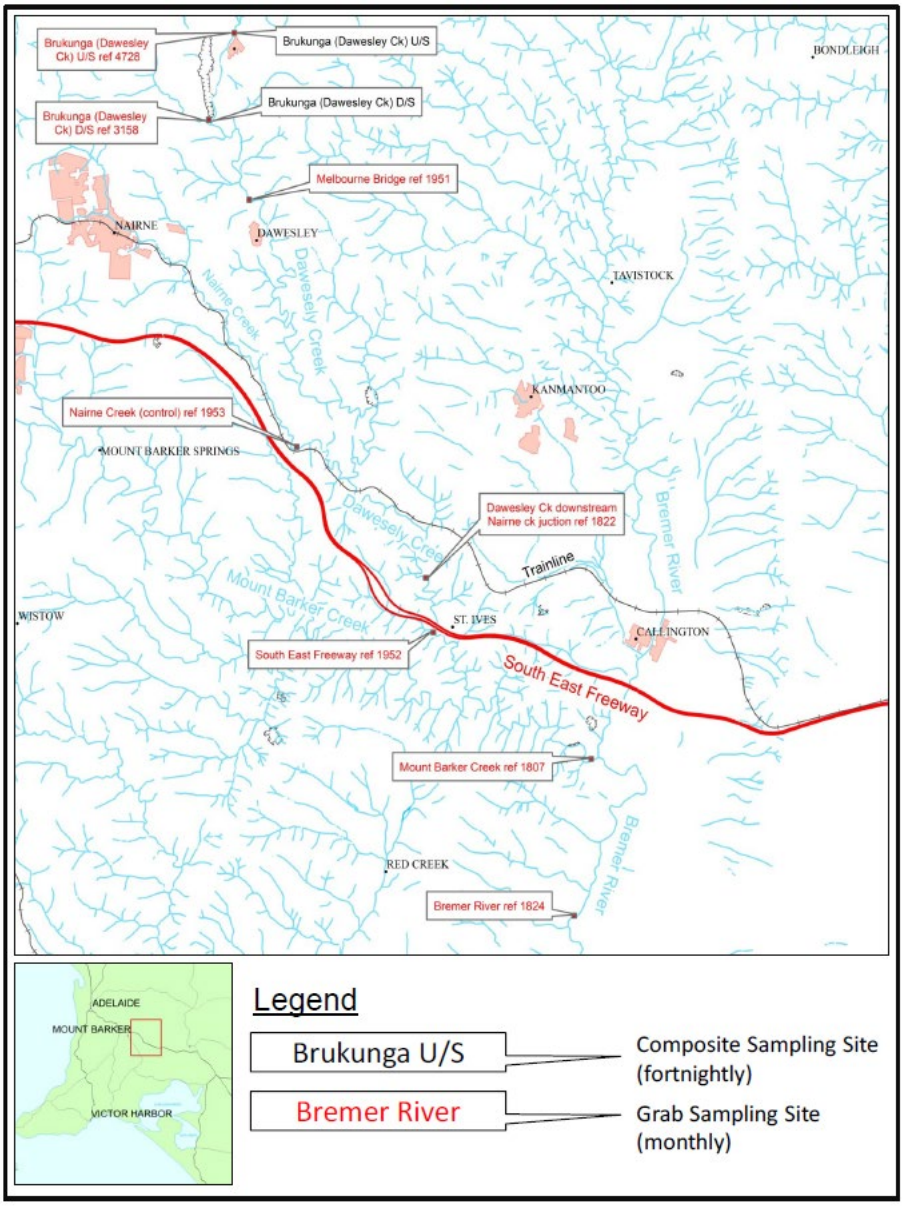

Figure 116: Monitoring sites as part of the catchment monitoring program.

The last published report from the Department for Energy and Mining demonstrated the below results for the water quality in the area:

(Department for Energy and Mining, 2017)

- Brukunga rainfall for 2017 (705.6 mm) was significantly higher than the long-term average (585.0 mm). This resulted in an above average volume of AMD being treated (182.11 ML) by the acid water neutralisation plant in 2017.
- The installation of the Dawesley Creek diversion drain (2014) and a new retention pond and pumps (commissioned July 2016) has increased storage capacity and helped mitigate potential downstream AMD impacts.
- Untreated acid flushes of low pH and metal-rich water are observed downstream of the mine in both grab and composite sampling data. These flushes usually occur immediately after the drier summer months and to varying degrees sporadically in the wetter months during flood events.
- Water quality downstream of the mine generally improves with distance from the mine, with the zone of impact of AMD contamination mostly contained within Dawesley Creek (as opposed to the downstream creeks and rivers).
- Metal and sulfate concentrations in Dawesley Creek downstream of the mine exceed the ANZECC/ARMCANZ safe levels for potable, irrigation and stock water at certain periods of time in 2017 and in most years (usually autumn and winter). Exceeded values relate to sulfate, aluminium, cadmium, manganese and iron. This presently precludes the use of Dawesley Creek water for any beneficial use downstream of the mine at certain periods of the year.
- A number of overflow events were notified to the EPA in 2017 due to high annual rainfall and storm events in winter and spring.

Table 35: Water Quality downstream of Brukunga in 2017 from (Department for Energy and Mining, 2017)

DATE	pH	EC	TDS by EC	TSS	SULPHATE	ALUMINIUM	ARSENIC	CADMIUM	CHROMIUM	COPPER	IRON	LEAD	MANGANESE	NICKEL	ZINC
		us/cm	total mg/l	total mg/l	total mg/l	total mg/l	total mg/l	total mg/l	total mg/l	total mg/l	total mg/l	total mg/l	total mg/l	total mg/l	total mg/l
11/01/2017	dry														
1/02/2017	7.60	2520	1400		483	0.614	0.0008	0.001	0.0002	0.0069	0.735	0.0002	0.742	0.0167	0.059
14/02/2017	7.80	2400	1300		540	0.451	0.0006	0.0007	0.0001	0.0088	0.497	0.0002	0.499	0.014	0.0472
1/03/2017	dry														
15/03/2017	4.60	4250	2400		2120	9.103	0.0013	0.0055	0.0002	0.0186	0.368	0.0006	7.2	0.0856	1.634
23/03/2017	7.30	2420	1360		441	1.488	0.0005	0.0007	0.0005	0.1011	1.340	0.0005	0.884	0.0105	0.241
12/04/2017	6.60	3620	2000		1630	0.345	0.0007	0.0021	0.0002	0.0266	0.207	0.0002	2.52	0.0399	0.5089
27/04/2017	7.20	2330	1300		624	0.956	0.0006	0.0009	0.0004	0.0092	0.486	0.0001	0.928	0.0175	0.1309
23/05/2017	7.60	2630	1500		510	5.783	0.0005	0.002	0.0005	0.011	2.102	0.0007	1.36	0.0247	0.2463
6/06/2017	7.80	2240	1200		516	0.797	0.0007	0.0008	0.0004	0.0075	0.316	0.0001	0.713	0.0151	0.0597
21/06/2017	7.90	2260	1200		522	0.666	0.0006	0.001	0.001	0.0085	0.314	0.0002	0.68	0.0145	0.096
11/07/2017	7.30	2290	1300		780	3.292	0.0009	0.0023	0.0007	0.0468	1.808	0.0027	2.22	0.0283	0.3607
25/07/2017	4.30	2360	1300		1040	71.63	0.0063	0.0131	0.0161	0.0621	33.36	0.0085	3.73	0.106	1.813
9/08/2017	4.40	1870	1000		624	58.61	0.0044	0.0089	0.0138	1.817	23.17	0.0829	2.38	0.0698	2.841
22/08/2017	4.40	654	360		157	18.6	0.0015	0.005	0.0066	0.0444	8.825	0.0027	0.937	0.0386	0.8035
6/09/2017	4.60	1090	600		234	15.96	0.0015	0.004	0.0038	0.022	5.407	0.0008	1.07	0.0362	0.6547
19/09/2017	7.70	2720	1500		711	2.903	0.0005	0.0021	0.0006	0.0098	2.012	0.0004	0.848	0.0156	0.1823
4/10/2017	7.40	3150	1700		993	2.256	0.0007	0.00025	0.0005	0.0143	1.184	0.0007	1.12	0.0179	0.2065
18/10/2017	7.80	1500	2650		630	1.889	0.0009	0.0015	0.001	0.0148	1.236	0.0006	0.632	0.0131	0.1221
8/11/2017	8.00	2450	1400		444	1.69	0.0012	0.0015	0.0004	0.0128	0.963	0.0005	0.531	0.0134	0.1004
21/11/2017	4.30	1730	950		513	58.93	0.0057	0.0101	0.0184	0.3238	20.86	0.0229	3.61	0.1161	1.798
19/12/2017	7.60	2180	1200		567	2.276	0.0008	0.0022	<0.0001	0.0267	1.952	0.0026	0.714	0.0186	0.1649
31/12/2017	dry														
Aquatic Ecosystems			<6.5/>9.0			0.08	0.04	0.0004		0.0018		0.006	2.5	0.013	0.02
Adjusted for Hardness (Based on 210mg/L as $CaCO_3$)								0.00228		0.00936		0.0708		0.0676	0.10
Potable						0.2	0.007	0.002		2	0.3	0.01	0.5	0.02	3
Irrigation	<6.0/>9.0					5	0.1	0.01	1	0.2	1	0.2	2	0.2	2
x10						50		0.1			10				
Livestock			2500		1000	5	0.5	0.01	1	0.5		0.1		1	20
x10															
ANZECC 2000 irrigation short-term trigger value											0.2	2	0.2		

Learnings from Brukunga Mine

- Once you oxidise iron sulfide minerals like pyrite – consequences can be ongoing for hundreds of years. In 1993-94 the Australian Nuclear Scientific and Technology Organisation (ANSTO) were engaged to provide an estimate of how long the oxidation would continue. Temperature and oxygen concentrations were monitored in a series of boreholes drilled into the tailings and rock piles, and results indicated that acid-forming reactions are likely to continue for between 240 and 750 years.
- Site has caused significant environmental and socio-economic problems across a large watershed area
- Major engineering solutions were to existing creeks were needed to protect environmental values
- Agencies have implemented strategies for handling sulfidic mining waste (segregation, neutralisation, selective placement, co-disposal/blending/encapsulation) but this cost of several millions of dollars, ongoing treatment needed
- Prevention is better than the cure! Proactive management to prevent AMD legacy – MORE COST EFFECTIVE

REFERENCES

Baker A.K (2006). New approaches to investigate and construct biogeochemical models of inland acid sulfate soils: Linkages to environmental degradation processes and mineral exploration. PhD Thesis, The University of Adelaide

Baker A.K.M. and R.W. Fitzpatrick (2003). Lead isotopes for constructing geochemical dispersion models in sulfidic wetlands. In: Roach I. C. ed. 2003. Advances in Regolith, pp. 2-7. CRC-LEME. ISBN 0-7315-4815-9 (CD-ROM).

Baker, KM and Fitzpatrick, RW (2010) A Multidisciplinary Approach to Base Metal Exploration in an area of Extreme Anthropogenic Disturbance; Mt Lofty Ranges, South Australia. CSIRO Land and Water Science Report 9/10, 44 pp. http://www.clw.csiro.au/publications/science/2010/sr9-10.pdf

Bigham, J.M., Carlson, L., Murad, E., (1994). Schwertmannite, a new iron oxyhydroxysulphate from Pyhasalmi, Finland, and other localities. Mineral. Mag. 58, 641–648.

Bigham JM, Schwertmann U, Carlson L. and. Murad E (1990). A poorly crystallized oxyhydroxysulfate of iron formed by bacterial oxidation of Fe(II) in acid mine waters. Geochim. Cosmochim. Acta 54:2743-2758.

Bigham, JM, Schwertmann U, Traina, S.J, Winland R. L, and Wolf. M. (1996). Schwertmannite and the chemical modeling of iron in acid sulfate waters. Geochim. Cosmochim. Acta 60:2111-2121.

Cox JW, Fritsch E and Fitzpatrick RW, (1996). Interpretation of soil features produced by ancient and modern processes in degraded landscapes: VII. Water duration. Australian Journal of Soil Research 34, 803-824.

Cox, R., Grindley, P., Taylor, J., & Pape, S. (2006). *Successfully lowering the risks and costs associated with the legacy of the abandoned Brukunga Pyrite Mine, South Australia*. 365–377. https://doi.org/10.21000/JASMR06020365

Department for Energy and Mining. (2017). *Brukunga mine site water monitoring report 2017* (2018/00020,). Mineral Resources Division. Department for Energy and Mining,.

Dittmann, S., Mosley, L., Stangoulis, J., Nguyen, V. L., Beaumont, K., Dang, T., Guan, H., Gutierrez-Jurado, K., Lam-Gordillo, O., & McGrath, A. (2022). Effects of Extreme Salinity Stress on a Temperate Mangrove Ecosystem. *Frontiers in Forests and Global Change*, *5*. https://doi.org/10.3389/ffgc.2022.859283

Drexel, J. F., & Preiss, W. V. (1995). *The Geology of South Australia, The Phanerozoic* (Vol. 2). Geological Survery of South Australia, Bulletin 54. Department of Primary Industries and Resrouces SA.

Dyson IA, Gatehouse CG, Jago JB (1994) The significance of the sequence boundary at the base of the Early Cambrian Talisker Calc-siltstone and its relationship to mineralisation in the Kanmantoo Trough. In 'Geoscience Australia; 1994 and beyond.'. (Eds Freeman, Michael) pp. 92-93. (Geological Society of Australia: Sydney, N.S.W., Australia).

Fitzpatrick RW (1991). How rising water-tables cause productive soils to alter to saline mangrove swamp like-soils. CSIRO Division of Soils Technical Report No. 16/1991. 6pp.

Fitzpatrick RW, Fritsch E and Self PG (1996). Interpretation of soil features produced by ancient and modern processes in degraded landscapes. V. Development of saline sulfidic features in non-tidal seepage areas. Geoderma 69, 1–29.

Fitzpatrick RW, Cox JW and Bourne J (1997). Managing Waterlogged and Saline Catchments in the Mt Lofty Ranges, South Australia: a soil-landscape and vegetation key with on-farm management options. Catchment Management Series No. 1. CSIRO Publishing, Melbourne.

Fitzpatrick RW, Cox JW, Munday B and Bourne J (2003). Development of soil - landscape and vegetation indicators for managing waterlogged and saline catchments. Australian Journal of Experimental Agriculture 43, 245–252.

Fitzpatrick RW, WH Hudnall, PG Self and R Naidu (1993). Origin and properties of inland and tidal saline acid sulfate soils in South Australia. p. 71 - 80. In D. L. Dent and M. E. F. van Mensvoort (eds.). Selected papers of the Ho Chi Minh City Symposium on Acid Sulfate Soils. International Inst. Land Reclamation and Development Publication 53.

Fitzpatrick RW and Merry RH (2002). Soil-regolith models of soil-water landscape degradation: development and application. In Regional water and soil assessment for managing sustainable agriculture in China and Australia. (Eds TR McVicar, L Rui, RW Fitzpatrick and L Changming) pp. 130–138. Australian Centre for International Agricultural Research 84, Canberra.

Fitzpatrick RW, Naidu R and Self PG (1992). Iron deposits and microorganisms occurring in saline sulfidic soils with altered soil water regime in the Mt. Lofty Ranges, South Australia. p. 263-286. In H.C.W. Skinner and R.W. Fitzpatrick (eds.) Biomineralization Processes of Iron and Manganese -Modern and Ancient Environments. Catena Supplement 21. Catena Verlag, Reiskirchen, Germany.

Fitzpatrick, R.W., Merry, R.H. and Cox, J.W., (2000a). What are saline soils? What happens when they are drained? Journal of the Australian Association of Natural Resource Management (AANRM). Special Issue (June 2000): 26-30.

Fitzpatrick RW, Raven M, Self PG, McClure S, Merry RH and Skwarnecki M (2000b). Sideronatrite in acid sulfate soils in the Mt. Lofty Ranges: First occurrence, genesis and environmental significance. In New Horizons for a New Century. (Eds. JA Adams and AK Metherell). Australian and New Zealand Second Joint Soils Conference Volume 2: Oral Papers. 3-8 December 2000, Lincoln University, New Zealand Society of Soil Science. pp. 109-110.

Fitzpatrick, R., & Self, P. G. (1997). Iron oxyhydroxides, sulfides and oxyhydroxysulfates as indicators of acid sulfate weathering environments. *Advances in GeoEcology*, *30*, 227–240.

Fitzpatrick RW and Skwarnecki MS (2005). Mount Torrens, eastern Mount Lofty Ranges, South Australia: Regolith Models of Soil-Water Landscape Degradation In Regolith Landscape Evolution Across Australia: A compilation of regolith-landscape case studies and landscape evolution models. (Eds RR Anand and P de Broekert) pp. 220–225.CRC LEME, Perth.

Fitzpatrick Rob and Shand Paul (2008). Inland Acid Sulfate Soils: Overview and conceptual models. In Inland Acid Sulfate Soil Systems Across Australia (Eds. Rob Fitzpatrick and Paul Shand). pp 6-73. CRC LEME Open File Report No. 249 (Thematic Volume) CRC LEME, Perth, Australia.

Foden JD, Turner SP, Morrison RS (1990) Tectonic implications of Delamerian magmatism in South Australia and western Victoria. In 'The evolution of a late Precambrian-early Palaeozoic rift complex; the Adelaide Geosyncline.'. (Eds Jago, B, Moore) pp. 465-482. (Geological Society of Australia: Sydney, N.S.W., Australia)

Flottmann T, Gum J, Haines PW (1996) Kanmantoo Tectonics, Sedimentology and Metallogeny Excursion. Department of Mines and Energy, South Australia, Field Guide No. 96/40, Adelaide.

Fritsch E and Fitzpatrick RW, (1994). Interpretation of soil features produced by ancient and modern processes in degraded landscapes. I. A new method for constructing conceptual soil-water-landscape models." Australian Journal of Soil Research 32, 880–885, 889–907.

Skwarnecki Marian and Rob Fitzpatrick (2008). Geochemical Dispersion in Acid Sulfate Soils: Implications for Mineral Exploration in the Mount Torrens-Strathalbyn area, South Australia. In Inland Acid Sulfate Soil Systems Across Australia (Eds Rob Fitzpatrick and Paul Shand). pp 86-107. CRC LEME Open File Report No. 249. (Thematic Volume) CRC LEME, Perth, Australia.

Skwarnecki MS and Fitzpatrick RW (2003). Regional geochemical dispersion in materials associated with acid sulfate soils in relation to base-metal mineralisation of the Kanmantoo Group, Mt Torrens-Strathalbyn region, eastern Mt Lofty Ranges, South Australia. Cooperative Research Centre for Landscape Environments and Mineral Exploration. CRC LEME Restricted Report No 185R; 193pp
Reissued in 2008 as: CRC LEME Open File Report No 205; 193 pp

Skwarnecki, M., Fitzpatrick R.W., and Davies P.J (2002). Geochemical dispersion at the Mount Torrens lead-zinc prospect, South Australia, with emphasis on acid sulfate soils. Cooperative Research Centre for Landscape Environments and Mineral Exploration. CRC LEME Restricted Report No 174. pp. 68 (volume 1) (plus 13 appendices: volumes 2 and 3).
Reissued in 2008: Open File Report No 204 68pp (Volume 1) (plus 13 appendices: volumes 2 and 3).

Soil Survey Staff, 1999. Soil Taxonomy - a basic system of soil classification for making and interpreting soil surveys. 2nd edn. United States Department of Agriculture, Natural Resources Conservation Service, USA Agriculture Handbook No. 436. 869 pp.

Soil Survey Staff, 2003. Keys to Soil Taxonomy. 9th edn. United States Department of Agriculture, Soil Conservation Service, Blacksburg. http://soils.usda.gov/technical/classification/tax_keys/

Seccombe PK, Spry PG, Both RA, Jones MT, Schiller JC (1985) Base metal mineralization in the Kanmantoo Group, South Australia; a regional sulfur isotope study. Economic Geology and the Bulletin of the Society of Economic Geologists 80, 1824-1841.

Toteff S (1999) Cambrian sediment-hosted exhalative base metal mineralisation, Kanmantoo Trough, South Australia. Geological Survey, Report of Investigations No. Report of Investigations, 57.